Migration and bioenergetics of juvenile Snake River fall Chinook salmon

Daniel Widener

A thesis submitted in partial fulfillment of

the requirements for the degree of

Master of Science

University of Washington

2012

Committee:

James Anderson

Dave Beauchamp

Julian Olden

Program Authorized to Offer Degree:

Aquatic and Fishery Sciences

University of Washington

Abstract

Migration and Bioenergetics of Juvenile Snake River Fall Chinook Salmon

Daniel Widener

Chair of the Supervisory Committee:
Professor James J. Anderson
School of Aquatic and Fishery Sciences

While general patterns in the juvenile outmigration of Pacific salmon are well known, the proximate mechanisms informing migration in individuals are still poorly understood. This thesis describes a complex of individually-based bioenergetic and migration initiation models and their application to fall Chinook salmon. We used the Wisconsin bioenergetics model combined with PIT tag and temperature data to model the growth of individual fish within the rearing habitat. We then created and tested a series of mechanistic models of migration initiation using individual fish mass and growth efficiency as proximate triggers of migration. We examined the performance of these models using CPUE data and maximum likelihood optimization methods and found that the model with both fish mass and growth efficiency as possible trigger methods performed the best; we refer to this model as the Mass-Growth model. To further test this model, we then created a correlative model of migration initiation which we refer to as the Age-Growth model. We found the predictions of the Mass-Growth and Age-Growth models to be comparable. We then applied the Mass-Growth and bioenergetic models to PIT data from ocean-type and reservoir-type fall Chinook to examine possible triggers that result in the two different life history strategies when fish enter Lower Granite Reservoir. Our models predicted that reservoir-type fish were more likely to initiate migration later and at smaller sizes than ocean-type fish,

and that the proximate triggers for migration were more likely to be reversed for reservoir-type fish after they entered Lower Granite Reservoir. We determined that the stratified temperature regime in Lower Granite Reservoir was the primary cause of the reversal of modeled migration triggers; for this reason, we then assert that the cool-water pools in Snake and Columbia River reservoirs provide temperature refuges with favorable growing conditions that result in slower-growing fall Chinook salmon following a reservoir-type life history.

Table of Contents

Acknowledgements

The author wishes to express sincere appreciation to the University of Washington School of Aquatic and Fishery Sciences, the Keeler Endowment for Excellence, and the Bonneville Power Administration for providing the funding that made this research possible. I would also like to give my heartfelt thanks to Professor James Anderson, my advisor and mentor, who has turned me into a real scientist over the last few years, and without whom this project would not have existed. I would also like to thank Billy Connor of the Idaho Department of Fish & Game and Nick Beer and Chris Van Holmes at Columbia Basin Research for providing the data and groundwork necessary for this research. Lastly, I would like to thank my friends and labmates for their continual advice and support.

Chapter 1: Introduction

1.1 Background and Chinook Life History

Migration plays a central role in the life history of anadromous salmon. Chinook salmon (*Oncorhynchus tshawytscha*) rear in riverine habitats, then migrate as subyearling or yearling juveniles through riverine and estuarine habitats to the ocean (Quinn 2005). There are several distinct life history types present in Chinook salmon in the Snake River basin, characterized by differences in timing of their juvenile outmigration and the return migration as adults (Quinn 2005, Waples et al. 1991, Connor et al. 2005). Spring-summer Chinook spawn and rear in small order streams in tributaries of the Snake River (Matthews and Waples 1991) and follow a "stream-type" life history characterized by rearing for a full year in the spawning habitat and migrating in early to mid spring as age-1 smolts (Healy 1991). Fall Chinook spawn and rear in the main stem of the Snake River and in the lower reaches of some Snake River tributaries (Connor et al. 2003a) and generally have been assumed to follow an "ocean-type" life history (NMFS 1992) wherein juveniles rear for only a few months after emergence from the gravel and migrate in the summer as age-0 smolts (Healy 1991). However, it has recently been discovered that significant numbers of fall Chinook juveniles arrest their seaward migration and overwinter in reservoirs on the Snake and Columbia Rivers, then resume migration and enter the ocean in early spring as age 1 smolts (Connor et al. 2005). Connor termed this life history strategy

"reservoir-type." As there were no dams on the Snake or Columbia rivers prior to the 1950s, the development of this reservoir-type life history is likely fairly recent (Connor et al. 2005).

The reservoir-type life history has not yet been well-studied, and the mechanisms that result in the reservoir-type life history as opposed to the ocean-type life history are not fully understood. However, it appears that the reservoir-type life history has become consequential to the fall Chinook population spawning in the Snake River basin (Connor et al. 2005, Williams et al. 2008). Work by Connor has revealed that a significant proportion of the overall population currently follows the reservoir-type life history. The percentage of juvenile Chinook that follow the reservoir-type life history seems to be quite variable, ranging from 1% to 25% depending on specific subpopulation in the Snake River and year (Connor et al. 2002); the percentage of returning adults that were reservoir-type juveniles is also quite variable, but averages 41% for wild fish and 51% for hatchery fish (Connor et al. 2005). Additionally, the reservoir-type life history appears to result in higher smolt-to-adult return rates than the ocean-type life history, as predicted by optimal life history models (Williams et al. 2008) and demonstrated by return rates (Connor et al. 2005). These studies demonstrate that reservoir-type fall Chinook have become a significant component of the Snake River population, and make clear the importance of gaining an understanding of this life history to efforts to restore the Snake River population of fall Chinook salmon. Snake River fall Chinook salmon are listed as threatened under the Endangered Species Act (NMFS 1992), and over the last several decades significant resources have been allocated to research and efforts to restore and protect fall Chinook salmon, as well as other populations of salmon in the Columbia River basin. Many agencies and stakeholders hold an interest in preserving Columbia River salmon; numerous federal and state government agencies are tasked with managing various aspects of the river and its resources, and many academic,

private, and tribal agencies contribute to research and management efforts as well. More than $7 billion has been spent in total in efforts to research, protect and manage salmon and restore runs to their historical sizes (Williams 2008). This Master's research intends to contribute to these efforts to understand and restore salmon populations, specifically fall Chinook salmon. The primary goal of this research is to investigate what factors influence migratory decision-making in individual fall Chinook juveniles, and to relate these factors to the ocean-type and reservoir-type life histories to gain a deeper understanding of the mechanisms controlling life history and how individual fish may follow one or the other. While the exact mechanisms underlying the life histories observed in Snake River fall Chinook salmon are unknown, there is a great deal of prior research in salmonid ecology and Columbia River basin dynamics that provides a background and framework for this research.

The single most important factor affecting salmon life history in the Snake and Columbia Rivers is anthropogenic modification of the river habitat. Since the beginning of the 20th century, numerous dams have been built on the Snake and Columbia Rivers and their tributaries (Williams 2008). The largest dams on the mainstem Snake and Columbia Rivers that lie between fall Chinook spawning habitat and the ocean were built starting in the 1950s. Currently, fall Chinook must pass eight dams to reach the ocean: Lower Granite, Little Goose, Lower Monumental, and Ice Harbor dams on the Snake River, and McNary, John Day, The Dalles, and Bonneville dams on the Columbia River (Figure 1.1). The creation of these dams has had numerous direct and indirect effects on Chinook salmon. Direct effects on salmon include impeding and slowing the migration of both adults and juveniles (Williams 2008), direct mortality of outmigrating juveniles due to turbine blade strikes (Deng et al. 2011), and denying access to salmon spawning habitat via inundating spawning habitat under reservoirs and blocking

access to spawning reaches via impassable dams (Williams 2008). Juvenile fall Chinook salmon in the Snake River incur significant direct mortality during their outmigration due to turbine blade strikes. Fish passing through the powerhouse of a single dam generally incur around 10% mortality (Deng et al. 2011); since fall Chinook must migrate past eight dams, this mortality has the potential to be very costly. Significant research and resources have gone into designing and building various redirection and bypass systems to prevent juvenile salmon from passing through turbine passageways, but none of these systems is completely effective (Johnson and Dauble 2006). Dam construction has also resulted in changing and limiting the spawning habitat available to fall Chinook salmon in the Snake River (Dauble and Geist 2000). Brownlee Dam, constructed in the middle Snake in 1958, is impassable to salmon and blocked access of the Snake River fall Chinook population to their historical spawning grounds near Marsing, Idaho (Connor et al. 2005, Williams 2008). Today, fall Chinook salmon are confined to spawning in the lower 224 km of the Snake River; since much of the lower Snake is inundated by reservoirs, only 163 km of this reach is usable for spawning, most of it located in the reach of the Snake River from Hell's Canyon Dam to Lewiston, Idaho (Dauble and Geist 2000, Dauble et al. 2003, Connor et al. 2005). While few data are available on the quality of the original spawning and rearing habitat, Connor and Burge (2003) concluded that the temperature regime was slightly warmer than that observed currently in the portion of the Snake River upstream of Lower Granite Reservoir. It is uncertain how productivity and suitability for growth of the current rearing habitat compare to the original habitat, but Connor and Burge (2003) speculated that growth was faster in the Marsing reach, and recent research has concluded that portions of the Marsing reach are still suitable rearing habitat (Dauble et al. 2003). Similarly, recent research has also found that suitable Chinook salmon spawning habitat still remains above impassable dams on the

Columbia River (Hanrahan et al. 2004). Hydrosystem operations significantly affect the suitability and extent of the current spawning habitat (Williams 2008); reservoir drawdown can have the effect of increasing available spawning habitat (Tiffan et al. 2006) and flow release schedules are timed to manage temperature regimes for redd and fry survival (Dauble et al. 2003, Williams 2008, Yates et al. 2008).

The construction of the hydropower system has also had numerous indirect effects on Snake River salmon. Dam construction has created reservoir habitat suitable for native and invasive salmon predators (Petersen and DeAngelis 2000, Harvey and Kareiva 2005, Waples et al. 2007); this has had a potentially large impact on the predation mortality migrating juvenile salmon face in the Columbia River. Modeling has shown that migrating salmon face a gauntlet of predators, where predation mortality varies depending on the distance salmon must migrate, predator density, and the migration rate of the salmon (Petersen and DeAngelis 2000, Anderson et al. 2005). Reservoirs created by Snake and Columbia dams can increase predator density by providing suitable habitat for native species (Petersen and DeAngelis 2000) and invasive species such as lake trout (Harvey and Kareiva 2005, Carey et al. 2011). These changes in predator regime are complicated, and their impacts on salmon are not easy to manage (Fritts and Pearsons 2008, Carey et al. 2011).

Another, potentially more important, indirect effect dam construction has had on Snake and Columbia River salmon is that the dams have radically altered temperature and flow regimes through much of the river (Connor et al. 2005). Changes in the hydrosystem resulting from dam construction have resulted in lower survival and increased travel time for migrating fall Chinook juveniles; research has linked these changes to increased water temperature, decreased flow, and decreased turbidity (Smith et al. 2003). William Connor and others have hypothesized that water

temperature also plays an important role in determining the outmigration timing of fall chinook (Connor et al. 2003a, Connor and Burge 2003); prior work has linked temperature and associated growth opportunity to life history variability in Chinook salmon (Brannon et al. 2004). Laboratory studies have demonstrated that salmon react to changes in water temperature by increasing activity levels and propensity for movement, showing that there definitely are proximate linkages between temperature and salmon behavior (Bellgraph et al. 2009). Field and laboratory studies have also shown that juvenile Chinook salmon behaviorally thermoregulate by choosing specific temperature ranges in reservoirs or in stratified laboratory tanks (Sauter et al. 2001, Tiffan et al. 2009). However, the physiological mechanisms by which temperature influences migration, and ultimately, life history, are unknown. In summation, while the mechanisms which govern migration and life history in salmonids are incompletely understood, temperature, flow, and growth have all been identified as important in previous research on salmonid life history (Hutchings and Jones 1998, Metcalfe 1998, McCormick et al. 1998, Thorpe et al. 1998, Morinville and Rasmussen 2003, Mangel and Satterthwaite 2008, Sykes et al. 2009), and changes in these environmental and biological characteristics stemming from dam construction are thought to have played an important role in the recent emergence of the reservoir-type life history (Connor et al. 2005, Williams et al. 2008). Our research is focused on using numerical modeling methods to test individually-based mechanistic linkages between water temperature, fish growth, and life history. We created a complex of models to simulate the growth, bioenergetics, and movement of fall Chinook juveniles from the rearing habitat to Lower Granite Dam, using data on water temperature in the free-flowing river and the reservoir and data from tagged fall Chinook; these models were created by applying theory from previous research on salmonid life history.

1.2 Prior Models of Salmonid Migration

The most widely accepted theory for the existence of migratory behavior posits that such behavior must provide a fitness advantage over a non-migratory behavior pattern (Gross 1987). Consequently, a common method of modeling migration has been via maximization models that track fitness (or fitness proxies such as foraging efficiency) over multiple habitats and predict migration based on strategies that maximize the statistics being modeled (Thorpe et al. 1998, Werner and Gilliam 1984). This modeling process is based on how natural selection operates; the model assumes that selective pressures direct behavior into the most optimal schema (Gross 1987). Habitat shifts of rearing juvenile salmon have been modeled using this approach (Jager et al. 1997), however, while this modeling approach incorporates the ultimate reasons for migration, it does not necessarily capture the proximate mechanisms that are directing migration in individuals (Metcalfe 1998, Thorpe et al. 1998). It only makes sense to conjecture that fitness may be informing an individual's migration in the case of small-scale habitat shifts where an individual can sample the habitats available, such as shifting between surface orientation and bottom orientation in a lake (Werner et al. 1983). Anadromous salmon migrate thousands of miles through diverse habitats (Quinn 2005); an individual salmon has no firsthand knowledge of what the conditions are or what its fitness will be in those habitats. Furthermore, the reservoir-type life history currently observed in Snake River fall Chinook has emerged very recently, so a modeling process that implies behavior optimization over evolutionary timescales is not ideal.

Rather, we focus on modeling the proximate mechanisms informing migratory decision-making. Since an individual salmon has no foreknowledge of the fitness outcome a decision will produce, it must make these decisions using locally obtained information. Models of the

cognitive process of decision-making demonstrate that the brain interprets sensory information via statistical processes to extract signal from noise and to determine if the signal satisfies a criterion to initiate behavior (Bogacz 2007, Gold and Shadlen 2007). In the context of fish migration, while the predisposition to migrate may be partially under the control of genetics, most salmonids display a continuum of potential life history strategies and an individual must make a selection of when (or if) to migrate. The proper timing of this decision has significant impact on the individual's fitness, as migrating when the fish is physiologically unprepared or environmental conditions are unfavorable is very costly (Hansen 1987, McCormick et al. 1998). Many prior models of salmonid life history utilize threshold processes in these important physiological and environmental variables to time important transitions such as initiation of migration (Metcalfe 1998, Thorpe et al. 1998, Mangel and Satterthwaite 2008), smoltification (Metcalfe 1998, Thorpe et al. 1998, Mangel and Satterthwaite 2008), and maturation (Hutchings and Jones 1998, Thorpe et al. 1998). These threshold models of behavior are not incompatible with fitness maximization models; if the proximate mechanism governing migration is thresholds in physiological and environmental variables, then the ultimate mechanism becomes the genetic factors that govern the magnitude of the thresholds and the fish's perception of the relevant variables, which can be modified by evolutionary forces (Metcalfe 1998, Thorpe et al. 1998).

Metcalfe (1998) and Thorpe et al. (1998) developed one of the most complete mechanistic models of Atlantic salmon life history to date. Their model proposes that growth rate and energetic status are the primary determinants of migration. The model is also notable in that it proposes that an individual's decision of which life history strategy to follow occurs significantly prior to migration; in Thorpe et al.'s model, an individual salmon parr will decide in August whether or not to migrate the following spring. The fish uses its current mass and growth

rate to project its mass at the time of migration. If the fish's projected mass is greater than the 'emigration threshold,' then the fish will decide to migrate and enter a pre-migratory behavior pattern characterized by high metabolic rate and rapid growth in preparation for the migration and smolt transformation (Thorpe et al. 1998). If the fish's projected mass does not meet the emigration threshold, then the fish is modeled to instead adopt a conservative feeding strategy and not migrate the next year. There is considerable empirical evidence to support this model of Atlantic salmon life history (references in Thorpe et al. 1998 and Metcalfe 1998); for instance, the smolt transformation and maturation are processes that take months and start significantly before either migration or reproduction, but not in all fish – i.e., according to Thorpe et al.'s model, differences in behavior are observed because some fish begin to prepare for the transition after they decided to migrate or mature during the relevant decision window.

Mangel and Satterthwaite (2008) adapted the model and theory from Thorpe et al. (1998) to describe age at return migration in Coho salmon and smolting migration in steelhead trout. Their modeling demonstrated that in coho salmon, different ages at return would be favored depending both on individual growth parameter and on environmental resource distribution. They also modeled the juvenile life history of central California steelhead trout; they modeled growth using a von Bertalanffy function and used the theory from Thorpe et al. and survival estimates to select optimal threshold sizes for smoltification and the resulting expected life histories for steelhead trout. They then examined how potential scenarios for anthropogenic modification of the habitat and climate change would impact modeled optimal thresholds for smoltification, and demonstrated how different temperature or food availability scenarios could produce different optimal juvenile life histories.

1.3 Modeling Strategy

The goal of this thesis is to develop an individually-based mechanistic model of the early stages of migration for juvenile fall Chinook in the Snake River using theory developed by prior researchers (especially Thorpe et al. 1998 and Mangel and Satterthwaite 2008). Prior research has indicated that bioenergetics, including fish mass and growth rate, are critical to successful migration and smolting in salmonids, and these statistics have figured highly in previous threshold-based models of salmon migration (Thorpe et al. 1998). Therefore, bioenergetics and the environmental factors that affect it are also at the core of our modeling, and we apply much of the theoretical framework developed by Thorpe et al. in our models. However, several aspects of Snake River fall Chinook necessitated departures from Thorpe et al.'s theories.

Thorpe et al.'s (1998) model of decision-making in Atlantic salmon proposes that individuals make their decisions about which life history strategy to follow months before the transition in question actually occurs. This model works well for Atlantic salmon (Thorpe et al. 1998), which rear for one or more years before initiating migration and smoltification (McCormick et al.1998). However, ocean-type fall Chinook in the Snake River emerge in late spring, grow rapidly, and then initiate migration and smoltification only a few months later in late summer (Waples et al. 1991). This compressed time schedule does not allow for a decision window very much prior to initiation of migration, and we treat the decision to migrate and the initiation of migration as the same event in our modeling of fall Chinook.

A second complication involved in modeling Snake River fall Chinook is the fact that Snake River temperatures can reach lethal levels. Temperatures above about 20 degrees Celsius cause significant thermal stress to Chinook salmon, resulting in disruption of physiological processes and refuge-seeking behavior (Connor et al. 2003a, Richter and Kolmes 2005). The

incipient lethal temperature for Chinook salmon is about 25 degrees Celsius (Richter and Kolmes 2005). Daily mean temperatures in the free-flowing portion of the Snake River routinely reach 20 degrees Celsius in July and August and in some years can even reach above 24 degrees (Anderson 2000, this thesis). In Thorpe et al.'s model, the only consideration for initiation of migration is the attainment of a growth or size threshold; while their model accounts for reduced feeding and activity during winter dormancy, there is no consideration for what a fish will do if growth becomes negative during the growth season. We propose that there is a second mechanism that can initiate migration; if the environment becomes so hostile that growth is negative, fish will be forced to initiate migration regardless of whether or not they have reached the growth/size threshold. Anecdotal evidence wherein Connor observed that juvenile fall Chinook tended to leave the nearshore of the riverine rearing habitat when river temperatures exceeded 18 degrees Celsius supports this hypothesis (Connor et al. 2002). Additionally, a previous model of fall Chinook salmon in the Sacramento River also incorporated mechanisms for juvenile salmon to respond to hostile warm temperatures by seeking a cooler refuge (Jager et al. 1997); however, this model used simple threshold water temperatures as the trigger, while in our model, we test physiological mechanisms via thresholds in bioenergetic statistics.

Lastly, while Thorpe et al. (1998) and Mangel and Satterthwaite (2008) used von Bertalanffy growth models, we use the Wisconsin bioenergetics model (Hanson et al. 1997) since it better suits our individually–based approach. Since we are explicitly modeling the migration of Chinook and Chinook do not mature as parr, we are also ignoring the portions of the Thorpe et al. model that pertain to precocious maturation. Mangel and Satterthwaite (2008) have stated that it is difficult to determine which growth statistics - lipid or total mass, absolute or rate parameters - are most important to the fish's assessment and decision process; in light of this

uncertainty, we created a several mechanistic and correlative models attempting to explain initiation of migration using a variety of energetic statistics, but chiefly fish mass, growth rate, and growth efficiency.

We here present the terminology we will use to distinguish the components of our models and data through the remainder of this thesis. We divide the habitat of the Snake River into two broad reaches for the purposes of our modeling. We define the reach of the Snake River from Hell's Canyon Dam to the confluence with the Clearwater River as the free-flowing 'River' portion of the Snake River habitat, and the reach from the confluence of the Snake and Clearwater Rivers to Lower Granite Dam as the 'Reservoir' reach of the Snake River. We assume the environmental conditions within each reach are homogenous, meaning our habitat model is a simple compartment model, with two compartments: the 'River' and the 'Reservoir.' We will elaborate on the reasons for this decision in section 2.2.1 of this thesis. Figure 1.2 displays the region of the Snake River habitat used in this study, with the relevant features labeled.

We define the times and locations of juvenile fish life history transitions based on these broad habitat delineations. The individual fish data for our modeling comes from a study conducted by Connor (Connor et al. 2005) from 1992-2000 in which many wild fall Chinook were sampled and tagged with PIT (Passive Integrated Transponder) tags. We define the day a fish is tagged as time T0. Some of the fish were recaptured within the rearing habitat and detected or recaptured at Lower Granite Dam and at dams further downstream on the Snake and Columbia rivers. We define the day a fish is recaptured by Connor within the 'River' reach as time T1, the day a fish is recaptured or detected at Lower Granite Dam as time T3, and capture dates at downstream dams as time T4. To simplify our modeling, we assume that all fish within

the rearing habitat (the ‘River’ reach) are parr and non-migratory; this assumption is supported by the fact that most fish recaptured within the ‘River’ reach were recaptured at the tagging location (Connor et al. 2003a). We define the day a fish transitions from the ‘River’ reach to the ‘Reservoir’ reach as time T2; in our models, this is the initiation of migration. There is no point of data that directly corresponds to T2; there is a juvenile fish trap near the confluence of the Snake and Clearwater Rivers maintained by the Idaho Department of Fish and Game (Marvin and Nighbor 2009), but exceedingly few fall Chinook are captured in the trap. We also do not explicitly model distance or the exact location of individual fish; since our habitat model is a compartment model, all fish within each reach experience the same environmental conditions regardless of their exact position within the reach. We also treat the transition of fish from the ‘River’ box to the ‘Reservoir’ box at time T2 as instantaneous, meaning that as soon as fish initiate migration at time T2 they enter the reservoir. This assumption is supported by evidence that Chinook juveniles migrate very rapidly in the free-flowing portion of the Snake River, then slow down when they reach the reservoir (Connor et al. 2003a). Figure 1.3 displays the locations of points T0-T4 on the habitat map from Figure 1.2; Figure 1.4 displays a simplified, iconic version. We will use the layout from Figure 1.4 through the remainder of this thesis to illustrate and organize the components of our data and models.

1.4 Chapter 1 Figures

Figure 1.1

Map of the Columbia River Basin showing the locations of the major dams on the Columbia River and its tributaries. Fall Chinook salmon in the Snake River must migrate past Lower Granite Dam, Bonneville Dam, and all the dams in between.

Figure 1.2

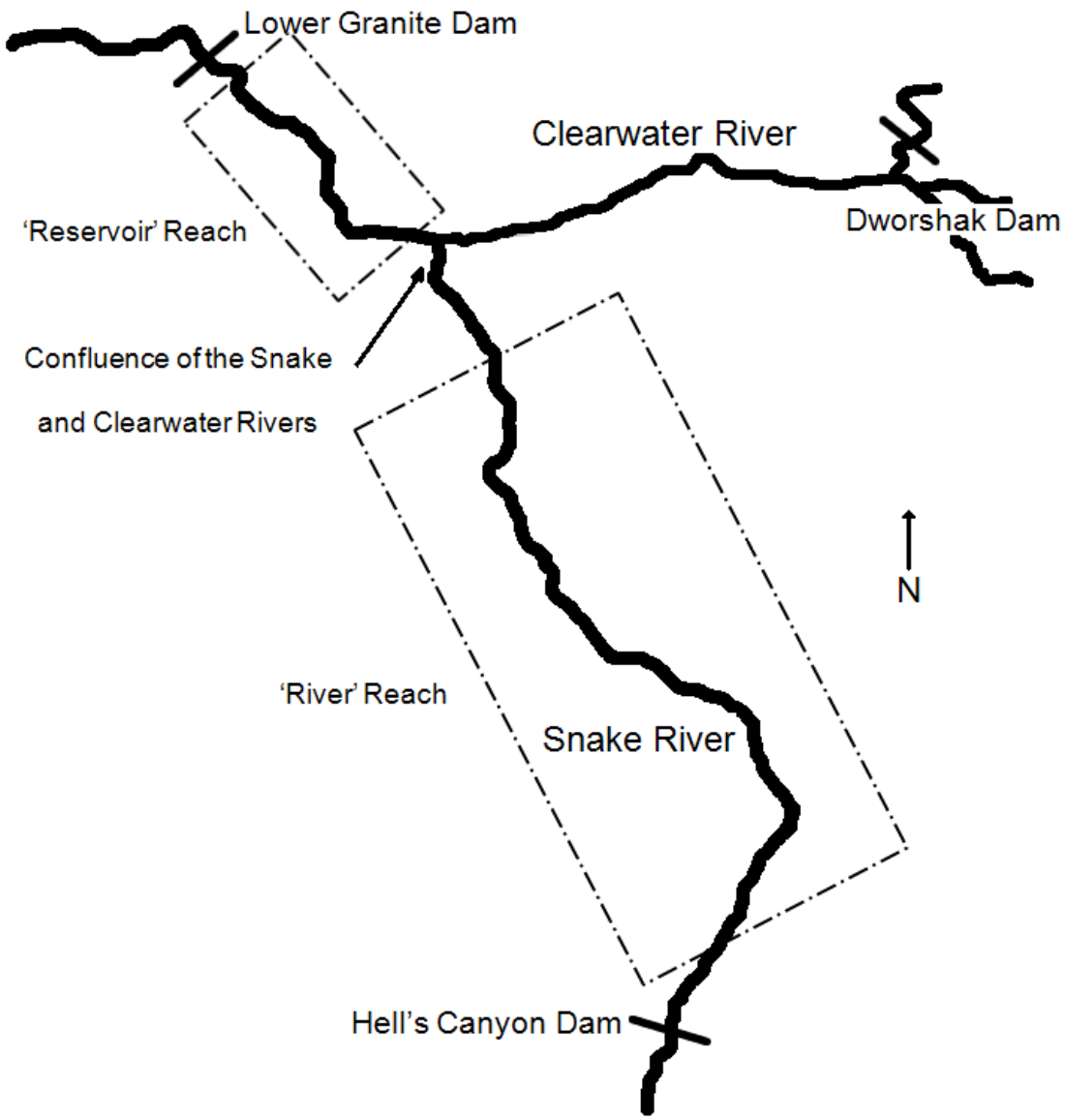

The portion of the Snake River habitat relevant to this study. Labeled are the Snake and Clearwater Rivers, the major dams mentioned in this thesis, and the confluence of the Snake and Clearwater Rivers. The two dashed boxes indicate the broad habitat regions modeled in this thesis.

Figure 1.3

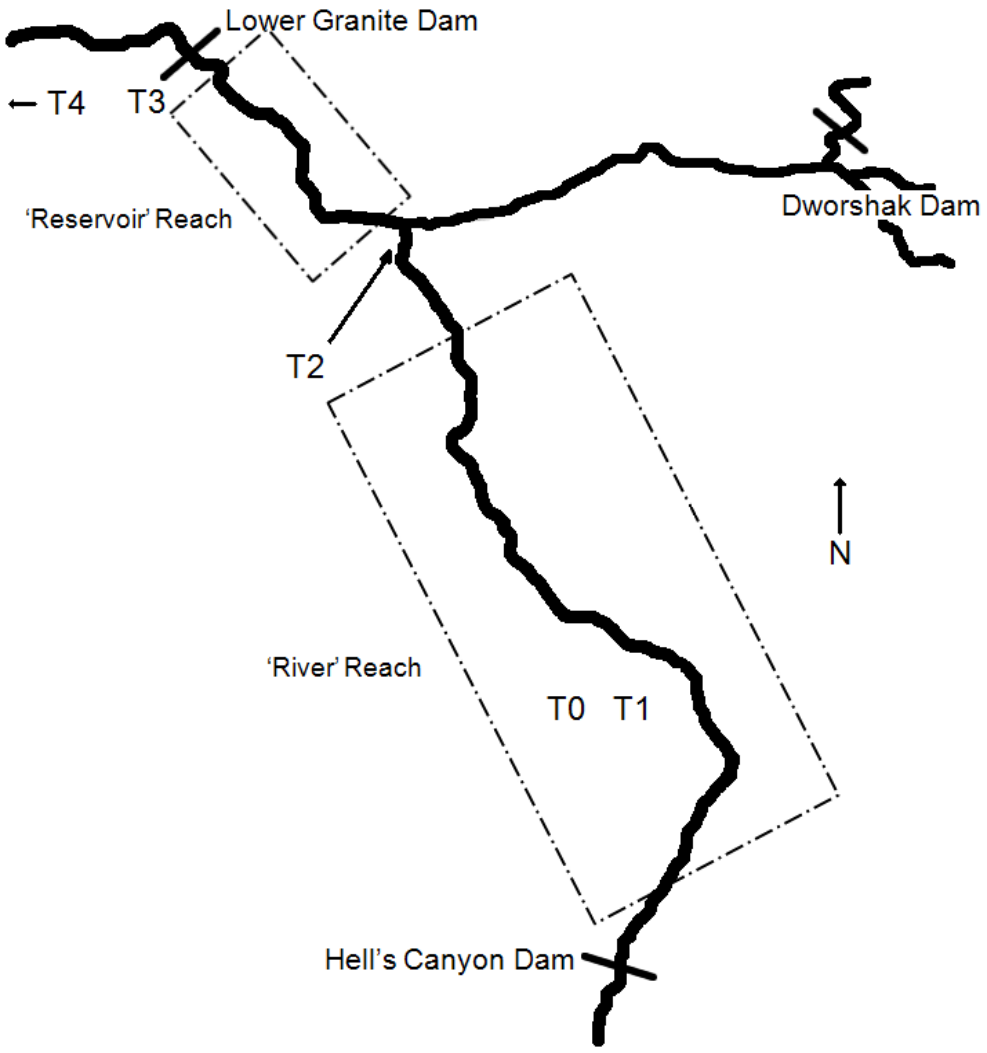

The habitat and the locations of the critical points in time of juvenile fall Chinook life history in our data and models. Points T0 and T1 (tagging and in-river recapture) occur at many sampling locations within the 'River' reach of the Snake River. Point T2 (initiation of migration) is the point where a fish transitions from the 'River' reach to the 'Reservoir' reach. Point T3 (recapture or detection at Lower Granite Dam) is the point where a fish passes Lower Granite Dam. Point T4 (other recapture or detection) is the point where a fish passes dams downstream of Lower Granite Dam (not shown on map).

Figure 1.4

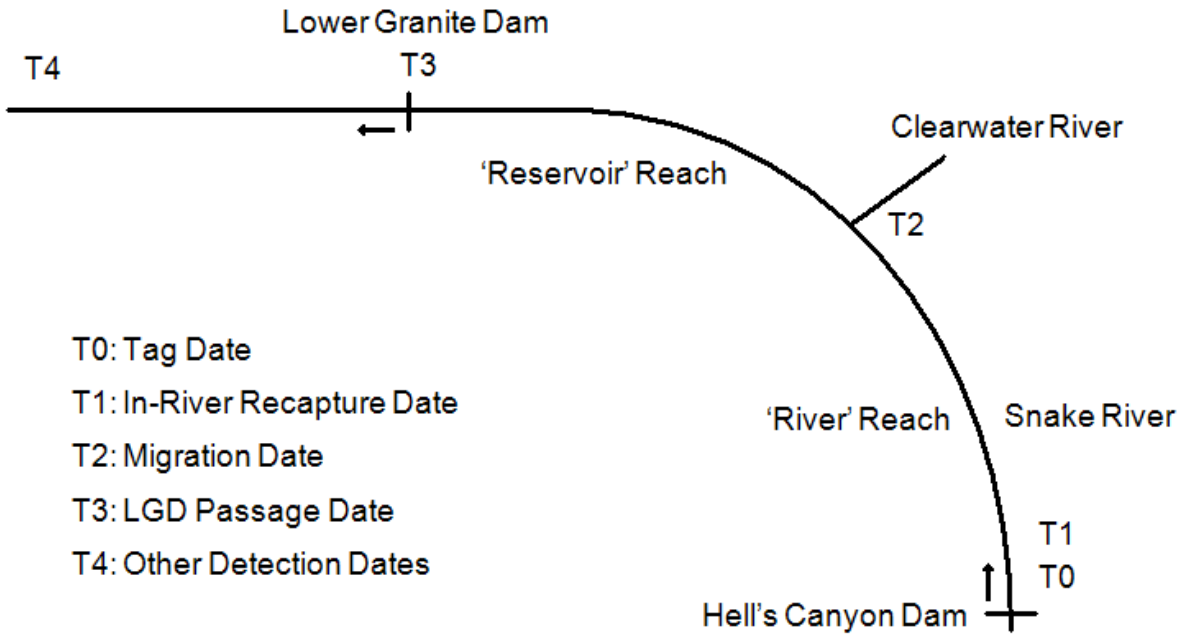

A simplified, iconic representation of the Snake River habitat used in our model. The main habitat features and the critical points in time in our models and data are labeled.

Chapter 2: Bioenergetic Models and Thermal Wall Model

2.1 Introduction

The first step in our life history modeling of juvenile Chinook was to build an individually-based bioenergetic model and parameterize it for use with our data. We chose to use the Wisconsin bioenergetics model (Hanson et al. 1997) as the core of our growth model; this model has been parameterized specifically for Chinook salmon (Stewart and Ibarra 1991) and used extensively for modeling salmonids in freshwater environments (Beer 1993, Madenjian et al. 2009). From data, we have dates of tagging and recapture within the 'River' reach (denoted as T0 and T1 respectively) as well as the fish's mass at those dates (denoted as M0 and M1) for a number of fish; in this chapter, we describe how we used the bioenergetics model to model growth within the 'River' reach (denoted as G1) and describe a model of migration initiation that predicts T2 based on G1 (Figure 2.1). This model of migration initiation applies theory from Morinville and Rasmussen (2003). Morinville and Rasmussen proposed that growth efficiency may be an important determinant of life history in salmonids by providing an index of how much benefit an individual is receiving from its current habitat. The migration model we describe in this chapter, which we term the Thermal Wall model, incorporates this theory; the Thermal Wall model assumes that positive growth efficiency indicates that an individual is benefiting from its current habitat and will continue rearing. We propose that zero growth efficiency is the threshold

which indicates an individual is no longer benefitting from its habitat; thus the Thermal Wall model predicts that fish will initiate migration once their growth efficiency falls below zero. Henceforth, in this chapter and subsequent chapters in this thesis, whenever we refer to an important statistic that comes from data, it will be in red, while any statistic coming from a model will be in blue.

2.2 Methods

2.2.1 Overview of Data

Environmental Data

As discussed in section 1.3, we represent the habitat occupied by fall Chinook in the Snake River as a compartment model with two primary compartments (Figure 1.3). Temperature and flow data was sourced from the USGS gauge near Anatone, WA (USGS 13334300) for the 'River' reach of the model. Daily mean temperatures in degrees Celsius and flows in cubic feet per second from the Anatone gauge were assumed to adequately describe the reach of the Snake River from Hell's Canyon Dam (river kilometer 399) to the confluence with the Clearwater River (river kilometer 224), the entirety of the 'River' reach. This also contains the reach of the mainstem Snake River used by spawning and rearing fall Chinook salmon (Connor et al. 2002). Figure 2.2 provides yearly plots of the water temperature recorded at the Anatone gauge over the rearing season of juvenile fall Chinook salmon. While the Clearwater River is not a compartment of our habitat model, input from the Clearwater River at the confluence of the Snake and Clearwater Rivers has a large impact on the thermal regime of Lower Granite Reservoir (Cook et al. 2006). For this reason, we use the temperature differential between the Clearwater River and the 'River' reach of the Snake River as one index of thermal stratification in Lower Granite

Reservoir. Temperature and flow data for the Clearwater River were taken from the USGS gage at Peck, Idaho (USGS 13341050) and was assumed to describe adequately the temperature of the Clearwater River at the confluence with the Snake River. Daily mean temperature data for the Lower Granite Reservoir (the 'Reservoir' reach) was taken from the DART database maintained by Columbia Basin Research of the University of Washington. This data contains separate temperature readings from Lower Granite Dam forebay, tailrace, and scroll case. Data for the forebay and tailrace readings begins in 1995, so for the years 1992-1994 the only temperature measure available for the Lower Granite Reservoir is the scroll case measure. During the summer, the scroll case temperature reading is generally the coolest while the forebay reading is generally the warmest, so for periods where both readings are available we use the difference between the two as a second index of thermal stratification in the reservoir.

Missing values in temperature or flow data from the USGS datasets were filled in by interpolating linearly between the values on either end of the gap. Since most gaps in the data were only one or two days, and there were only two gaps longer than one week over the nine years of data, this simple method is sufficient to repair the data. Small gaps in the temperature data from Lower Granite Dam were repaired in the same manner; however, no readings were taken at Lower Granite Dam during the winter, and this gap cannot be repaired by interpolation both because it is too long and because it contains the yearly temperature minimum. Since all of our modeling takes place in late spring and summer, it was decided to ignore the missing winter data.

PIT Tag Data

The data to enable our individually based model come from records of fish tagged with passive integrated transponder (PIT) tags in the Snake River. We retrieved records of juvenile Fall Chinook salmon tagged by William Connor (Connor et al. 2005) in the years 1991-2000 from the PTAGIS database of the Pacific States Marine Fish Commission. Some records were unusable for various reasons, but a total of 75,969 individual fish records over the nine year period were deemed usable. Of these fish, 58,314 fish were hatchery-reared and released into the Snake River rearing habitat by Connor; 17,655 fish were captured by Connor from the rearing habitat and are presumed to be wild. In our modeling, we preferentially use the wild fish. In some analyses where sample sizes were too small, we expanded the sample size by including the hatchery reared fish; it will be noted where this is the case. Subsets of these fish were detected or recaptured one or more times; Tables 2.1 and 2.2 provide summaries of the numbers of tagged wild fish and tagging date and size recorded at tagging by year of the study. In our modeling, we term the day a fish is tagged as tagging date T0 (Figure 1.3).

The fish tagged by Connor are ideal for this study because they were captured from the wild. Connor captured and tagged rearing fish in the Snake and Clearwater rivers (Connor et al. 2002). This sampling method results in a mixture of wild and hatchery origin fish, and for most fish their true origin cannot be determined since many hatchery fish released at small size are not adipose fin-clipped. However, since all of these fish were captured in-river and not taken directly from hatcheries, we assume that all of these fish have reared in the wild. Thus, even though we have excluded from our modeling any fish that could be determined to be of hatchery origin, the remaining sample which we have assumed to be of wild origin likely still contains some

hatchery-spawned individuals; we assume that this portion of hatchery individuals are similar enough to the wild individuals that they do not adversely impact our modeling.

Connor conducted beach seines weekly at multiple sampling sites spanning the reach of the Snake River from river kilometer 224 (upper end of Lower Granite Reservoir) to river kilometer 397 (Hell's Canyon Dam). Connor sampled each year starting in April when fall Chinook begin to emerge from the gravel and ending on a site-by-site basis when no juvenile Chinook were captured in consecutive samples at a particular site, typically in late June to early July (Connor et al. 2002, Connor et al. 2005). Connor PIT tagged all juvenile Chinook longer than 60 millimeters and released them back into the river on the same day they were captured. Tagging date and length at tagging were recorded for all fish; weight at tagging was recorded for 10,713 fish of the 17,655 wild fish.

Tagged fish could then be detected by PIT tag detectors located in the juvenile fish bypass systems and in sampling at the juvenile fish facilities at dams on the Snake and Columbia rivers and a handful of other sampling sites. Sampling effort and schedule varied by location and by year; additionally, the structure and operations at each dam as well as river conditions affect detection and survival probabilities (Muir et al. 2001, Connor et al. 2002). Table 2.3 summarizes the distribution of detections. Besides being detected, some fish were recaptured and measured at the juvenile fish facilities at dams. Recapture and detection at Lower Granite Dam in particular are important components in our modeling; we refer to the date of such recapture or detection as T3 (Figure 1.3). Recapture and detection at other dams downstream of Lower Granite have some use in our modeling, and we term the date of such events as T4 (Figure 1.3). Additionally, Connor recaptured some fish that had previously been tagged in his sampling. In our modeling, we refer to the date a fish is recaptured in-river as T1 (Figure 1.3). Most recapture events have

fish length, but as with tagging data, weight at recapture is only available in a portion of the recapture data.

CPUE Data

To supplement the PIT tag data, we requested records of the catch per unit effort (CPUE henceforth) from Connor. Connor conducted a large-scale study of juvenile fall Chinook in the Snake River from 1992 to 2000. The study sampled many sites along the Snake River by beach seining and tagging juvenile Chinook (Connor et al. 2002 and 2005). All of the fish tagged were labeled with Connor's tag code (WPC) in the PTAGIS database; however, not all sites were sampled in the same manner. Some sites were sampled on a regular basis (referred to as permanent sites); other sites were sampled on an irregular basis (referred to as supplemental sites) (Connor et al. 2003). Connor provided us with CPUE data for permanent sites, but the data was unavailable for supplemental sites. Additionally, no complete record of sampling sites and dates sampled was available for the supplemental sites.

2.2.2 Wisconsin Model

The Wisconsin Model (Hansen et al. 1997) is a generalized bioenergetics model encompassing a family of equations intended to simulate the different components of bioenergetics in different species. This model simulates the physiological processes of an individual fish, yielding a daily estimate of energy the fish has available for growth (or potentially negative growth). The model follows the general energy balance framework:

$$G = C - (R + F + U + S)$$

In this formulation, *G* refers to the total energy available for growth, *C* is the total energetic intake from consumption, *R* is the energy lost to metabolism and activity, *F* and *U* are the energy lost to egestion and excretion respectively, and *S* is the energy lost to specific dynamic action (SDA), the cost of digestion. For each of the components listed above, the Wisconsin model has several potential equations for use with different species or under different assumptions.

For the consumption term of the bioenergetics model, we used equation set 3 from the Wisconsin model (Hanson et al. 1997), parameterized for Chinook salmon by Stewart and Ibarra (1991). This equation set follows the form:

$$C = C_{max} \times T \times P \times E_{prey}$$

$$C_{max} = 0.303 \times Mass^{-0.275}$$

$$T = \left(\frac{0.36 \times L1}{1 + 0.36 \times (L1 - 1)}\right) \times \left(\frac{0.01 \times L2}{1 + 0.01 \times (L2 - 1)}\right)$$

$$L1 = e^{(0.4467 \times (Temperature - 5))} \quad L2 = e^{(1.4145 \times (24 - Temperature))}$$

In this formulation, C_{max} is the theoretical maximum consumption rate of the organism in grams per gram of fish per day, *T* is a function that describes the temperature dependence of consumption, *P* is an estimate of the fish's consumption rate (represented as a proportion of the

theoretical maximum), and E_{prey} is the energy density of the prey the salmon consumes, in joules per gram.

We used equation set 1 for the respiration term of the bioenergetics model (Hanson et al. 1997, Stewart and Ibarra 1991). This equation set follows the form:

$$R = B \times T \times A$$

$$B = 0.00264 \times Mass^{-0.217}$$

$$T = e^{(0.06818 \times Temperature)}$$

$$A = e^{(0.0234 \times VEL)}$$

$$VEL = (9.7 \times Mass^{0.13}) \times e^{(0.0405 \times Temperature)} \quad \text{when temperature} \leq 25^{o}\text{C}$$

$$VEL = (9.7 \times Mass^{0.13}) \times e^{(0.0405 \times 25)} \quad \text{when temperature} > 25^{o}\text{C}$$

In this formulation, *B* is the basal metabolic rate in joules per day, *T* is a function that describes the temperature dependence of respiration, and *A* is an adjustment for the organism's activity level. We modified the activity function, however, in order to align the two halves of the function (which uses separate equations for temperatures above and below 25 degrees Celsius for Chinook salmon). Instead of using: $(mass^{0.13})$ we used: $9.7*(mass^{0.13})*e^{(0.0405*25)}$ for the upper half of the function. Since 25 degrees Celsius is very near the lethal limit for Chinook salmon (Richter and Kolmes 2005, Geist et al. 2009) and temperatures rarely go above this level in the Snake River, we assume this change had no significant impact on the outcome of our modeling.

We used equation set 2 for the egestion and excretion terms of the bioenergetics model (Hanson et al. 1997, Stewart and Ibarra 1991). These equation sets follow the form:

$$F = (0.212 \times Temperature^{-0.222}) \times e^{(0.631 \times 0.68)} \times C$$

$$U = (0.0314 \times Temperature^{0.58}) \times e^{(-0.299 \times 0.68)} \times (C - F)$$

In this formulation, *F* is the energy lost to egestion in joules per day, *U* is the energy lost to excretion, and *C* is the total energy intake from consumption. The equation for SDA follows the following form:

$$S = 0.172 \times (C - F)$$

In this formulation, *C* is the total energy consumed and *F* is the total energy lost to egestion. As the equations demonstrate, *F* is calculated as a temperature-dependant proportion of the total energy consumed, while *U* is calculated as a temperature-dependant proportion of the total energy assimilated, and *S* is calculated as a constant proportion of the total energy assimilated.

Explanation of Growth Model Operation

To model the growth of a fish, we combine the Wisconsin model with our compartment model of the habitat. The Wisconsin model takes as inputs a fish's mass and energy density, the fish's consumption rate, the temperature, and diet energy density and returns the fish's modeled daily growth. A fish's initial mass comes from the PIT tag dataset; we term the fish's mass at tagging (T0) as M0. We determine the compartment of the habitat the fish occupies to get the daily mean temperatures the fish experiences. We determine the fish's energy density and the diet energy density from prior research and estimations using PIT data. We fit consumption rate individually for fish with a T1 data point and use a model to estimate consumption rate for others. By combining these components, the Wisconsin model produces daily estimates of

growth of an individual fish. By incrementing the fish's mass by the amount of growth predicted by the model in each daily timestep, the mass of a fish can be modeled over time.

From the PIT tag dataset, we have the date a fish was tagged and released, its mass (potentially converted from length) on that date, and the reach in which it was located. We also have the daily mean temperature on that date and the surrounding dates from the environmental dataset. Assuming estimates for consumption rate and the diet energy density, individual fish can be modeled. For example, assume a hypothetical fish capture and tagged in the Snake River on June 1st 1995 (T0), weighed 10 grams (M0). From the environmental dataset, we know that the daily mean temperature of the Snake River was 14.5 degrees Celsius on June 1st 1995. Assuming the fish's consumption rate (P) was 0.6 and that the prey energy density was 5400 joules per gram, then the Wisconsin model predicts a growth increment for June 1st of 0.339 grams (Figure 2.3a). The fish then starts at 10.339 grams on June 2nd, the temperature on June 2nd is read in and the growth increment for June 2nd is modeled (Figure 2.3b). This process can be repeated in forward or in reverse given temperature data and assumptions on the habitat, consumption rate, and diet (Figure 2.3c).

2.2.3 Assumptions and Sub-Components

Weight to Length Conversion

The Wisconsin model requires mass as an input, but for a large portion of our tagging and recapture data points only fork length is available. Therefore, we used a weight-to-length relationship to convert lengths into masses where necessary. N. Beer (personal communication, unpublished data) fitted the following weight-to-length model for juvenile fall Chinook in the Snake River:

$$Mass = e^{-12.17} \times Length^{3.179}$$

This model closely fits the weight to length relationship seen in the juvenile Chinook in this study (Figure 2.4). 10,713 wild fish had both weight and length recorded at tagging; fork length at tagging ranges from 60 mm to slightly over 120 mm, and mass at tagging from 2 g to more than 30 g. The weight-to-length conversion model describes 94% of the variance observed in this data, so we assumed that weights derived from converted lengths were suitable for use in our modeling for fish that do not have weight recorded at tagging.

Consumption Rate

Since the Wisconsin model requires a consumption rate (P) as an input, and we had no independent estimate of consumption rate, we used records of fish that were recaptured to iteratively generate estimates of consumption rates. We assumed that fish that were recaptured by Connor's beach seining (a T1 data point was present) had not migrated out of the Snake River reach in between release and recapture; therefore, for those fish recaptured within the Snake River, we have a known start weight and end weight from the PIT tag data and a known temperature history. We had estimates of prey energy density from literature values (described below), leaving consumption rate as the only unknown remaining. For these fish we modeled growth over the period between release and recapture, iterating over a range of consumption rates. The two-decimal consumption rate that produced a modeled final mass closest to the recapture mass was selected as an individual's consumption rate and assumed to be constant over the period modeled. A total of 2,447 fish recaptured within the Snake River could be fitted with a consumption rate. In addition, 62 fish had strong negative growth and could not be fitted closely under any of the prey energy density values tested. Since the model cannot fit a consumption rate

below 0, these fish were assumed to be sick or otherwise strongly affected by some non-bioenergetic factor and were excluded from future simulations. Even though the theoretical maximum value of consumption rate is 1.00, the model will fit consumption rates above 1 without issue.

Energy Density

The Wisconsin model requires as inputs estimates of the energy density of the fish and its prey. We used the following linear equation to generate a juvenile salmon's energy density based on its mass:

$$E_{predator} = 5764 + (Mass \times 0.5266)$$

This relationship was calculated for juvenile fall Chinook by N. Beer at Columbia Basin Research (unpublished data).

We generated estimates of prey energy density from two studies of diet composition of juvenile Snake River Chinook and literature energy density values for prey taxa (Curet 1993, Muir and Coley 1996). Curet (1993) provided calorific estimates of the taxa he identified in his study of diet contents, but he did not provide the wet weight/ dry weight ratio necessary to convert his units into joules per gram wet weight required in the Wisconsin model (Hanson et al. 1997). Therefore, literature values of wet-to-dry weight ratios were necessary to produce an estimate of prey energy density (Table 2.4). The overall estimate of the energy density of the diet of juvenile Chinook we generated from Curet (1993) is 4,371 joules per gram of prey. Muir and Coley (1996) also conducted a study of the diet of juvenile Fall Chinook from the Snake River, but they did not provide any calorific estimates, so we used literature values for energy density to produce a second estimate of the energy density of the juvenile salmon diet (Table 2.5). The

overall estimate of the energy density of the juvenile fall Chinook diet we generated from Muir and Coley (1996) is 3,992 joules per gram of prey.

We assumed that all fish consumed the same diet, so we needed to select a single value for prey energy density. We selected a prey energy density by using the Wisconsin model to estimate consumption rates using test values of prey energy density. Individual consumption rates were fitted for the 2,447 fish for which a T1 data point was present for each of the prey energy density values tested. First, the two estimates of prey energy density generated from Curet (1993) and Muir and Coley (1996) were used to generate distributions of consumption rates (Figures 2.5, 2.6). Both of the resulting distributions had a large number of consumption rates fitted above the theoretical maximum- 19.7% of all consumption rates in the 4,371 (Curet) distribution and 30.9% in the 3,992 (Muir and Coley) distribution. The distributions produced from these estimates of prey energy density are clearly fitting far outside the bounds of the model, as the tail of the main distribution easily surpasses 150% consumption in both. However, prior research using bioenergetic models to fit growth of fishes feeding in freshwater lakes have found similar results, with fitted consumption rates exceeding theoretical maximum rates (Luecke and Brandt 1993, Stockwell et al. 1999). These researchers concluded that the salmonids they modeled have the ability to reduce the water content of Cladoceran prey in the mouth or the foregut, thus effectively increasing the energy density of the diet. For this reason, rather than use either of the prey energy density estimates generated from the diet analyses and literature values, we decided to fit a prey energy density that produced a small percentage of fitted consumption rates above 1. 5400 joules per gram was selected because it is a round number that results in only 1.6% of fish fitted with over 100% consumption (Figure 2.7), and because this estimate was used in prior modeling of fall Chinook conducted by N. Beer at Columbia Basin Research (Beer

1998). Note that while the value used for prey energy density changes the fitted consumption rate for individuals, it affects all individuals equally; i.e., each individual's growth rate is known and comes directly from data, so the relationship between fitted consumption rates of different individuals remains the same regardless of the prey energy density used.

2.2.4 Thermal Wall Model

The first model of migration we created to test our hypothesis that hostile environmental factors will cause juvenile salmon to initiate migration. Temperatures above 21 degrees Celsius cause severe thermal stress to Chinook salmon (Richter and Kolmes 2005), and peak summer temperatures usually reach this level in the Snake River. Since we use the equation sets of the Wisconsin model designed to simulate the effects of temperature on bioenergetics, we use the growth statistics produced by the Wisconsin model as an indicator of how temperature is affecting the physiology of the salmon. Our 'Thermal Wall' model of migration initiation states that an individual salmon will initiate migration when its growth efficiency falls below zero; we denote the date of migration initiation T2, and refer to a T2 predicted by the Thermal Wall model as T2b. Since the Thermal Wall model relies completely on the Wisconsin model, we confined our testing of the Thermal Wall model to only those 2,385 fish for which an individual consumption rate could be fitted.

We initially modeled T2b as the first day when a fish's growth efficiency fell below zero; however, in some years, brief temperature spikes lasting only a day or two could produce modeled migration much earlier than in other years. To explore the resulting predictions, we also tested a version of the Thermal Wall model that would predict T2b after a predetermined number of continuous days of below-zero growth. We somewhat arbitrarily settled on five days as the

limit for this version of the model, as this was longer than most of the short temperature spikes and also limited exposure to very high temperatures to no more than a few days.

Response Variables

While growth magnitude is produced directly by the Wisconsin model and is the most obvious variable to examine with regards to determining when growth reaches zero, we used growth efficiency as our primary indicator metric for the Thermal Wall model. In theory proposed by Morinville and Rasmussen (2003), growth efficiency provides an indicator of how well an individual is performing within its current habitat; they propose that fish that perform inefficiently may be more likely to initiate migration. In the Thermal Wall model, we slightly redefine this theory to instead propose that growth efficiency can provide an indicator of when the current habitat becomes hostile to an individual. This is incorporated into our zero threshold; when growth or growth efficiency fall below zero, an individual can no longer grow and the Thermal Wall model predicts that it will initiate migration. We defined growth efficiency as energy available for growth divided by total energy consumed, or:

$$G_{efficiency} = \frac{G}{C}$$

We chose this metric because it displays a strong signal when growth approaches and falls below zero with increasing temperature and because of its use in prior studies (Morinville and Rasmussen 2003). Due to our model assumptions, energy density of the salmon diet remains constant across time and for all individuals, and while consumption rates are fitted on an individual basis, they remain constant over time for each individual for the duration of the rearing period. Therefore, the only inputs to the Wisconsin model that remain variable on an

individual basis are mass and temperature. Over the size ranges seen in our data, the Wisconsin model is insensitive to changes in mass relative to changes in temperature, as an order of magnitude change in mass only results in a 5% change in growth efficiency, while a change over the range of temperatures commonly seen in the Snake River during spring and summer results in a change of orders of magnitude in growth efficiency (Figure 2.8). Since temperature has the largest impact on the bioenergetic model, we chose metrics based on how they responded to temperature. Over the course of the spring-summer period when fall Chinook are rearing, temperatures in the Snake River increase in a linear manner (Anderson 2000). Growth magnitude varies very little across temperatures from 10-20 degrees Celsius, and then declines at higher temperatures (Figure 2.9). Energy consumed displays the same pattern, and the result of combining the two curves into growth efficiency is a steepening of the curve as it declines at high temperatures (Figure 2.10). Since the signal in growth efficiency when growth is approaching zero is very strong, we used it as the metric informing the Thermal Wall model.

Validating Model Predictions

Unfortunately, as very few fall Chinook are captured at the juvenile fish trap at the confluence of the Snake and Clearwater Rivers, there is no data point for the initiation of migration (T2) in the PIT tag dataset with which to compare the T2b predicted by the Thermal Wall model. What we do have for 2,385 individual Chinook is a date of recapture within the 'river' reach (denoted as T1). Connor et al. (2003) in their study of migration of fall Chinook assumed that this date was the date that Chinook initiated migration in order to estimate travel time from the rearing grounds to Lower Granite Dam. However, since these fish are recaptured within the rearing habitat, we do not make this assumption; instead, we assume T1 is a date when

the fish was known to be in the rearing habitat and has not yet initiated migration. 534 of these 2,385 fish are also detected or recaptured while passing Lower Granite Dam (denoted as T3). Since these fish have left the rearing habitat, we know that the initiation of migration took place prior to T3. So, for the subset of 534 fish for which both a T1 and a T3 data point are present, there is a range of valid T2 dates between T1 and T3. By comparing modeled T2b for these fish with this range, T2b can be determined to be valid or invalid for each fish.

A second method to examine the validity of modeled T2b dates is to compare the distributional properties of T1 dates and CPUE data. On a yearly basis, both T1 and CPUE display a normal distribution. We assume that the distribution begins to climb as fish in the rearing habitat grow into the tagging size threshold of 60mm, and then begins to decline as fish initiate migration and leave the rearing habitat. Thus, if the model of migration initiation is accurate, we expect it to predict an increase in migration aligning with the decline observed in recapture and CPUE data. Lastly, the decline in CPUE and recapture data to zero is indicative of the true end of the rearing season, as Connor continued sampling for two weeks after the last fish was capture to ensure that he sampled the entire rearing season (Connor et al. 2003); therefore, if the model is accurate, it should predict a mean migration date prior to the date of the last recorded recapture.

Modeling Process

The first step in modeling these fish was to fit a consumption rate (P) using the mass of the fish at T0 and T1 and the temperature history of the Snake River between those dates (Figure 2.11). Once a fish's consumption rate was determined, its daily growth was modeled and its growth efficiency tracked until growth efficiency fell below zero (Figure 2.12), or in the case of

the 5-day alternative, until its growth efficiency fell below 0 for 5 consecutive days (Figure 2.13). According to the Thermal Wall model, this date is the date of migration initiation T2b. After T2b, the model predicts that the fish enters Lower Granite Reservoir; we treat the transition from the 'River' reach to the 'Reservoir' reach as instantaneous. If growth in the reservoir is then modeled, the model then uses temperature data from the reservoir instead of the Snake River; however, we did not model in-reservoir growth in our validation of the Thermal Wall model.

2.3 Results

2.3.1 Validation of the Thermal Wall Model

The relative timing of the rearing season and thus the distributions of tagging, passage, and modeled migration varied by year, so yearly data was examined individually. Additionally, the total of 534 fish used to test the Thermal Wall model was not distributed evenly across years (Table 2.6). Years with fewer than 30 fish were excluded from analysis; these years were 1992, 1996, and 2000, with 2, 22, and 0 fish respectively. The Thermal Wall model with the one day alternative predicted a very compact period for initiation of migration. Within each year, greater than 90% of fish modeled were predicted to initiate migration within a one-week period, with a handful of early outliers (Figure 2.14). There were few or no late outliers. The Thermal Wall model with the five day alternative predicted a slightly more widely distributed period of initiation of migration (Figure 2.15). Since the only difference from the one-day alternative is that fish will initiate migration four or more days later under the five day alternative, the mean migration date is also later (Table 2.6).

Significant numbers of modeled fish were modeled with an invalid T2b (Table 2.7). A T2b modeled to occur prior to T1 was invalid due to predicting migration too early; a T2b

modeled to occur after T3 was invalid due to predicting migration too late. Overall, the Thermal Wall model tends to predict migration late. While there are early predictions, the number seldom exceeds 10% of all fish in a given year (Table 2.7). There are very many late predictions, with many years exceeding 50% of all T2bs invalidated (Table 2.7). The Thermal Wall model with the five-day alternative predicts slightly fewer early migrants, but at the cost of predicting many more late migrants. Additionally, the mean migration date in 1993, 1996, and 1999 is later than the mean T3 date in both versions of the Thermal Wall model (Table 2.6). The cumulative plots of T2b and T3 display how T2b is late compared to T3 (Figures 2.14 and 2.15); portions of the plot where cumulative T3 crosses above cumulative T2b indicate many late migrants predicted at that time.

Comparisons of CPUE data and T2b predicted by the Thermal Wall model also reveal a general trend of late prediction of migration (Figures 2.16 and 2.17). As a decline in CPUE is indicative of fish leaving the rearing habitat, we would expect the model to predict the bulk of migration initiation over this period. Instead, in every year but 1994, the vast majority of fish are not predicted to initiate migration until very late in the CPUE distribution, or even until several weeks after the end of the CPUE data (Figure 2.16). Using the five-day alternative instead of the one-day alternative makes the fits even later; fish in 1994 are now predicted not to migrate until the tail of the CPUE distribution, and in most other years, the bulk of migrants are not predicted to leave until several weeks after the end of the CPUE data (Figure 2.17). Lastly, the decline in CPUE data to zero indicates that very few fish remain in the rearing habitat at that time; the Thermal Wall model instead predicts that the bulk of the population remains in the rearing habitat until that time or later.

2.3.1 Sensitivity Analysis of the Thermal Wall Model

The Thermal Wall model produces very compact distributions of initiation of migration within years due to the mechanics of growth efficiency. As growth efficiency is produced from the Wisconsin model, the factors that impact growth efficiency are the inputs to the Wisconsin model – temperature, diet energy density, fish mass, and fish consumption rate (P). Within a given year, all fish experience the same temperature regime and we assume that all fish consume the same diet; therefore, the only factors that vary on an individual basis are fish mass and consumption rate. Assuming that temperature increases linearly through the rearing season, individual fish mass and consumption rate affect the temperature at which growth efficiency drops below zero, and thus the predicted date of T2b. The Wisconsin Model is not very sensitive to changes in fish mass, so changes in mass do not have much effect on resulting T2b (Figures 2.18, 2.19). The majority of fish captured within the 'River' reach of the Snake River are between 1 and 10 grams in mass; a change of this magnitude in mass results in just a 3 day difference in predicted T2b (Figure 2.19). Consumption rate has a much larger impact on predicted T2b, but only when consumption is low (Figures 2.20, 2.21). A change in consumption rate from 1.0 to 0.4 results in a 13 day difference in predicted T2b, while a change from 0.4 to 0.2 results in a 49 day difference (Figure 2.21).

2.4 Discussion

The sensitivity analysis of the Thermal Wall model shows why it predicts such a compact period of migration initiation within years. Changes in fish mass have little effect on the modeled day of migration initiation, and while very low consumption rates do have a large impact, only a small proportion of fish are fitted with a consumption rate below 0.4 (Figure 2.7). This results in

the majority of the population reaching the zero-growth threshold at about the same time, and is the reason why we termed this model the ‘Thermal Wall’ model.

The validation of the Thermal Wall model reveals that it is not predicting migration at the time the data suggests the fish are migrating. The model produces very many ‘late’ predictions; these predictions are direct evidence of a failure to predict migration, as the fish were known from data to have already passed through Lower Granite Reservoir before the model even predicts the fish to leave the free-flowing portion of the Snake River. Additionally, the distributional properties of both CPUE data and T3 suggest that the initiation of migration is a much more gradual distribution than predicted by the Thermal Wall model. The CPUE distributions all have a gradual decline from peak CPUE lasting more than a month (Figures 2.16, 2.17), and cumulative passage of Lower Granite Dam takes generally about 2 months before the bulk of the population has passed (Figures 2.14, 2.15). We concluded that the Thermal Wall model was not sufficient to describe initiation of migration in fall Chinook salmon, and that most fish were initiating migration via a different mechanism. We then proceeded to create another model to examine a growth efficiency threshold with a relaxed assumption on the value of the threshold as well as threshold mass as potential triggers of migration.

2.5 Chapter 2 Tables

Table 2.1

Distribution of fish tagged, detected, and recaptured by year. Since fish could be recaptured more than once, the total number of recaptures is also included.

Year	# Tagged	# Detected	# Recaptured	Total Recaptures
1992	1010	68	83	88
1993	1404	393	388	477
1994	2344	340	455	599
1995	6603	3479	945	1104
1996	465	203	100	120
1997	641	223	165	196
1998	2058	1024	449	522
1999	1917	1062	342	394
2000	1213	507	147	189

Table 2.2

Mean and standard deviations by year of tagging date and fork length at tagging for wild fall Chinook in the Snake River. Minimum size for tagging was 60 mm fork length.

Year	Mean Tag Date	Tag Date SD	Mean Tag Length	Tag Length SD
1992	24 May	10 days	72 mm	11 mm
1993	13 June	13 days	75 mm	13 mm
1994	2 June	10 days	74 mm	12 mm
1995	4 June	6 days	72 mm	7 mm
1996	6 June	23 days	75 mm	13 mm
1997	14 June	14 days	77 mm	13 mm
1998	31 May	15 days	74 mm	11 mm
1999	5 June	12 days	75 mm	11 mm
2000	25 May	14 days	76 mm	12 mm

Table 2.3

Distribution of detections of wild juvenile fall Chinook by dam and by year. Total Detected = total number of fish detected in that year; numbers of detections at the various locations are not additive since fish can be detected at more than one location. LGD = Lower Granite Dam, LGS = Little Goose Dam, LMN = Lower Monumental Dam, IHA = Ice Harbor Dam, MCN = McNary Dam, JDA = John Day Dam, BON = Bonneville Dam, Traps = Snake and Clearwater River juvenile traps.

Year	Total Detected	LGD	LGS	LMN	IHA	MCN	JDA	BON	Traps
1992	68	39	20	0	0	9	0	0	1
1993	393	270	68	54	0	40	0	0	3
1994	340	202	60	64	0	52	5	0	1
1995	3479	2097	1344	1303	0	946	31	11	0
1996	203	145	76	45	0	27	2	1	0
1997	223	135	106	47	0	32	2	2	0
1998	1024	571	631	295	0	217	75	19	1
1999	1062	608	544	364	0	142	73	40	0
2000	507	336	269	145	2	142	31	11	1
Total	7299	4403	3118	2317	2	1607	219	84	7

Table 2.4

Summary of the diet composition from Curet (1993) and energy density estimates derived from it. %TD is the percent of the total diet by mass of each prey taxon. DW ED is the energy density of ash-free dry weight in joules per gram converted from Curet (1993). %DW is the percent ash free dry weight of wet weight from literature values. 20% was used for taxon where a source could not be found and the percent total diet was less than five percent. Source is the source for the %DW value. For those entries with (order) or (subclass), a literature value for the next highest taxonomic group was used instead of the group listed under Prey Taxon. WW ED is the energy density in joules per gram wet weight calculated from DW ED and %DW.

Prey Taxon	%TD	DW ED	%DW	Source	WW ED
Collembola	<0.01	23998	20.0	NA	4800
Chironomidae/Simuliidae	0.25	21388	17.0	Groot 1995 (order)	3636
Cecidomyiidae	<0.01	19886	17.0	Groot 1995 (order)	3381
Ceratopogonidae	<0.01	19924	17.0	Groot 1995 (order)	3387
Coleoptera	<0.01	19585	23.7	Chen 2003	3094
Drosophilidae	<0.01	20920	17.0	Groot 1995 (order)	3556
Ephemeroptera	0.33	25172	23.0	Hanson 1997	5789
Homoptera	0.03	21334	20.0	NA	4267
Cicadellidae	<0.01	21489	20.0	NA	4298
Isoptera	<0.01	21757	20.0	NA	4351
Hodotermitidae	<0.01	41840	20.0	NA	8368
Odonata	<0.01	23135	22.8	Groot 1995	5275
Hymenoptera	<0.01	23745	20.0	NA	4749
Plecoptera	<0.01	21365	20.0	NA	4273
Psocoptera	<0.01	20920	20.0	NA	4184
Thysanoptera	<0.01	21525	20.0	NA	4305
Thripidae	<0.01	14428	20.0	NA	2886
Trichoptera	0.01	20068	20.7	Groot 1995	4154
unknown insects	<0.01	20969	20.0	NA	4194
insect parts	0.02	21090	20.0	NA	4218
Amphipoda	<0.01	16348	26.0	Hanson 1997	4250
Annelida	<0.01	19416	18.2	Groot 1995 (subclass)	3534
Araneae	<0.01	19819	20.0	NA	3964
Copepoda	<0.01	22985	19.6	Groot 1995	4505
Cladocera	0.11	20590	11.0	Hanson 1997	2265
Hirudinea	<0.01	20477	20.0	Hanson 1997	4095
Hydracarina	<0.01	21429	20.0	NA	4286
Isopoda	0.03	11863	20.0	NA	2373
larval fish	0.19	21493	21.0	Groot 1995	4514

Table 2.5

Summary of the diet composition from Muir and Coley (1996) and the literature values of energy density used to estimate energy density of the juvenile salmon diet. %TD is the percent of the total diet for each taxon from Muir and Coley (1996). WW ED is the literature value for energy density in joules per gram wet weight used for the analysis, and Source is the source for the literature value. For those taxa with Curet (1993) listed as source, no estimate of wet mass/dry mass ratio was available, so a value of 0.2 was used to produce an estimate of wet mass energy density from the dry mass energy densities provided by Curet (1993).

Prey Taxon	%TD	WW ED	Source
Diptera	0.44	3859	Groot 1995
Coleoptera	0.16	5010	Chen 2003
Homoptera	0.02	4267	Curet 1993
Hymenoptera	0.08	4748	Curet 1993
Thysanoptera	0.01	4305	Curet 1993
Trichoptera	0.03	4554	Groot 1995
Amphipoda	0.22	3582	Groot 1995

Table 2.6

Summary of the results of the Thermal Wall model, shown by year. # Fish is the number of individual fish used to test the model in a given year. Mean T2b (1D) and Var (1D) are the mean and variance of the day of year of the predicted T2b produced by the Thermal Wall model with the one day alternative; Mean T2b (5D) and Var (5D) are the mean and variance of the predicted T2b produced with the five day alternative. Mean T1 and Mean T3 are the mean in-river recapture date and recapture/detection date at Lower Granite Dam for the fish in that year.

Year	# Fish	Mean T2b (1D)	Var (1D)	Mean T2b (5D)	Var (5D)	Mean T1	Mean T3
1992	2	173.5	0.5	177.5	0.5	141	184
1993	30	205.5	299.9	210.4	272.4	152.2	204.4
1994	34	177.9	24.3	191.8	25.8	146	202.2
1995	103	199.8	37.4	203.9	35.7	150.5	207.6
1996	22	196.2	255.3	201.6	259.7	144.8	199.2
1997	82	196.2	149.7	201.3	150.1	162.1	205.5
1998	187	185.9	69.6	190.7	74.4	157.7	201.8
1999	74	203.2	5.9	211.2	6.2	153.2	198.1
2000	0	-	-	-	-	-	-

Table 2.7

Summary of the validation of the Thermal Wall model, shown by year. # Fish is the number of individual fish used to test the model in a given year. % T2b Before T1 (1D) and (5D) are the percentage of individual fish fitted with a T2b prior to the date of T1 under the one-day and five-day alternatives of the Thermal Wall model; i.e., the fish was modeled to begin migration before a point where it was known to be in the rearing habitat, an 'early' invalid prediction. % T2b After T3 (1D) and (5D) are the percentage of individual fish fitted with a T2b after the date of T3 under the one-day and five-day alternatives of the Thermal Wall model; i.e., the fish was modeled to initiate migration after it was known to pass Lower Granite Dam, a 'late' invalid prediction.

Year	# Fish	% T2b Before T1 (1D)	% T2b After T3 (1D)	% T2b Before T1 (5D)	% T2b After T3 (5D)
1992	2	0%	0%	0%	0%
1993	30	13%	50%	7%	57%
1994	34	0%	6%	0%	38%
1995	103	1%	36%	1%	45%
1996	22	5%	50%	5%	55%
1997	82	10%	45%	0%	52%
1998	187	14%	22%	7%	30%
1999	74	0%	57%	0%	72%
2000	0	-	-	-	-

2.6 Chapter 2 Figures

Figure 2.1

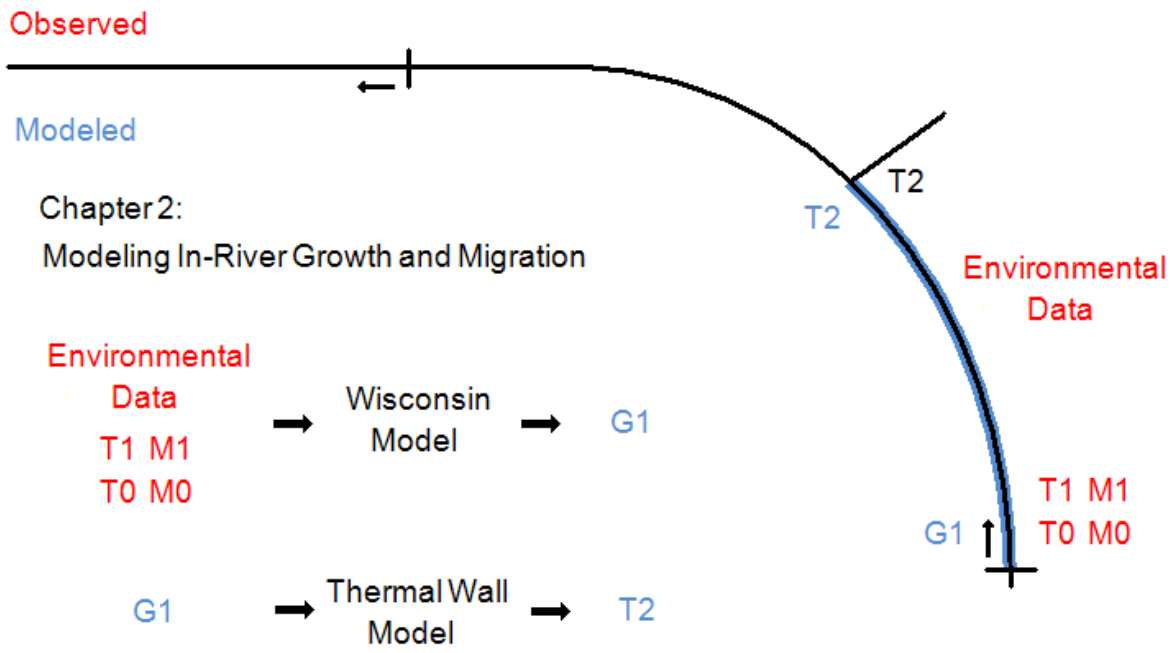

A depiction of the major modeling and data components presented in chapter 2 of this thesis within the iconic schema introduced in figure 1.3. Values from data are in red, components produced by models are in blue. Note that as there is no direct value for T2 from data, it is presented in black. T0 and T1 are the dates of tagging and in-river recapture from PIT tag data, M0 and M1 are the recorded mass on those dates. In combination with environmental data, the Wisconsin model is used to model growth for fish for which all data is present, yielding modeled growth G1. G1 is then used in our Thermal Wall model of migration initiation to yield a modeled migration initiation date, T2.

Figure 2.2

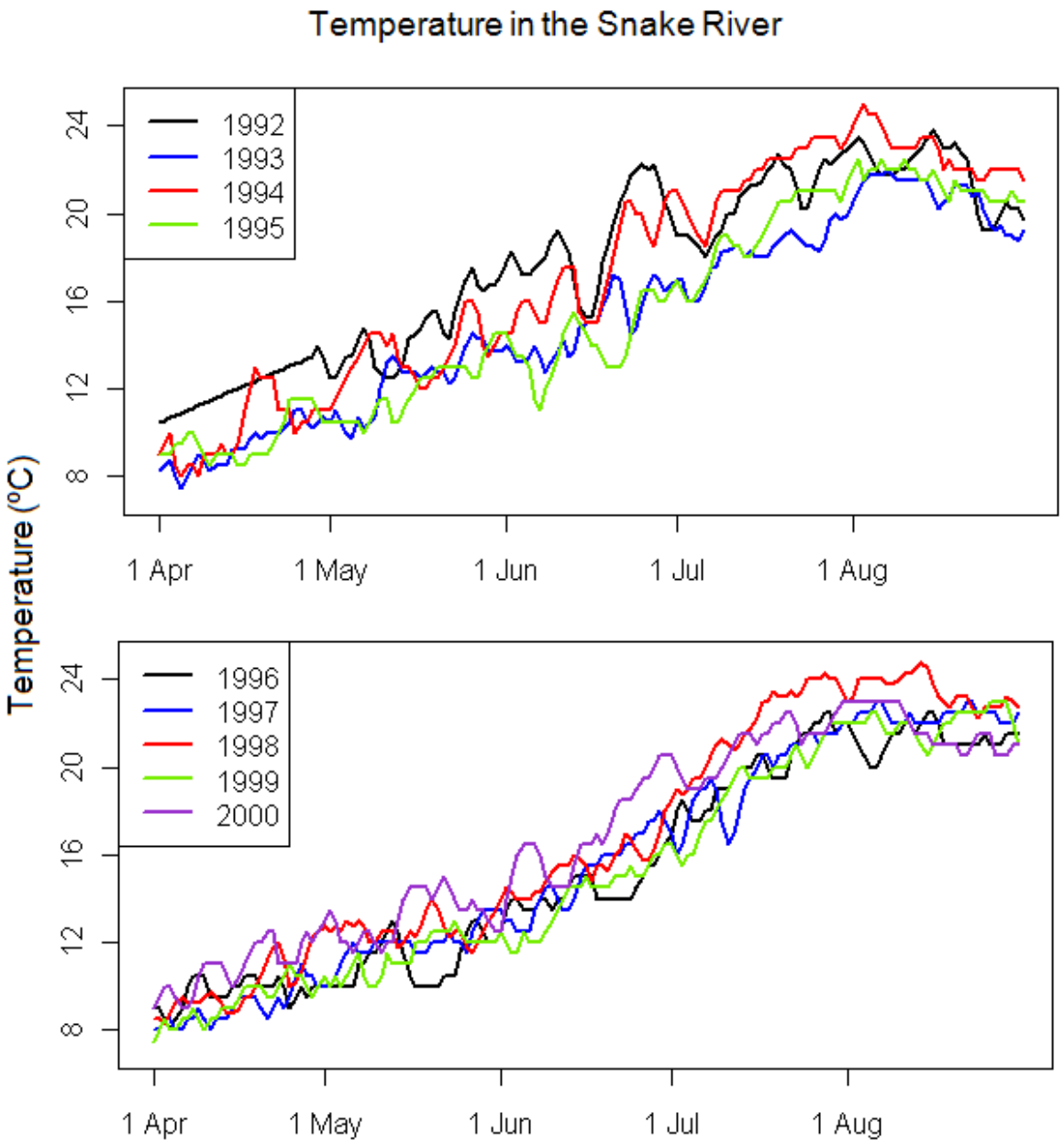

Graph of daily mean water temperature recorded at the USGS gauge at Anatone, WA from April through August for the nine years of the study. Water temperatures during the rearing season of Snake River fall Chinook vary from around 8 degrees Celsius to more than 24 degrees Celsius. Temperatures start low at the beginning of the rearing season and peak in early to mid August.

Figure 2.3a

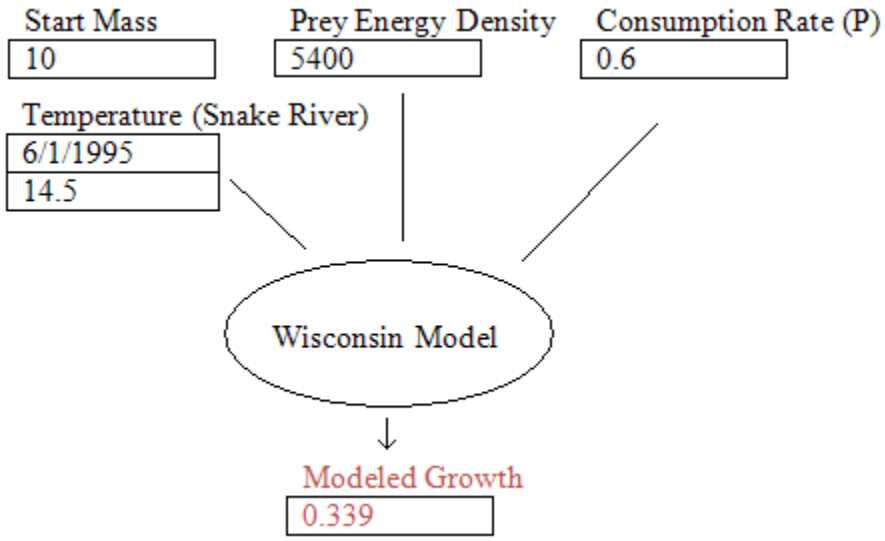

Depiction of the operation of the growth model. Values from data are in black, modeled values are in red. The first step is initialization of the model with data, which produces an estimate of the growth for the first day.

Figure 2.3b

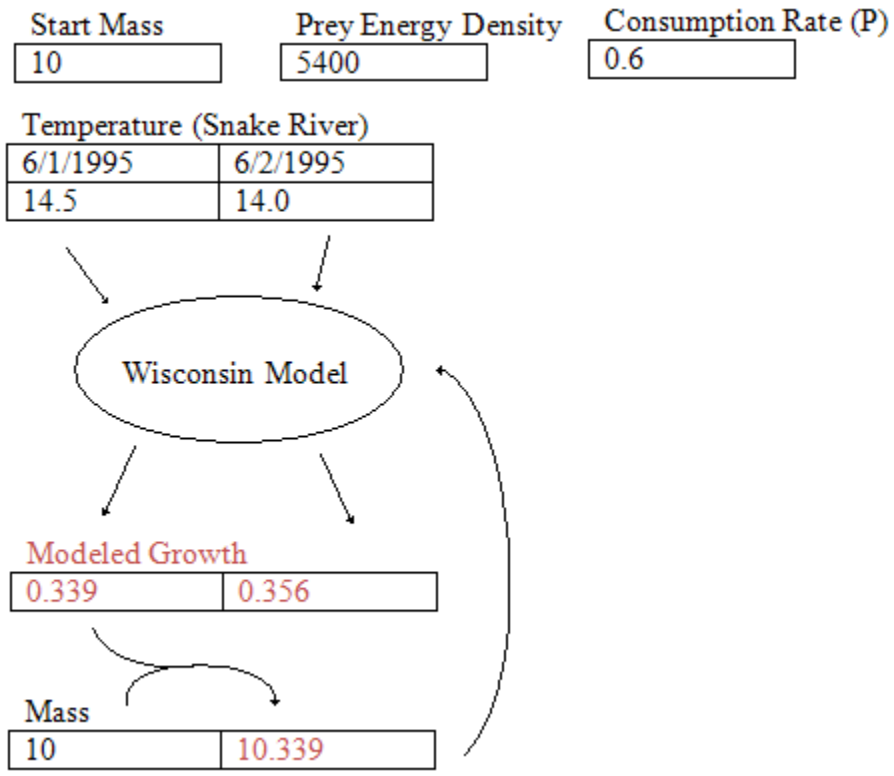

Depiction of the operation of the growth model. Values from data are in black, modeled values are in red. The modeled growth is added to the initial mass to yield the mass on day two. The mass on day two is then fed back into the Wisconsin model along with the temperature on day two of the simulation to generate the growth on day two.

Figure 2.3c

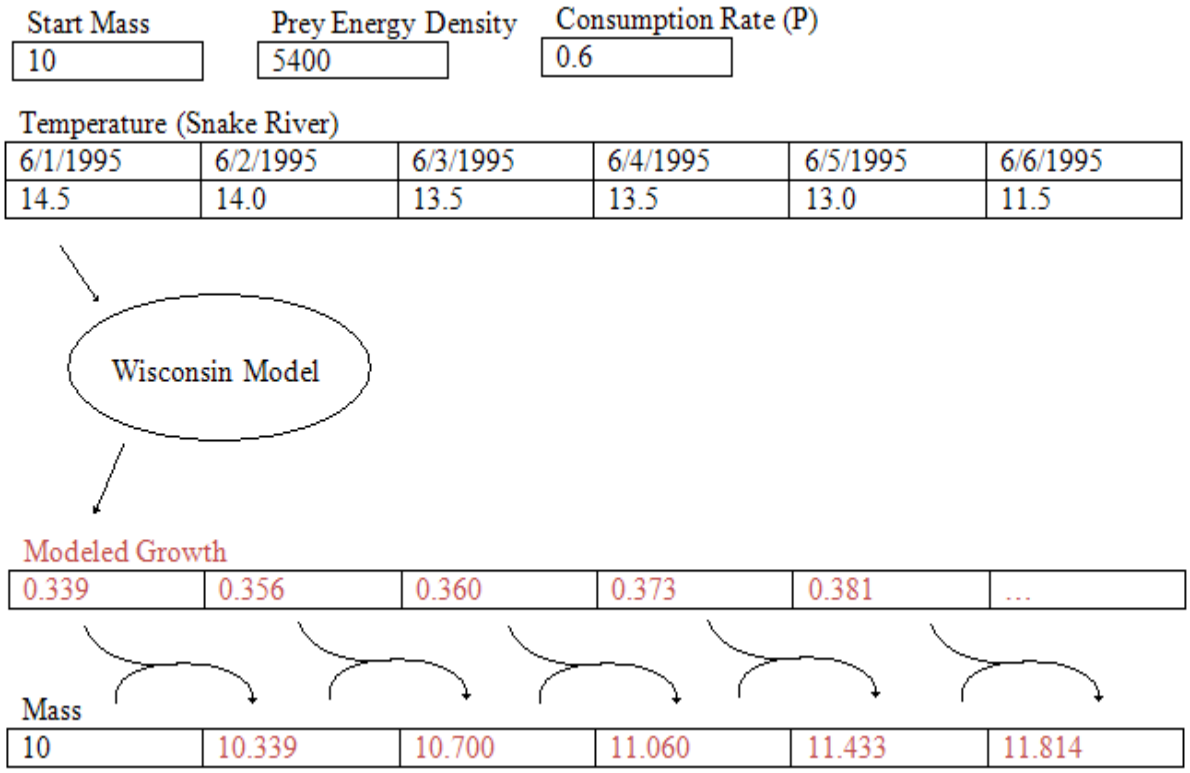

Depiction of the operation of the growth model. Values from data are in black, modeled values are in red. Modeled growth is continually added to mass to generate modeled mass.

Figure 2.4

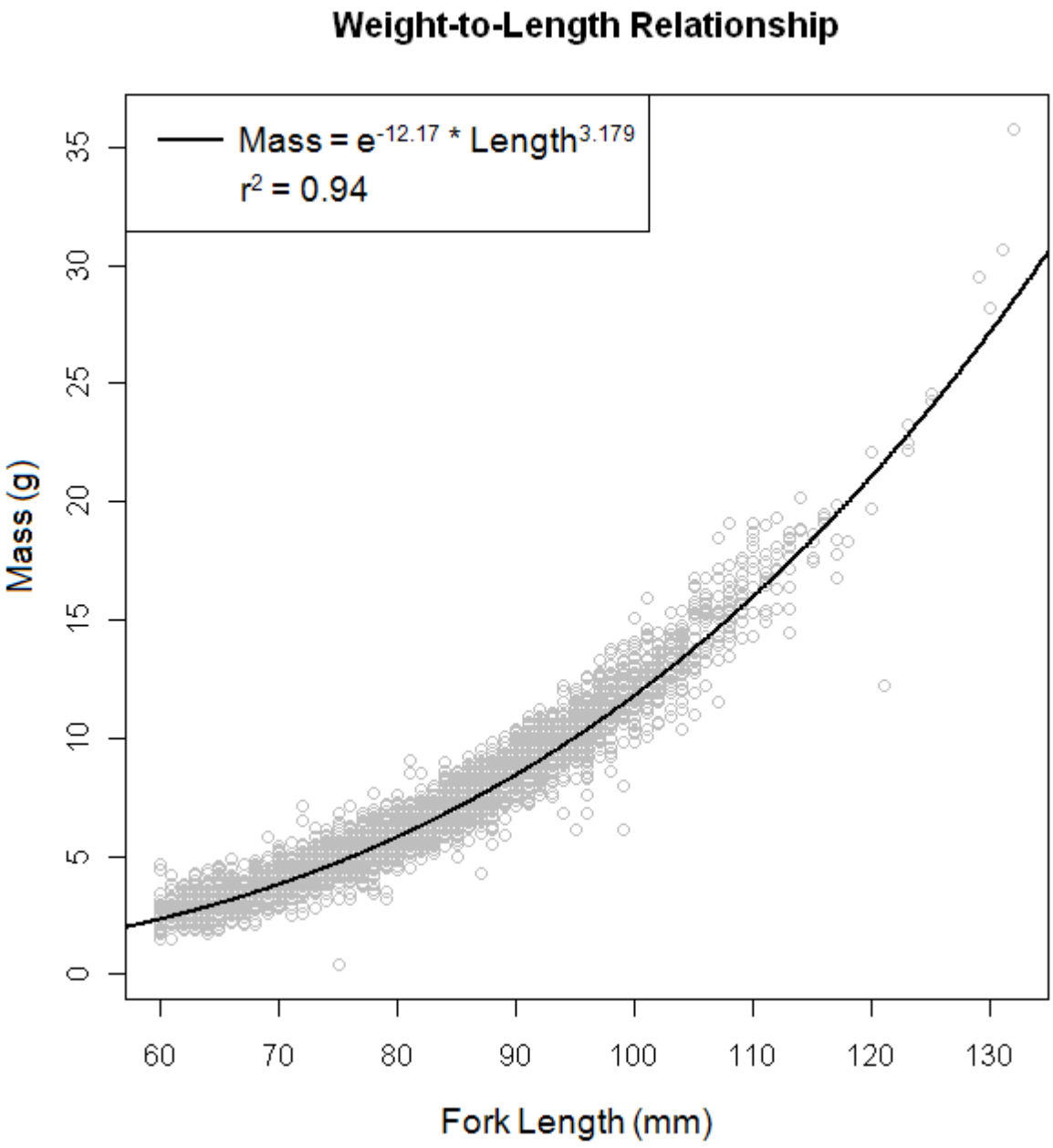

Distribution of weight and length values for 10,713 fish for which both length and weight was recorded at tagging. The weight-to-length relationship used to interconvert lengths and weights is shown in black.

Figure 2.5

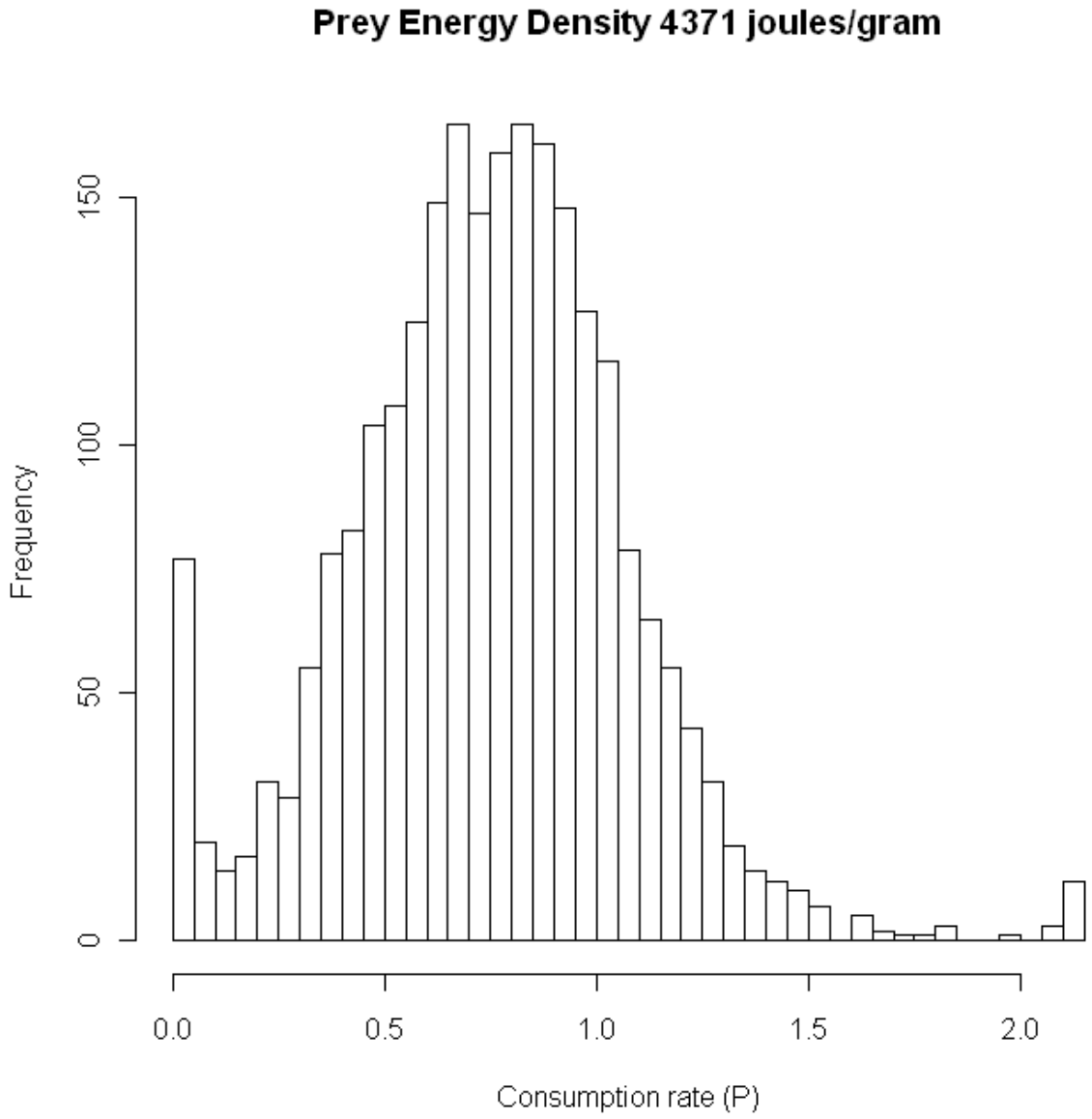

Distribution of consumption rates (P) generated using the Wisconsin model and a prey energy density of 4,371 joules per gram. This prey energy density was generated from a diet analysis performed by Curet (1993). This distribution of consumption rates has mean 0.754 and variance 0.109, and 19.7% of all fish are fitted with a consumption rate greater than 1.

Figure 2.6

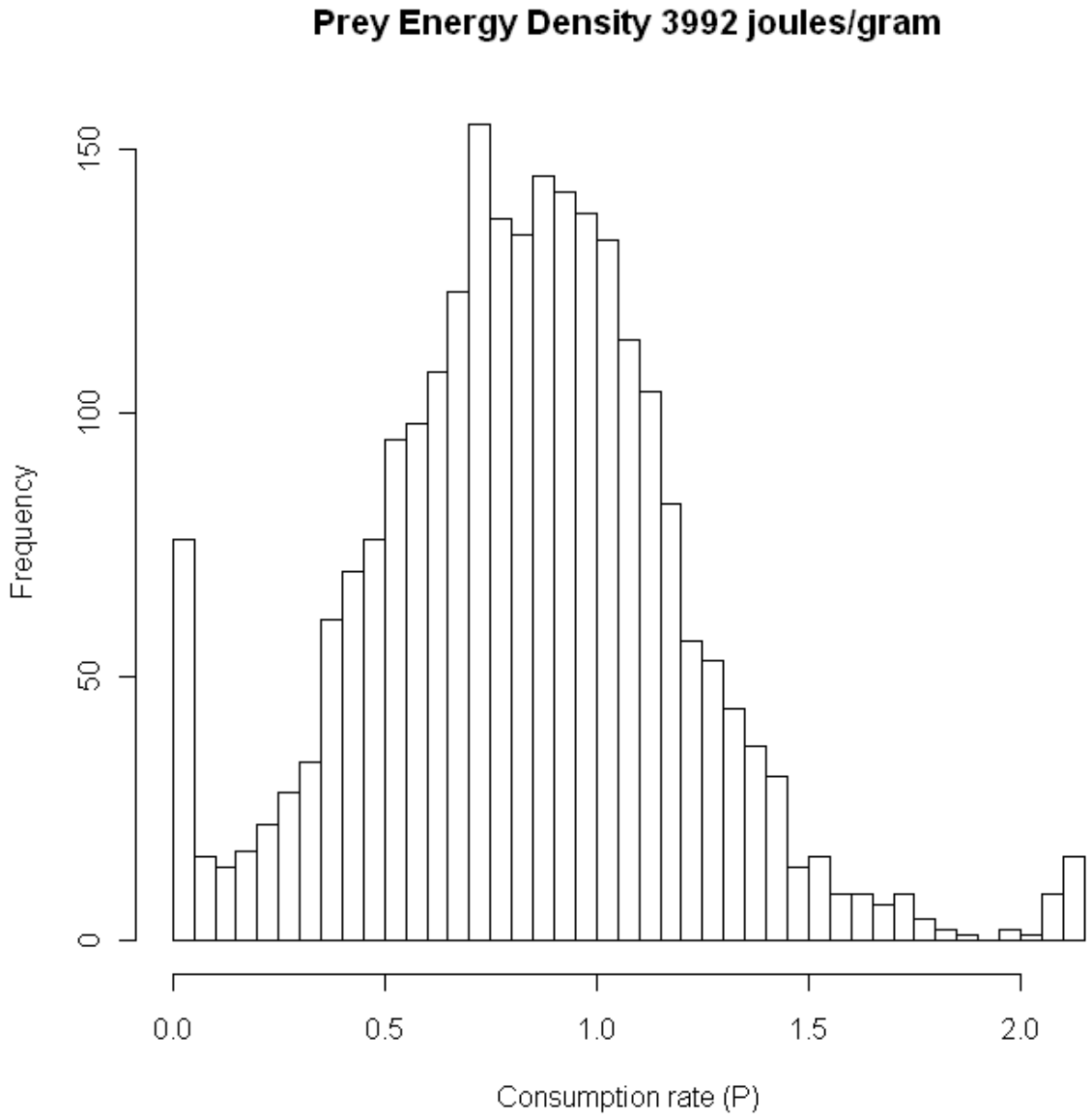

Distribution of consumption rates (P) generated using the Wisconsin model and a prey energy density of 3,992 joules per gram. This prey energy density was generated from a diet analysis performed by Muir and Coley (1996). This distribution of consumption rates has mean 0.837 and variance 0.137, and 30.9% of all fish are fitted with a consumption rate greater than 1.

Figure 2.7

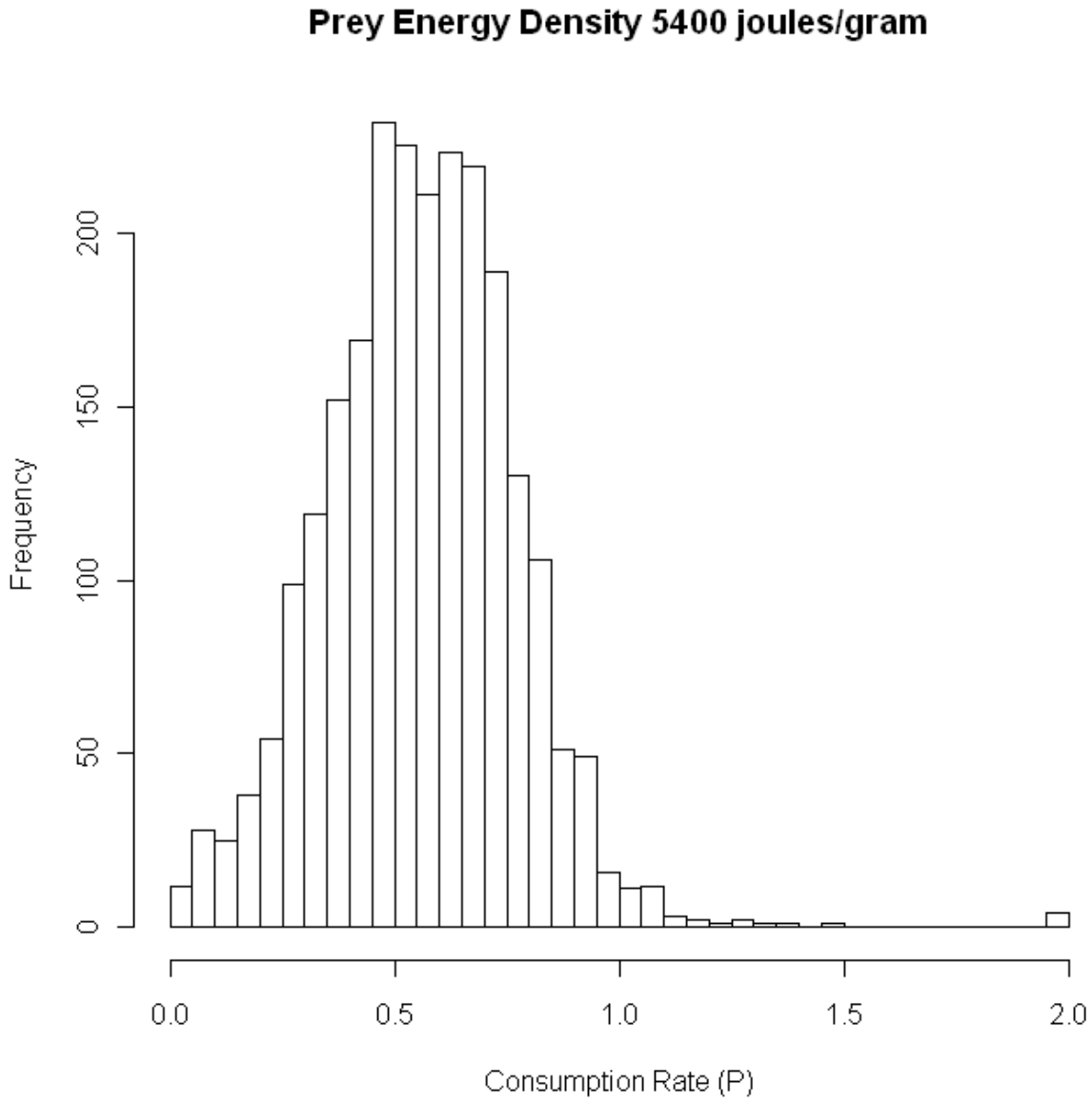

Distribution of consumption rates (P) generated using the Wisconsin model and a prey energy density of 5,300 joules per gram. This prey energy density was selected to produce less than 5% of fish fitted above 1. This distribution of consumption rates has mean 0.564 and variance 0.045 and 1.6% of all fish are fitted with a consumption rate greater than 1.

Figure 2.8

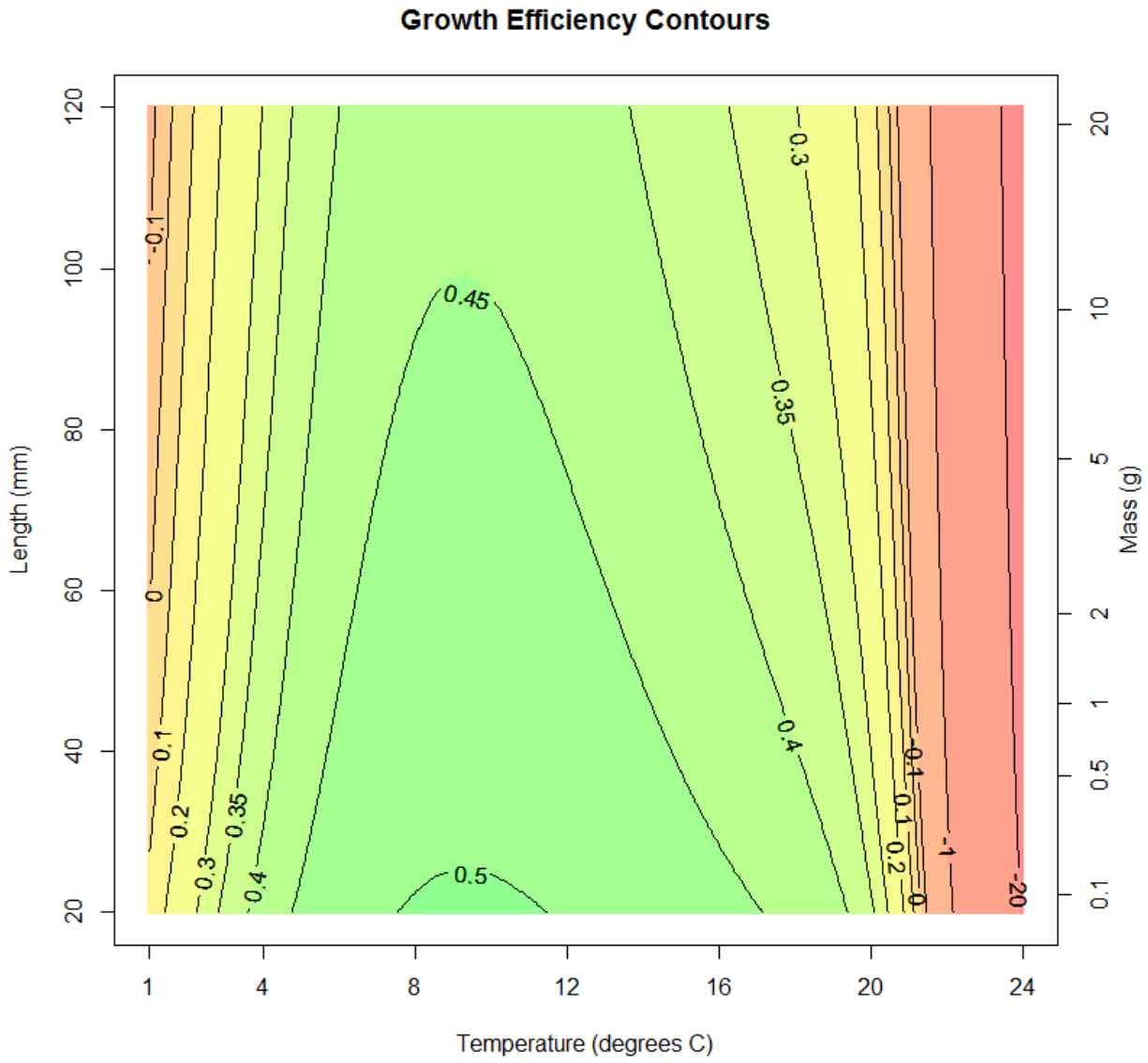

Contour plot of growth efficiency across varying temperature and mass. Prey energy density was held constant at 5400 joules per gram and consumption rate was held constant at 0.7. Spring and summer temperatures in the Snake River generally range from 10-24 degrees Celsius (Anderson 2000). Over that range of temperatures, growth efficiency declines with increasing temperatures. Growth efficiency also declines with increasing mass or length.

Figure 2.9

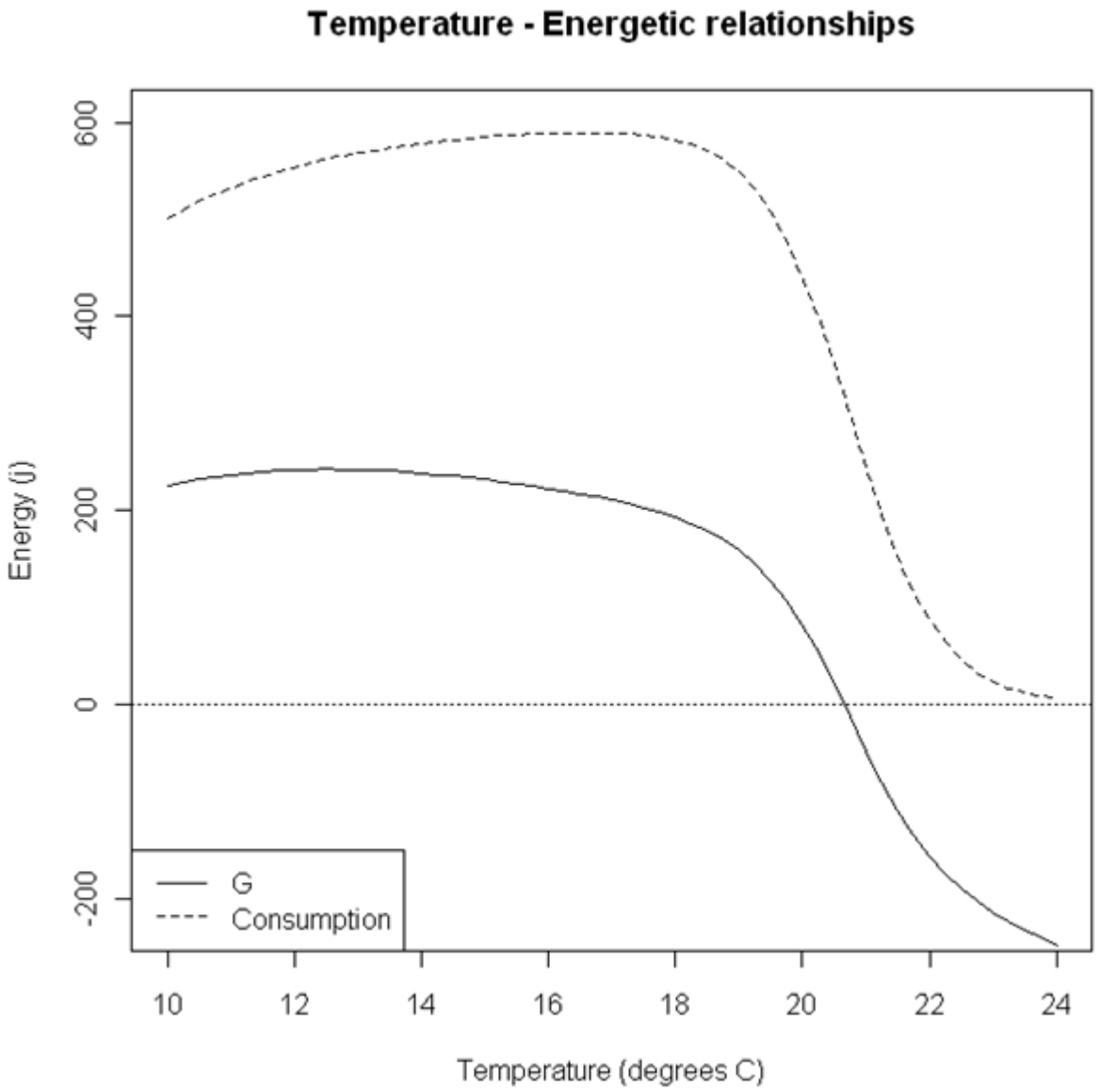

Relationships between total energy consumed (*C*) and total energy available for growth (*G*) and temperature in the Wisconsin model. Mass was held constant at 10 grams, prey energy density at 5400 joules per gram, and consumption rate at 0.7. Both curves follow similar relationships of little change from 10-20 degrees to steep decline from 20-24 degrees. Note that energy applied to growth passes zero near 21 degrees Celsius.

Figure 2.10

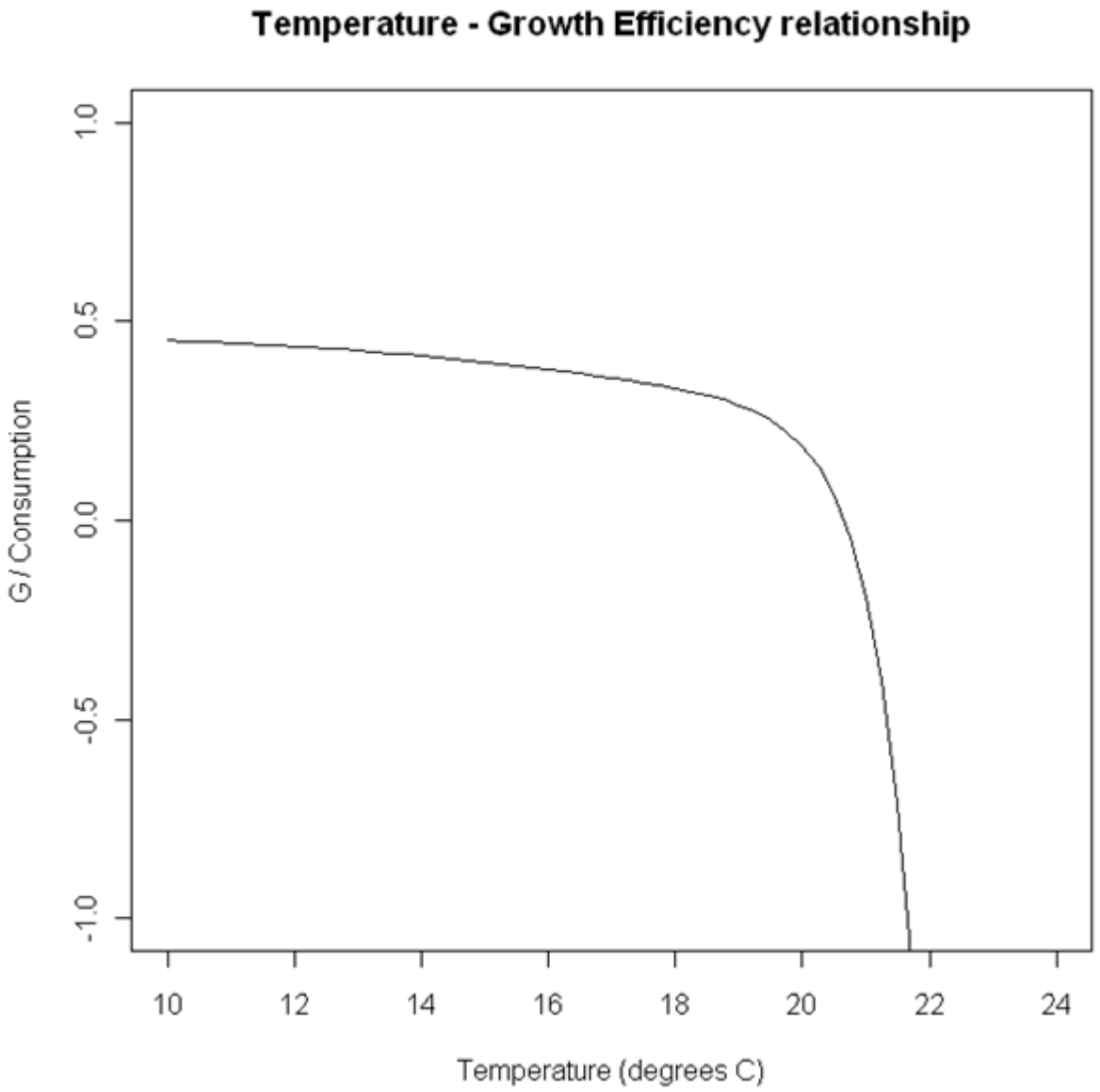

Relationship between growth efficiency and temperature (Mass was held at 10g, prey energy density at 5400 j/g, and P at 0.7). This relationship is monotonic over the temperature range experienced by rearing fall Chinook; it declines slowly from 10-20 degrees, then sharply from 20 degrees and higher. Note that growth efficiency is equal to zero when energy applied to growth is equal to zero (Figure 2.8).

Figure 2.11

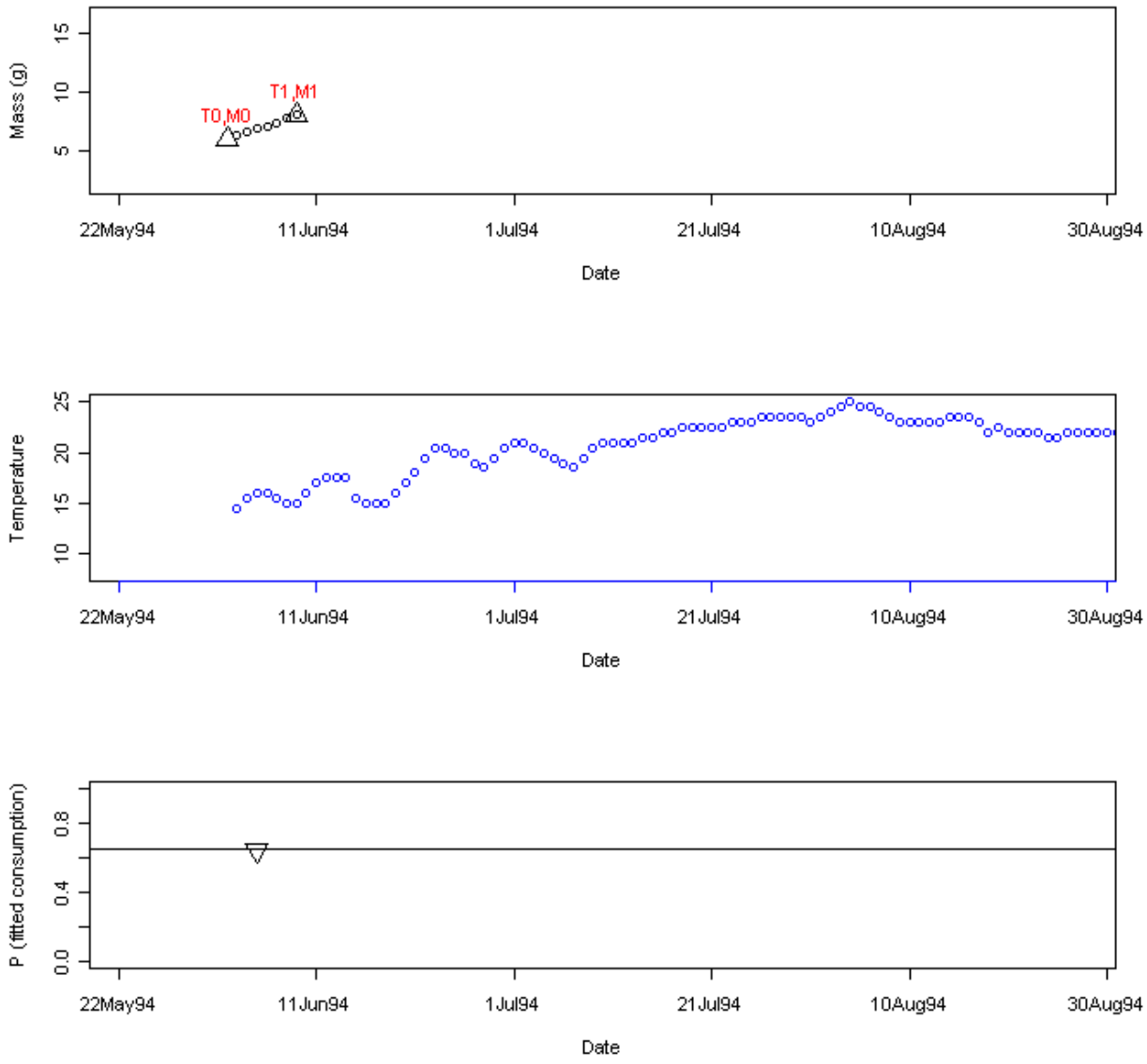

Plots depicting the process of fitting a consumption rate for an individual fish. T0, M0, T1, M1, and the temperature in the Snake River over that period are used to fit a consumption rate (P). The fitted daily masses are shown between T0 and T1.

Figure 2.12

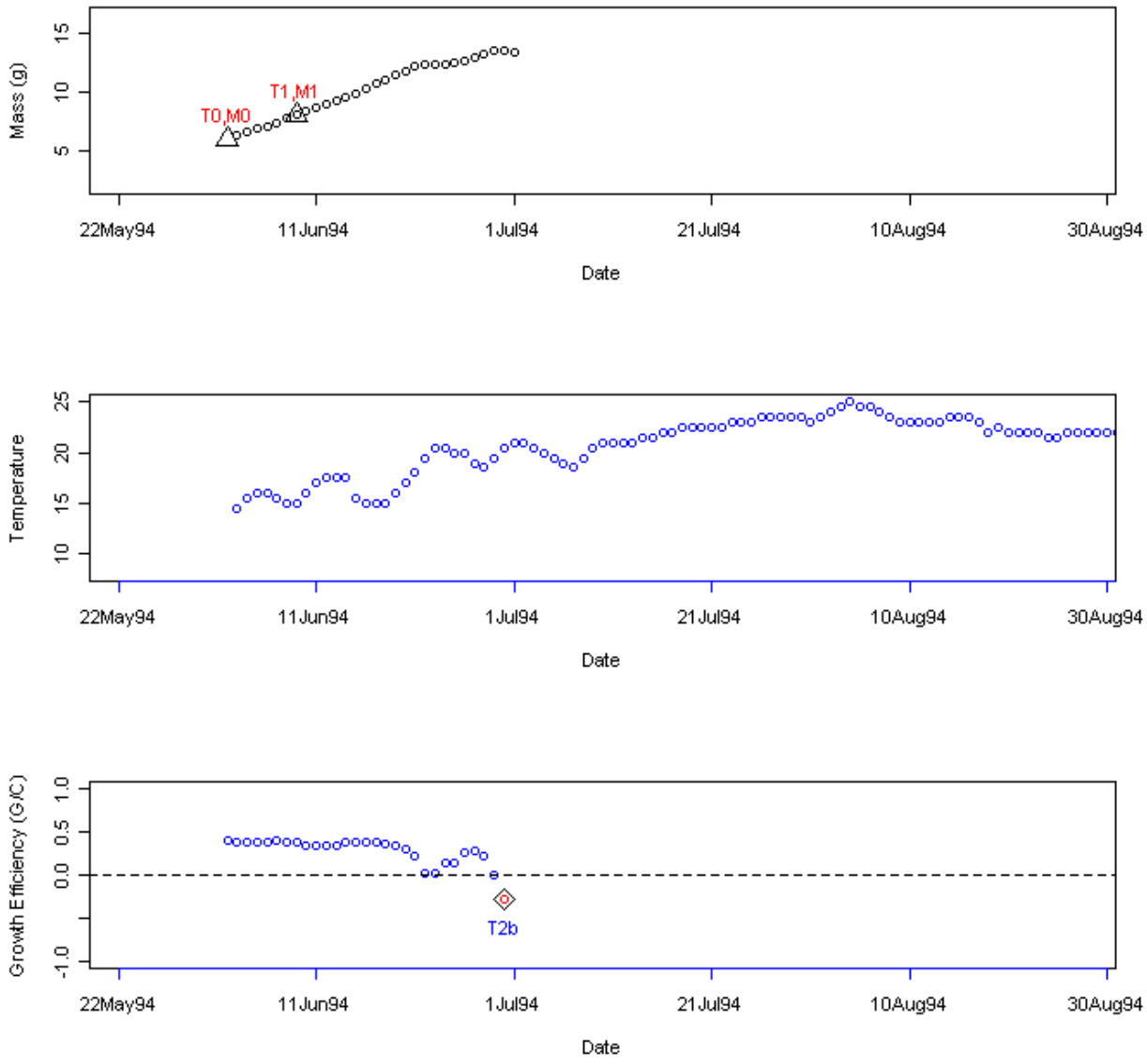

Plots depicting the process of generating a fish's growth efficiency data and predicting the initiation of migration via the Thermal Wall model. The previously estimated consumption rate is used to model the fish beyond T1 and the fish's growth efficiency is tracked until it falls below zero, at which point the model predicts T2b.

Figure 2.13

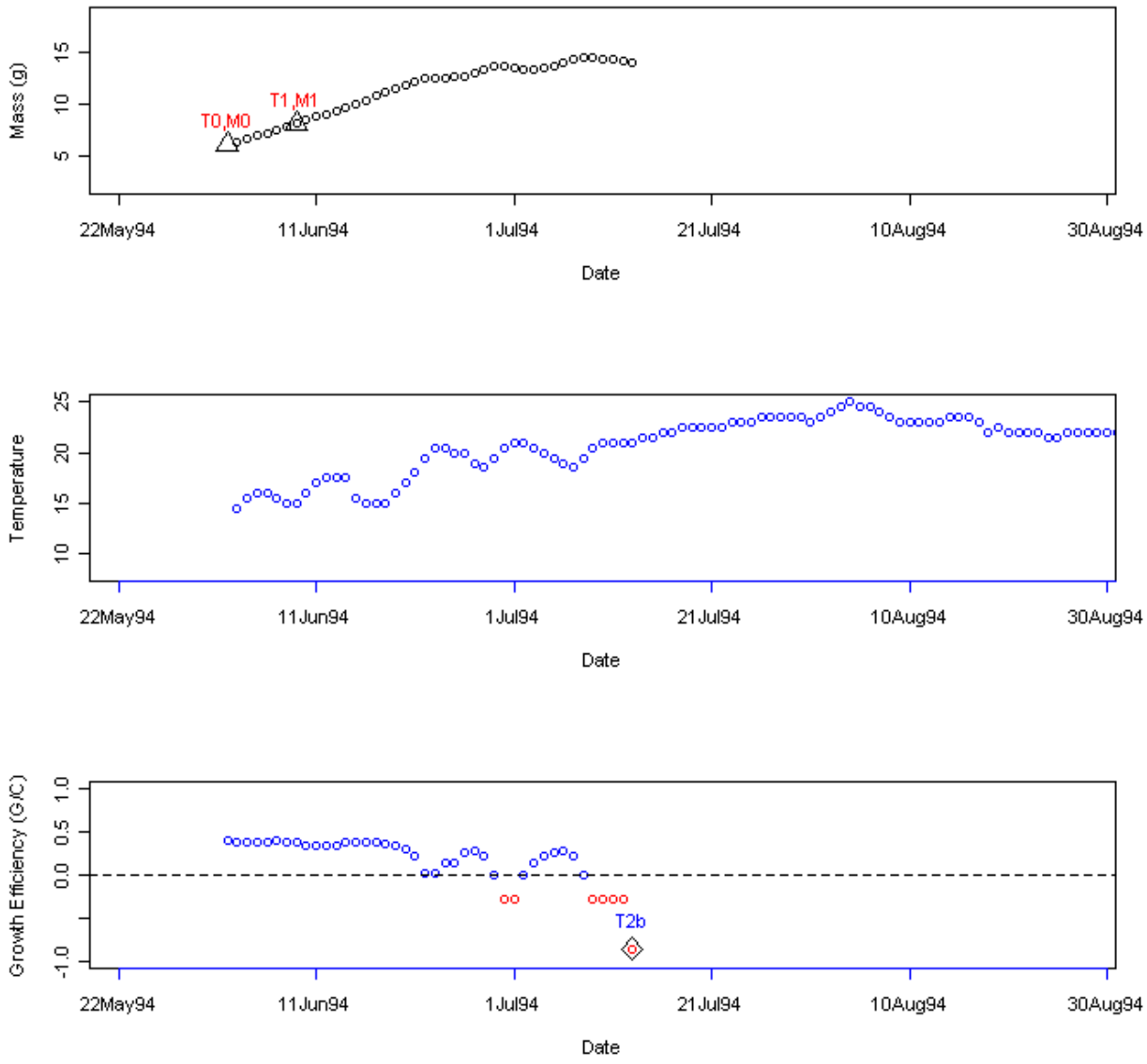

Plots depicting the process of predicting the initiation of migration via the Thermal Wall model with the 5 day alternative. The previously estimated consumption rate is used to model the fish beyond T1 and the fish's growth efficiency is tracked until it falls below zero for five consecutive days, at which point the model predicts T2b. For clarity, growth efficiencies below zero are in red.

Figure 2.14

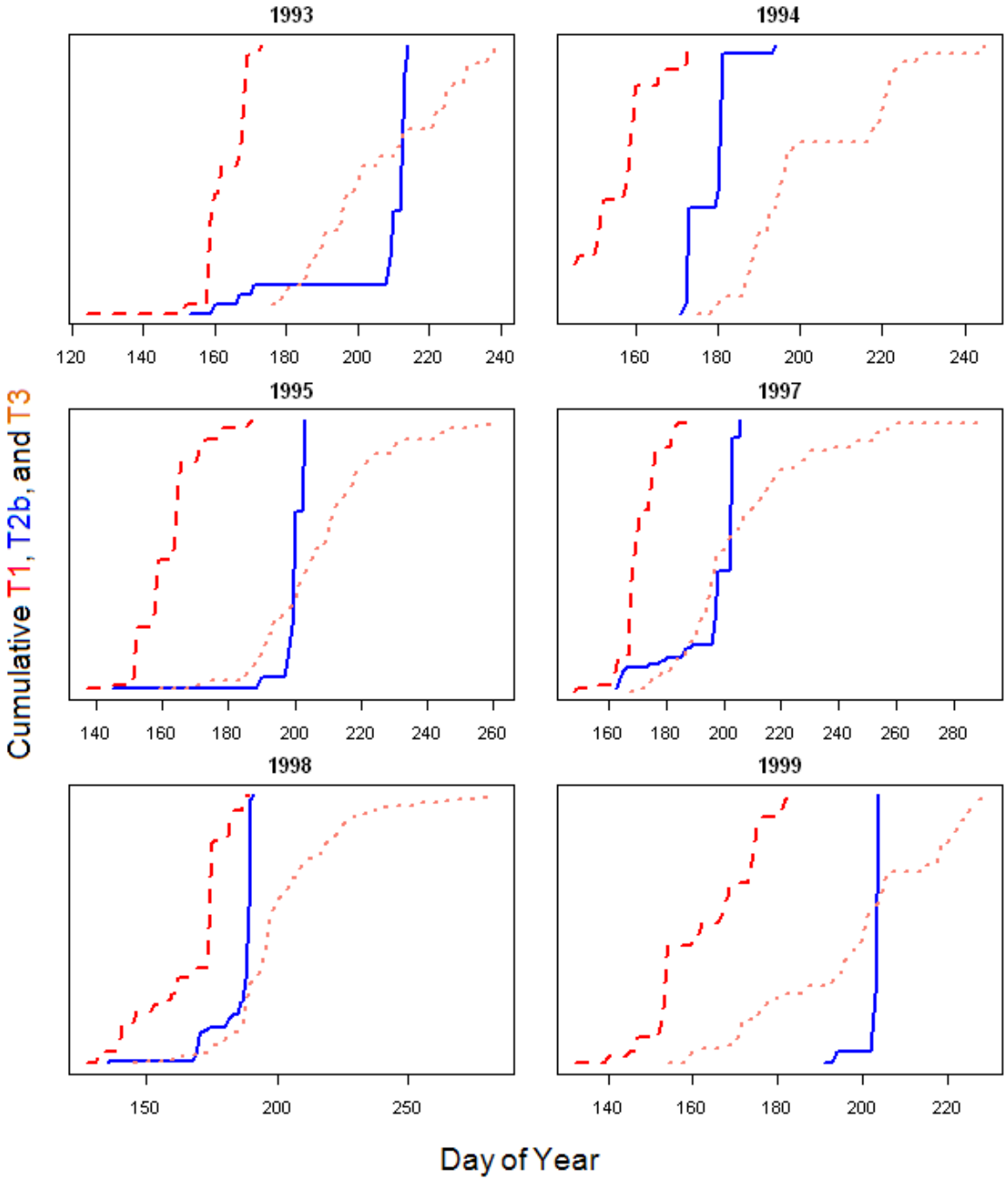

Yearly cumulative plots of the day of year of observed T1 and T3 and modeled T2b using the Thermal Wall model with the one day alternative.

Figure 2.15

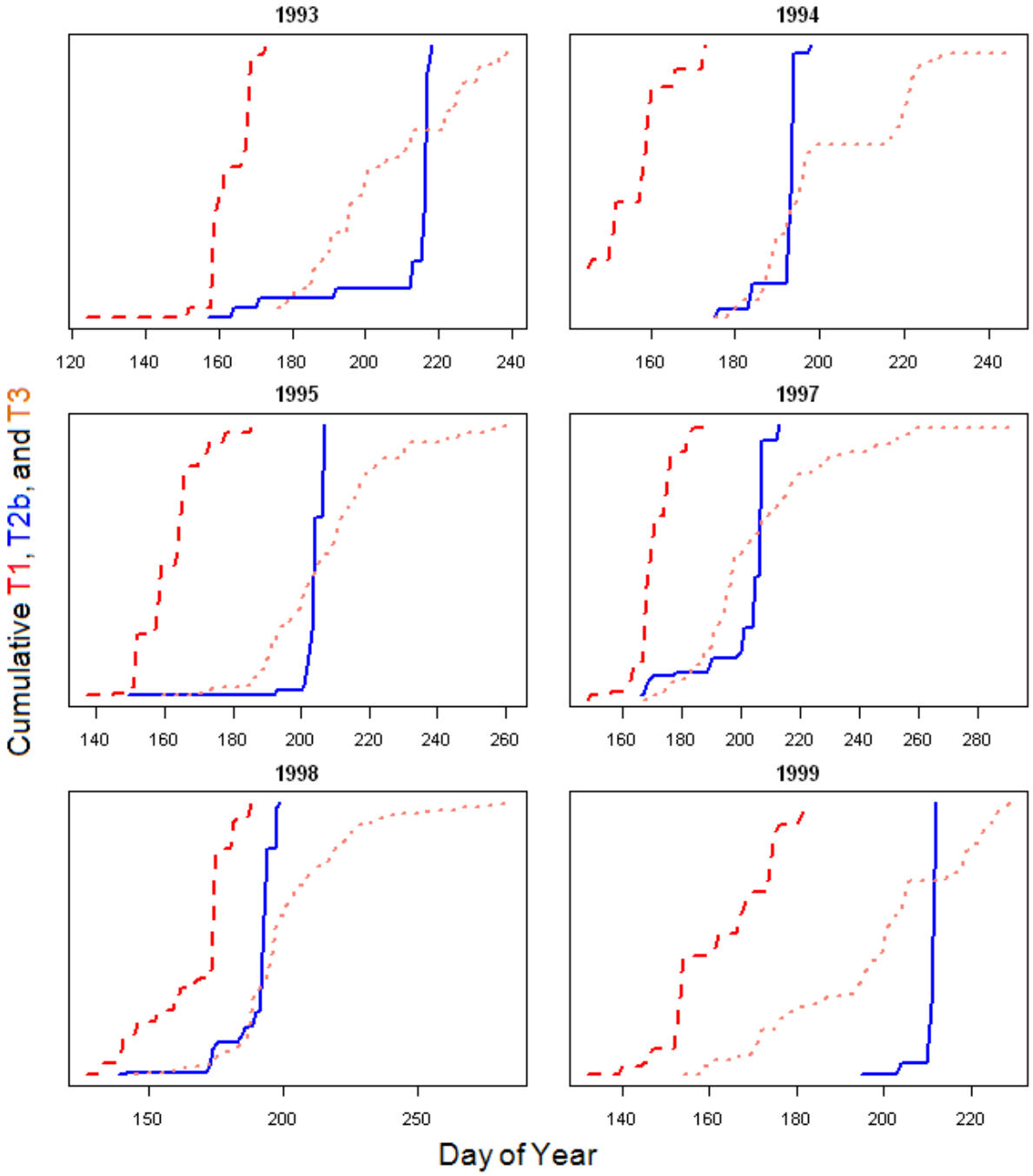

Yearly cumulative plots of the day of year of observed T1 and T3 and modeled T2b using the Thermal Wall model with the five day alternative.

Figure 2.16

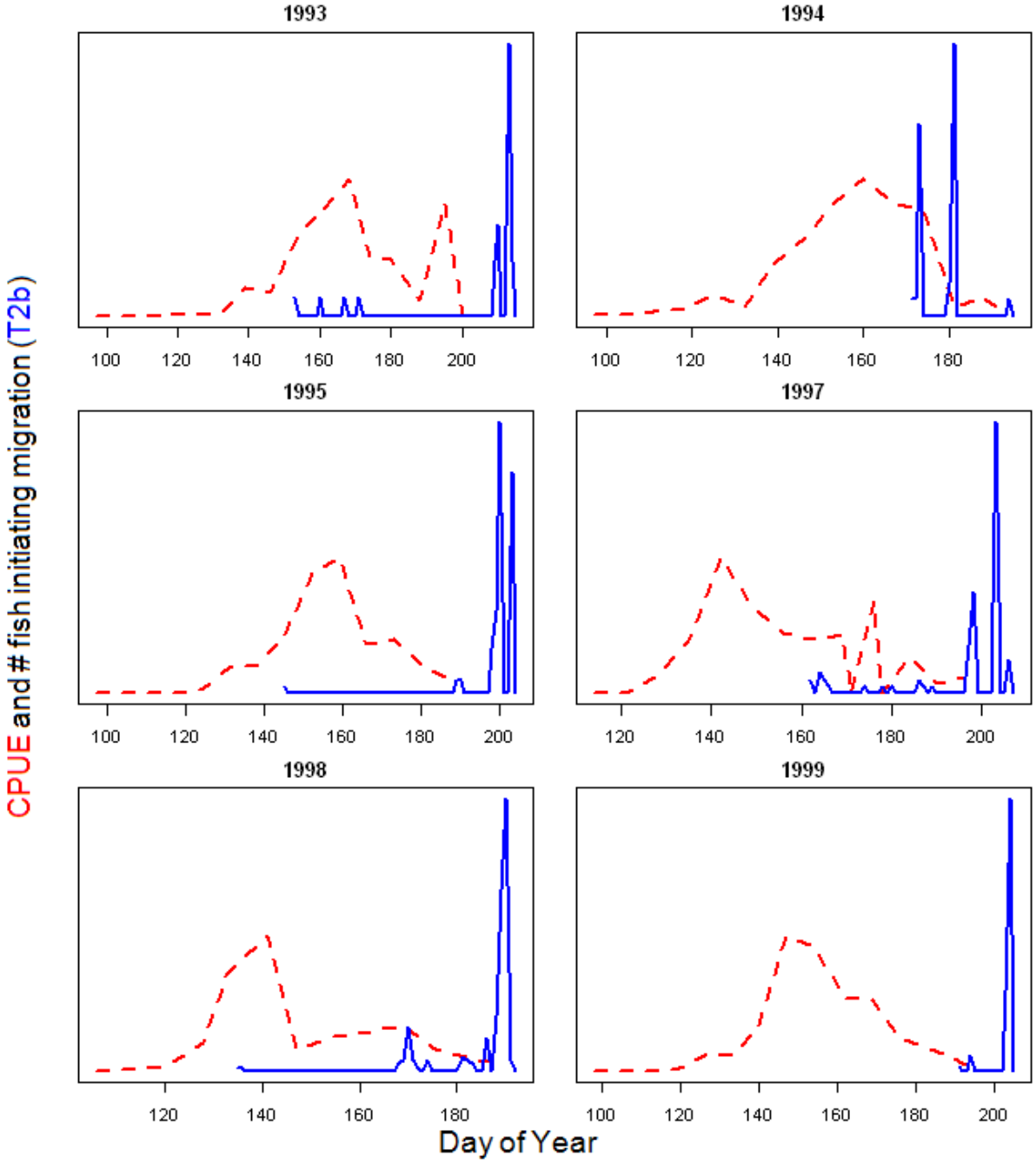

Yearly plots of CPUE from Connor's beach seining and number of fish modeled to initiate migration (T2b) using the Thermal Wall model with the one day alternative. Connor sampled on a weekly basis, so CPUE data from all sites sampled in a given week is averaged on a weekly basis.

Figure 2.17

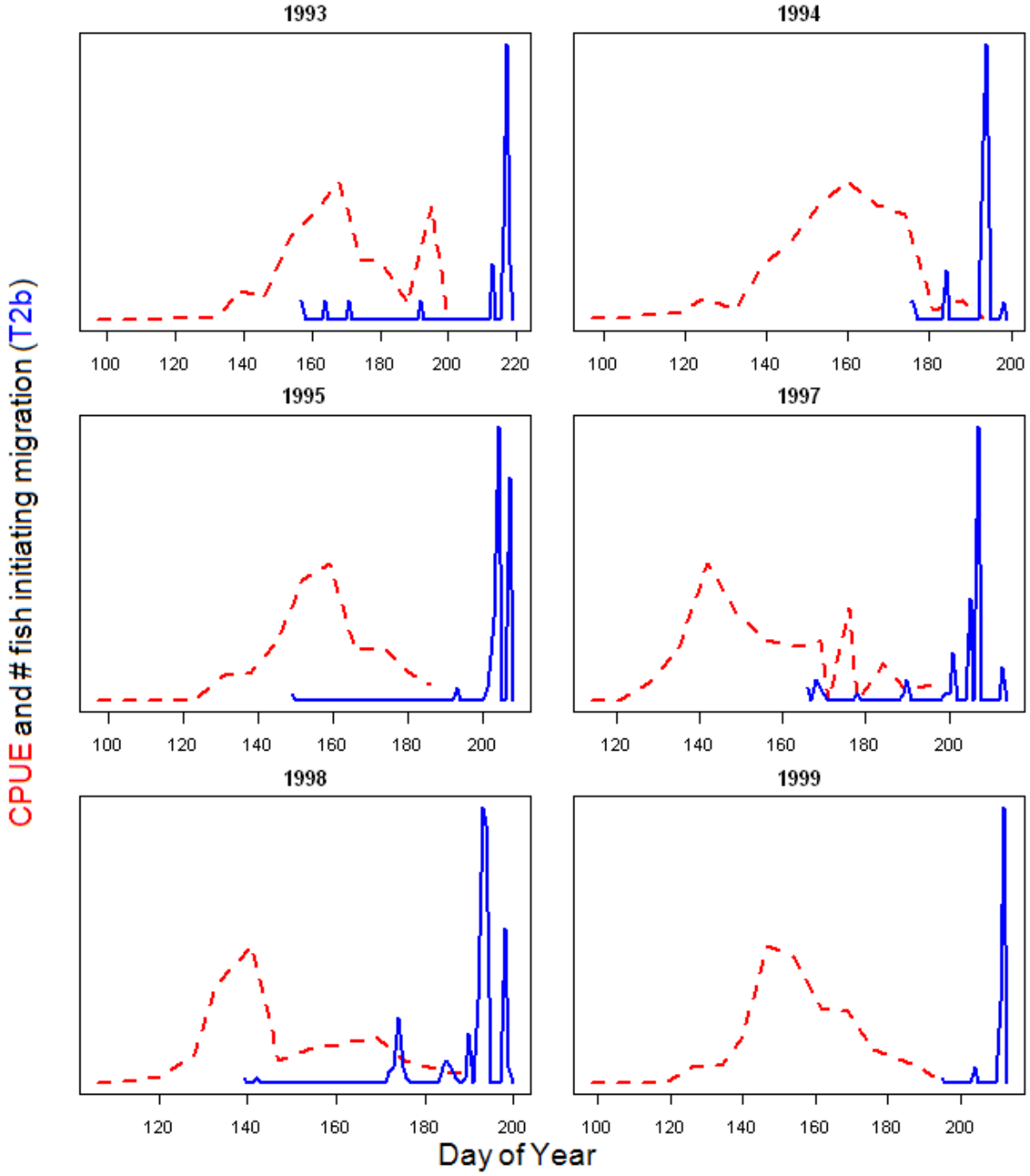

Yearly plots of CPUE from Connor's beach seining and number of fish modeled to initiate migration (T2b) using the Thermal Wall model with the five day alternative. Connor sampled on a weekly basis, so CPUE data from all sites sampled in a given week is averaged on a weekly basis.

Figure 2.18

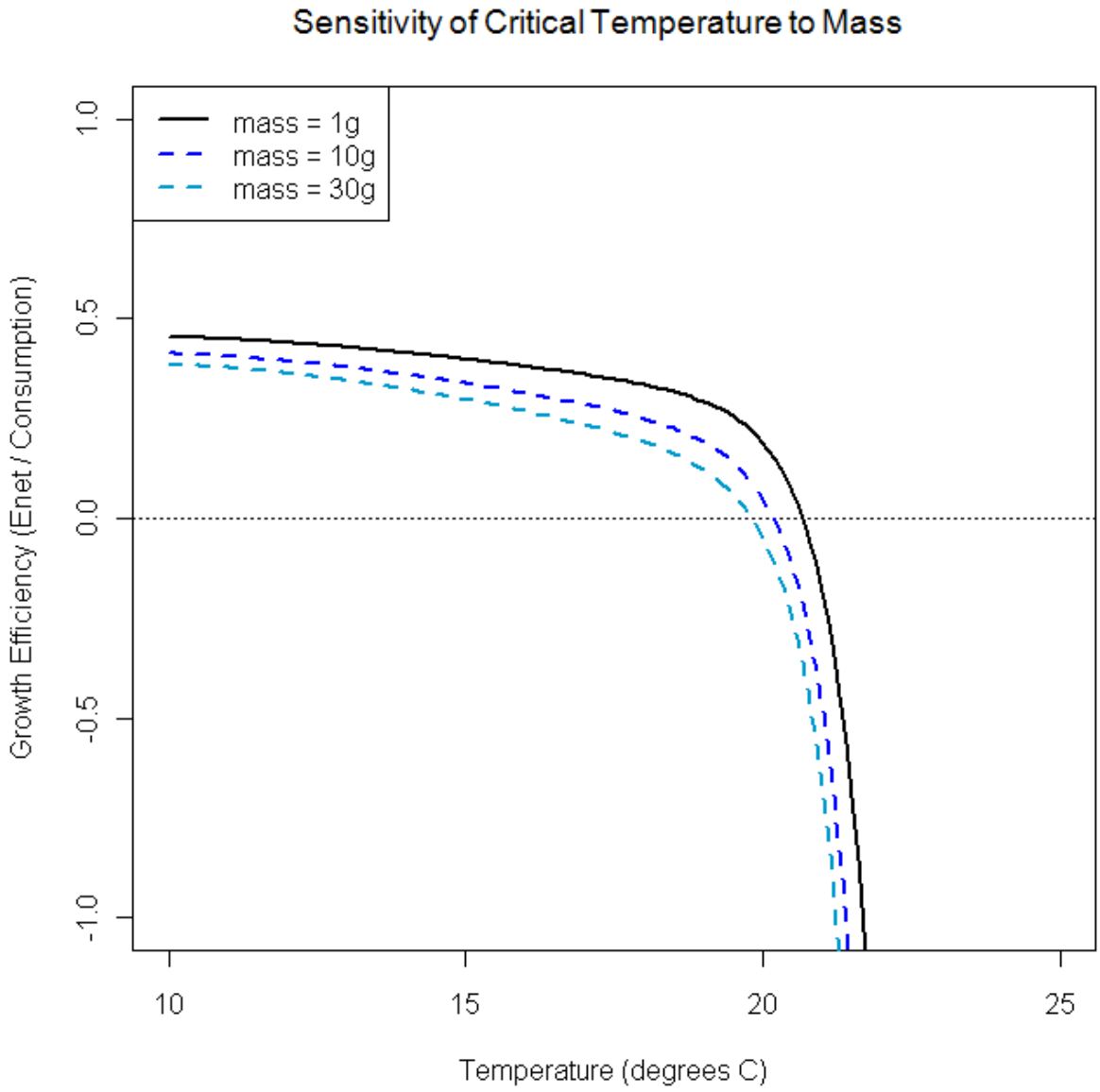

Plot depicting how the growth efficiency – temperature relationship responds to changes in fish mass. Prey energy density was held at 5400 joules/gram, and consumption rate (P) at 0.5. The critical temperature (the point where the growth efficiency curve crosses zero) is 20.7 degrees for a 1 gram fish, 20.2 degrees for a 10 gram fish, and 19.8 degrees for a 30 gram fish.

Figure 2.19

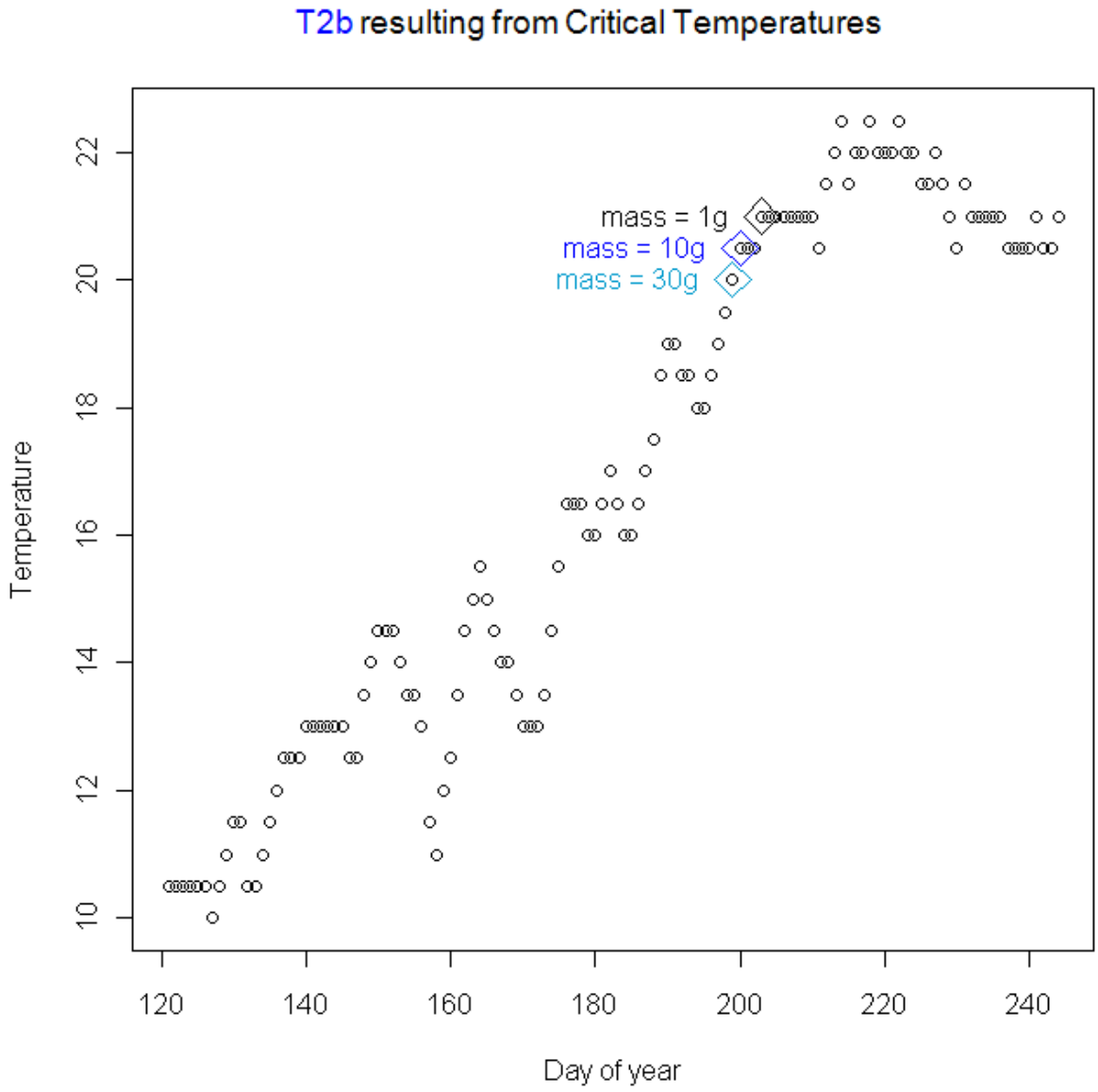

Plot depicting how changes in the critical temperature resulting from changes in mass produce different predicted T2b dates in the Thermal Wall model (the one-day alternative was used here). The temperatures used are temperatures from the 'River' reach in 1995. A mass of 1 gram resulted in T2b on day 203 (July 22nd), a mass of 10 grams resulted in T2b on day 200 (July 19), and a mass of 30 grams resulted in T2b on day 199 (July 18).

Figure 2.20

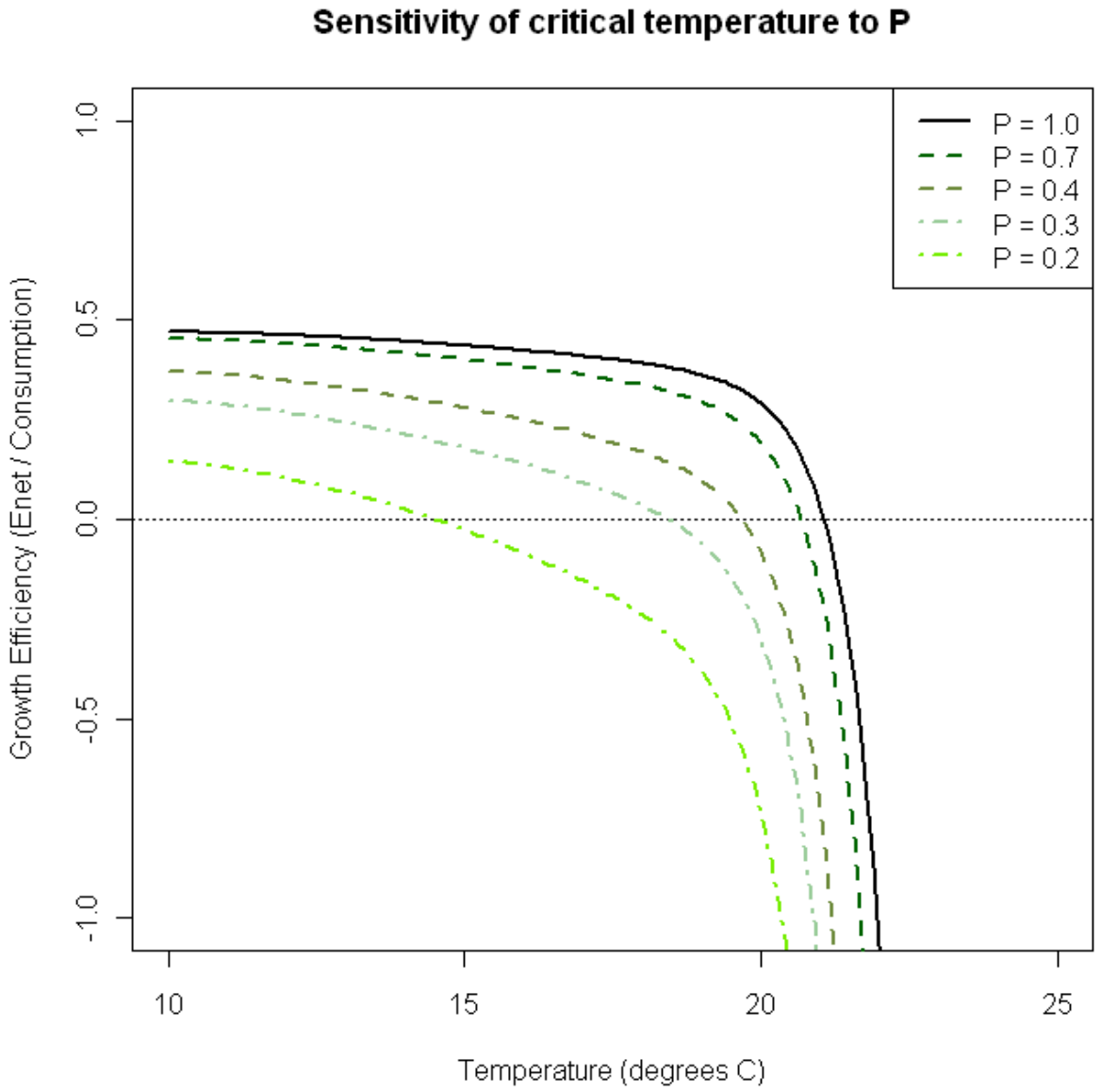

Plot depicting how the growth efficiency – temperature relationship responds to changes in fish consumption rate (P). Prey energy density was held at 5400 joules/gram, and mass at 10 grams. The critical temperature (the point where the growth efficiency curve crosses zero) is 21.1 degrees for P of 1.0, 20.7 degrees for a P of 0.7, 19.7 degrees for a P of 0.4, 18.4 degrees for a P of 0.3, and 14.5 degrees for a P of 0.2.

Figure 2.21

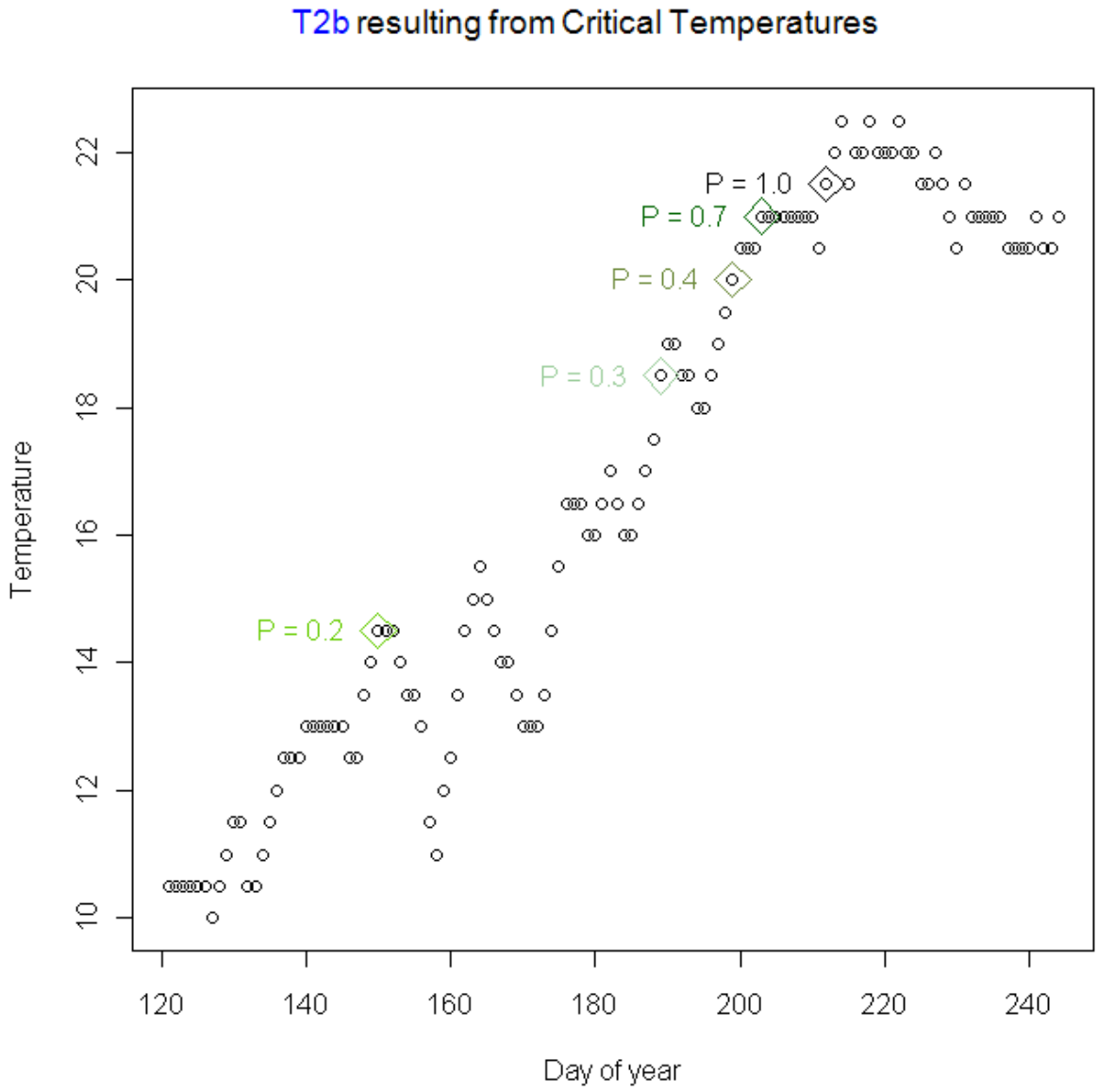

Plot depicting how changes in consumption rate produce different predicted T2b dates in the Thermal Wall model (the one-day alternative was used here). The temperatures used are temperatures from the 'River' reach in 1995. A P of 1.0 resulted in T2b on day 212 (July 31), a P of 0.7 resulted in T2b on day 203 (July 22), a P of 0.4 resulted in T2b on day 199 (July 18), a P of 0.3 resulted in T2b on day 189 (July 8), and a P of 0.2 resulted in T2b on day 150 (May 30).

Chapter 3: Mass-Growth Model of Migration Initiation

3.1 Introduction

After the Thermal Wall model was found to be inadequate to explain migration initiation, the second modeling project we undertook was the creation of a mechanistic model of migration initiation incorporating the theory proposed by Thorpe et al. (1998) and Mangel and Satterthwaite (2008). This mechanistic model uses the growth model we created in Chapter 2 to model the growth of individual fish, then predicts initiation of migration T2 when a fish's modeled mass passes a mass threshold. We refer to this model as the 'Mass-Growth' model, and we denote T2 predicted by this model as T2m. We tested several versions of the Mass-Growth model; in the first version a threshold mass was the only trigger for migration; in the second version both threshold mass and threshold growth efficiency could trigger migration; lastly, we modified the second version with a more complex catchability coefficient to improve fits.

3.2 Methods

3.2.1 Modeling Consumption Rate

The first step in the construction of the Mass-Growth model was expanding our original growth model to support modeling more fish. As described in section 2.2.3 of this thesis, we fitted consumption rates (P) individually for fish for which all of T0, M0, T1 and M1 data points

were present. Only a small percentage of all fish had a T1 and M1 data point, limiting the number of fish which could be modeled in this way. The method we use to fit the Mass-Growth model requires growth data for all fish tagged at a subset of tagging locations, including fish for which no T1 or M1 data is present. In order to model the growth of these fish, we needed a method to estimate consumption rate other than by a direct fit. We tested a multivariate linear model regressing fitted consumption rates (P) against T0, M0, and environmental data to attempt to create a model to predict P for fish lacking T1 and M1 data.

A total of 2,385 individual fish had a fitted consumption rate and were used to fit the linear model. We started with a full model including as predictors every piece of data available to fish with only a T0 and M0 data point from the PIT tag dataset. These data comprise T0 and M0 from the PIT tag data, the temperature and CPUE at the tag location on T0, and the river kilometer of the tag location. Additionally, squared terms were included for temperature and CPUE to allow for a potential nonlinear relationship, and interaction terms between T0 and M0, temperature, and CPUE were included. Tables 3.1 and 3.2 show a summary of the full model fit and the ANOVA table of the full model fit. To reach a parsimonious model, we used sequential deletion; the least explanatory predictor was removed from the model sequentially until removing another predictor would result in an increase in Akaike's Information Criterion (AIC) estimate of greater than two. The predictors removed from the model were, in sequence: T0-CPUE interaction term, and T0-M0 interaction term. Tables 3.3 and 3.4 show a summary and ANOVA table of the reduced model.

While there are statistically significant relationships between most of the predictor variables and fitted consumption rate, overall the available data does not explain enough of the variation in fitted consumption rate to be useful for making accurate predictions. The total

adjusted R^2 of both the full and reduced models are only 0.12; we decided that this model was inadequate to predict consumption rates for use in our modeling. As a fallback option, we decided to use the mean value of all fitted consumption rates (0.564) for any fish which did not have an individual fit.

3.2.2 Mass-Growth Model of Migration

To facilitate confronting our models of the migration initiation of juvenile fall Chinook with our data, we created a generalized modeling framework to model the number of tagged fish present in the rearing habitat over time. This model has the following structure:

$$N_i = N_{i-1} + T_i - L_i$$

In this formulation, N_i is the number of tagged fish at large within the rearing habitat on day i, so N_{i-1} is the number of fish that were present within the rearing habitat on the previous day. T_i is the number of fish tagged and released back into the rearing habitat on day i, and L_i is the number of fish that initiate migration and leave the habitat on day i. T_i is generated from the T0 data points of individual fish and is an external forcing. L_i is generated by our models of migration initiation, described below. We use N_i to validate the model by comparing it to CPUE data. We assume that N_i is related to CPUE via the following relationship:

$$CPUE_i = N_i \times cc$$

In this formulation, N_i is directly proportional to $CPUE_i$, and catchability coefficient cc describes the relationship between the two. We then test the model fit by comparing $CPUE_i$ produced by the model to $CPUE_i$ from data.

3.2.3 CPUE and PIT Data

CPUE data was only available for a subset of all sites sampled by William Connor. Some sites were sampled on a regular basis, others were sampled on an irregular basis (Connor et al. 2003). CPUE data is available for a subset of sites that were sampled on a weekly basis. The set of sites sampled each year is not exactly the same, but CPUE data is available for 10-14 sites in each year of data from 1992 to 2000. These sites were sampled and CPUE recorded on a weekly basis, with subsets of sites sampled on different days of the week. To yield a single estimate of CPUE, the CPUE recorded at all sites was averaged over each weekly sampling period. The days between each weekly mean were then backfilled by linear interpolation between the mean CPUE points. Both averaged data points and interpolated points were used to verify model results, but averaged data points were weighted three times heavier than interpolated points.

For the individual fish data used in the Mass-Growth model, we used all fish tagged at the river kilometers for which CPUE data is available in each year. As the CPUE data is derived from initial capture and recapture of these fish (fish too small to be PIT tagged were not included in CPUE data, William Connor, personal comm.), the CPUE data reflects the presence of these fish in the rearing habitat. By using this subset of the PIT data to run the model, the CPUE data can provide an accurate indicator of how well the Mass-Growth model is predicting the movement of the fish. As described in section 3.2.1, many of the fish tagged at these sampling locations lack a T1 and M1 data point; they only have a T0 and M0 data point. For these fish, the mean of fitted consumption rates is used in the growth model.

3.2.4 Mass Only Model

The first version of the model we tested used only mass to trigger migration. For ease of reference through the rest of this chapter, we will refer to this version of the model as the Mass Only Model. Growth of all fish was modeled from tagging through the end of the rearing season; when an individual's mass passed a critical mass, that fish was modeled to initiate migration. So, for this version of the mass-growth model, the leaving function L_i follows the following structure:

$$L_i = \sum_{fish[\,j\,]}^{\max\, j} \left(mass[\,j,i\,] > Mcrit \right)$$

In this formulation, the number of fish leaving on day i (L_i) is equal to the sum of all fish j for which their modeled mass on day i is greater than the critical mass, *Mcrit*. *Mass* is a matrix of modeled masses with two dimensions; dimension j is the individual fish modeled, and dimension i is time, in days. *Mcrit* simulates a genetic threshold size which must be surpassed for a fish to decide to initiate migration, as proposed in Thorpe et al. (1998). The theory in Thorpe et al. (1998) proposes that, as a genetically controlled threshold, the magnitude of the threshold likely varies among individuals due to variation in genes; however, to support parameter estimation via optimization fitting, we treat *Mcrit* as a constant for all fish within a given year.

3.2.5 Mass and Growth Efficiency Model

We then created a second version of the model in which either mass or growth efficiency could trigger migration. For ease of reference, we will refer to this version of the model as the Mass & Growth Model through the remainder of this chapter. Both mass and growth efficiency were modeled for all fish from tagging through the end of the rearing season; an individual

would be modeled to initiate migration when its mass was greater than a critical mass or when its growth efficiency was less than a critical growth efficiency. The leaving function L_i for this model follows the following form:

$$L_i = \left(\sum_{fish[j]}^{\max j} \left(mass[j,i] > Mcrit \right) \right) + \left(\sum_{fish[j]}^{\max j} \left(growtheff[j,i] < Gcrit \right) \right)$$

In this formulation, the first term of the leaving function is identical to that in the mass only version of the model. However, there is also a second term with a similar structure to the first to account for fish leaving due to the growth efficiency threshold. The total number of fish leaving on day *i* is equal to the sum of all fish for which their modeled mass is greater than the critical mass *Mcrit*, plus the sum of all fish for which their modeled growth efficiency on day *i* is less than the critical growth efficiency, *Gcrit*. In order to prevent double counting, any fish that initiated migration by the mass threshold was ineligible to initiate migration by the growth efficiency threshold. Again, *Mcrit* and *Gcrit* are fitted as constant parameters for all fish in a given year.

3.2.6 Adding a Mass-Based Covariate to the Catchability Model

Model fits of both versions of the Mass-Growth model tended to underestimate CPUE in the early portion of the season, so the catchability portion of the model was expanded to include a term that modifies catchability depending on the mean mass of the population of fish in the

rearing habitat. For ease of reference, we will refer to this version of the model as the Mass, Growth, & Catchability Model. This expanded catchability term has the following structure:

$$CPUE_i = N_i \times \left(cc \times \left(\frac{\sum_{fish[j]}^{\max j} mass[j,i]}{\max j} \right)^B \right)$$

In this formulation, the term inside the inner set of parenthesis calculates the mean mass of all fish present in the rearing habitat on day *i*. The term sums the mass of fish on day *i* across all fish *j*, then divides by the number of fish *j* to yield the mean mass. Exponential parameter *B* then describes how mean mass impacts the catchability coefficient *cc*. If *B* is zero, then population mass has no impact on catchability. If *B* is larger than zero, then increasing population mass will result in increasing catchability. If *B* is less than zero, then increasing population mass will reduce catchability.

3.2.7 Maximum Likelihood Parameter Estimation

We used a maximum likelihood method to estimate the parameters on a yearly basis for each version of the model. For the maximum likelihood implementation of our model, we assumed that the deviations between observed CPUE and CPUE predicted by our model come from a Gaussian distribution with mean 0 and variance σ. Thus, for our model:

$$CPUE_{observed} = N_i \times cc \times \ldots + \varepsilon$$

Modeled CPUE is generated from the modeled number of fish in river N_i and the catchability term *cc*, as well as the additional mass catchability term in one version of the model. Then, for each day *i*, a deviation ε between modeled and observed CPUE is generated. For each deviation ε, the likelihood that the deviation came from Gaussian distribution with mean 0 and variance σ

is then calculated. The negative log of these likelihoods is then taken, to yield negative log likelihood. Due to the log transform, these negative log likelihoods are additive; the sum of the negative log likelihoods for each day *i* yields a single estimate of negative log likelihood for a given set of parameters. The negative log likelihood is then minimized via an iterative parameter estimation process to yield a single maximum likelihood parameter set.

We tested three versions of the Mass-Growth model. The first version tested was the Mass-Only Model: a mass-only leaving function with a constant catchability coefficient. The second was the Mass & Growth Model: a mass and growth efficiency driven leaving function with constant catchability. The last version tested was the Mass, Growth, & Catchability Model: both a mass and growth efficiency driven leaving function and a mass-varying catchability coefficient. The optim function from the stats package in the statistical computing language 'R' was used for the minimization process. The optim function implements several different minimization methods; for the parameter estimations of the Mass Only and Mass & Growth versions of the model, the Nelder-Mead method (Nelder and Mead 1965) was used as the primary method, with the L-BFGS-B (Byrd et al. 1995) method being used if the Nelder-Mead method had difficulty converging. The Nelder-Mead method is unbounded, so it searches the entire parameter space. The L-BFGS-B method is bounded; bounds were selected to be as large as possible, but often had to be tweaked to reach convergence. For the parameter estimation of the Mass, Growth & Catchability version of the model, the L-BFGS-B method was the primary method used, with the Nelder-Mead as a fallback if the L-BFGS-B method did not converge. The starting parameters used for the optimizations were: 10 grams for *Mcrit*, 0.0 joules *G/C* for *Gcrit*, 0.02 for *cc*, -1 for *B* if the mass-varying catchability coefficient was used, and 2 for σ. In some

years for some versions of the model these starting parameters were modified slightly if optim had difficulty converging.

3.3 Results

3.3.1 Mass Only Model

Table 3.5 presents the results of the maximum likelihood parameter estimation of the Mass Only Model (mass driven leaving, constant catchability). The Nelder-Mead optimization method (Nelder and Mead 1965) was used for most years; in 1994 and 1996, the Nelder-Mead method had difficulty converging and the L-BFGS-B method (Byrd et al. 1995) was used instead. Fitted *Mcrit* values are fairly consistent across years (Table 3.5), ranging from 3.13 grams to 6.74 grams. The average fitted *Mcrit* is 4.99 grams. Fitted catchability coefficients vary relatively more across years, ranging from 0.0088 to 0.0867. The mean fitted catchability coefficient is 0.0316. Fitted σ is an index of how close the fit is to the observed data; in most years fitted σ is less than one, but in 1998 and 2000 a larger fitted σ indicates a poorer fit. The theory behind the model states that achieving a critical mass is the trigger for migration; therefore, fish that were larger than fitted *Mcrit* at tagging are evidence of a model failure, as these fish have clearly not yet initiated migration even though they are larger than the threshold mass. Significant numbers of fish were larger than *Mcrit* at tagging in each year of data (Table 3.5), ranging up to half of the fish modeled in some years.

In most years, the Mass Only version of the Mass-Growth Model does an adequate job of fitting observed CPUE data (Figures 3.1, 3.2); however, some years have noticeably poor fits. In 1993 and 1996, many fish are modeled to never grow larger than the growth threshold for migration *Mcrit*, resulting in the modeled CPUE distribution never reaching close to zero. In the

other years this is only true for a handful of fish, and the modeled CPUE distribution approaches zero at the same time as the observed CPUE distribution. Additionally, in most years the fitted CPUE distribution lags slightly behind the observed CPUE distribution. This effect is most visible in 1997. Observed CPUE data displays mostly monotonic patterns with little jaggedness in the pattern of CPUE over time; however, model fits display significant jaggedness (Figures 3.1, 3.2). This is largely due to the large proportion of fish that were larger than fitted *Mcrit* values at tagging. Due to the stratified nature of sampling, sampling events tend to be clustered together in blocks of three to four days, with spaces of several days with no sampling between each cluster. After each sampling event, many fish which were larger than *Mcrit* at tagging are then modeled to immediately initiate migration. This leads to jaggedness in modeled CPUE values; modeled CPUE tends to climb rapidly due to a sampling event, then rapidly drop after the sampling event.

Modeled leaving illustrates how the large number of fish larger than *Mcrit* at tagging leads to jagged modeled CPUE (Figures 3.3, 3.4). Distributions of modeled leaving dates (T2m) predicted by the Mass Only model are very spiky. While these leaving distributions are located within the declining portion of the CPUE data, which the Thermal Wall model was unable to achieve, this spikiness is a symptom of a high rate of model failure with regards to fitted *Mcrit* values being smaller than the mass of many fish at tagging.

3.3.2 Mass & Growth Model

Table 3.6 presents the results of the maximum likelihood parameter estimation of the Mass & Growth model (mass and growth efficiency leaving, constant catchability). The Nelder-Mead optimization method (Nelder and Mead 1965) was used for most years; in 1995 and 1997,

the Nelder-Mead method had difficulty converging and the L-BFGS-B method (Byrd et al. 1995) was used instead. While a maximum likelihood fit was found for 2000, the nature of the fitted parameter values and the distributions of the fit are markedly different from the other years. We concluded that the fit for 2000 was not working very well and attempted to find a local minimum with parameters closer to those fitted in other years, but we were unsuccessful. Fitted *Mcrit* values are fairly consistent across years (Table 3.6), with the exception of 1996 and 2000. Fitted *Mcrit* values range from 9.19 grams to 12.53 grams excluding 1996 and 2000, with those years fitted at 7.86 grams and 5.54 grams respectively. The average fitted *Mcrit* is 9.79 grams. Fitted *Gcri*t values are also very consistent, with the exception of 1994 and 1996. Fitted *Gcrit* ranges from 0.30 to 0.41 excluding 1994 and 1996, with 1994 fitted at -0.015 and 1996 at 0.16. As in the Mass Only version of the Mass-Growth model, fitted catchability coefficients vary relatively more across years, ranging from 0.0034 to 0.09. The mean fitted catchability coefficient is 0.0236. Fitted σ again follows a similar pattern as in the Mass Only version of the Mass-Growth model; in most years fitted σ is less than one, but in 1998 and 2000 a larger fitted σ indicates a poorer fit. As fitted *Mcrit* values were much larger in this version of the model than in the mass-only version, many fewer fish were larger than *Mcrit* at tagging in each year of data (Table 3.6). The one exception is 2000, which is fitted with the same *Mcrit* as in the mass-only version of the Mass-Growth model (Table 3.5).

The Mass & Growth version of the Mass-Growth model does a better job of fitting observed CPUE data than the Mass Only version. The problem of jagged fits observed in the Mass Only fits is mostly absent in the Mass & Growth fits (Figures 3.5, 3.6). This is largely due to the much larger fitted *Mcrit* values, which lead to many fewer fish being larger than fitted *Mcrit* at tagging (Table 3.6). Additionally, the problem observed in the Mass Only version of the

model with some fish never modeled to initiate migration is absent in the Mass & Growth version of the model. The growth efficiency leaving term of the Mass-Growth model behaves in the same manner as the Thermal Wall model; the only difference is that the critical growth efficiency *Gcrit* is free to be fitted at any value in the Mass-Growth model, where it was constrained to zero in the Thermal Wall model. Since temperature strongly impacts the growth efficiency of all fish as discussed in Chapter 2 of this thesis, *Gcrit*-initiated leaving tends to be tightly grouped into short periods. As discussed in Chapter 2, temperature increases over the rearing season resulting in generally declining growth efficiency. This results in *Gcrit* acting in the same manner as the Thermal Wall model, where beyond a certain date temperature will drive the growth efficiency of virtually all fish below the threshold and no fish will be modeled to remain in the river. This solves the problem of some fish being modeled to never migrate, but it introduces another problem as in some years *Gcrit*-driven leaving produces a poor fit of the tail of the CPUE distribution. This is especially visible in 1993 and 1998 (Figures 3.5, 3.6), where modeled CPUE rapidly drops to near zero after the peak of the distribution, while the observed CPUE distribution declines much more gradually. Jaggedness is then observed in the fitted CPUE distributions, resulting from small numbers of tagged fish being captured and released back into the river, then immediately initiating migration due to the *Gcrit* threshold. There are clearly still some fish in the river at this point, as evidenced by the observed CPUE distributions and records of tagged fish, but the model has predicted that virtually no fish should remain in the river, so this can be considered a partial failure of the fit.

Examination of the leaving distributions predicted by the fitted *Mcrit* and *Gcrit* values illustrates the differences between how the two leaving processes operate (Figures 3.7, 3.8). As in the Thermal Wall model, *Gcrit* driven leaving displays a very spiky distribution, with leaving

packed into short periods of a few days. In contrast, *Mcrit* driven leaving displays a much more diffuse distribution, with fish growing into the threshold gradually. Additionally, the percentage of fish that initiate migration by the two processes varies greatly depending on the year (Table 3.8). For most years, the majority of fish initiate migration due to the *Gcrit* threshold; only in 1996 and 2000 do majorities of fish initiate migration due to the *Mcrit* threshold. This *Gcrit*-dominated leaving is very visible in the leaving distributions (Figure 3.7, 3.8).

3.3.3 Mass, Growth & Catchability Model

Table 3.7 presents the results of the maximum likelihood parameter estimation of the Mass, Growth & Catchability Model (mass and growth efficiency driven leaving, mass-varying catchability). The L-BFGS-B optimization method (Byrd et al. 1995) was used for every year except 2000, for which the Nelder-Mead (Nelder and Mead 1965) optimization method was used. Achieving convergence was much more difficult for this version of the model, and starting parameters had to be modified slightly for most years. Unlike the previous versions of the model, the maximum likelihood fit for 2000 was not markedly different from the other years. Fitted *Mcrit* values seem to break into two groups, with some years fitted around 7.5 grams and other years fitted near 11 grams (Table 3.7). Fitted *Mcrit* values range from 7.36 grams to 11.53 grams; the average fitted *Mcrit* is 9.44 grams. Fitted *Gcri*t values are very consistent, with the exception of 1994 and 1996 again. Fitted *Gcrit* ranges from 0.27 to 0.4 excluding 1994 and 1996, with 1994 fitted at -0.015 and 1996 at 0.049. As in the other versions of the Mass-Growth model, fitted catchability coefficients vary relatively more across years, ranging from 0.015 to 0.19. The mean fitted catchability coefficient is 0.102. Fitted *B* is fairly consistent, ranging from -0.46 to -1.82, with a mean of -0.99. Fitted σ again follows a similar pattern as in the other versions of the

Mass-Growth model; in most years fitted σ is less than one, but in 1998 and 2000 a larger fitted σ indicates a poorer fit. Fitted *Mcrit* values were larger in this version of the model than in the Mass Only version but smaller than in the Mass & Growth version. Some fish were larger than *Mcrit* at tagging in each year of data, ranging as high as 19% of all fish modeled in 1995.

The Mass, Growth & Catchability version of the Mass-Growth Model produces the best fits of observed CPUE data of the three versions tested. Where both of the previous versions of the model produced fits that tended to lag behind observed CPUE in the early part of the distribution (Figures 3.1, 3.2 and 3.5, 3.6), this problem is much lessened in the fits produced using the mass-varying catchability coefficient (Figures 3.9, 3.10). The mass exponential term *B* in the catchability coefficient has the effect of increasing modeled catchability in the early portion of the rearing season, improving the model's ability to match the observed increases in CPUE. Since the fitted value of *B* is negative in all years, catchability in this version of the model declines as fish mass increases. The mean population mass tends to increase over the rearing season, leading to declining catchability (Figures 3.13, 3.14). Modeled mass and catchability tend to be quite spiky near the end of the rearing season; this is because the number of fish remaining in the habitat is very low, and the tagging or migration of even a handful of fish can have a large impact on the mean population mass. Leaving distributions produced by this version of the model are similar to those produced by the Mass & Growth model; *Mcrit*-driven leaving tends to follow a more gradual distribution spread out across the rearing season, while *Gcrit*-driven leaving is compacted into short periods with many fish leaving at once (Figures 3.11, 3.12). Since fitted *Mcrit* values are significantly lower than those in the Mass & Growth version of the model, the percentages of fish that initiate leaving by the two processes is much

more even (Table 3.8). *Gcrit*-driven leaving is dominant in 1992, 1993, and 1998; *Mcrit*-driven leaving is dominant in 1996; the remaining years show a balance of the two processes.

While overall the fits produced by this version of the model are better, some of the problems present in the previous versions persist. In particular, *Gcrit*-driven leaving still produces a poor fit of the tail of the CPUE distribution in many years. *Gcrit* as a leaving process produces compact leaving distributions where many fish are modeled to initiate migration at once (Figures 3.11, 3.12), and due to how growth efficiency changes over the rearing season, past a certain point in the rearing season *Gcrit*-driven leaving will drive all fish out of the rearing habitat. This produces a sharp decline to zero at the tail of most of the modeled CPUE distributions, while observed CPUE distributions mostly show a much more gradual decline. In 1993 and 1998 this phenomenon has the largest impact on the fit; modeled CPUE declines sharply to zero several weeks before observed CPUE does, and there are even several tagging events after *Gcrit* driven leaving has driven all fish from the rearing habitat, leading to brief spikes in modeled CPUE.

3.4 Discussion

3.4.1 Observed Problems

The largest problems observed in the fits of the three versions of the Mass-Growth model were fitted *Mcrit* values smaller than the mass of many fish at tagging and a tendency for *Gcrit*-driven leaving to drive modeled fish out of the rearing habitat before observed CPUE reaches zero. The Mass Only version suffered the most from large number of fish with tagging mass larger than fitted *Mcrit* values. In every year fitted, twenty to fifty percent of all fish were larger at tagging than the fitted *Mcrit* (Table 3.5). Each of these fish can be considered a model failure;

our model proposes that reaching the *Mcrit* threshold is the trigger for migration; therefore any fish that has grown larger than *Mcrit* and has not yet initiated migration is evidence that the *Mcrit* threshold fitted is in error. If the model were working perfectly, we would expect no fish in the rearing habitat to be larger than *Mcrit*, and therefore no fish could be captured and tagged with a larger mass than *Mcrit*. This being the ideal outcome, no model is a perfect representation of reality and the Mass-Growth model is no exception. For reasons including parsimony and ease of estimating the parameter, our model fits *Mcrit* as a single value constant for all fish; however, as a representation of a genetic threshold, the theory motivating the model suggests that there would most likely be significant variability in *Mcrit* on an individual basis corresponding with genetic variability in the population (Thorpe et al. 1998). In this case, what the Mass-Growth model is actually fitting is the population mean of the individual *Mcrit* values. Some rate of failure would be expected under this circumstance, as some fish will have a true mass threshold larger than the fitted *Mcrit*, and they could be captured and tagged after they have grown larger than the fitted *Mcrit* but before they have reached their individual threshold. However, the very high rate of failure displayed by the Mass Only version of the Mass-Growth model is almost certainly evidence that the fitted *Mcrit* thresholds are too low. The two versions of the model with both mass-driven leaving and growth efficiency-driven leaving have significantly higher fitted *Mcrit* values and correspondingly a much lower rate of failure with respect to tagging masses larger than the fitted *Mcrit* values. For this reason, we conclude that the Mass Only version of the Mass-Growth model is insufficient to explain migration in juvenile Chinook, and both mass and growth efficiency thresholds are necessary.

Both the Mass & Growth and the Mass, Growth & Catchability versions of the model display a tendency for *Gcrit*-driven leaving to drive modeled fish out of the rearing habitat

before observed CPUE reaches zero. As discussed in section 3.3, this is especially visible in the fits for 1993 and 1998 in both versions of the model (Figures 3.5, 3.6 and 3.9, 3.10). The *Gcrit* parameter behaves as the Thermal Wall model, discussed in the sensitivity analysis in section 2.3.2; due to the increasing trend in temperature over the course of the rearing season, eventually the growth efficiency of all fish will fall below *Gcrit*. *Gcrit*-driven leaving thus acts as a termination of the rearing season, forcing all fish to initiate migration with an abrupt, large migration pulse (Figures 3.7, 3.8 and 3.11, 3.12). In contrast, observed CPUE distributions display gradual declines, sometimes with a marked tail. Again, assumptions and simplifications we have made in our modeling are likely responsible for the difficulty the Mass-Growth model has in fitting a gradual tail. *Gcrit* affects the majority of the population at once because many of the factors that determine individual growth efficiency are constant across fish in our modeling. In reality, individual growth efficiencies are affected by individual variation in temperature experience and consumption rate, and genetic variation in *Gcrit*.

In our modeling, we use only the daily mean temperature from a single source to describe the temperature experience of all fish. In reality, there is spatial and diurnal variation in temperature through the reach of the Snake River used as rearing habitat by fall Chinook (Anderson 2000, Cook et al. 2006). Additionally, in the nearshore habitat used by rearing juvenile Chinook, the salmon are vulnerable to being caught in entrapment pools caused by anthropogenic modification of flow rates (Geist et al. 2010). Temperatures within entrapment pools vary much more than temperatures within the river (Geist et al. 2010). These variations in individual temperature experience will affect each fish's growth efficiency, resulting in greater variation in when individual fish pass the growth efficiency threshold *Gcrit* than captured by our modeling.

While we fit individual consumption rates for any fish for which a T1 and M1 data point is present, many fish used in the Mass-Growth model did not have a T1 and M1 data point. Since our multivariate linear model of consumption rate was unsatisfactory, we used the mean fitted consumption rate for all of these fish. Unfortunately, this assumption removes much individual variation in growth rate and growth efficiency, which results in less variation in migration dates predicted by *Gcrit*.

Lastly, similarly to our modeling of *Mcrit*, we model *Gcrit* as a constant parameter for all fish. However, we employ Thorpe et al.'s (1998) theory that the triggering mechanisms driving migratory behavior are under genetic control, and as a representation of a genetically-determined threshold, *Gcrit* in reality will vary according to an individual's genetic makeup. Since the Mass-Growth model can only estimate a single, constant value for *Gcrit*, this genetic variability is not modeled. This individual variation in temperature experience, consumption rate, and *Gcrit* threshold which the Mass-Growth model does not capture would all work to spread out the migration dates predicted by the *Gcrit* threshold. If such improvements could be made to the model, the large pulse that the model currently predicts would be more dispersed, greatly improving the model's ability to fit a gradual tail in the observed CPUE distribution.

The last question arising from the model fits concerns the fitted relationship between fish mass and catchability in the Mass, Growth & Catchability version of the model. In every year fitted, the fitted relationship predicts decreasing catchability with increasing mass (Figures 3.13, 3.14). While no prior studies explicitly evaluate the relationship between catchability and fish mass with beach seine gear, a study examining catchability of juvenile salmonids with electrofishing gear found a positive relationship between fish mass and catchability (Ruiz and Laplanche 2010). The mass coefficient *B* was added to the model to address the tendency for

model fits to lag behind observed CPUE, but it is possible that a different factor is impacting catchability, or even some factor other than catchability may be responsible for the lagging fits. The fitted mass-catchability relationship cannot be discounted entirely however, because catchability relationships are known to vary widely depending on the gear type and fishing method used (Arreguin-Sanchez 1996). It is likely that differences between beach seine and electrofishing processes could result in opposite relationships between fish mass and catchability; in electrofishing, larger fish are more vulnerable due to the physics of the fishing gear- the waveform generated by the electric probes intersects larger bodies more frequently, resulting in a more severe stun effect. In contrast, beach seining has very different sampling dynamics. In a large habitat such as the mainstem Snake River, habitat nearer to shore is easier to sample, and habitat further from shore is comparatively more difficult due to increasing depth and a longer cast distance. Additionally, fish can see the oncoming net and attempt to escape it; fish with a faster swimming speed are better able to escape the net. If larger fish tend to occupy rearing habitat farther from shore or are better able to escape the net, then the negative relationship fitted between fish mass and catchability in our model is likely accurate.

3.4.2 Overall Performance

The Mass Only version of the Mass-Growth model produced reasonable fits of observed CPUE data for some years; notably, the AIC scores for 1993 and 1995 compare favorably to the other models (Table 3.9). However, the fits produced for many other years had notable problems, and this version had a high rate of model failure with many fish larger at tagging than the low fitted *Mcrit* values. Ultimately, due to the model failures, we conclude that a mass threshold alone is insufficient to describe migration initiation in fall Chinook in the Snake River. Both the

Mass & Growth and the Mass, Growth & Catchability versions of the Mass-Growth model produced much better fits of observed CPUE data with fewer systemic problems with the fits. However, modifying the catchability term of the model significantly changed the fitted values of the other parameters and the distributions of fish that initiated migration via the two processes. With a constant catchability term, fitted *Mcrit* values were quite large, averaging 9.79 grams (Table 3.6). While these large *Mcrit* values resulted in a low rate of failure with regards to fish being larger than *Mcrit* at tagging, it also resulted in the mass-driven leaving process being unimportant to overall migration, as most fish initiated migration via the *Gcrit* process (Table 3.8). Using a mass-varying catchability term resulted in smaller fitted *Mcrit* values, averaging 9.44 grams, but produced little change in fitted *Gcrit* values. This results in the two parameters being equally important to the overall migration pattern, with one or the other process producing a majority of migrants depending on the year. These lower fitted *Mcrit* values do produce a slightly higher failure rate with fish larger than *Mcrit* at tagging, but overall the failure rate is much more acceptable, with less than ten percent of all fish larger at tagging than their fitted *Mcrit* (Table 3.7).

The quality of the fits produced and the low rate of failure lead us to select the Mass, Growth & Catchability version of the Mass-Growth model as the most successful version. For most years, the AIC scores produced by this model are superior to those of the other versions (Table 3.9); the largest exceptions are 1998 and 2000, which are not fitted well by any version of the Mass-Growth model. The model produces very consistent estimates for the critical growth efficiency initiating migration. With the exception of two years, the fitted values of *Gcrit* suggest that growth efficiencies between 0.3 and 0.4 are a trigger for migration. The fitted values of the mass threshold are more ambiguous; some years seem to cluster around 7.5 grams, while others

cluster around 11 grams. It is interesting to note that the three years with the lowest fitted *Mcrit* values- 1995, 1997, and 1998- are also three years when Connor released significant numbers of tagged subyearling hatchery fish into the Snake River rearing habitat in a study related to his study of wild fall Chinook. In 1995, 7,681 hatchery subyearlings were released; in 1997, 29,783 were released, and 25,470 were released in 1998. No hatchery subyearlings were released by Connor in the other years. These three years also have the lowest fitted *Mcrit* values, at 7.61, 7.36, and 7.60. These values are markedly lower than the fitted *Mcrit* values for the other years (with the exception of 1996); it is possible that amplified density dependent effects resulting from the large number of hatchery subyearlings released reduced the optimal mass for migration.

The end result of combining the mass-driven and growth-efficiency driven leaving processes into one leaving function is a fairly constant, low-level amount of fish initiating migration through the bulk of the rearing season, capped by large pulses of migration at the end of the rearing season. Depending on whether the constant or mass-varying catchability term is used, the dynamics of the two processes change. If the constant catchability term is used (Mass & Growth Model), the number of fish migrating in the diffuse portion of the season (produced by *Mcrit*) is insignificant compared to the large leaving pulses at the end (produced by *Gcrit*). If the mass-varying catchability term is used (Mass, Growth & Catchability Model), the number of fish leaving by the two processes is much more balanced, though one or the other can be dominant depending on the year.

3.5 Chapter 3 Tables

Table 3.1

Summary table of the full model with all predictors for the multivariate linear model of fitted consumption rate (P). T0 is the day of year a fish was tagged, M0 is the fish's mass at tagging, T0 RKM is the river kilometer the fish was tagged at, T0 CPUE is the catch per unit effort recorded at the site and day on which the fish was tagged, CPUE^2 is a squared term of CPUE, T0 Temp is the daily mean Snake River temperature on the day the fish was tagged, Temp^2 is a squared term of temperature, and T0:M0, T0:CPUE and T0:Temp are interaction terms. Year effects are estimated as offsets from the base year (1992). The T-statistics of T0 Temp, T0:M0 and T0:CPUE and the year offset for 1993 are not significant at the 0.05 level; the slope coefficients of all other terms are significantly different from zero. The total adjusted R^2 is 0.12.

Predictor	Estimate	Std. Error	T	P
Y-Intercept	-1.516	0.398	-3.81	0.00014
T0	0.0169	0.00337	5.01	5.8e-7
M0	-0.0627	0.0295	-2.13	0.0335
T0 RKM	0.000894	0.000114	7.78	1.1e-14
T0 CPUE	0.00849	0.00360	2.36	0.019
CPUE^2	-0.000028	0.0000095	-2.96	0.0031
T0 Temp	0.0631	0.0418	1.51	0.13
Temp^2	0.00571	0.00194	2.95	0.0032
Year (1993)	0.0142	0.0338	0.42	0.67
Year (1994)	0.157	0.0290	5.40	7.6e-8
Year (1995)	0.0761	0.0319	2.39	0.017
Year (1996)	0.169	0.0399	4.24	2.3e-5
Year (1997)	0.0955	0.0335	2.85	0.0043
Year (1998)	0.0626	0.0315	1.99	0.047
Year (1999)	0.120	0.0338	5.91	3.7e-9
Year (2000)	0.166	0.0369	4.50	7.2e-6
T0:M0	0.000333	0.000186	1.79	0.073
T0:CPUE	-0.000041	0.000024	-1.71	0.087
T0:Temp	-0.00132	0.000259	-5.11	3.6e-7
		R^2: 0.1288		**Adjusted R^2: 0.1222**

Table 3.2

ANOVA Table of the full model with all predictors for the multivariate linear model of fitted consumption rate (P). The table includes a list of the predictor variables, the degrees of freedom used by each predictor, the sum of squares and mean sum of squares explained by each predictor, the resulting F statistics and the P values of the F statistics. T0 is the day of year a fish was tagged, M0 is the fish's mass at tagging, T0 RKM is the river kilometer the fish was tagged at, T0 CPUE is the catch per unit effort recorded at the site and day on which the fish was tagged, CPUE^2 is a squared term of CPUE, T0 Temp is the daily mean Snake River temperature on the day the fish was tagged, Temp^2 is a squared term of temperature, Year is a year effect, and T0:M0, T0:CPUE and T0:Temp are interaction terms. The F-statistics of T0, Temp^2, T0:M0 and T0:CPUE are not significant at the 0.05 level, all other predictors are statistically significant. All predictors combined explain 13.715 of 106.453 total variance in the response variable, fitted consumption rate (P).

Predictor	D.F.	SS	Mean SS	F	P
T0	1	0.00000236	0.00000236	0.0001	0.994
M0	1	0.377	0.377	9.614	0.00195
T0 RKM	1	3.296	3.296	84.088	< 2.2e-16
T0 CPUE	1	0.406	0.406	10.345	0.00131
CPUE^2	1	0.831	0.831	21.206	4.34e-6
T0 Temp	1	0.309	0.309	7.889	0.00501
Temp^2	1	0.116	0.116	2.959	0.0855
Year	8	7.303	0.913	23.290	< 2.2e-16
T0:M0	1	0.009	0.009	0.224	0.636
T0:CPUE	1	0.046	0.046	1.180	0.278
T0:Temp	1	1.022	1.022	26.074	3.55e-7
Error	2366	92.738	0.039		
Total	2384	106.453			

Table 3.3

Summary table of the reduced multivariate linear model of fitted consumption rate (P), produced by sequential deletion from the full model. T0 is the day of year a fish was tagged, M0 is the fish's mass at tagging, T0 RKM is the river kilometer the fish was tagged at, T0 CPUE is the catch per unit effort recorded at the site and day on which the fish was tagged, CPUE^2 is a squared term of CPUE, T0 Temp is the daily mean Snake River temperature on the day the fish was tagged, Temp^2 is a squared term of temperature, and T0:Temp is an interaction term. Year effects are estimated as offsets from the base year (1992). The T-statistics of T0 Temp and the year offsets for 1993 and 1998 are not significant at the 0.05 level; the slope coefficients of all other terms are significantly different from zero. The total adjusted R^2 is 0.12.

Predictor	Estimate	Std. Error	T	P
Y-Intercept	-1.410	0.395	-3.57	0.00037
T0	0.0158	0.00334	4.74	2.3e-6
M0	-0.00998	0.0236	-4.24	2.4e-6
T0 RKM	0.000939	0.000111	8.44	< 2e-16
T0 CPUE	0.00218	0.000789	2.76	0.0058
CPUE^2	-0.000027	0.0000095	-2.81	0.0050
T0 Temp	0.0464	0.0407	1.14	0.25
Temp^2	0.00545	0.00193	2.82	0.0048
Year (1993)	0.0108	0.0336	0.32	0.75
Year (1994)	0.154	0.0290	5.31	1.2e-7
Year (1995)	0.0703	0.0317	2.23	0.026
Year (1996)	0.164	0.0398	4.12	3.9e-5
Year (1997)	0.0918	0.0334	2.75	0.0061
Year (1998)	0.0612	0.0315	1.94	0.052
Year (1999)	0.195	0.0334	5.83	6.3e-9
Year (2000)	0.167	0.0363	4.6	4.4e-6
T0:Temp	-0.00117	0.000250	-4.68	3.1e-6
		R^2: 0.1268		**Adjusted R^2: 0.1209**

Table 3.4

ANOVA Table of the reduced multivariate linear model of fitted consumption rate (P), produced by sequential deletion from the full model. The table includes a list of the predictor variables, the degrees of freedom used by each predictor, the sum of squares and mean sum of squares explained by each predictor, the resulting F statistics and the P values of the F statistics. T0 is the day of year a fish was tagged, M0 is the fish's mass at tagging, T0 RKM is the river kilometer the fish was tagged at, T0 CPUE is the catch per unit effort recorded at the site and day on which the fish was tagged, CPUE^2 is a squared term of CPUE, T0 Temp is the daily mean Snake River temperature on the day the fish was tagged, Temp^2 is a squared term of temperature, Year is a year effect, and T0:Temp is an interaction term. The F-statistics of T0 and Temp^2 are not significant at the 0.05 level, all other predictors are statistically significant. All predictors combined explain 13.496 of 106.453 total variance in the response variable, fitted consumption rate (P).

Predictor	D.F.	SS	Mean SS	F	P
T0	1	0.00000236	0.00000236	0.0001	0.994
M0	1	0.377	0.377	9.614	0.00195
T0 RKM	1	3.296	3.296	84.088	< 2.2e-16
T0 CPUE	1	0.406	0.406	10.345	0.00131
CPUE^2	1	0.831	0.831	21.206	4.34e-6
T0 Temp	1	0.309	0.309	7.889	0.00501
Temp^2	1	0.116	0.116	2.959	0.0855
Year	8	7.303	0.913	23.290	< 2.2e-16
T0:Temp	1	0.858	0.858	21.860	3.10e-6
Error	2366	92.738	0.039		
Total	2384	106.453			

Table 3.5

Table of yearly fitted parameter values for the Mass Only version of the Mass-Growth model (mass driven leaving function, constant catchability coefficient). Year is the year modeled, # Fish is the number of individual fish tagged at the sites sampled in CPUE data and used to fit the model. # Fitted P is the number of individual fish which had a T1 and M1 data point and had an individually fitted consumption rate; other fish used the mean consumption rate. Fitted *Mcrit*, *cc*, and σ are the parameters of the Mass-Growth model estimated via maximum likelihood. Method is the optimization method used to reach the fit; N-M refers to the Nelder-Mead method (Nelder and Mead 1965), L-BFGS-B is the method of Byrd et al. 1995. # T0 > *Mcrit* is the number of fish which had a larger mass at tagging than the critical mass for migration, which is a model failure; the model predicts that these fish initiate migration immediately after tagging, leading to spikiness in the modeled CPUE fits.

Year	# Fish	# Fitted P	Fitted *Mcrit*	Fitted *cc*	Fitted σ	Method	# T0 > *Mcrit*
1992	633	43	3.13 g	0.0358	0.964	N-M	358
1993	751	141	4.53 g	0.0178	0.633	N-M	324
1994	1177	213	4.68 g	0.0088	0.548	L-BFGS-B	494
1995	692	144	5.83 g	0.0227	0.661	N-M	207
1996	389	61	6.74 g	0.0162	0.01	L-BFGS-B	83
1997	291	54	4.38 g	0.0348	0.574	N-M	146
1998	1298	203	4.17 g	0.0461	1.734	N-M	665
1999	1129	221	5.90 g	0.0151	0.803	N-M	220
2000	1078	142	5.54 g	0.0867	3.958	N-M	356

Table 3.6

Table of yearly fitted parameter values for the Mass & Growth version of the Mass-Growth model (mass and growth efficiency leaving function, constant catchability coefficient). Year is the year modeled, # Fish is the number of individual fish tagged at the sites sampled in CPUE data and used to fit the model; the number is the same as in Table 3.5. The number of fish with a fitted consumption rate is also the same as in Table 3.5; it has been omitted from this table. Fitted *Mcrit*, *Gcrit*, *cc*, and σ are the parameters of the Mass-Growth model estimated via maximum likelihood. Method is the optimization method used to reach the fit; N-M refers to the Nelder-Mead method (Nelder and Mead 1965), L-BFGS-B is the method of Byrd et al. 1995. # T0 > *Mcrit* is the number of fish which had a larger mass at tagging than the critical mass for migration, which is a model failure; the model predicts that these fish initiate migration immediately after tagging, leading to spikiness in the modeled CPUE fits.

Year	**# Fish**	**Fitted *Mcrit***	**Fitted *Gcrit***	**Fitted *cc***	**Fitted σ**	**Method**	**# T0 > *Mcrit***
1992	633	10.74 g	0.36	0.019	0.69	N-M	11
1993	751	11.29 g	0.34	0.011	0.71	N-M	69
1994	1177	12.53 g	-0.015	0.0034	0.43	N-M	41
1995	692	9.19 g	0.37	0.018	0.77	L-BFGS-B	83
1996	389	7.86 g	0.16	0.012	0.23	N-M	59
1997	291	11.08 g	0.30	0.010	0.41	L-BFGS-B	7
1998	1298	9.49 g	0.41	0.040	2.52	N-M	84
1999	1129	10.39 g	0.37	0.0090	1.33	N-M	47
2000	1078	5.54 g	0.35	0.090	3.95	N-M	356

Table 3.7

Table of yearly fitted parameter values for the Mass, Growth & Catchability version of the Mass-Growth model (mass and growth efficiency leaving function, mass-varying catchability coefficient). Year is the year modeled; # Fish and # Fitted P have been omitted from this table, as they are the same as in Table 3.5. Fitted *Mcrit*, *Gcrit*, *cc*, *B*, and σ are the parameters of the Mass-Growth model estimated via maximum likelihood. Method is the optimization method used to reach the fit; N-M refers to the Nelder-Mead method (Nelder and Mead 1965), L-BFGS-B is the method of Byrd et al. 1995. # T0 > *Mcrit* is the number of fish which had a larger mass at tagging than the critical mass for migration, which is a model failure; the model predicts that these fish initiate migration immediately after tagging, leading to spikiness in the modeled CPUE fits.

Year	Fitted *Mcrit*	Fitted *Gcrit*	Fitted *cc*	Fitted *B*	Fitted σ	Method	#T0>Mcrit
1992	10.0	0.35	0.044	-0.91	0.70	L-BFGS-B	13
1993	11.53	0.34	0.025	-0.99	0.72	L-BFGS-B	64
1994	10.61	-0.015	0.015	-1.15	0.33	L-BFGS-B	82
1995	7.61	0.37	0.087	-1.30	0.66	L-BFGS-B	131
1996	8.23	0.049	0.065	-1.82	0.18	L-BFGS-B	53
1997	7.36	0.27	0.10	-0.88	0.31	L-BFGS-B	49
1998	7.60	0.40	0.19	-0.63	3.98	L-BFGS-B	154
1999	10.61	0.30	0.19	-0.46	0.58	L-BFGS-B	40
2000	11.44	0.34	0.20	-0.77	4.43	N-M	50

Table 3.8

Table showing the percentage of fish that initiated migration via *Mcrit* and via *Gcrit* in the two versions of the model with both thresholds present. In both versions of the model with a mass and growth driven leaving function, a fish can initiate migration by either growing larger than *Mcrit* or by having its growth efficiency fall below *Gcrit*. Since each fish initiates migration only once, the first threshold criteria met becomes the mechanism to initiate migration for an individual fish. The columns % *Mcrit* and % *Gcrit* show the percentage of all fish modeled in each year and model run for which the relevant threshold was the mechanism that resulted in migration initiation.

	Mass & Growth Model		**Mass, Growth & Catchability Model**	
Year	% *Mcrit*	% *Gcrit*	% *Mcrit*	% *Gcrit*
1992	0%	100%	4%	96%
1993	6%	94%	5%	95%
1994	14%	86%	24%	76%
1995	26%	74%	41%	59%
1996	81%	19%	82%	18%
1997	26%	75%	70%	30%
1998	3%	97%	8%	92%
1999	27%	73%	76%	24%
2000	71%	29%	16%	84%

Table 3.9

Table showing the AIC scores of the maximum likelihood fitted models for each year and all three versions of the Mass-Growth Model.

Year	Mass Only AIC	Mass & Growth AIC	Mass, Growth & Catchability AIC
1992	308.1	237.2	275.6
1993	306.6	339.2	412.2
1994	239.8	172.6	89.2
1995	275.8	352.5	305.1
1996	516.9	1.0	-60.2
1997	135.2	140.5	72.8
1998	498.4	598.1	649.0
1999	352.0	499.2	291.6
2000	766.6	774.6	805.5

3.6 Chapter 3 Figures

Figure 3.1

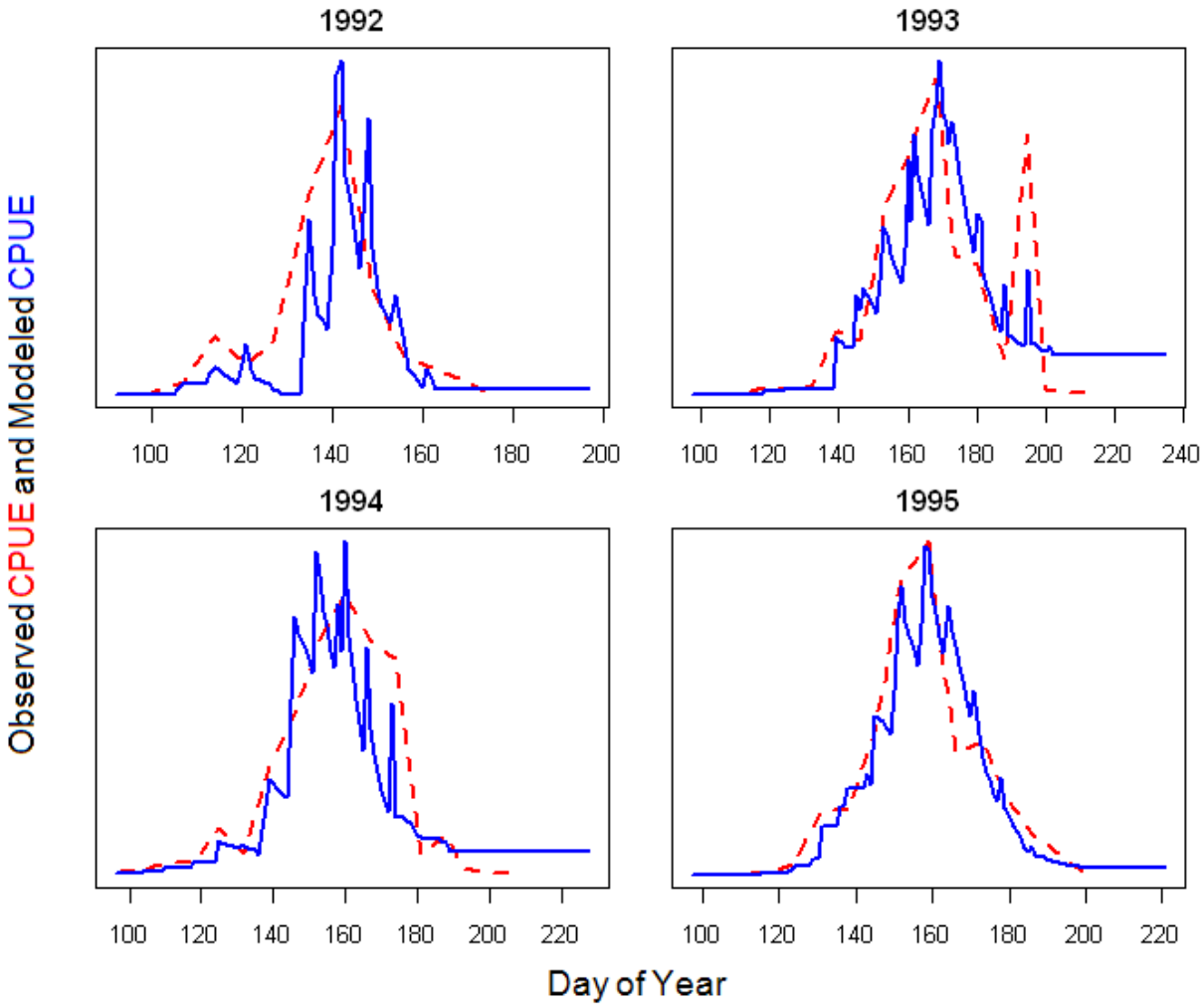

Yearly plots showing observed CPUE and modeled CPUE produced by the Mass Only version of the Mass-Growth model (mass driven leaving, constant catchability) for the years 1992-1995. Model parameters were estimated independently for each year via a maximum likelihood method. Modeled CPUE tracks observed CPUE fairly well in most years. In 1993 and 1996, many fish are never modeled to grow larger than *Mcrit* and are thus modeled to never initiate migration, resulting in modeled CPUE distributions not approaching zero when observed CPUE distributions are approaching zero.

Figure 3.2

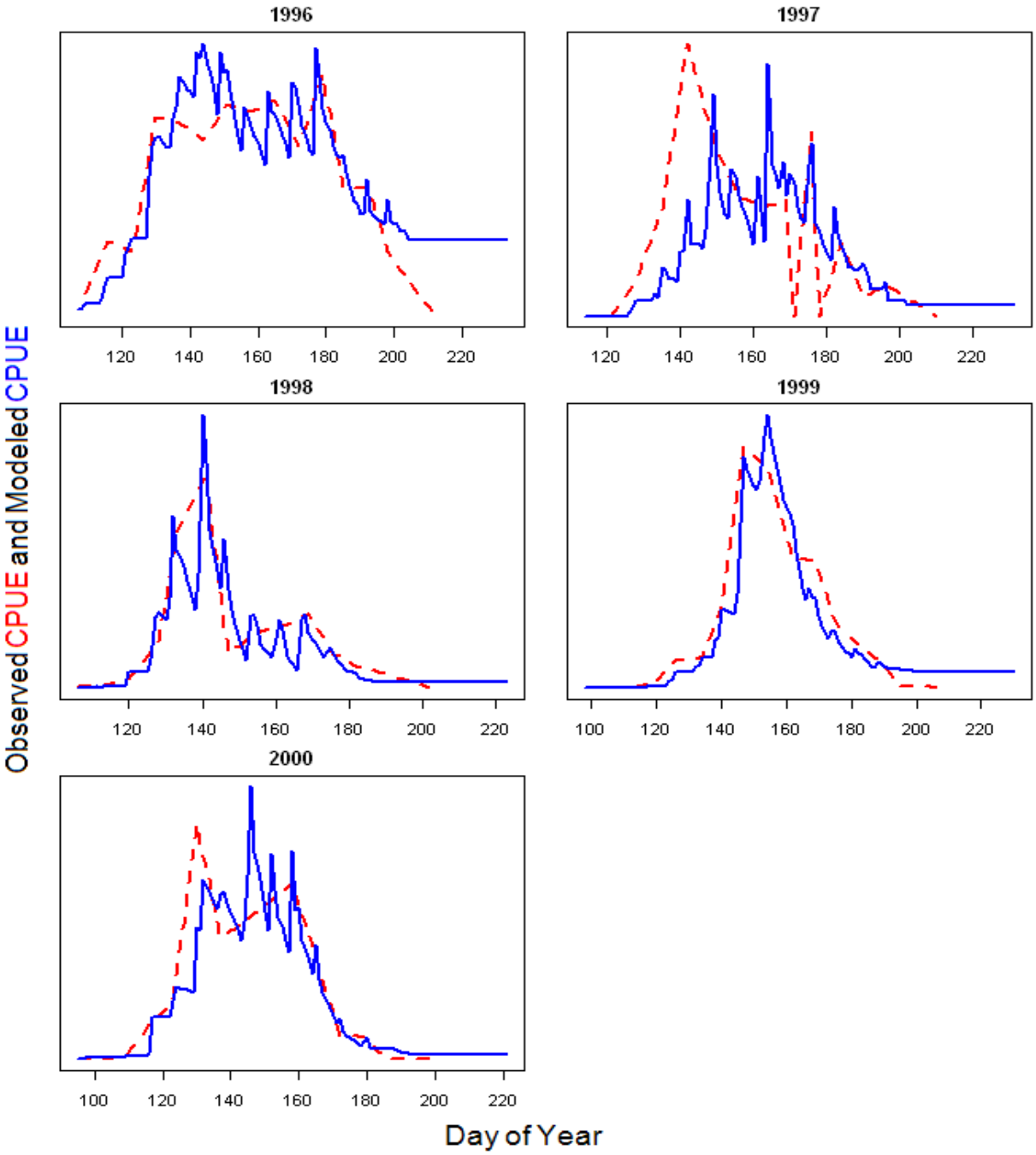

Yearly plots showing observed CPUE and modeled CPUE produced by the Mass Only version of the Mass-Growth model (mass driven leaving, constant catchability) for the years 1996-2000.

Figure 3.3

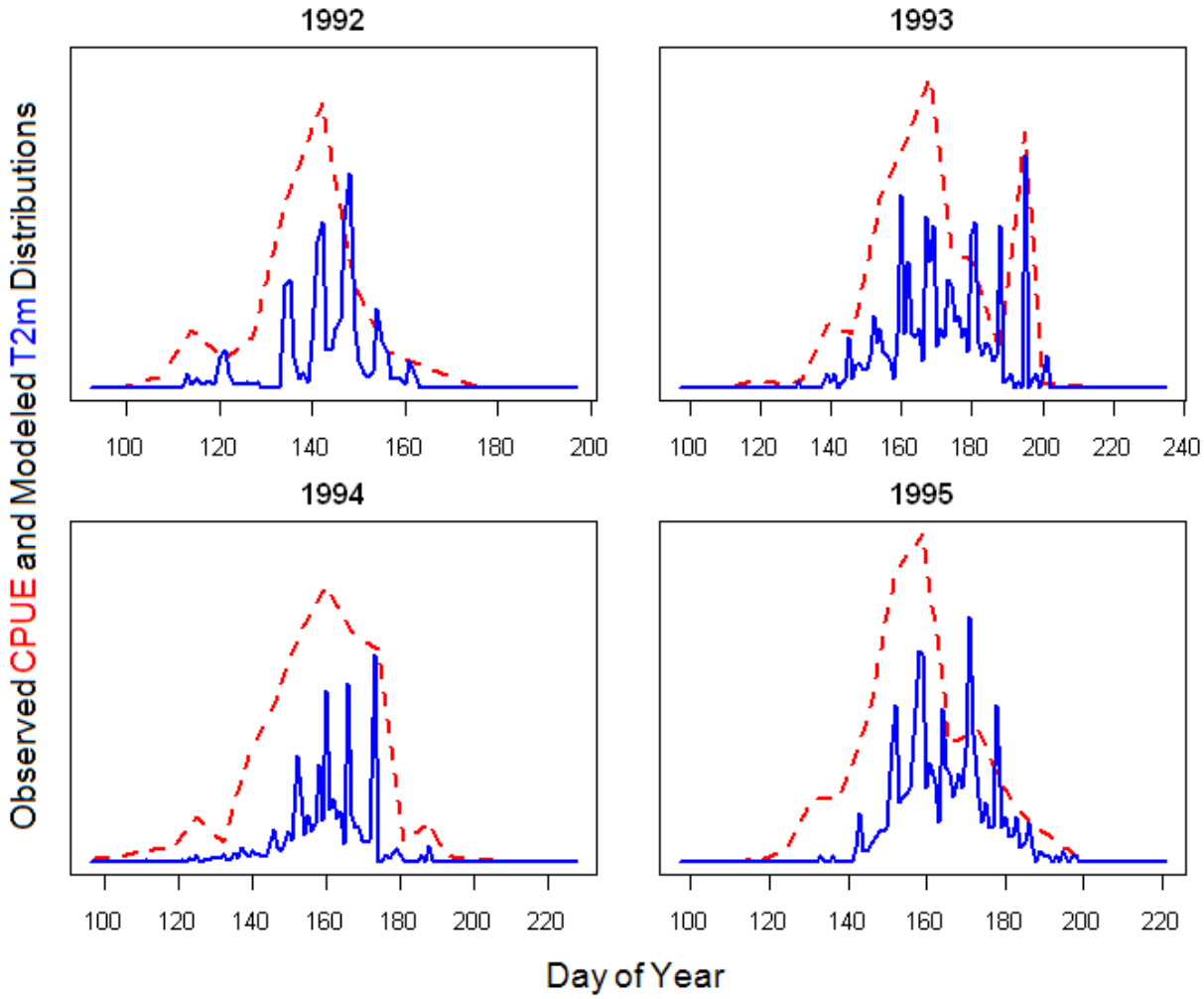

Yearly plots showing observed CPUE and modeled T2m distributions produced by the Mass Only version of the Mass-Growth model (mass driven leaving function, constant catchability) for the years 1992-1995. Leaving occurs within the CPUE distribution as opposed to after the end of the distribution like the T2b produced by the Thermal Wall model. Distributions of T2m tend to be very spiky due to low fitted *Mcrit* thresholds; many fish are larger than *Mcrit* at tagging, leading to spikes in modeled T2m coinciding with sampling events where many fish were tagged and then modeled to immediately initiate migration.

Figure 3.4

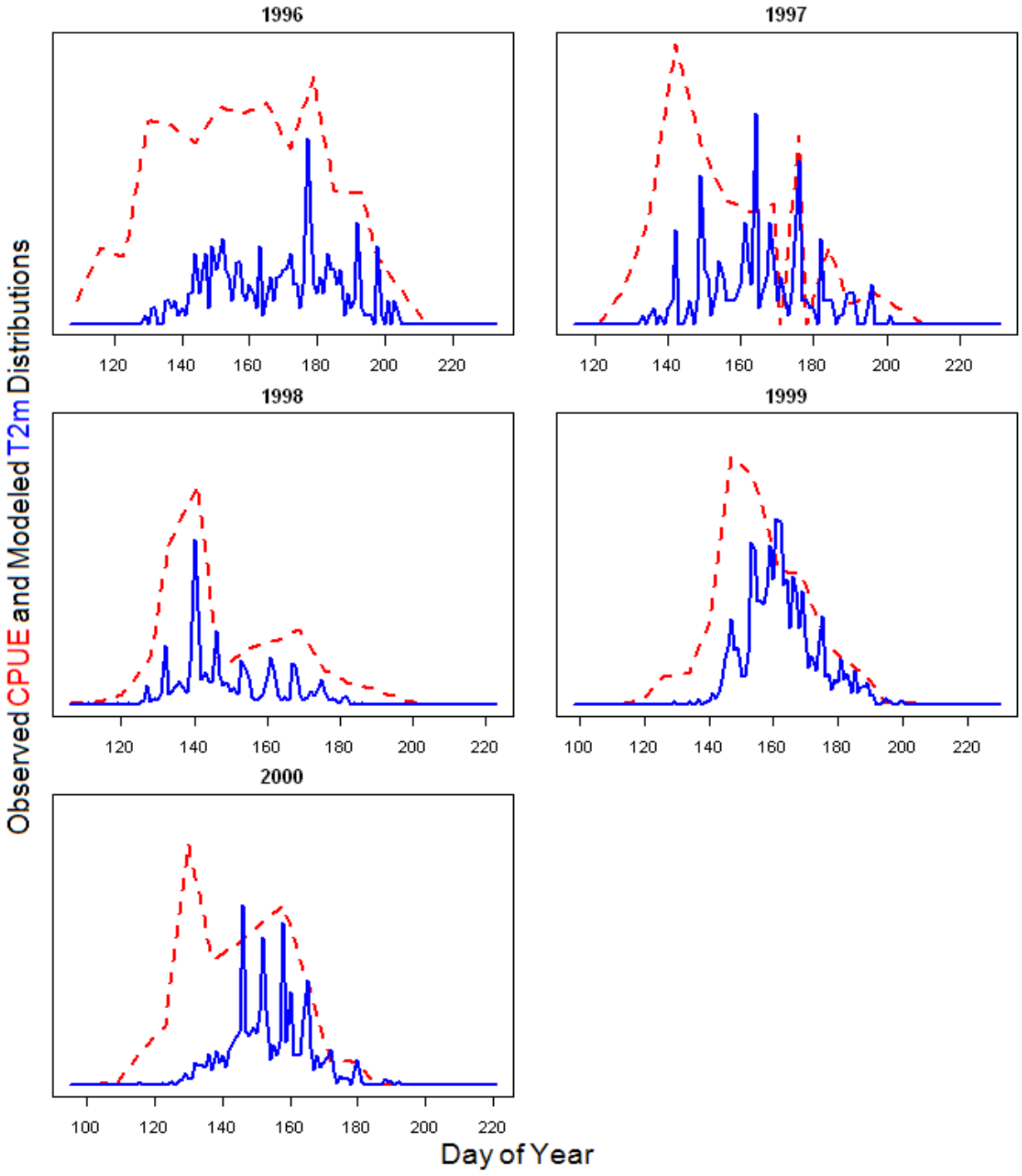

Yearly plots showing observed CPUE and modeled T2m distributions produced by the Mass Only version of the Mass-Growth model (mass driven leaving function, constant catchability) for the years 1996-2000.

Figure 3.5

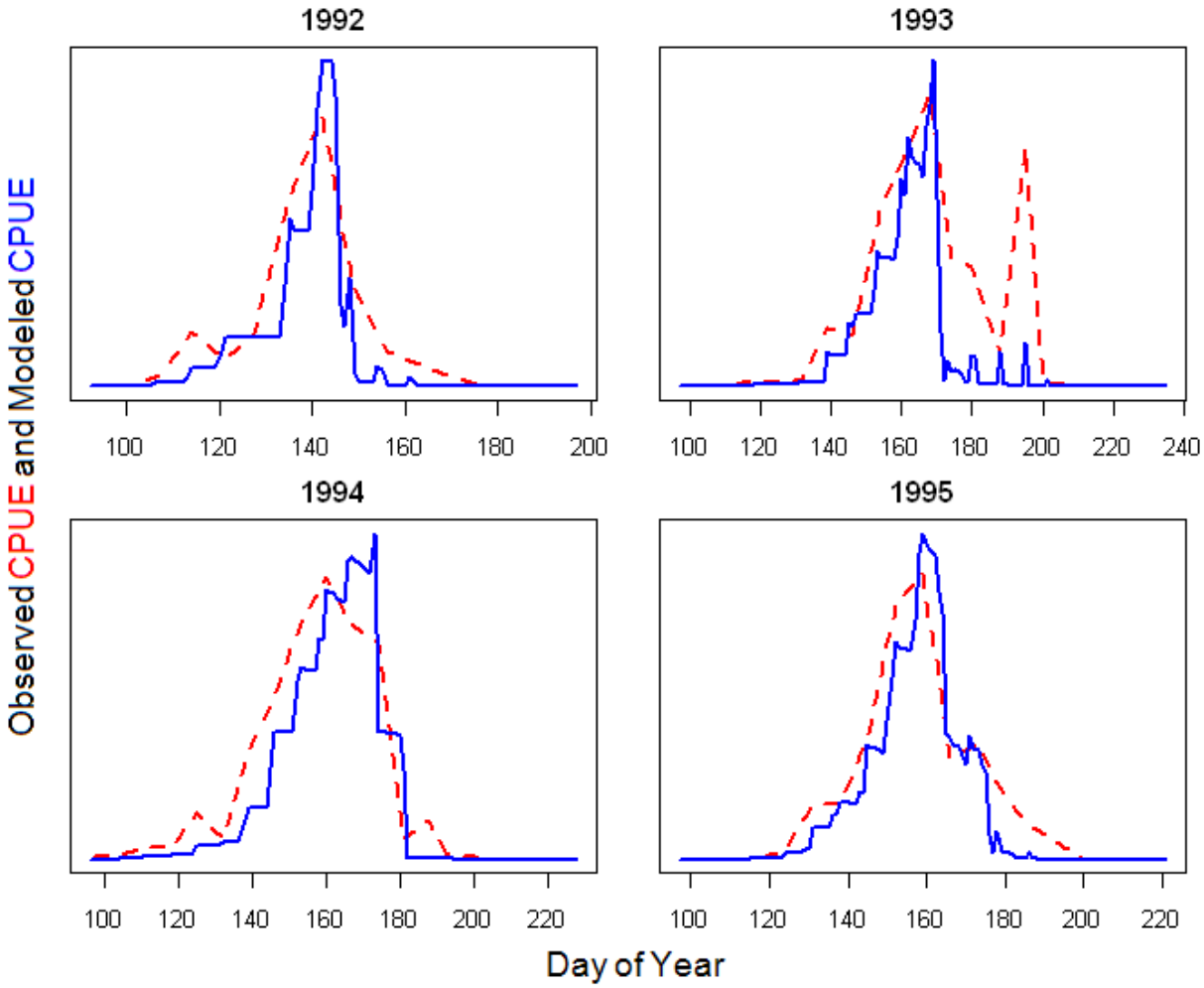

Yearly plots showing observed CPUE and modeled CPUE produced by the Mass & Growth version of the Mass-Growth model (mass and growth efficiency driven leaving, constant catchability) for the years 1992-1995. Model parameters were estimated independently for each year via a maximum likelihood method. Modeled CPUE tracks observed CPUE fairly well in most years.

Figure 3.6

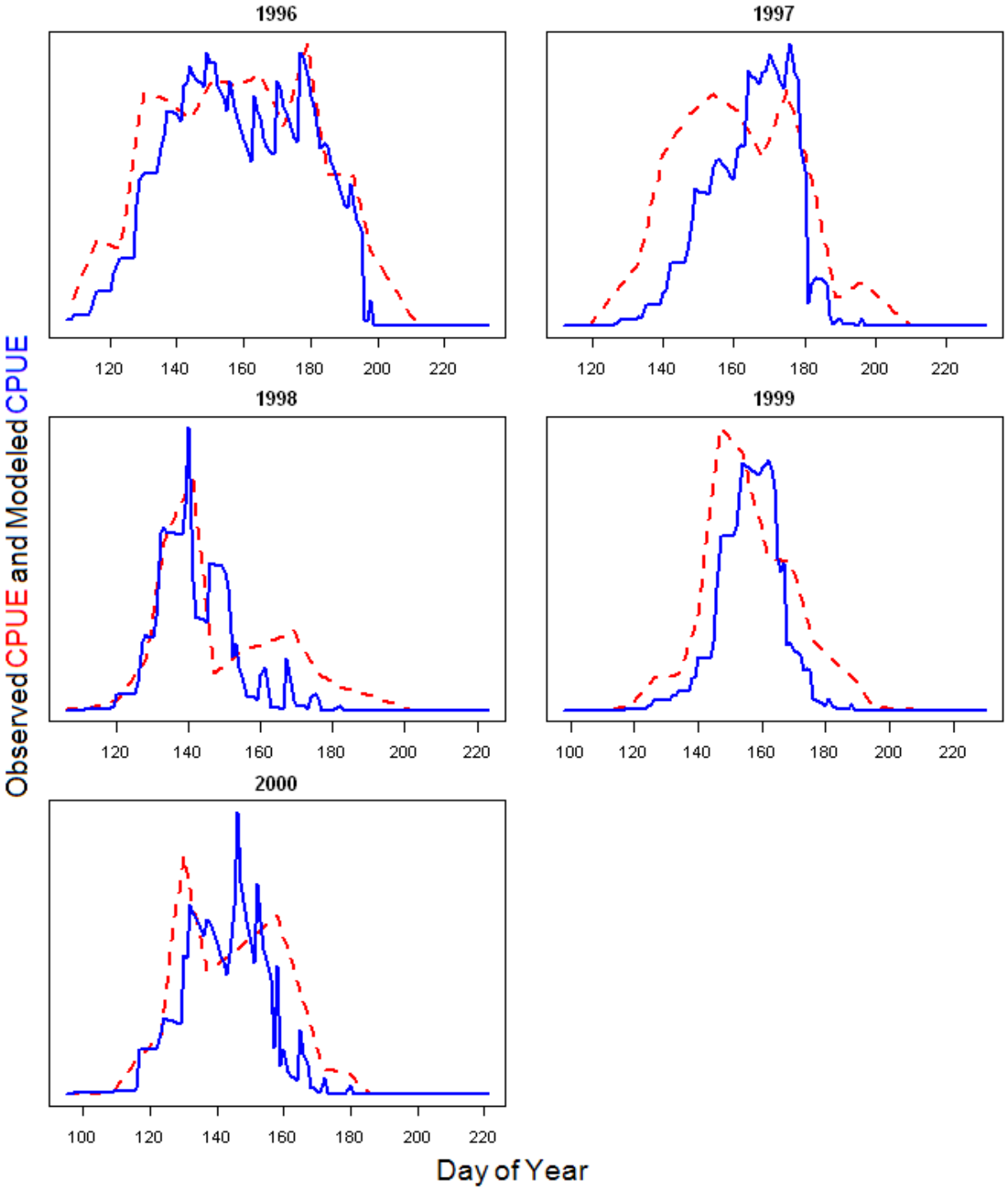

Yearly plots showing observed CPUE and modeled CPUE produced by the Mass & Growth version of the Mass-Growth model (mass and growth efficiency driven leaving, constant catchability) for the years 1996-2000.

Figure 3.7

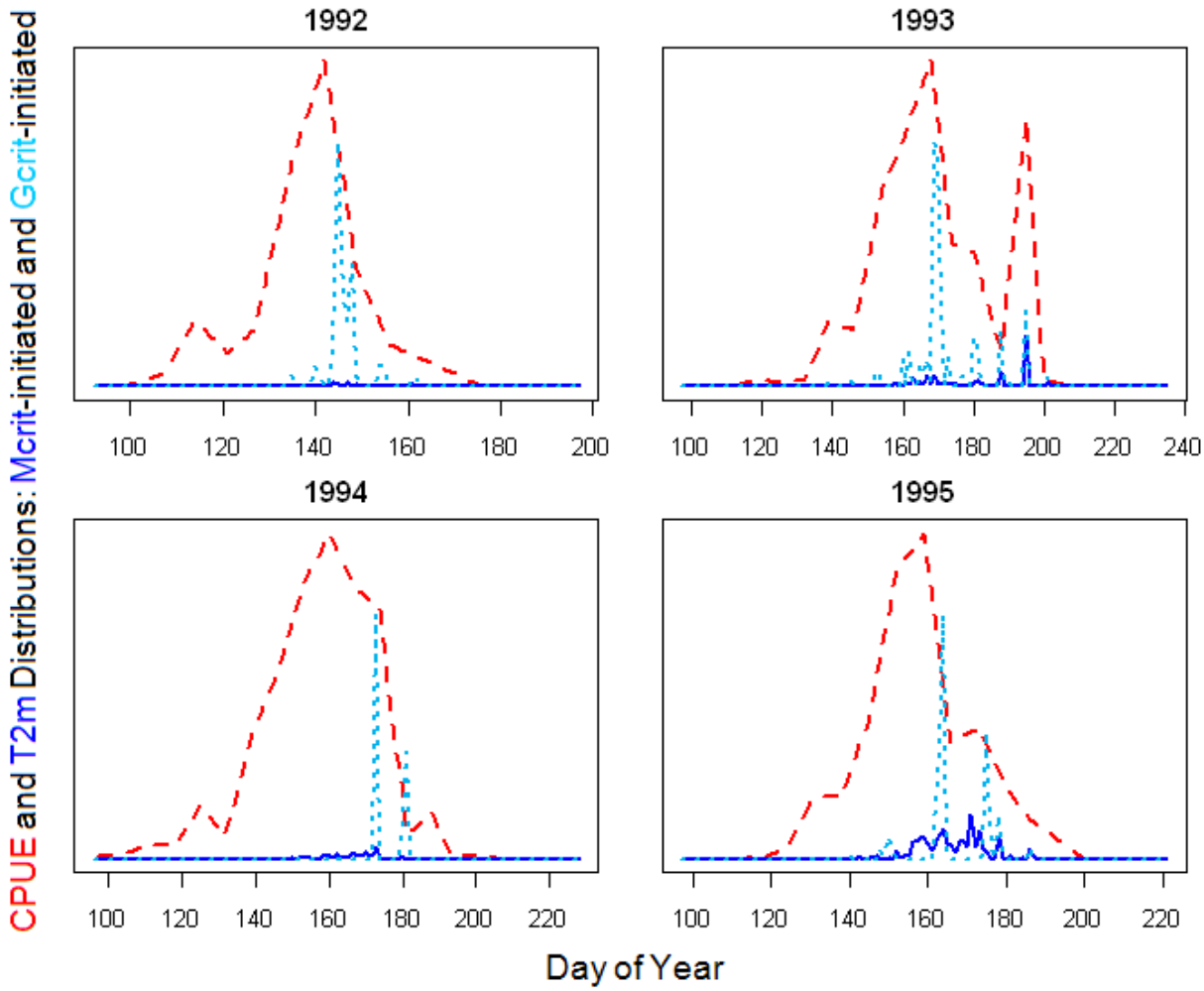

Yearly plots showing observed CPUE and modeled T2m distributions produced by the Mass & Growth version of the Mass-Growth model (mass and growth efficiency driven leaving, constant catchability) of the years 1992-1995. T2m is broken into separate distributions of fish that initiated migration due to growing larger than *Mcrit* and fish that left due to growth efficiency falling below *Gcrit*. The leaving distributions are proportional to each other, but not directly proportional to CPUE.

Figure 3.8

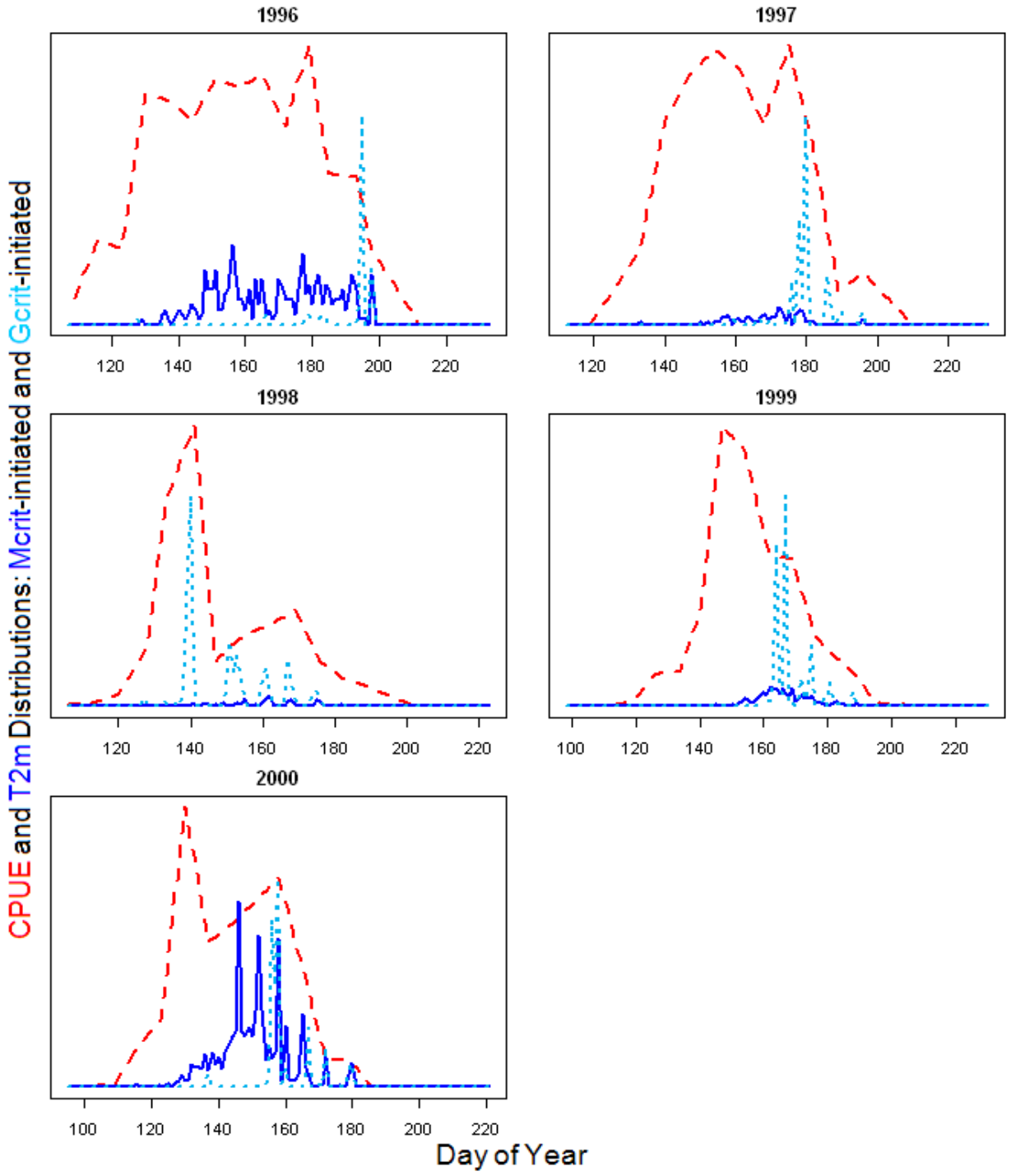

Yearly plots showing observed CPUE and modeled T2m distributions produced by the Mass & Growth version of the Mass-Growth model (mass and growth efficiency driven leaving, constant catchability) of the years 1996-2000.

Figure 3.9

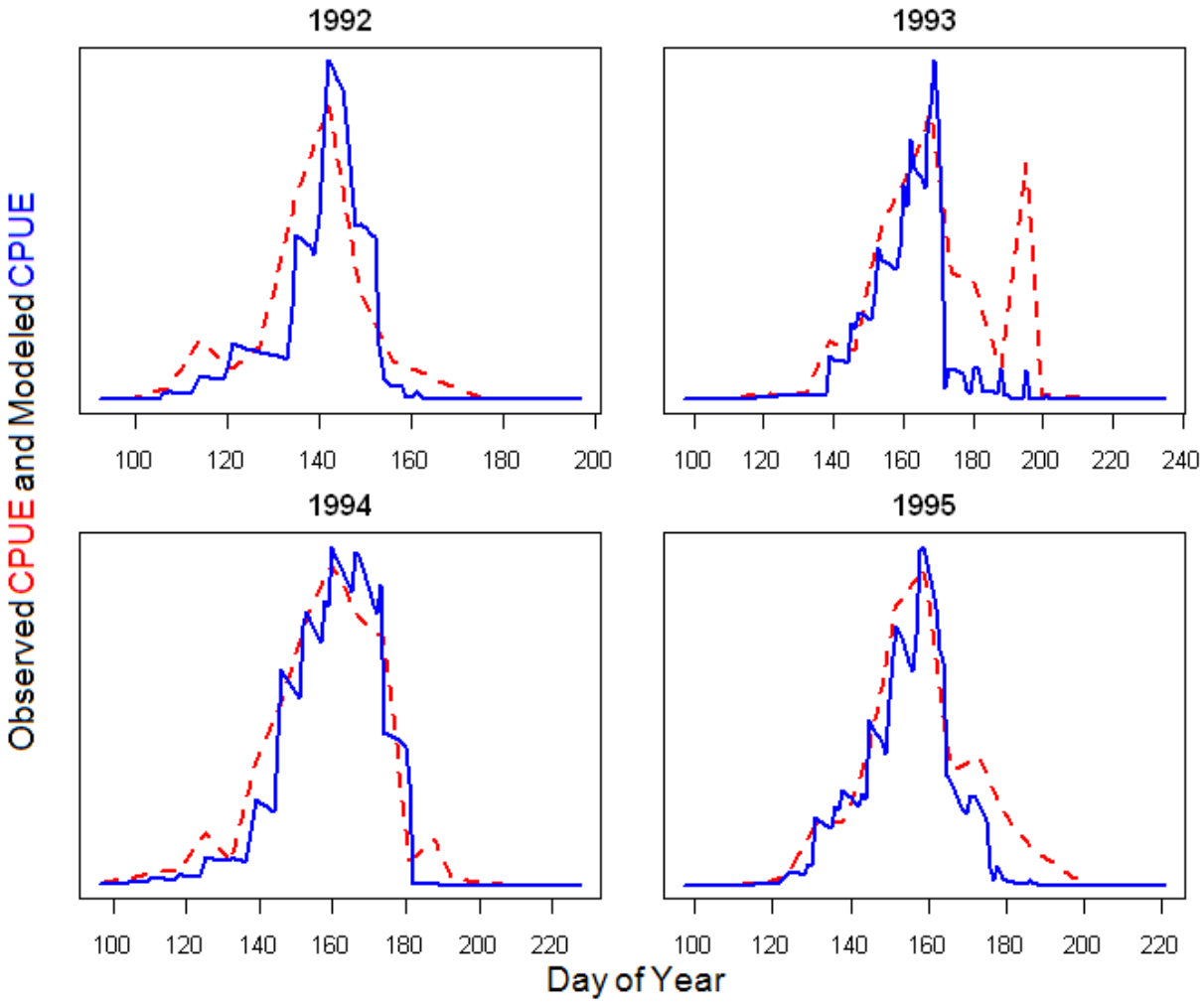

Yearly plots showing observed CPUE and modeled CPUE produced by the Mass, Growth & Catchability version of the Mass-Growth model (mass and growth efficiency driven leaving, mass varying catchability) for the years 1992-1995. Model parameters were estimated independently for each year via a maximum likelihood method. Modeled CPUE tracks observed CPUE fairly well in most years.

Figure 3.10

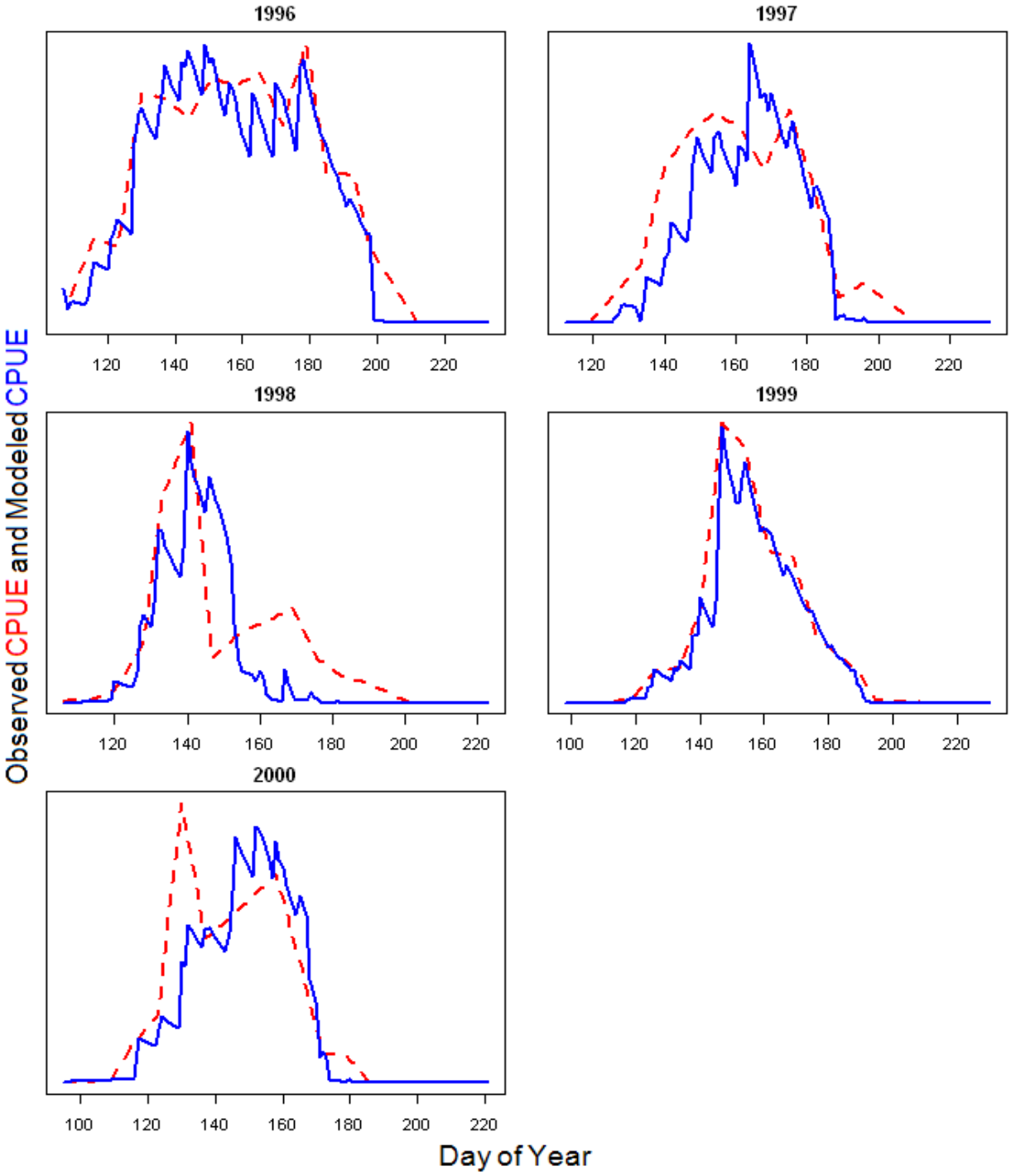

Yearly plots showing observed CPUE and modeled CPUE produced by the Mass, Growth & Catchability version of the Mass-Growth model (mass and growth efficiency driven leaving, mass varying catchability) for the years 1996-2000.

Figure 3.11

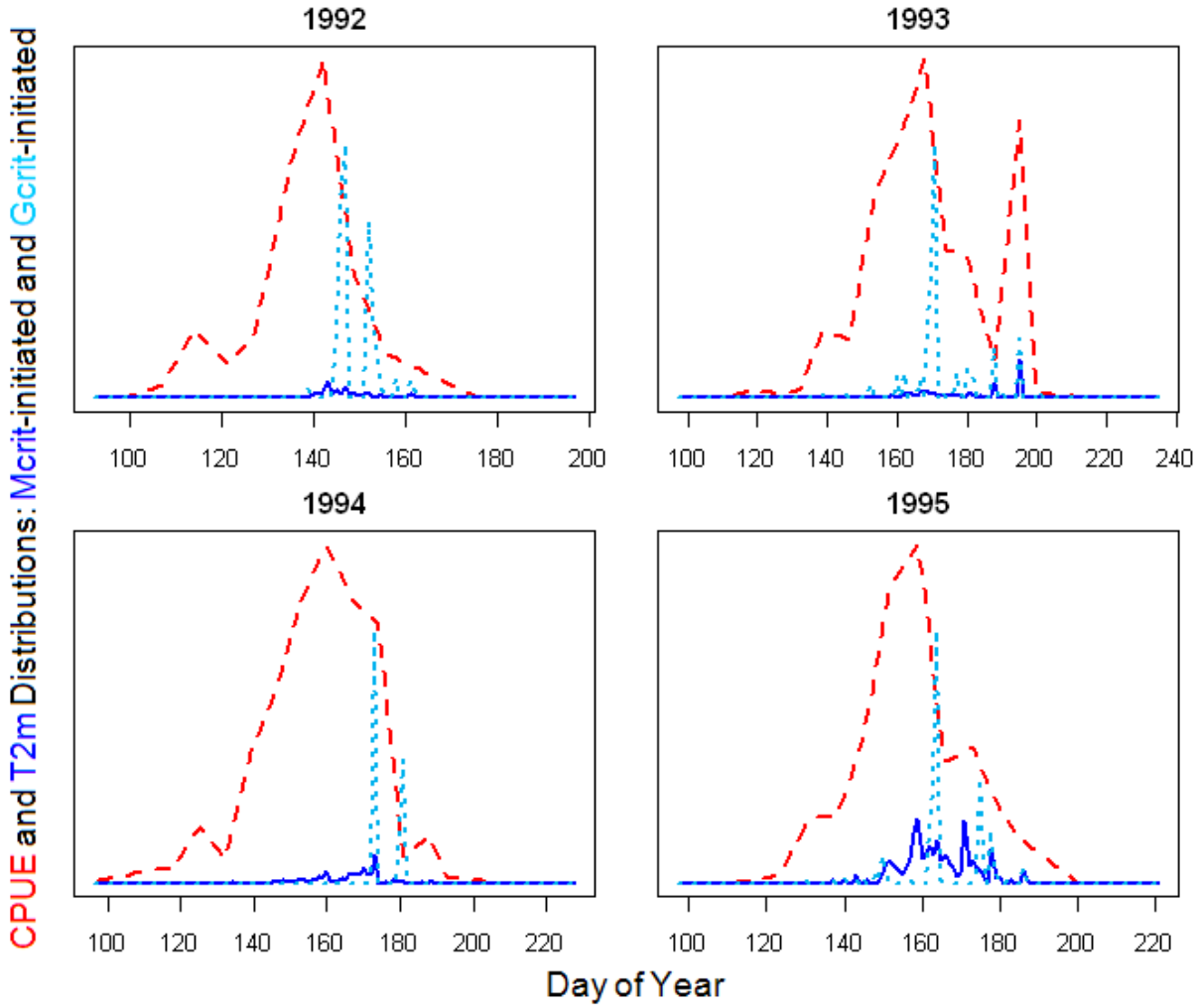

Yearly plots showing observed CPUE and modeled T2m distributions produced by the Mass, Growth & Catchability version of the Mass-Growth model (mass and growth efficiency driven leaving, mass varying catchability) for the years 1992-1995. T2m is broken into separate distributions of fish that initiated migration due to growing larger than *Mcrit* and fish that left due to growth efficiency falling below *Gcrit*. The leaving distributions are proportional to each other, but not directly proportional to CPUE; CPUE distributions are only shown to indicate where in the rearing season modeled leaving occurs.

Figure 3.12

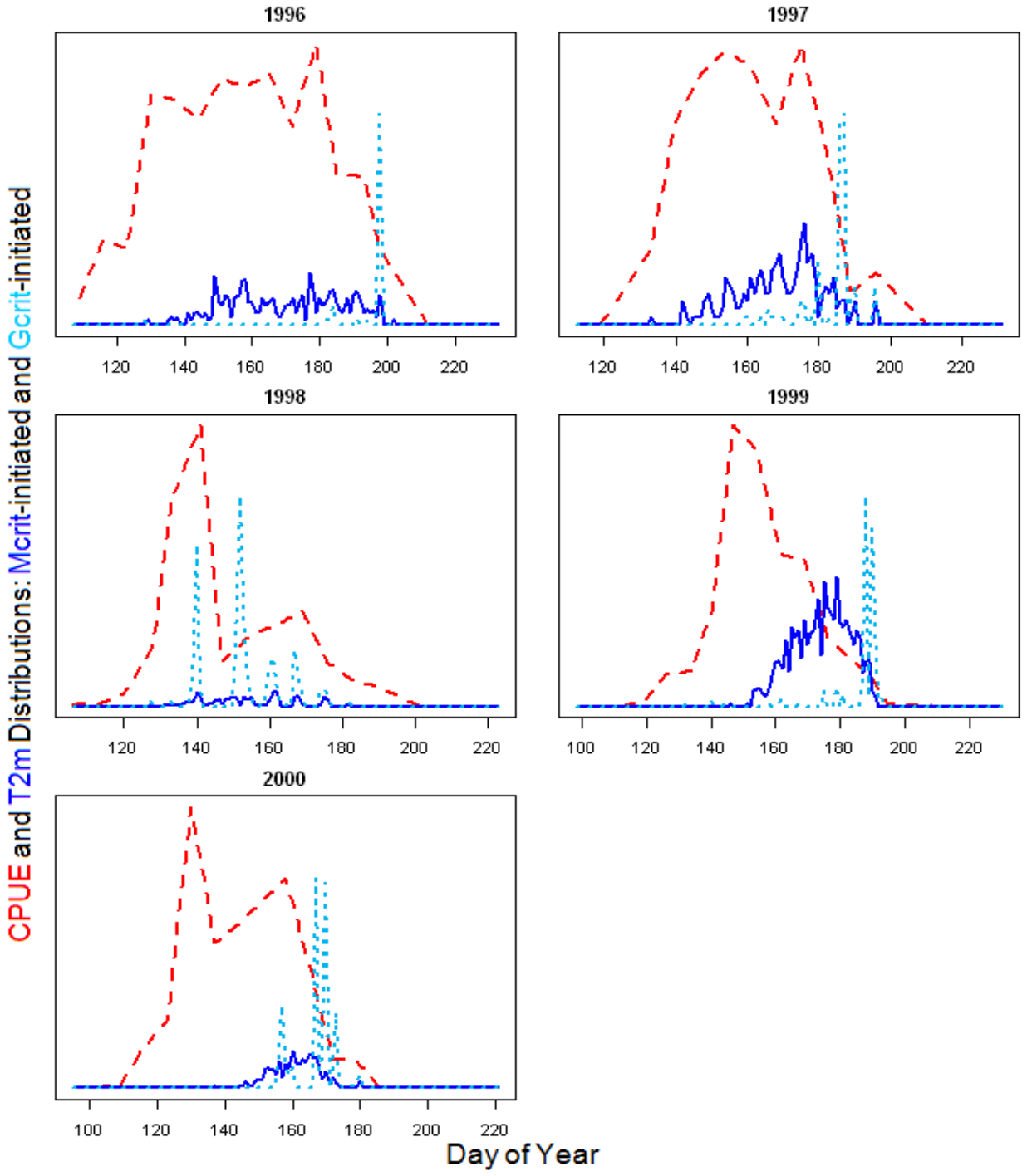

Yearly plots showing observed CPUE and modeled T2m distributions produced by the Mass, Growth & Catchability version of the Mass-Growth model (mass and growth efficiency driven leaving, mass varying catchability) for the years 1996-2000.

Figure 3.13

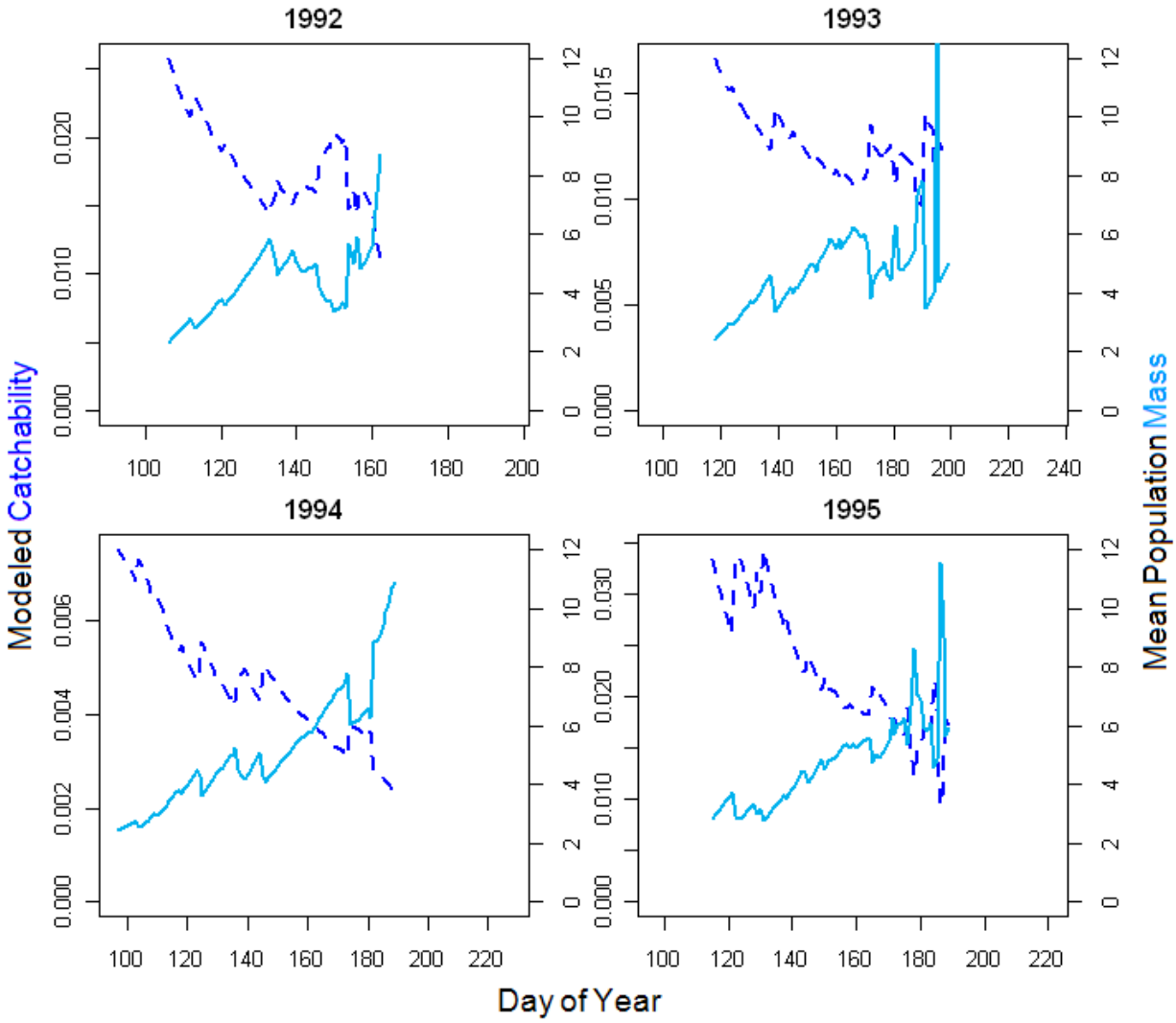

Yearly plots for 1992-1995 showing mean modeled Mass of fish present in the rearing habitat and modeled Catchability for the Mass, Growth & Catchability version of the Mass-Growth model. Catchability is a function of each year's individually fitted catchability coefficient *cc*, the mean population Mass, and the fitted exponential coefficient *B* (see section 3.2.6 and Table 3.7). Mean Mass tends to increase over the rearing season as fish grow, but it is also affected as fish are tagged and added into the population or initiate migration and leave the population. Large tagging or migration events can have large impacts on mean population Mass.

Figure 3.14

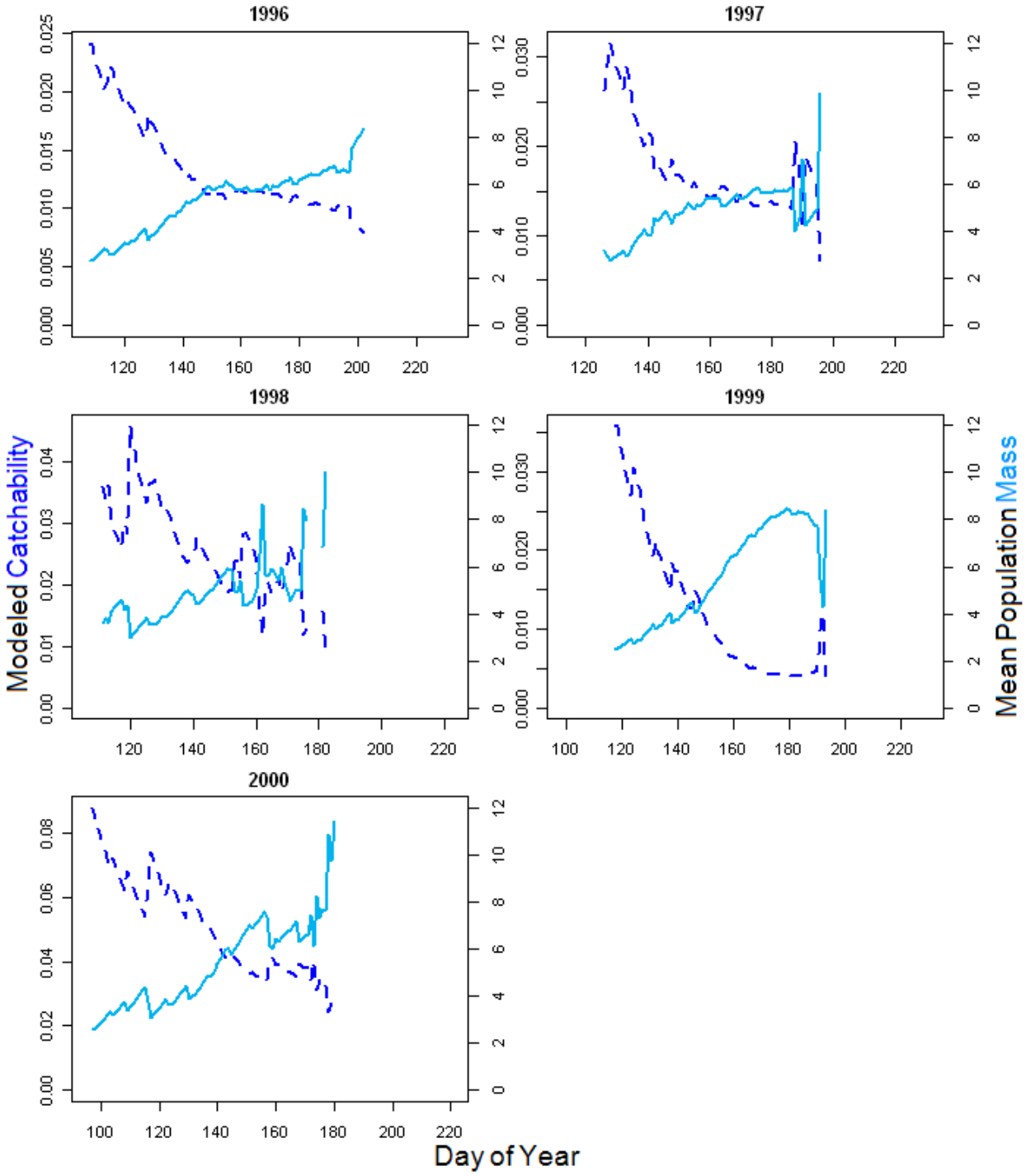

Yearly plots for 1996-2000 showing mean modeled Mass of fish present in the rearing habitat and modeled Catchability for the Mass, Growth & Catchability version of the Mass-Growth model.

Chapter 4: Age-Growth Model of Migration Initiation

4.1 Introduction

After the Thermal Wall model was found to be inadequate to explain migration and the Mass-Growth model produced reasonable predictions of migration, we undertook a third modeling project to compare to the results of the Mass-Growth model. This third model is a correlative model that regresses tagging and environmental data against recapture time T0:T1 in a generalized linear modeling framework, and then predicts T2 using modeled recapture time. We refer to this model as the 'Age-Growth' model and denote T2 predicted by this model as T2a. The two major steps in the creation of the Age-Growth model were the creation of the generalized linear model of recapture time T0:T1 and creating a theoretical framework to estimate T2a from modeled recapture time.

4.2 Methods

4.2.1 PIT Data

The Age-Growth model is a correlative model that extrapolates T2 from a generalized linear model of recapture time, the number of days between T0 and T1. The generalized linear model of T1 was fit using the records of 2,451 fish for which a T1 data point was present. These

fish are largely the same as those used to fit the Thermal Wall model, described in section 2.2.3 of this thesis. All 2,385 fish used to fit the Thermal Wall model are present in the 2,451 fish used to fit the Age-Growth model. Slightly more fish are used to fit the Age-Growth model because more data points were usable. Unlike the Thermal Wall model, the Age-Growth model only requires a T1 data point; no M1 data point is necessary. Four fish had a T1 data point with no length or mass recorded at recapture; these fish were unable to be used for the Thermal Wall model, but they were used for the Age-Growth model. Additionally, the Thermal Wall model required a fitted consumption rate for every fish. Since the Age-Growth model does not require fitted consumption rates, the 62 fish which were discarded in the Thermal Wall model are used to fit the Age-Growth model.

4.2.2 Generalized Linear Model of Recapture Date

The first component of the Age-Growth model is a generalized linear model that predicts the number of days between tagging and recapture T0:T1 using environmental data and tagging data from the PIT tag dataset. The goal of this model was to produce the best prediction of recapture time possible using only data available from the tagging data point. Thus, while the model is fitted using the records of fish for which a T1 data point is present, it will be capable of predicting recapture time for fish with only a T0 and M0 data point, along with environmental data.

To determine the error distribution to use for the generalized linear model, we examined the characteristics of the data. On an individual basis, recapture of tagged fish follows a Poisson process. Each fish is tagged on date T0 and released back into the river; the fish then remains in the rearing habitat until the initiation of migration at unknown date T2. During the period T0-T2,

on any given day, sampling may occur at the tagged fish's location, and if sampling occurs, the fish may be recaptured, producing a T1 data point. Thus, for a given day *i*, the probability of a fish being recaptured is:

$$\mathrm{P_r} = P_s \times P_c \qquad [4.1]$$

In this formulation, $\mathrm{P_r}$ is the probability of recapture, P_s is the probability of sampling occurring, and P_c is the probability a fish is captured if sampling occurs. If P_s is constant over time and P_c does not vary according to individual fish characteristics, then recapture follows a homogenous Poisson process; if these probabilities vary over time or between individual fish, then recapture follows a non-homogenous Poisson process.

While a complete record of all sampling events is not available, tagging and recapture data displays fairly regular patterns. According to Connor et al. (2003), some sampling sites were sampled on a regular, weekly basis, while other sites were sampled on an irregular basis. The bulk of tagging and recapture data comes from sites sampled on a regular basis. Plots of the distribution of tagging events (Figures 4.1, 4.2) by day of year and river kilometer sampled display regular, weekly patterns in sampling. There are some departures from the weekly sampling schedule- particularly in the first three years of data, and not all regularly sampled sites are sampled on the same schedule, but overall the pattern of tagging data suggests regularity in sampling. Additionally, a histogram of recapture time T0:T1 (Figure 4.3) displays distinct peaks at 7, 14, 21, and 28 days, displaying that the bulk of recaptured fish are recaptured at sites with a weekly sampling schedule. For this reason, we assume that P_s remains uniform across time. As for P_c, we assume that it remains constant for all fish. Though the mass-varying catchability coefficient of the Mass-Growth model estimated a negative relationship between individual fish

mass and catchability, assuming uniform catchability greatly simplifies the Age-Growth model, as individual fish mass then does not need to be modeled.

Since recapture follows a Poisson process, the natural error distribution to use for the generalized linear model was the Poisson distribution. The first generalized linear model we created used the Poisson distribution with a log link to regress day of recapture T1 against tag day T0, mass at tagging M0, length at tagging L0, CPUE at the tagging location on the tag date, daily mean temperature of the Snake River on the tag date, and a year effect. Interaction terms between tag day and length at tagging, CPUE, and temperature were included as well as squared terms for length at tagging, CPUE and temperature. Table 4.1 provides a summary of parameter estimates and significance and Table 4.2 provides an analysis of deviance table for the full model. A parsimonious reduced model was then generated from this full model via sequential deletion. The least explanatory predictor was removed from the model if removal did not increase the AIC score of the model by more than 2, then the model was re-fitted and the new least explanatory predictor examined. Once removal of the least explanatory predictor would increase the AIC of the model by more than 2, we determined that a parsimonious model had been reached. The parameters removed from the full model were, in sequence: L0 squared term, T0:L0 interaction term. Table 4.3 provides a summary of parameter estimates and significance and Table 4.4 provides an analysis of deviance table for the reduced model.

There was concern that the Poisson model of recapture time was inadequate because the Poisson distribution did not fit observed recapture time well. The mean of the Poisson distribution is also the variance of the Poisson distribution; observed recapture time is over-distributed with respect to the Poisson distribution. The mean recapture time is 10.34 days, while the variance in observed recapture time is 40.89 days. Since the negative binomial distribution is

often used in place of the Poisson distribution for over-distributed statistics, we compared the distributions of a maximum likelihood negative binomial fit and Poisson fit of observed recapture time. The Poisson fit (Figure 4.3) clearly does not adequately match the variance of the observed recapture time distribution (Figures 4.1, 4.2); the Poisson fit underpredicts the number of short recapture times in the 1-5 day range and the tail of the observed distribution in the 20-40 day range. In contrast, the negative binomial distribution (Figure 4.4) fits the early and later portions of the observed recapture time distribution much better.

We then created a second generalized linear model of recapture time using the negative binomial error distribution with a log link and compared the AIC score of the model to the AIC of the Poisson log-link generalized linear model. The full negative binomial model used the same set of predictors as the full Poisson model. Tables 4.5 and 4.6 provide a summary of parameter estimates, significance, and analysis of deviance of the full model. A reduced, parsimonious negative binomial model was then generated from the full model via the same sequential deletion process used for the Poisson model. The predictors removed were, in sequence: L0 squared term, T0:L0 interaction term, CPUE squared term, temperature squared term, T0:temperature interaction term, and temperature. Tables 4.7 and 4.8 provide a summary of parameter estimates, significance, and analysis of deviance of the reduced model. The AIC scores of both the full and reduced negative binomial models are significantly lower than those of the respective Poisson models. The full negative binomial model has an AIC of 14776.9 compared to an AIC of 16976.4 for the full Poisson model; the reduced models have slightly lower AIC scores, with 14773.4 for the reduced negative binomial model and 16973.8 for the reduced Poisson model. Since it has the lowest AIC score, uses the error distribution that best fits the data, and has

statistically significant parameter estimates for all predictors, we used the reduced negative binomial generalized linear model for the Age-Growth model.

4.2.3 Linking Recapture Time and Residence Time

Once a satisfactory model of recapture time was found, it was necessary to create a theoretical framework to relate recapture time to residence time. As discussed in section 4.2.2, a fish's residence time is defined as the number of days between tagging T0, known from data, and the date the fish initiates migration T2, which is unknown. Recapture follows a Poisson process where a fish is subject to a probability of being recaptured for each day of the fish's residence time. As described in section 4.2.2, we assume that the probability of recapture is uniform with time and identical for all fish. For a single sampling event, the day of recapture could be located at any date within the residence time, resulting in a recapture time ranging from one day to equivalent to residence time. This means that for an individual sampling event, the relationship between recapture time and residence time is unknown. However, the assumption of uniform probability of recapture means that as the number of hypothetical sampling events becomes large, the mean recapture time approaches one half of residence time.

Unfortunately, this only holds if there is no variation in residence time among fish. Variation in residence time introduces bias, as fish with longer residence times are more likely to be recaptured than fish with shorter residence times. A fish's probability of being recaptured follows the following relationship:

$$P_{T1} = 1 - (1 - P_r)^R \quad [4.2]$$

In this formulation, P_{T1} is the probability a fish is recaptured at least once during its residence time and a T1 data point is generated, P_r is the probability that a fish is recaptured on any given

day, and R is the length of the fish's residence time in days. As residence time R increases, the probability a fish is recaptured P_{T1} also increases. This means that there is some amount of bias in the relationship between observed recapture times and the true population mean residence time. While the mean of observed recapture times approaches one half of the true residence times of those recaptured fish, the recaptured fish are a biased subset of the total population, with a mean residence time larger than the mean residence time of the population at large.

To address this issue of bias, we applied theory from a classical study in probability and queuing theory on waiting time paradoxes (Feller 1966). The original theory arose to address the issue of bias in expected residual waiting time for customers of an arrival process. For an arrival process such as buses arriving at a bus stop, a passenger's residual waiting time is the amount of time between when the passenger arrives at the stop and when the next bus arrives. If the passenger's arrival time is independent of the bus arrival time, then for a single interarrival period, the mean expected waiting time is one-half the interarrival period; the passenger could arrive at any time between the two bus arrivals, and over many samples the waiting time will average to one-half the length of the interval. The paradox arises when examining more than one interarrival period when interarrival periods are not uniform. Over a given time interval, the probability of the passenger's arrival is uniform, but if the length of the interarrival periods is not the same, then the passenger is more likely to arrive at the stop during a long interarrival period than a short interarrival period. The result is that longer interarrival periods contribute more to mean waiting time and mean waiting time is greater than one-half the mean interarrival period length (Feller 1966).

To illustrate how we apply this method to recapture of fish and approximate this bias, we treat the residence and potential recapture of an individual fish as a triangular surface, and the

residence and recapture of multiple fish as a sawtooth curve (Figure 4.6). For an individual fish, residence time is presented on the x-axis beginning with tagging T0 at the origin and ending with initiation of migration T2 at *R*. This residence time of a single fish approximates a single interarrival period from an arrival process. Recapture time is presented on the y-axis; as recapture at any date within the residence time produces a recapture time equivalent to the number of days to that point, potential recapture time follows a one-to-one increasing relationship with a maximum potential recapture time equal to the length of the residence time, *R*. This is the opposite of residual waiting time; rather than counting from the passenger arrival time to the end of the interarrival period, we count from the beginning of the residence period to the recapture time; however, the end result is still comparable, just mirrored on the bus arrival/ fish residence time axis. We then place the residence times of multiple fish in sequence, producing a sawtooth curve of potential recapture time. This approximates the curve of residual waiting time for an arrival process over multiple arrival periods; however, unlike the arrival process example, the x-axis no longer directly relates to time. Instead, the x-axis becomes an abstract representation of the population of tagged fish. Here is where the assumptions of uniformity of sampling effort and uniformity of catchability among fish become important; these assumptions mean that any single sampling event has a uniform probability of occurring at any point on the fish-day axis of the population sawtooth curve. The mean potential recapture time $\bar{r}$ then becomes the average height of the sawtooth curve; as the number of actual sampling events becomes large, realized mean recapture time will approach $\bar{r}$. The average height of the sawtooth curve is described by the following equation:

$$\bar{r} = \frac{1}{\sum R} \sum_{i=1}^{n} \frac{1}{2} {R_i}^2 \qquad [4.3]$$

In this formulation, $\bar{r}$ is the mean recapture time, R_i is the residence time of a fish *i*, *n* is the number of fish in the population, and ΣR is the sum of all residence times, the total number of fish-days in the population. Mean residence time $\bar{R}$ is equal to $\Sigma R/n$, yielding:

$$\bar{r} = \frac{1}{\bar{R}n}\sum_{i=1}^{n}\frac{1}{2}R_i{}^2 \quad [4.4]$$

This formula reduces to:

$$\bar{r} = \frac{1}{2}\frac{\overline{R^2}}{\bar{R}} \quad [4.5]$$

In this formulation, $\bar{r}$ is mean recapture time; $\overline{R^2}$ is mean squared residence time, and $\bar{R}$ is mean residence time. Mean squared residence time is equal to the variance in residence time plus mean residence time squared, yielding:

$$\bar{r} = \frac{1}{2}\frac{Var(R)+\bar{R}^2}{\bar{R}} \quad [4.6]$$

Thusly, the relationship between mean recapture time and mean residence time depends on the variance in residence time. As discussed above, if all residence times are equal, then the variance in residence time is zero, and mean recapture time is equal to one half of mean residence time. As variance in residence time increases, mean recapture time approaches mean residence time.

Though true residence time is unknown, we estimated some potential relationships between recapture time and residence time by assuming a hypothetical distribution of residence times equal to observed recapture times multiplied by two. As the mean observed recapture time is 10.34 days, the hypothetical residence time distribution has a mean of 20.68 days and a variance of 163.51. We then used the MASS library in the statistical computing language R to produce maximum likelihood fits of this hypothetical residence time distribution to both Poisson and negative binomial distributions. We then used the mean and variance predicted by the fits and equation 4.6 to produce predictions of mean recapture time under each scenario. Table 4.9

presents the fitted parameter values, the resulting predicted mean recapture time, and the relationship between predicted mean recapture time and hypothetical mean residence time. The Poisson and negative binomial distributions both underpredict the variance in hypothetical residence time, but the negative binomial distribution does so by much less. The Poisson fit predicts low variance, and thus predicts that mean residence time will be only slightly less than twice the mean recapture time. The negative binomial fit predicts much larger variance, resulting in the prediction that mean residence time is 1.51 times longer than mean recapture time.

While the true residence time distribution is unknown, we assume that initiation of migration can be represented as a Poisson process, and thus the Poisson family of distributions is appropriate to fit the data. Since observed recapture time is overdistributed with respect to the Poisson distribution, we assume that residence time likely is as well. For this reason, we decided that the negative binomial model likely provides the best estimate of the relationship between observed mean recapture time and true mean residence time. We combine this relationship with the generalized linear model of recapture time to predict residence time for individual fish via the following relationship:

$$R_i = 1.51 \times GLM(T0, L0, M0, T0\ CPUE, Year) \quad [4.7]$$

In this formulation, R_i is the predicted residence time for an individual fish, and *GLM()* is the reduced log-link negative binomial model of recapture time described in Tables 4.7 and 4.8. We recognize that using the 1.51 conversion factor estimated between mean recapture time and mean residence time does not necessarily predict individual residence time well, but we assume that the sample sizes of our data are large enough that it will be sufficient to represent the distributional properties of true residence time. We then use predicted residence time R_i and

known date of tagging $T0_i$ to yield an individual prediction of date of migration initiation $T2a_i$ via the following relationship:

$$T2a_i = T0_i + R_i \quad [4.8]$$

Equations 4.7 and 4.8 together comprise the Age-Growth model of migration initiation.

4.2.4 Validating the Age-Growth Model

To validate the Age-Growth model, we use T2a predicted by the Age-Growth model to predict CPUE and compare modeled CPUE distributions to observed CPUE. Similarly to the Mass-Growth model, we use the records of all fish tagged at the sites for which CPUE data is available. This ensures that we are comparing model predictions and data from the same group of fish, and also makes the model results directly comparable to results from the Mass-Growth model. We use the modeling framework presented in section 3.2.2 of this thesis to track the number of tagged fish in the river. This framework has the following structure:

$$N_i = N_{i-1} + T_i - L_i \quad [4.9]$$

In this formulation, N_i is the number of tagged fish in the rearing habitat on day i, N_{i-1} is the number of tagged fish in the rearing habitat on the previous day, T_i is the number of fish that are tagged and released back into the rearing habitat on day i, and L_i is the number of tagged fish that initiate migration and leave the rearing habitat on day i. T_i is generated from the tagging dates T0 from data, and L_i is generated from T2a predicted for each fish using the Age-Growth model. N_i, the number of tagged fish in the river, relates to CPUE via the following equation:

$$CPUE_i = N_i \times cc \quad [4.10]$$

In this formulation, cc is a catchability constant describing how the population of fish in the rearing habitat relates to catch per unit effort. Since we assume that catchability is constant for

all fish in the Age-Growth model, we did not include a mass-varying term in catchability like in the Mass-Growth model.

We used a maximum likelihood method to fit modeled CPUE to observed CPUE. We assumed that the deviations between observed CPUE and CPUE predicted by our model come from a Gaussian distribution with mean 0 and variance σ. Thus, for our model:

$$CPUE_i = N_i \times cc + \varepsilon \quad [4.11]$$

For each day *i*, a deviation ε between modeled and observed CPUE is generated. For each deviation ε, the likelihood that the deviation came from Gaussian distribution with mean 0 and variance σ is then calculated. The negative log of these likelihoods is then taken, to yield negative log likelihood. Due to the log transform, these negative log likelihoods are then additive; the sum of the negative log likelihoods for each day *i* yields a single estimate of negative log likelihood for a given set of parameters. The negative log likelihood is then minimized via an iterative parameter estimation process using the statistical computing language R. For the Age-Growth model, since the leaving function is wholly predetermined by the Age-Growth model of migration initiation, the catchability constant *cc* and the variance parameter σ are the only free parameters fitted in the maximum likelihood process.

4.3 Results

Table 4.10 presents the yearly predictions of the Age-Growth model. For most years, mean modeled residence time was around 15 days. Shorter residence time was modeled in 1992, with a mean of 11.45 days, and longer residence time was modeled in 1997 and 2000, with mean residence times of 23.52 days and 19.80 days respectively. Though mean residence time was quite consistent, mean T2a displayed more variation between years. More variation in T2a was

not unexpected; the relative timing of the rearing season shifts from year to year due to differences in temperature regime that affect growth and development and variation in spawning date (Quinn 2005). Fitted catchability coefficient was very consistent, with the exception of 2000; catchability coefficients vary from 0.0052 to 0.0144 excluding 2000. Fitted σ is small in most years, indicating a good fit. Fitted σ is larger in 1998 and 2000, indicating poorer fits of observed CPUE in those years.

In most years, the Age-Growth model produces respectable fits of observed CPUE data (Figures 4.7, 4.8). The closeness of the fits is reflected in the low σ fitted in most years. However, similarly to the Mass-Growth model without the mass-varying catchability coefficient, the Age-Growth model tends to underpredict CPUE early in the rearing season. This early underprediction is visible in the modeled CPUE distributions for 1992, 1997, 1998, and 2000. In 1992 and 1998 in particular, the modeled CPUE distribution looks like it is shaped similarly to the observed CPUE distribution, but lagging behind by a week or more. In most years, the fits produced by the Age-Growth model are comparable to fits produced by the Mass-Growth model with both mass and growth efficiency driven leaving (Figures 3.9, 3.10). The primary difference between the fits produced by the two models lies in the fact that the Mass-Growth model tends to have sudden drops in modeled CPUE resulting from surges in growth-efficiency driven leaving; while modeled CPUE distributions produced by the Age-Growth model decline much more gradually. This difference is most evident in the fits for 1993, 1995, and 1997 (Figures 3.9, 3.10 and 4.7, 4.8); in all these years, the Mass-Growth model predicts sharp declines to zero in CPUE, while the Age-Growth model predicts much more gradual declines with an evident tail in modeled CPUE.

The reasons for this difference in fits become evident when examining distributions of initiation of migration produced by the two models. The distribution of T2a predicted by the Age-Growth model tends to be gradual and fairly dispersed (Figures 4.9, 4.10). Predicted T2a distributions tend to start near the peak of observed CPUE distributions in most years, and the last modeled T2a occurs at nearly the same time as observed CPUE distributions reach zero in every year except 1994. These distributions of T2a strongly resemble distributions of mass-driven leaving predicted by the Mass-Growth model (Figures 3.11, 3.12); in every year where enough fish left via the mass threshold to produce a visible distribution, the location and characteristics of modeled T2m are quite comparable to T2a. While distributions of T2a more closely resemble the dispersed leaving produced by mass-driven leaving than the densely packed growth-efficiency driven leaving, a significant amount of spikiness is still observed in the distributions on T2a. Combined with stratified sampling, this results in significant spikiness in the curves of the modeled CPUE where observed CPUE displays much more monotonic properties; this is most obvious in the fits for 1994, 1996 and 1997.

4.4 Discussion

Overall, the Age-Growth model was successful at fitting observed data. To be confident that the model is producing accurate fits, we determined that modeled leaving should primarily coincide with observed declines in CPUE. We also expect few migrants early in the rearing season, and the model should not predict fish to remain in the rearing habitat beyond when fish are no longer observed there. The Age-Growth model's predictions definitely meet all of these criteria, meaning that the mechanics of the model merit further inspection.

However, as a correlative regression model, the conclusions that can be drawn from the Age-Growth model are unfortunately less clear than those that can be drawn from a mechanistic model like the Mass-Growth model. In particular, the assumptions made in the process of creating the Age-Growth model limit the ability to be confident in the model's predictions on an individual basis. The relationship established between mean recapture time and mean residence time is just that; a relationship between the means of the relevant statistics. Thusly, we examine the distributional characteristics of the resulting predictions rather than aspects of predictions for individual fish.

The negative binomial generalized linear model of recapture time is the primary determinant of modeled T2a. Most of the coefficients estimated in the model can be extrapolated fairly easily to a potential process (Table 4.7). There is a negative relationship between tag date T0 and recapture time; this makes sense, as tagging of fish is a random process. Later in the rearing season, most fish will be closer on average to their migration date, and thus the expected residual residence time of fish captured and tagged later is shorter. Interestingly, opposite relationships are fitted between length at tagging L0 and mass at tagging M0, both of which are measurements of fish size. The magnitude of the coefficient fitted for M0 is larger, but the magnitude of the measurement used for fish length (millimeters) scales much more rapidly than the metric for mass (grams), so the overall relationship between fish size and residence time is driven by the negative coefficient fitted for L0. This relationship makes sense in context of mass-driven leaving; fish that are larger at tagging will grow into a mass threshold more quickly, and would thus have less residual residence time. The difference in signs between the L0 and M0 coefficients likely captures nonlinearity in the fish size-residence time relationship; however, a squared term for L0 was included in the full model for just this possibility, so it is perplexing

why M0 was retained but L0^2 was not. The most likely explanation is that M0 contains some additional information that L0^2 does not; as explained in section 2.2.1 of this thesis, about 30% of all fish have both a mass and a length recorded at tagging. For the remainder of the fish, M0 is estimated directly from L0 via the weight-length relationship presented in section 2.2.3 and M0 offers no advantage over L0^2, but for the 30% of the fish which do have a M0 data point, it offers additional information about the condition of the fish.

A positive relationship is fitted between CPUE at tagging and modeled residence time (Table 4.7). This makes sense in the context of density dependence; if many fish are present in the rearing habitat, then competition for resources may restrict growth, and thusly delay migration since fish take longer to become bioenergetically prepared to migrate. A negative interaction is fitted between CPUE and tag date, suggesting that the importance of density dependence declines later in the tagging season. This could be because density dependent effects decline later in the season as fish leave the rearing habitat. It could also be an impact of our hypothesized growth efficiency driven leaving; in the fits produced by the Mass-Growth model, it was shown that growth efficiency driven leaving tends to impact all fish similarly regardless of their mass, and it tends to act as a termination factor driving fish out of the rearing habitat at the end of the growing season. Thusly, late in the season, any impacts of density dependent growth restriction would become nullified, as fish are forced to leave regardless of how quickly they are growing.

4.5 Chapter 4 Tables

Table 4.1

Summary of the full log-link Poisson model of recapture time with all predictors. T0 is the day a fish was tagged, L0 is the fish's length on the tag day in millimeters, L0^2 is a squared term of length, M0 is the fish's mass on the tag day in grams, T0 CPUE is the CPUE at the tag site on the tag date, CPUE^2 is a squared term of CPUE, T0 Temp is the daily mean temperature of the Snake River on the tag date, and Temp^2 is a squared term of temperature. Year 1993-2000 are year effects, estimated as offsets from the base year (1992). T0:L0, T0:CPUE, and T0:Temp are interaction terms. All parameter estimates except T0, L0^2, T0 Temp, and T0:L0 are significantly different from zero at the 0.05 level.

Predictor	Estimate	Std. Error	T Statistic	P
Y-Intercept	3.919	0.768	5.10	3.4e-7
T0	0.00777	0.00599	1.30	0.19
L0	-0.0343	0.0128	-2.68	0.0073
L0^2	-0.0000101	0.0000843	-0.12	0.90
M0	0.0468	0.0184	2.54	0.011
T0 CPUE	0.0301	0.00523	5.73	9.9e-9
CPUE^2	-0.0000501	0.0000155	-3.24	0.0012
T0 Temp	-0.0337	0.0645	-0.52	0.60
Temp^2	0.0102	0.00309	3.30	0.00098
Year (1993)	0.597	0.0559	10.67	< 2e-16
Year (1994)	0.463	0.0501	9.25	< 2e-16
Year (1995)	0.515	0.0534	9.63	< 2e-16
Year (1996)	0.529	0.0647	8.18	2.7e-16
Year (1997)	0.543	0.0562	9.66	< 2e-16
Year (1998)	0.513	0.0527	9.74	< 2e-16
Year (1999)	0.435	0.0562	7.73	1.1e-14
Year (2000)	0.792	0.0591	11.93	< 2e-16
T0:L0	0.0000792	0.0000680	1.17	0.24
T0:CPUE	-0.000176	0.0000352	-4.99	6.2e-7
T0:Temp	-0.00159	0.000398	-4.01	6.2e-5
			Null Deviance: 8494.4	**Degrees of Freedom: 2450**
			Residual Deviance: 7071.1	**Degrees of Freedom: 2431**
			AIC: 16976.4	**Parameters: 20**

Table 4.2

Analysis of deviance table of the full log-link Poisson model of recapture time with all predictors. All predictors combined explain 1423.3 of 8494.4 total deviance.

Predictor	D.F.	Deviance	Residual D.F.	Residual Deviance
Null			2450	8494.4
T0	1	822.9	2449	7671.6
L0	1	262.0	2448	7409.6
L0^2	1	3.9	2447	7405.7
M0	1	4.4	2446	7401.2
T0 CPUE	1	94.9	2445	7306.3
CPUE^2	1	7.3	2444	7299.0
T0 Temp	1	7.6	2443	7291.4
Temp^2	1	3.9	2443	7287.5
Year	8	179.2	2434	7108.3
T0:L0	1	0.0241	2433	7108.2
T0:CPUE	1	21.0	2432	7087.2
T0:Temp	1	16.1	2431	7071.1

Table 4.3

Summary of the reduced log-link Poisson model of recapture time. T0 is the day a fish was tagged, L0 is the fish's length on the tag day in millimeters, M0 is the fish's mass on the tag day in grams, T0 CPUE is the CPUE at the tag site on the tag date, CPUE^2 is a squared term of CPUE, T0 Temp is the daily mean temperature of the Snake River on the tag date, and Temp^2 is a squared term of temperature. Year 1993-2000 are year effects, estimated as offsets from the base year (1992). T0:CPUE, and T0:Temp are interaction terms. All parameter estimates except T0 Temp are significantly different from zero at the 0.05 level.

Predictor	Estimate	Std. Error	T Statistic	P
Y-Intercept	3.419	0.592	5.77	7.8e-9
T0	0.0114	0.00510	2.24	0.025
L0	-0.0240	0.00293	-8.20	2.5e-16
M0	0.0488	0.0138	3.55	0.00039
T0 CPUE	0.0293	0.00522	5.61	2.0e-8
CPUE^2	-0.0000488	0.0000155	-3.15	0.0016
T0 Temp	-0.0514	0.0626	-0.82	0.41
Temp^2	0.0101	0.00309	3.28	0.0010
Year (1993)	0.597	0.0559	10.67	< 2e-16
Year (1994)	0.463	0.0500	9.25	< 2e-16
Year (1995)	0.515	0.0534	9.63	< 2e-16
Year (1996)	0.526	0.0646	8.14	4.0e-16
Year (1997)	0.542	0.0562	9.65	< 2e-16
Year (1998)	0.515	0.0527	9.77	< 2e-16
Year (1999)	0.436	0.0562	7.75	9.3e-15
Year (2000)	0.712	0.0587	12.13	< 2e-16
T0:CPUE	-0.000172	0.0000352	-4.90	9.5e-7
T0:Temp	-0.00147	0.000382	-3.83	0.00013
			Null Deviance: 8494.4	**Degrees of Freedom: 2450**
			Residual Deviance: 7072.5	**Degrees of Freedom: 2433**
			AIC: 16973.8	**Parameters: 18**

Table 4.4

Analysis of deviance table of the reduced log-link Poisson model of recapture time. All predictors combined explain 1421.9 of 8494.4 total deviance. The removal of L0^2 and T0:L0 results in M0 explaining more deviance than in the full model, and T0:Temp slightly less.

Predictor	D.F.	Deviance	Residual D.F.	Residual Deviance
Null			2450	8494.4
T0	1	822.9	2449	7671.6
L0	1	262.0	2448	7409.6
M0	1	8.3	2447	7401.3
T0 CPUE	1	94.8	2446	7306.5
CPUE^2	1	7.4	2445	7299.1
T0 Temp	1	7.6	2444	7291.6
Temp^2	1	3.9	2443	7287.7
Year	8	179.4	2435	7108.3
T0:CPUE	1	21.0	2434	7087.2
T0:Temp	1	14.7	2433	7072.5

Table 4.5

Summary of the full log-link negative binomial model of recapture time with all predictors. T0 is the day a fish was tagged, L0 is the fish's length on the tag day in millimeters, L0^2 is a squared term of length, M0 is the fish's mass on the tag day in grams, T0 CPUE is the CPUE at the tag site on the tag date, CPUE^2 is a squared term of CPUE, T0 Temp is the daily mean temperature of the Snake River on the tag date, and Temp^2 is a squared term of temperature. Year 1993-2000 are year effects, estimated as offsets from the base year (1992). T0:L0, T0:CPUE, and T0:Temp are interaction terms. The intercept, T0 CPUE, all year effects, and the T0:CPUE and T0:Temp interaction terms are significantly different from zero at the 0.05 level.

Predictor	Estimate	Std. Error	z Statistic	P
Y-Intercept	3.784	1.318	2.87	0.0041
T0	0.00705	0.0102	0.69	0.49
L0	-0.0298	0.0210	-1.42	0.16
L0^2	-0.0000422	0.000136	-0.31	0.76
M0	0.0551	0.0291	1.89	0.059
T0 CPUE	0.0302	0.00915	3.30	0.00098
CPUE^2	-0.0000442	0.0000255	-1.73	0.083
T0 Temp	-0.0277	0.0110	-0.25	0.80
Temp^2	0.00944	0.00515	1.83	0.067
Year (1993)	0.593	0.0899	6.59	4.3e-11
Year (1994)	0.468	0.0788	5.93	3.0e-9
Year (1995)	0.508	0.0851	5.97	2.4e-9
Year (1996)	0.542	0.107	5.08	3.8e-7
Year (1997)	0.531	0.0894	5.94	2.9e-9
Year (1998)	0.511	0.0839	6.09	1.1e-9
Year (1999)	0.452	0.0900	5.02	5.2e-7
Year (2000)	0.711	0.0972	7.31	2.6e-13
T0:L0	0.0000710	0.000113	0.63	0.53
T0:CPUE	-0.000179	0.0000617	-2.91	0.0036
T0:Temp	-0.00150	0.000683	-2.19	0.028
			Null Deviance: 2926.1	**Degrees of Freedom: 2450**
			Residual Deviance: 2433.9	**Degrees of Freedom: 2431**
			Estimated θ: 5.62	**Standard Error: 0.24**
			AIC: 14776.9	**Parameters: 20**

Table 4.6

Analysis of deviance table of the full log-link negative binomial model of recapture time with all predictors. All predictors combined explain 492.16 of 2926.1 total deviance.

Predictor	D.F.	Deviance	Residual D.F.	Residual Deviance	P (>|Chi|)
Null			2450	2926.1	
T0	1	288.15	2449	2637.95	1.3e-64
L0	1	95.25	2448	2542.70	1.7e-22
L0^2	1	1.33	2447	2541.38	0.25
M0	1	2.11	2446	2539.27	0.15
T0 CPUE	1	28.70	2445	2510.57	8.5e-8
CPUE^2	1	2.14	2444	2508.43	0.14
T0 Temp	1	2.84	2443	2505.59	0.09
Temp^2	1	1.02	2443	2504.58	0.31
Year	8	59.18	2434	2445.39	6.7e-10
T0:L0	1	0.02	2433	2445.37	0.88
T0:CPUE	1	6.67	2432	2438.70	0.01
T0:Temp	1	4.76	2431	2433.94	0.03

Analysis of deviance table of the full log-link negative binomial model of recapture time with all predictors. All predictors combined explain 492.16 of 2926.1 total deviance.

Table 4.7

Summary of the reduced log-link negative binomial model of recapture time. T0 is the day a fish was tagged, L0 is the fish's length on the tag day in millimeters, M0 is the fish's mass on the tag day in grams, and T0 CPUE is the CPUE at the tag site on the tag date. Year 1993-2000 are year effects, estimated as offsets from the base year (1992). T0:CPUE is an interaction term. All predictors are significantly different from zero at the 0.05 level.

Predictor	Estimate	Std. Error	z Statistic	P
Y-Intercept	4.642	0.263	17.66	< 2e-16
T0	-0.00808	0.00105	-7.73	1.1e-14
L0	-0.0247	0.00475	-5.21	1.9e-7
M0	0.0523	0.0219	2.40	0.017
T0 CPUE	0.0229	0.00851	2.68	0.0075
Year (1993)	0.528	0.0795	6.64	3.1e-11
Year (1994)	0.423	0.0748	5.65	1.6e-8
Year (1995)	0.463	0.0753	6.15	8.0e-10
Year (1996)	0.460	0.0936	4.91	9.0e-7
Year (1997)	0.448	0.0761	5.89	3.7e-9
Year (1998)	0.432	0.0736	5.87	4.4e-9
Year (1999)	0.399	0.0766	5.21	1.9e-7
Year (2000)	0.657	0.0892	7.35	2.0e-13
T0:CPUE	-0.000151	0.0000597	-2.53	0.011
		Null Deviance:	**2915.7**	**Degrees of Freedom:** **2450**
		Residual Deviance:	**2433.9**	**Degrees of Freedom:** **2431**
		Estimated θ:	**5.59**	**Standard Error:** **0.24**
		AIC:	**14773.5**	**Parameters:** **14**

Table 4.8

Analysis of deviance table of the reduced log-link negative binomial model of recapture time. All predictors combined explain 481.76 of 2915.69 total deviance.

Predictor	D.F.	Deviance	Residual D.F.	Residual Deviance	P (>|Chi|)
Null			2450	2915.69	
T0	1	287.10	2449	2628.59	2.1e-64
L0	1	94.91	2448	2533.68	2.0e-22
M0	1	3.42	2447	2530.26	0.06
T0 CPUE	1	28.57	2446	2501.69	9.0e-8
Year	8	61.62	2438	2440.06	2.2e-10
T0:CPUE	1	6.14	2437	2433.93	0.01

Table 4.9

Table of estimated parameter values and the resulting mean residence times from fitting a hypothetical residence time distribution to Poisson and negative binomial distributions. $\bar{R}$ is the mean of the hypothetical residence time distribution; *Var* $\bar{R}$ is the variance of the hypothetical residence time distribution. λ is the maximum likelihood fitted mean and variance parameter of the Poisson distribution. μ and θ are the maximum likelihood fitted parameters of the negative binomial distribution, where μ is the mean parameter and variance is found by $\mu+\mu^2/\theta$. Var Fit is the variance in each fitted distribution, and $\bar{r}$ Fit is the mean recapture time resulting from applying the fitted variance and mean residence time to the equation 4.6. $\bar{R}/\bar{r}$ is the ratio between mean hypothetical residence time and mean predicted recapture time.

	Poisson	**Negative Binomial**
$\bar{R}$	20.68 days	20.68 days
$Var\ \bar{R}$	163.51	163.51
λ	20.68	-
μ	-	20.68
θ	-	3.61
Var Fit	20.68	139.15
$\bar{r}$ **Fit**	10.84 days	13.71 days
$\bar{R}/\bar{r}$	1.91	1.51

Table 4.10

Table of the results of the Age-Growth model. # Fish is the number of fish modeled; these fish were tagged at locations where CPUE data is available in the given year. $\bar{R}$ is the mean residence time produced by the Age-Growth model for the fish in the given year. *T2a*-bar is the mean day of year of migration initiation produced by the Age-Growth model in the given year. *cc* is the catchability coefficient fitted by maximum likelihood for each year, and σ is the error variance parameter fitted by maximum likelihood for each year.

Year	**# Fish**	$\bar{R}$	$\overline{T2a}$	***cc***	**σ**
1992	633	11.45 days	152.4	0.0107	1.23
1993	751	14.52 days	180.2	0.0095	0.69
1994	1177	14.37 days	168.6	0.0052	0.28
1995	692	15.21 days	170.1	0.0150	0.93
1996	389	15.46 days	171.4	0.0144	0.35
1997	291	23.52 days	184.7	0.0141	0.32
1998	1298	16.70 days	162.8	0.0114	3.12
1999	1129	14.96 days	167.5	0.0116	1.05
2000	1078	19.80 days	165.9	0.0346	5.89

4.6 Chapter 4 Figures

Figure 4.1

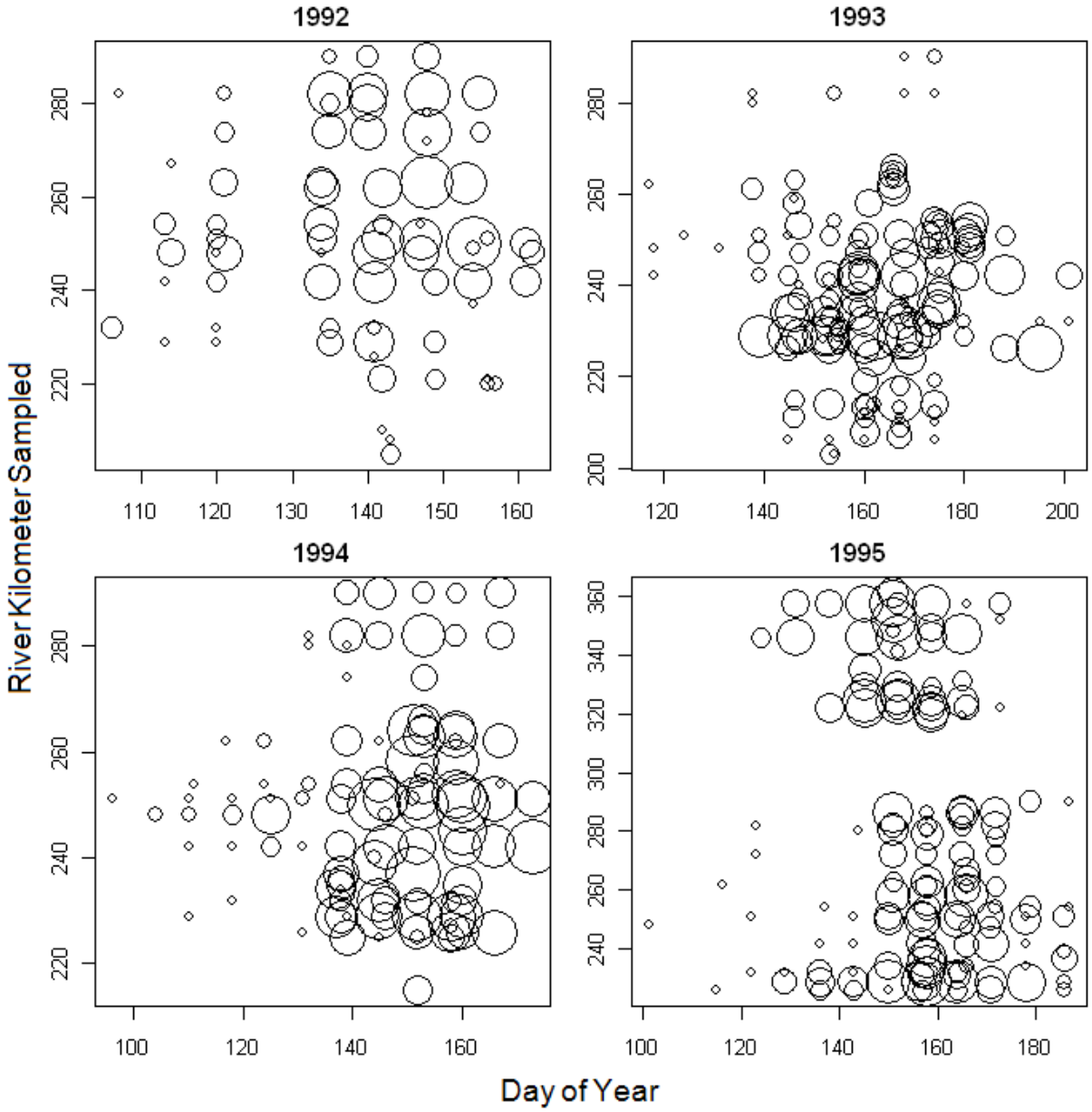

Yearly plots of the number of fish tagged by day of year and river kilometer sampled for the years 1992-1995. The size of each circle relates on a log scale to the number of fish tagged at a particular site on a particular day; the smallest circles correspond to a single fish, the largest to several hundred. Sampling distributions display regular, weekly patterns.

Figure 4.2

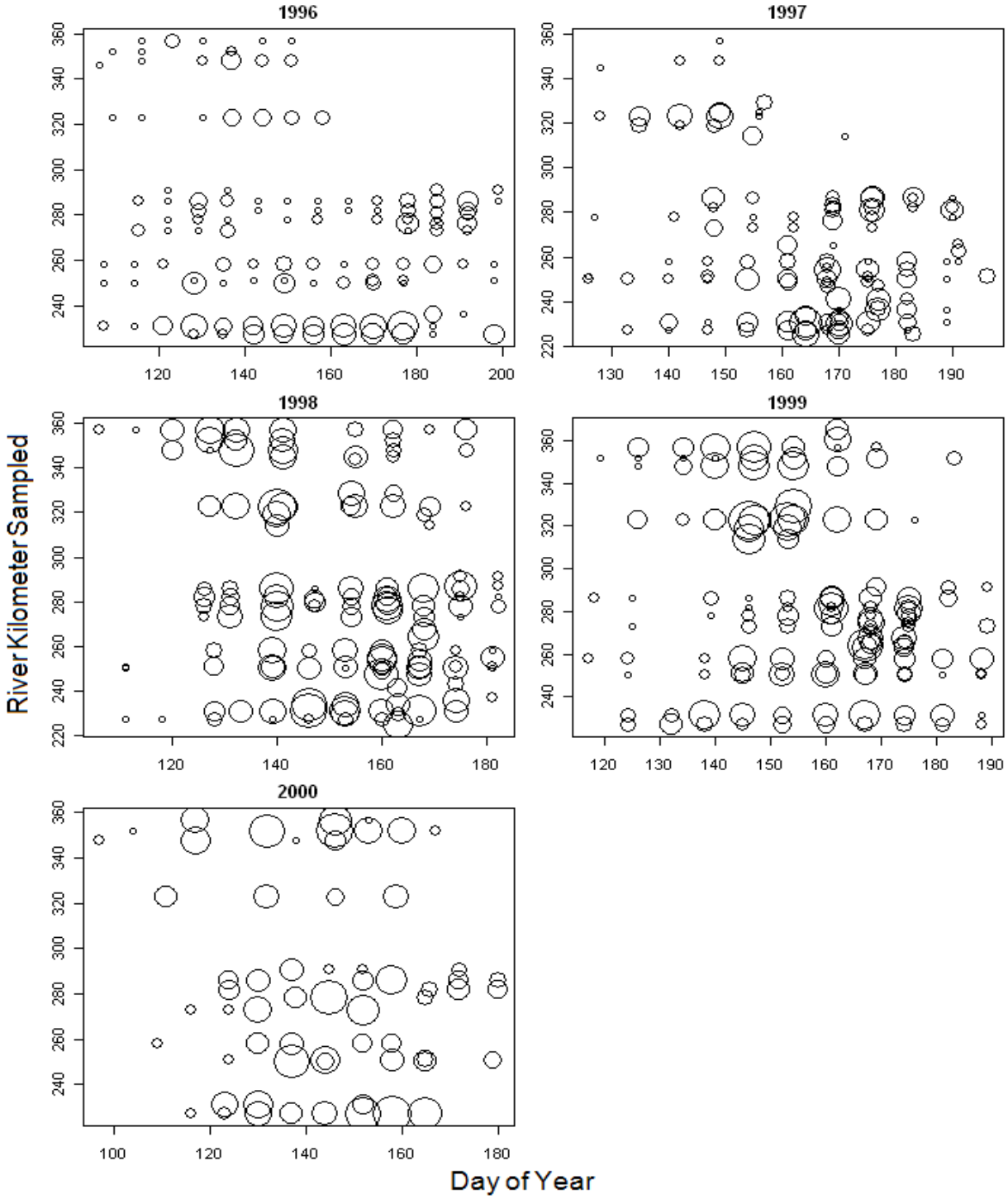

Yearly plots of the number of fish tagged by day of year and river kilometer sampled for the years 1992-1995. The size of each circle relates on a log scale to the number of fish tagged at a particular site on a particular day; the smallest circles correspond to a single fish, the largest to several hundred.

Figure 4.3

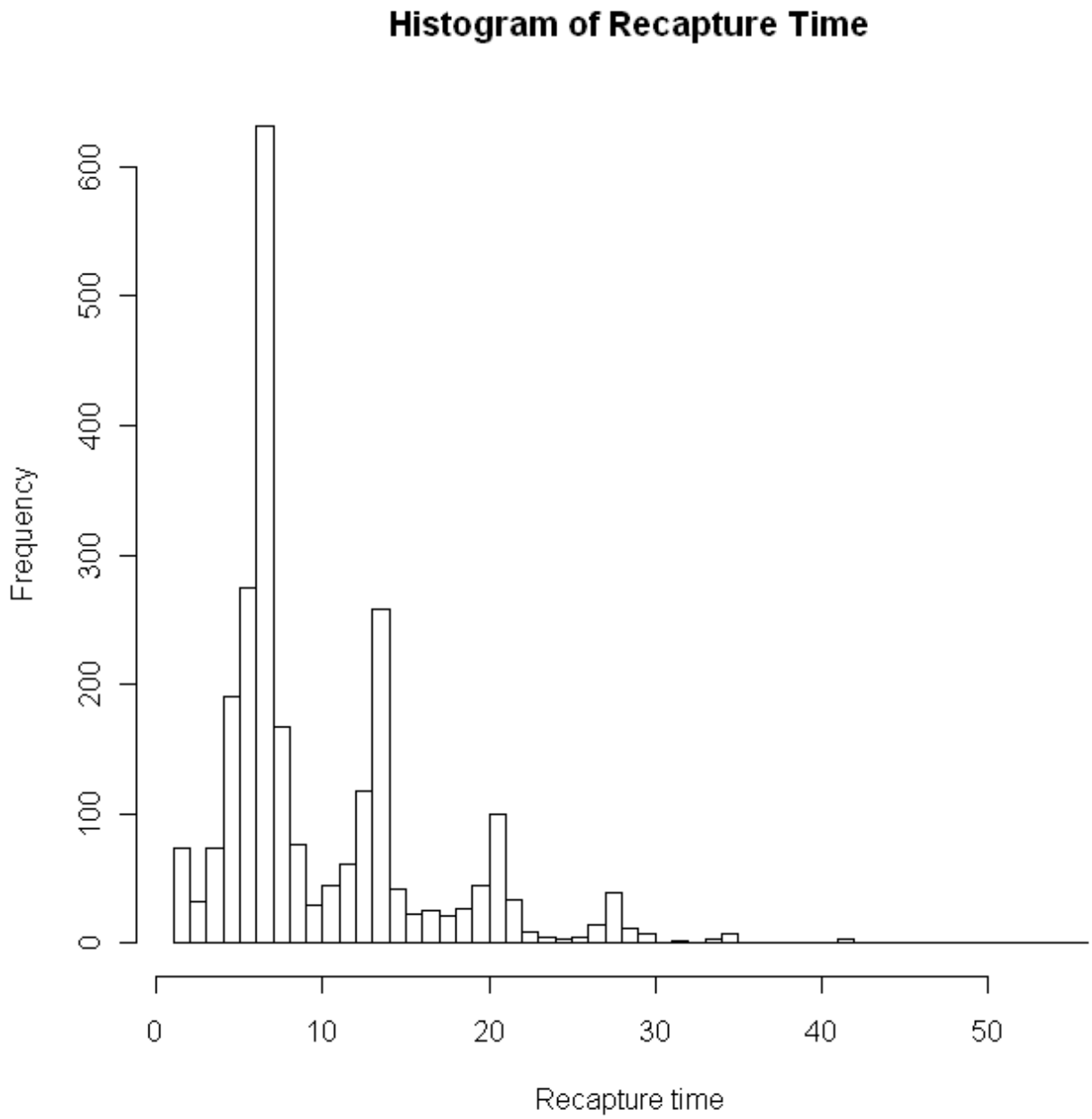

Histogram of observed recapture times for 2,451 fish for which a T1 data point is present. Observed recapture time is defined as the number of days between tagging (T0) and in-river recapture (T1) for each fish. Distinct peaks are seen at 7, 14, 21, and 28 days, indicating that many fish were recaptured at locations with weekly sampling.

Figure 4.4

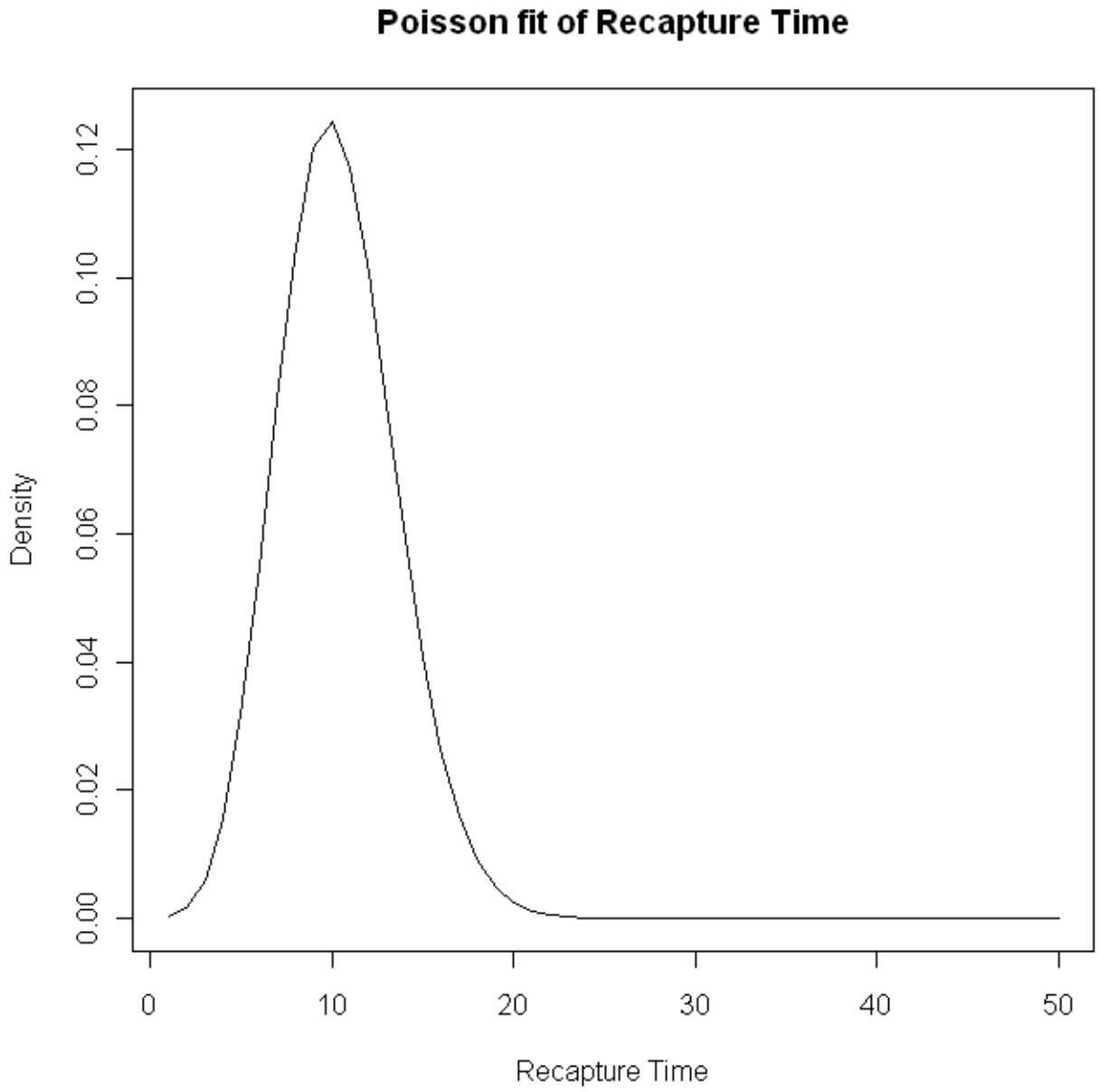

Plot of the Poisson fit of observed recapture time. Mean and variance parameter λ is equal to 10.34, the mean observed recapture time.

Figure 4.5

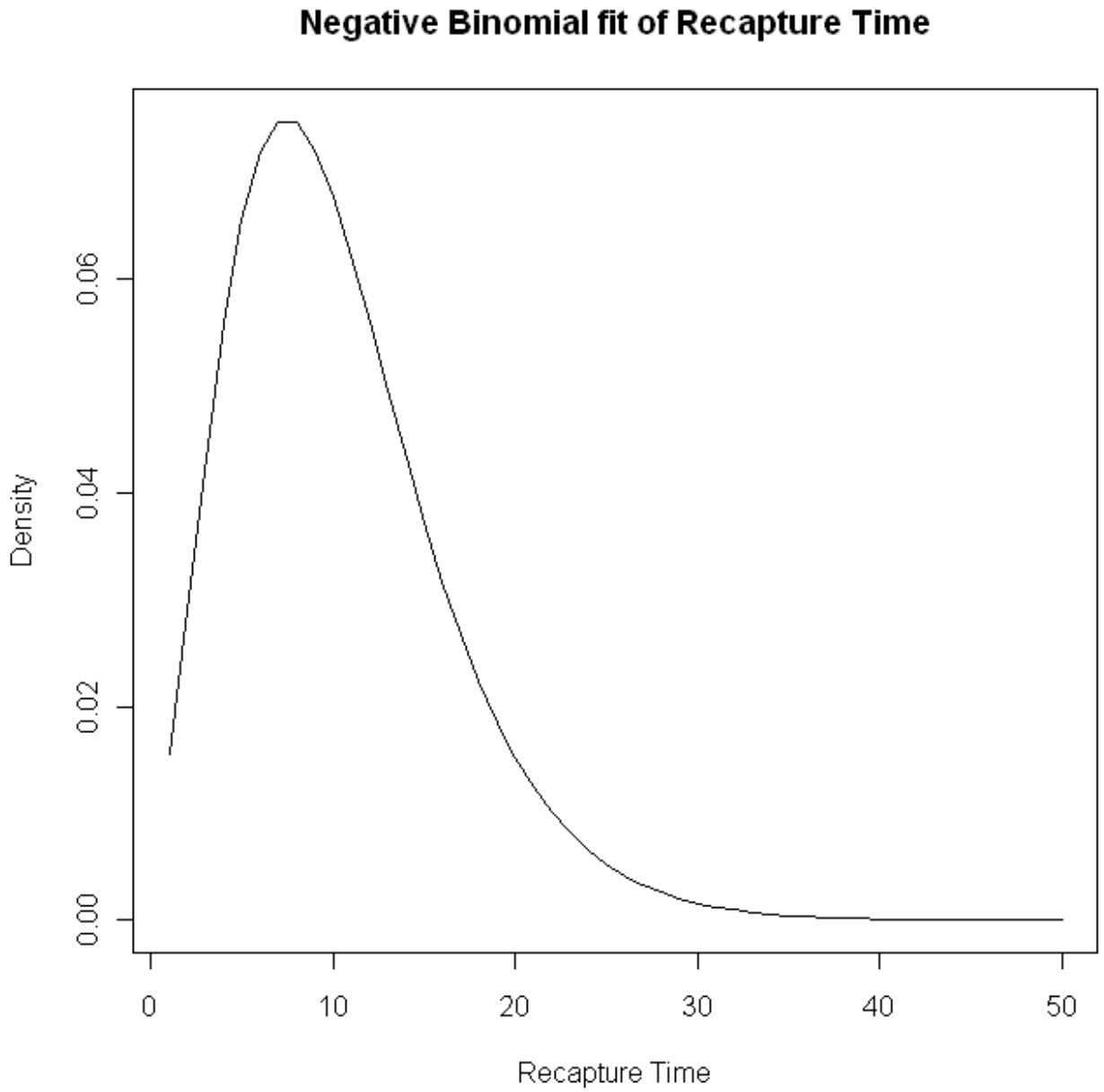

Plot of the negative binomial fit of observed recapture time. Mean parameter μ is equal to 10.34, the mean observed recapture time; dispersion parameter θ was fitted at 4.33 via maximum likelihood function using the MASS library in the statistical computing language 'R'.

Figure 4.6

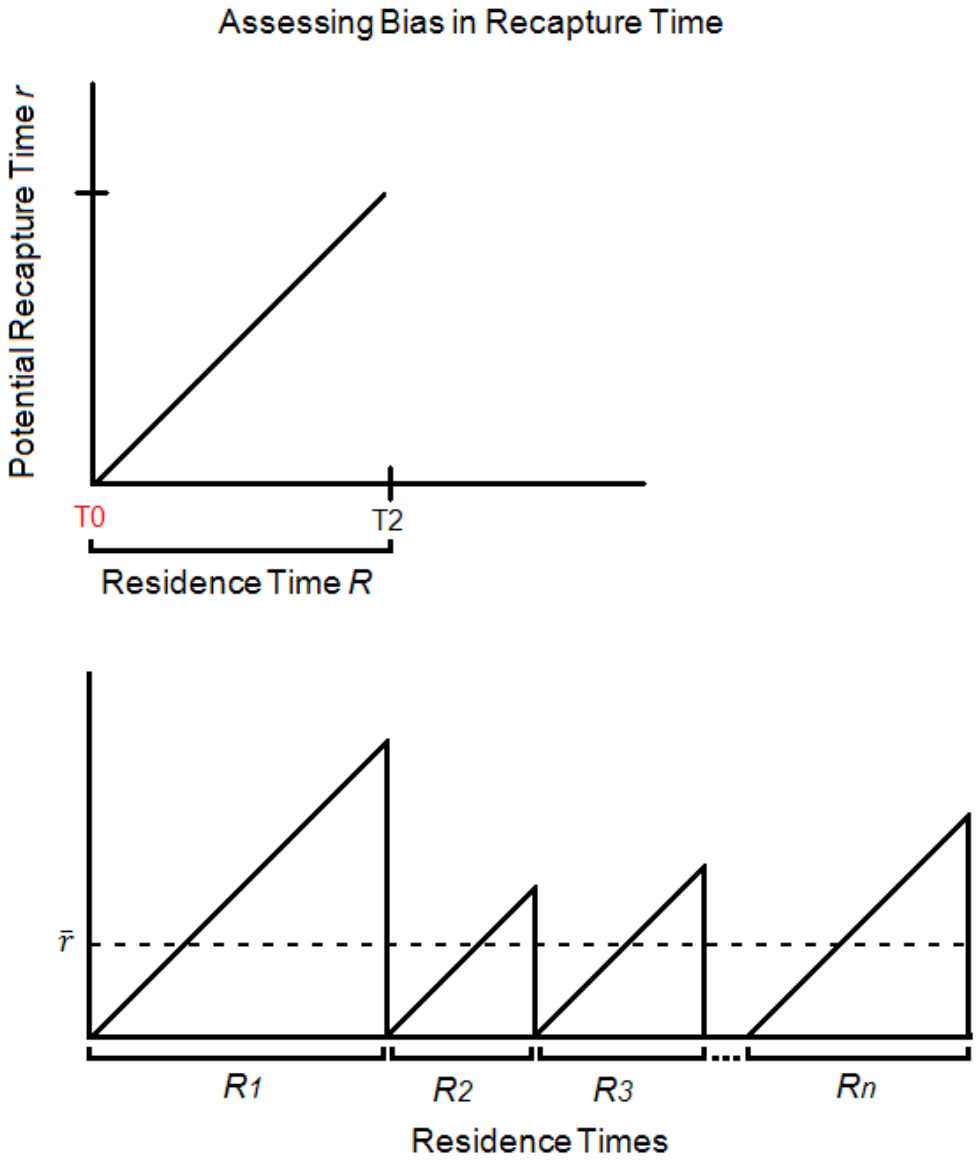

Depiction of the process of relating residence time *R* to recapture time *r* by representing potential recapture time as a sawtooth curve. For an individual fish, residence time *R* = T0:T2. Recapture can occur at any date within *R*, producing potential recapture time varying from 0 to *R* days. For a population of fish with varying residence times R_i, the mean recapture time $\bar{r}$ is the average height of the sawtooth curve.

Figure 4.7

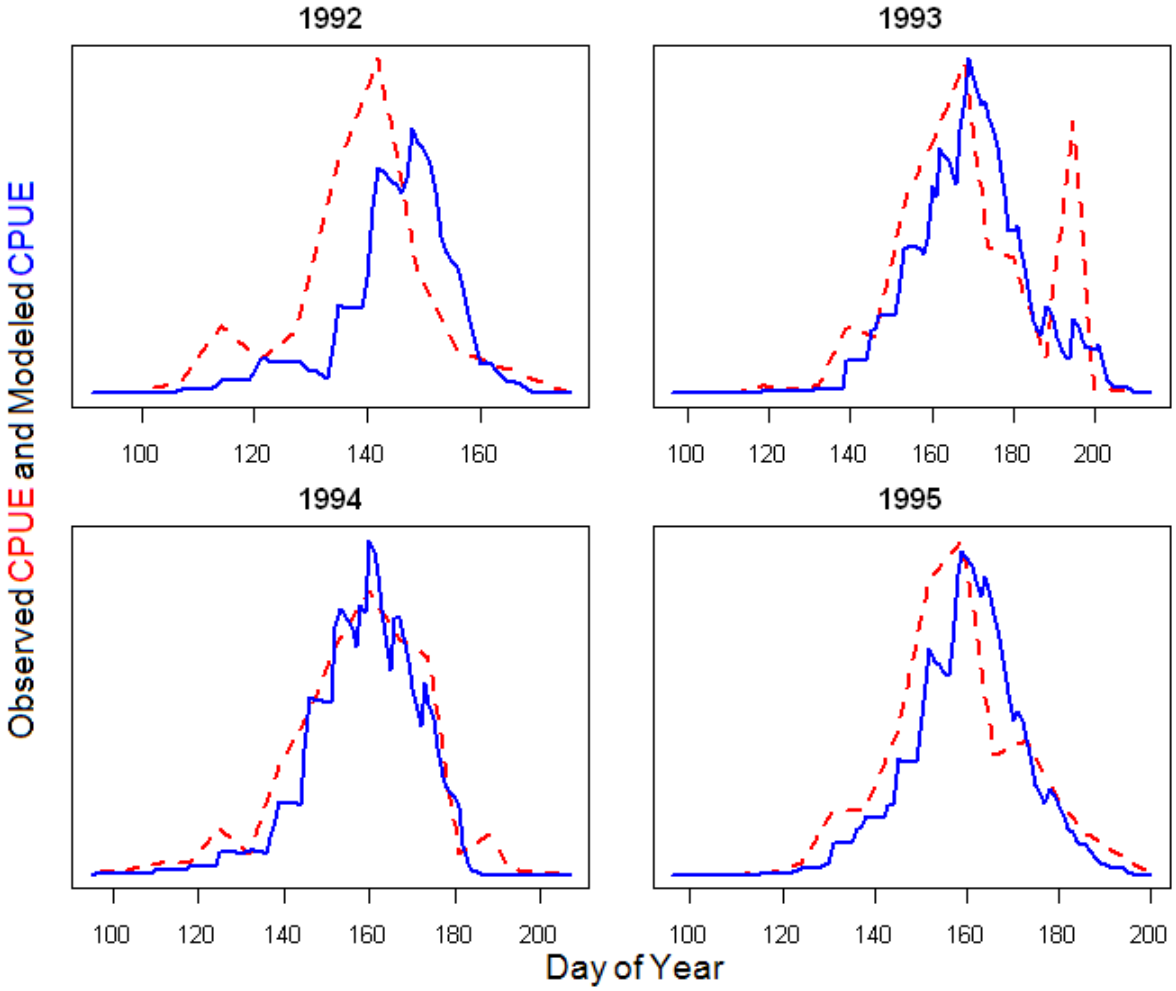

Yearly plots showing observed CPUE and modeled CPUE produced by the Age-Growth model for the years 1992-1995. Day of initiation of migration T2a is predicted for each fish using the negative binomial generalized linear model of recapture time and the 1.51 conversion factor. Modeled T2a and T0 are used to generate distributions of modeled number of fish in-river. These distributions are then fitted to observed CPUE via maximum likelihood fitting of catchability coefficient and variance. Catchability coefficient and variance were estimated independently for each year.

Figure 4.8

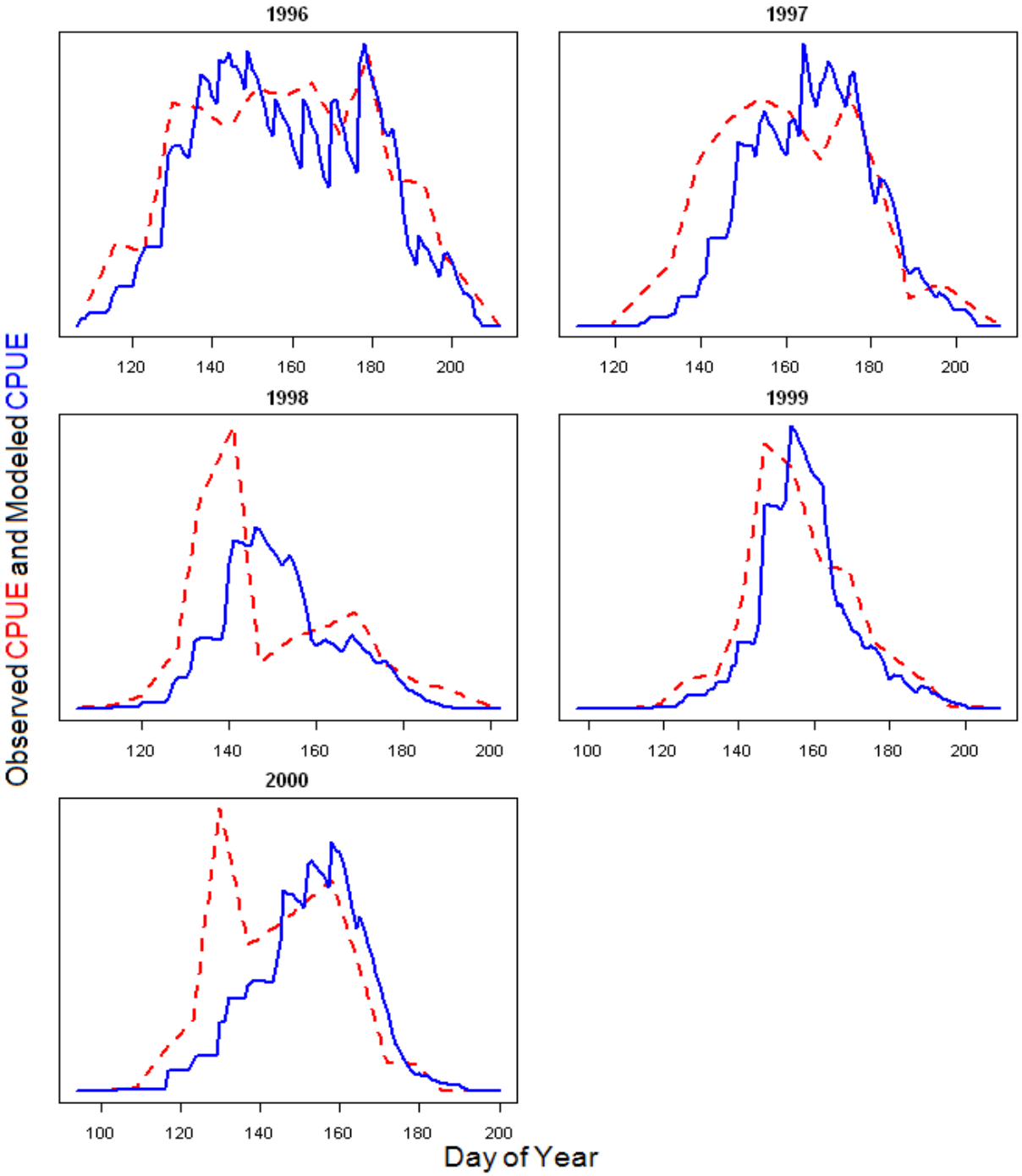

Yearly plots showing observed CPUE and modeled CPUE produced by the Age-Growth model for the years 1996-2000.

Figure 4.9

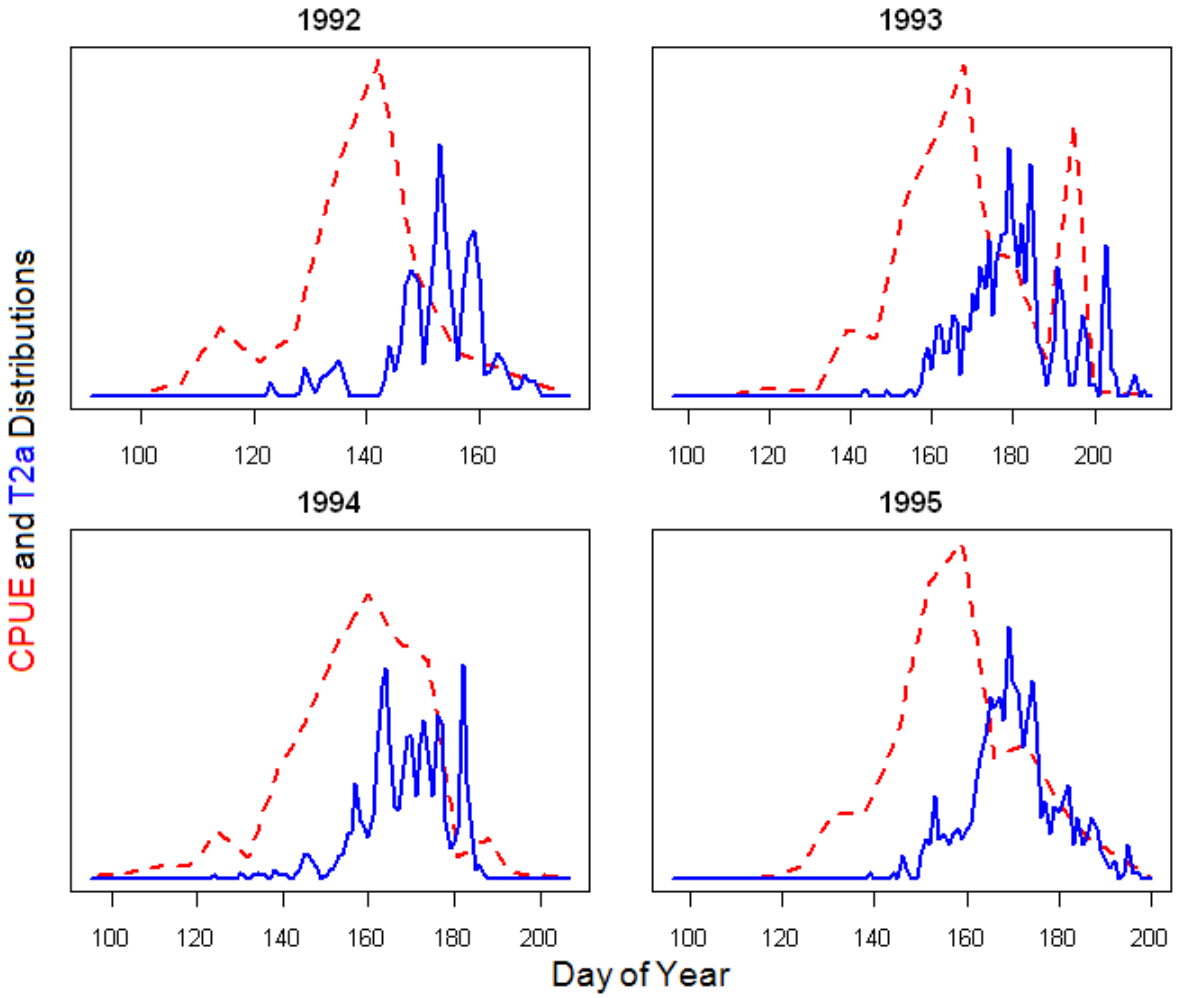

Yearly plots showing observed CPUE and distributions of modeled T2a produced by the Age-Growth model for the years 1992-1995. Day of initiation of migration T2a is predicted for each fish by first using the negative binomial generalized linear model of recapture time and the 1.51 conversion factor to predict residence time. Predicted residence time is then added to each fish's day of tagging T0 to yield modeled T2a.

Figure 4.10

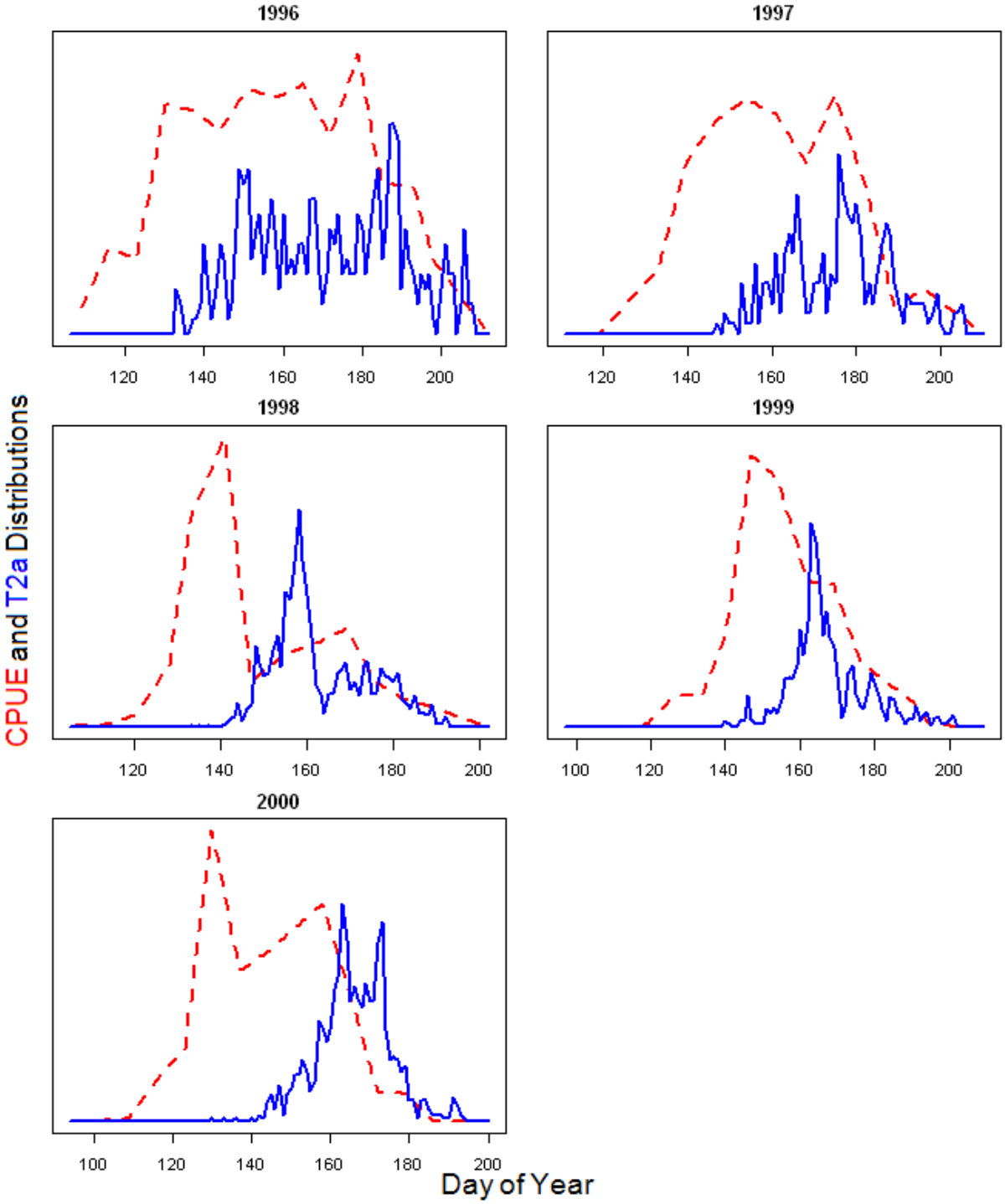

Yearly plots showing observed CPUE and distributions of modeled T2a produced by the Age-Growth model for the years 1992-1995.

Chapter 5: Applying Migration Models to Juvenile Life History

5.1 Introduction

After the Mass-Growth and Age-Growth models of migration initiation were completed, we applied these models with our other models to examine the early life history of fall Chinook. In particular, we examined fish that could be confidently labeled as either ocean-type or reservoir-type. As described in Chapter 1 of this thesis, ocean-type fall Chinook are fish that migrate to the ocean in the first summer after emergence (Healy 1991); reservoir-type fall Chinook arrest this seaward migration and overwinter in one of the reservoirs on the Snake or Columbia Rivers, then resume migrating the following spring (Connor et al. 2005). The mechanisms by which juvenile Chinook bifurcate into the ocean-type and reservoir-type life histories are unknown (Connor et al. 2005); to investigate what factors may be involved in determining which life history a fish follows, we used our models to examine these fish and identify differences in both modeled statistics and statistics from data. We also tested the fish using our models of migration initiation to see if fish fell back below the criterion for migration initiation after entering Lower Granite Reservoir. Lastly, we examine the results of these models in the context of the motivating theory to draw conclusions about the ecology of migration initiation in juvenile fall Chinook salmon and the role of reservoirs in the reservoir-type life history.

5.2 Modeling Fish Through Lower Granite Reservoir

5.2.1 Operation of the Model Complex

We combined our model of fish growth with our models of migration initiation to create a model complex to track the early life history of individual fall Chinook through the Snake River and Lower Granite Reservoir. We break down the migration and life history timing of juvenile Chinook salmon into distinct points in time and reaches in space relevant to our models and data (Figure 5.1). As discussed in section 2.2.1 of this thesis, we break the habitat of the Snake River into two broad reaches separated by the confluence of the Snake and Clearwater Rivers. The 'River' reach stretches from Hell's Canyon Dam to the confluence of the Snake and Clearwater Rivers. All tagging occurs within this reach, and in our modeling we assume that all fish within this reach are non-migratory parr. The 'Reservoir' reach covers the Lower Granite Reservoir and stretches from the confluence of the Snake and Clearwater Rivers to Lower Granite Dam. We assume in our modeling that fish instantaneously enter the reservoir reach once they begin to migrate. The critical points in time in our modeling of an individual fish are: T0, the day a fish was tagged; T1, the day a fish is recaptured within the river reach; T2, the day the fish initiates migration and transitions from the river reach into the reservoir reach; T3, the day a fish passes Lower Granite Dam; and T4, recapture and detection at other dams downstream of Lower Granite Dam (Figure 5.1).

The modeling process for an individual fish begins with the tagging data point T0 and mass at tagging M0. We then use our in-river growth model, described in section 2.2.2, to predict the growth of the fish during its period of in-river residence. We denote this period of modeled

growth as G1 (Figure 5.2). The end of the period of in-river growth is determined by the initiation of migration, for which we have two estimates; T2m from the Mass-Growth model and T2a from the Age-Growth model (Figure 5.3). At whichever T2 point is used for a particular run, we model the fish as instantaneously leaving the Snake River habitat and entering the Lower Granite Reservoir. We then model the growth of the fish in Lower Granite Reservoir using a growth model described in this section. We denote the period of modeled growth in Lower Granite Reservoir as G2.

To produce this model of the growth of individual fall Chinook in Lower Granite Reservoir, we combined the growth model used in-river with a new model of consumption rate and the estimates of migration initiation date produced by the migration initiation models. The core of the growth model is the Wisconsin bioenergetics model, parameterized for Chinook salmon by Stewart and Ibarra (1991). Section 2.2.2 of this thesis describes the Wisconsin model and the manner in which we used it in detail. To model the growth of a fish using the Wisconsin model, a number of inputs are required. Necessary inputs are the starting date and the starting mass of the fish, the water temperature on each day for which growth will be modeled, an estimate of the energy density of the fish's diet, and an estimate of consumption rate.

Since we treat the transition from the free-flowing river habitat to Lower Granite Reservoir as instantaneous in our modeling, the starting day of growth in the reservoir is determined by the modeled day the fish initiates migration, or day T2. We assessed the performance of the Mass-Growth and Age-Growth models to determine how different the predictions of the two models are and if one model should be preferentially used over the other, see section 5.2.2 for details. To get the fish’s starting mass upon entering Lower Granite Reservoir, we estimate the fish’s mass at the initiation of migration, which we denote as M2. M2

is generated using the in-river growth model, G1; the growth model is run until day T2, and the final modeled mass on day T2 becomes M2.

For temperature data, we used the daily mean temperature recorded in the scroll case at Lower Granite Dam. As discussed in section 2.2.1 of this thesis, there are three temperature readings available from Lower Granite Dam; temperatures are recorded at the scroll case, the forebay, and the tailrace. The scroll case reading is generally the coolest of the three readings, the forebay the warmest, and the tailrace intermediate between the two. The forebay reading provides an estimate of the surface temperature in Lower Granite Reservoir, and the scroll case temperature reading provides an estimate of the temperature at depth. However, it is not known how closely the forebay-scroll case temperature differential represents the actual thermal stratification of the reservoir. Most likely, the scroll case temperature reading represents a mixture of water from above and below the thermocline; dam operations and the flow rate of the river likely influence the mixture ratio over time. Radio tracking of tagged fall Chinook salmon indicates that outmigrating juveniles preferentially occupy intermediate temperatures in the thermocline (Tiffan et al. 2009). Since it provides the closest estimate of the temperatures available in the thermocline, we chose to assume in our modeling that all fish in Lower Granite Reservoir experience the temperature recorded at the scroll case. Additionally, the scroll case reading is the only reading available for every year modeled; the forebay and tailrace readings are only available from 1995 onwards.

For prey energy density, we used the same estimate used for the in-river growth model; see section 2.2.3 of this thesis for details. For the fish's consumption rate, we created a multivariate linear model of consumption rate in Lower Granite Reservoir using the records of fish recaptured at Lower Granite Dam. This model is described in detail below in section 5.2.3.

These inputs allow the growth of fish within Lower Granite Reservoir to be modeled, yielding G2 (Figure 5.4).

5.2.2 Relative Performance of the Mass-Growth and Age-Growth Models

We created two different models to predict the initiation of migration in juvenile fall Chinook salmon. The first model, described in Chapter 3 of this thesis, is the Mass-Growth model of migration initiation. This model is a mechanistic model that applies the theory proposed by Thorpe et al. (1998) and Mangel and Satterthwaite (2008); the model proposes that fish initiate migration when their mass exceeds a mass threshold or their growth efficiency drops below a growth efficiency threshold. The magnitude of these thresholds was fitted independently for each year of data using a maximum likelihood method.

The second model, described in Chapter 4 of this thesis, is the Age-Growth model of migration initiation. This model is a correlative model that predicts a fish's recapture time using a multivariate linear model with tagging data as predictors. This recapture time is then extrapolated into a residence time using a theoretical relationship between mean recapture time and mean residence time, and the modeled residence time is used to predict expected date of migration initiation.

These two models provide two independent estimates of date of migration initiation T2; T2m predicted by the Mass-Growth model, and T2a predicted by the Age-Growth model. To assess how congruent the predictions of these two models are, we compared predicted T2m and T2a for a set of fish. We used the records of the 7,438 fish which were used in the process of maximum likelihood fitting in both the Mass-Growth and Age-Growth models. For these fish, we used the fitted parameters from the version of the Mass-Growth model with mass and growth

efficiency driven leaving and a mass-varying catchability coefficient to predict T2m (see section 3.3.3). We also used the fitted parameters of the Age-Growth model to predict T2a for these fish (see section 4.2.4). We then plotted predicted T2a against predicted T2m and fitted a linear model to the resulting distribution (Figure 5.5).

In the ideal case where both models perfectly predict the initiation of migration, we would expect modeled T2a and T2m to be 100% correlated, with all points lying on the one-to-one line. As neither model can perfectly predict migration, there is significant deviation from the one-to-one line; however, the linear regression of T2a vs. T2m shows that the results of the two models are still comparable. The r^2 of the linear model fit is 0.565, meaning that the results of the two models are 56.5% correlated. The slope of the linear model fit is 0.823; since this departs from the expected slope of 1, this indicates differences in the distributional properties of fitted T2a and T2m. Mean T2a and T2m are very similar, as mean day of year of fitted T2a is 167.38, while the mean day of year of fitted T2m is 166.64. While the mean fitted T2a and T2m are very close, there is more variance in fitted T2m than in fitted T2a, which results in the fitted slope of the linear model being less than one. The variance of fitted T2a is 163.58, while the variance of fitted T2m is 195.96.

While this comparison showed that the individual predictions of the two models are fairly comparable, we decided that the results are different enough to warrant independent analysis. For this reason, in our modeling of juvenile Chinook through Lower Granite Reservoir, we create two versions of each analysis; one version using the Age-Growth model to predict migration, and the other using the Mass-Growth model to predict migration.

5.2.3 Modeling Growth in Lower Granite Reservoir

Fitting Reservoir Consumption Rate from Data

In order to model the growth of fish within Lower Granite Reservoir, individual estimates of consumption rate are necessary. To create a model capable of estimating consumption rates of individual fish, we created a multivariate linear model regressing consumption rate in the reservoir against T2, M2, tagging data and environmental data. To fit the model, we used the records of fish for which a consumption rate in Lower Granite Reservoir could be individually estimated. Estimating a fish's consumption rate in Lower Granite Reservoir required an estimate of the fish's growth over a known period within the reservoir; required components were the date of entry into the reservoir and mass at entry, date of exit of the reservoir and mass at exit, mean energy density of the composite diet, and the temperature of the reservoir for the period between reservoir entry and exit.

As we model the transition from the free-flowing habitat of the Snake River to the impounded reservoir habitat as instantaneous, date of entry to Lower Granite Reservoir is given by date of migration initiation T2. Since we have two models of migration initiation, we have two separate estimates of day T2: T2m from the Mass-Growth model and T2a from the Age-Growth model. We conducted two independent analyses of consumption rate in Lower Granite Reservoir; one using day T2m as the day of entry to the reservoir, the other using day T2a.

Mass at entry to the reservoir is denoted as M2. As we have two estimates of day of entry to the reservoir, each estimate of entry day is associated with an entry mass: M2m for entry day modeled by the Mass-Growth model and M2a for entry day modeled by the Age-Growth model. Each mass M2 is found by using the in-river growth model to model the growth of individual fish from the tag day T0 until the respective migration day T2. Section 2.2.2 of this thesis

describes the in-river growth model in detail. The in-river growth model is not able to model all fish with equal fidelity; some fish are recaptured in-river and have an in-river capture day T1 and capture mass M1. These fish have individually fitted in-river consumption rates, as described in section 2.2.3 of this thesis. Fish lacking a T1 and M1 data point have no individually fitted in-river consumption, and an attempt to model in-river consumption rate was unsuccessful (see section 3.2.1 of this thesis); so for these fish the mean fitted consumption rate was used in previous models in Chapters 3 and 4. In order to avoid compounding model error resulting from using mean in-river consumption to generate M2, then using this modeled M2 to fit the in-reservoir consumption model, we confined the fish used to fit the reservoir consumption model to only those fish with a T1 and M1 data point and individually fitted in-river consumption.

Day of exit of Lower Granite Reservoir is given by day of passage of Lower Granite Dam. This comes directly from PIT data; we denote the day a fish is detected passing Lower Granite Dam as day T3. Some of these fish are recaptured and measured as they pass Lower Granite Dam; for these fish, mass at passage M3 is known. As described in section 5.2.1 of this thesis, the temperature data we use for Lower Granite Reservoir comes from the scroll case temperature record at Lower Granite Dam. We used the same estimate of prey energy density used for the in-river growth model (section 2.2.3), 5400 joules per gram. Once all of these data are present, start day (T2m or T2a), start mass (M2m or M2a), end day T3, end mass M3, temperature and prey energy density, the Wisconsin model is used to estimate a consumption rate in Lower Granite Reservoir. As consumption rate is an input to the Wisconsin Bioenergetics Model, we solve for consumption rate using an iterative method. Test consumption rates are submitted to the model and modeled final mass M3 is compared to known final mass M3 until a suitable match is found.

Only a small percentage of all fish tagged were recaptured at Lower Granite Dam, and only a small percentage of these were also recaptured in-river. A total of 136 individual fish had all required data; as the sampling schedule at Lower Granite Dam varied by year, these fish are confined to the years 1992-1995. For these fish, the two-decimal consumption rate that most closely predicted the known mass at Lower Granite Dam M3 was selected as the fish's individual consumption rate. Some fish could not be satisfactorily fitted with a consumption rate; the number of fish varied depending on which migration model was used to predict T2 and the resulting M2. When the Mass-Growth Model was used, a total of 26 fish could not be fitted, resulting in a total of 110 fish with a fitted consumption rate. Table 5.1 provides a summary of the fitted consumption rates using the Mass-Growth model predicted reservoir entry. When the Age-Growth Model was used, a total of 2 fish could not be fitted, resulting in a total of 134 fish with a fitted consumption rate. Table 5.2 provides a summary of the fitted consumption rates using Age-Growth model predicted reservoir entry.

Fish that could not be satisfactorily fitted with a consumption rate were all tagged in 1994; the fish could not be fitted because observed growth was larger than could be matched with the Wisconsin model. While the theoretical maximum consumption rate is equal to one, the Wisconsin model can fit consumption rates larger than one; however, consumption peaks at two, and if a consumption rate of two does not match observed growth, then a fit could not be found. Previous researchers have found that bioenergetics model results may fit abnormally high consumption rates due to underestimation of diet energy density (Luecke and Brandt 1993, Stockwell et al. 1999). These researchers showed that salmonids are capable of reducing the water content of daphnid prey, meaning that field estimates of prey energy density can significantly underestimate the energy density of prey within the salmon stomach if the diet

consists in large part of daphnia. We already considered this phenomenon when fitting consumption rates within the in-river portion of the Snake River habitat, resulting in our estimate of a high prey energy density of 5400 joules per gram (section 2.2.3) in order to confine fitted consumption rates below the theoretical maximum. The consumption rates fitted within Lower Granite Reservoir used the same prey energy density, but resulted in significantly higher fitted consumption rates than those fitted in-river, and a number of fish that could not be fitted with a consumption rate high enough to match growth. A diet shift to a more daphnid-heavy diet when fish enter the impounded water of the reservoir could be responsible for this increase in fitted consumption rates. It is also possible that the temperature record we use in our model is not accurately capturing the thermal experience of the fish; even though the scroll case reading is the coolest of the three temperature readings available at Lower Granite Dam, we do not think it represents the coolest water available in Lower Granite Reservoir. Fish could potentially be occupying colder water than predicted in our model, which would be more optimal for growth; this may especially be the case in 1994, which has the highest fitted consumption rates, the most number of fish that could not be fitted, and also the warmest scroll case temperatures.

Multivariate Linear Models of Fitted Reservoir Consumption Rate

Once individually fitted consumption rates were identified for a set of fish, we then created a multivariate linear model of in-reservoir consumption rate by regressing these fitted consumption rates against tagging and environmental data. Since we have two separate models of migration initiation and two different sets of estimated in-reservoir consumption rates, two models of in-reservoir consumption rate were created. For ease of reference, we denote the reservoir consumption rate model created using Mass-Growth predicted migration as the

‘MGRC’ model, and the reservoir consumption rate model created using Age-Growth predicted migration as the ‘AGRC’ model. Both models regressed fitted in-reservoir consumption rate against: T0 and M0- tag date and mass at tagging; T0 RKM- the river kilometer of tagging; T0 CPUE- the CPUE at the tag location on the tag date; T0 Temp- the temperature in the Snake River (Anatone gauge) on the tag date; and three estimates of temperature in Lower Granite Reservoir. Squared terms were included for CPUE, river temperature, and all three estimates of reservoir temperature. Each model also included as predictors the T2 and M2 predicted by the relevant migration initiation model; T2m and M2m for the MGRC model and T2a and M2a for the AGRC model. Interaction terms were included between T0 and M0 and between the relevant T2 and M2 in each model. The three estimates of reservoir temperature were found by averaging temperature at the scroll case of Lower Granite Dam for different lengths of time following each fish’s individually predicted migration day T2. The first estimate was the mean temperature on day T2. The second estimate was the mean temperature for the first week after day T2, and the third was the mean temperature for the first month after day T2. Table 5.3 provides a summary of the parameter estimates and significance for the version of the full MGRC model. Table 5.6 provides a summary of parameter estimates and significance for the full AGRC model.

A parsimonious reduced model was then generated from each of these two full models via sequential deletion. The least explanatory predictor was removed from the model if removal did not increase the AIC score of the model by more than 2, then the model was re-fitted and the new least explanatory predictor examined. Once removal of the least explanatory predictor would increase the AIC of the model by more than 2, we determined that a parsimonious model had been reached. The parameters removed from the full MGRC model were, in sequence: reservoir temperature 2, T0 CPUE, CPUE squared term, reservoir temperature 3 squared term,

T0 RKM, T2m:M2m interaction term, T2m, T0:M0 interaction term, M0, reservoir temperature 2 squared term, river temperature, and T0. Tables 5.4 and 5.5 provide a summary of parameter estimates and significance and ANOVA tables of the reduced MGRC model. The parameters removed from the full AGRC model were, in sequence: T2a:M2a interaction term, T0 RKM, T0:M0 interaction term, CPUE squared term, reservoir temperature 3, T0 CPUE, reservoir temperature 1, reservoir temperature 1 squared term, T0, T2a, and M0. Tables 5.7 and 5.8 provide a summary of parameter estimates and significance and ANOVA tables of the reduced AGRC model.

The reduced models for both the MGRC and AGRC versions of the reservoir consumption rate model were successful at describing fitted reservoir consumption rate. Many of the predictors tested were not contributing very much to explaining consumption rate, resulting in the full models having no significant predictors despite having reasonable R^2 values. The reduced models eliminate the deadweight predictors, resulting in far fewer parameters than the full models, with all remaining parameter estimates significantly different from zero. The resulting AIC scores of the reduced models are better than their respective full models, and most of the R^2 value of the full models is retained. As the reservoir consumption rates used for the two models were fitted separately using the different migration models to predict reservoir entry, the results of the two models are not directly comparable, but their relative success at predicting consumption rate can be examined. While both the reduced MGRC model and the reduced AGRC model have decent R^2 scores, the AGRC model is better at predicting consumption rates fitted using Age-Growth migration than the MGRC model is at predicting consumption rates fitted using Mass-Growth migration. This is illustrated by the difference in R^2; the reduced MGRC model has an R^2 of 0.405, while the reduced AGRC model has an R^2 of 0.597, meaning

that the AGRC model explains almost 20% more of the variation in consumption rate. We decided that both models were successful enough to use in further analysis modeling the growth of fish in Lower Granite Reservoir. As described in section 5.2.1, we use the fitted parameters of the reduced MGRC and AGRC models to predict consumption rates of individual fish in Lower Granite Reservoir, which then enables the growth model to predict growth in Lower Granite Reservoir. For an analysis predicting reservoir entry using the Mass-Growth model, consumption rates are estimated using the reduced MGRC model; for analysis predicting reservoir entry using the Age-Growth model, consumption rates are estimated using the reduced AGRC model.

5.3 Differences Between Ocean-Type and Reservoir-Type Chinook

Once we had completed a model complex capable of modeling the growth and migration of juvenile salmon from the rearing habitat in the free-flowing Snake River into Lower Granite Reservoir, we applied this model complex to investigate the differences between the life history strategies employed by Snake River fall Chinook. Currently, two different juvenile life histories are observed in fall Chinook, labeled as ‘ocean-type’ (NMFS 1992) and ‘reservoir-type’ life histories. Ocean-type Chinook salmon juveniles rear for only a few months after emergence from the gravel and migrate in their first summer as age-0 smolts (Healey 1991). Reservoir-type juveniles initiate migration in late summer or early fall like the ocean-type fish and leave the natal rearing habitat, but then arrest migration and overwinter in one of the reservoirs along the Snake or Columbia Rivers (Connor et al. 2005). These fish resume migration early in the following spring and enter the ocean as age-1 smolts (Connor et al. 2005). The reservoir-type life history is thought to have emerged very recently; reservoir-type fall Chinook were first described

in 2002 (Connor et al. 2002), and prior to the discovery of the reservoir-type life history it was thought that all Snake River fall Chinook were ocean-type (NMFS 1992).

While researchers familiar with Snake River Chinook salmon have postulated that habitat modification resulting from damming and impounding the river is ultimately responsible for the emergence of the reservoir-type life history (Connor et al. 2002 & 2005, Williams et al. 2008), the proximate mechanisms by which individual salmon arrest their migration are unknown. Previous studies of salmon migration have speculated that growth opportunity and threshold size or mass inform the migratory tactic that juvenile salmon use (Thorpe et al. 1998, Brannon et al. 2004, Mangel and Satterthwaite 2008); we applied these principles in the creation of our models of salmon migration, expanding them to include growth efficiency. Our goal is to apply our models of salmon growth and migration initiation to juvenile Chinook of both life history types to identify and quantify plausible mechanisms that could result in selection of one life history strategy or the other by individual fish.

5.3.1 Identifying Ocean-Type and Reservoir-Type Fish

The first step in examining the different life history strategies observed in Snake River fall Chinook was to identify a set of individual fish as either ocean-type or reservoir-type using the PIT tag dataset. PIT tag detectors are located in the juvenile bypass systems at the dams on the Snake and Columbia Rivers (Marvin and Nighbor 2009). Outmigrating juvenile fall Chinook from the Snake River pass a total of eight dams on their way to the ocean: Lower Granite Dam, Little Goose Dam, Lower Monumental Dam, and Ice Harbor Dam on the Snake River, then McNary Dam, John Day Dam, The Dalles Dam, and Bonneville Dam on the Columbia River. PIT tag detectors are located at all of these dams except The Dalles Dam (Marvin and Nighbor

2009). Detection efficiency is not the same at each dam, as the configuration of the bypass system and detectors is different at each dam; additionally, the operation of the bypass systems varied by dam and by year. Consequently, the distribution of recorded detections in the PIT tag dataset varies by dam and by year (Table 5.9). Individual fish could be detected at multiple locations during their migration, and date of first and last detection at each location a fish was detected at is recorded in the PIT tag dataset.

To assign a life history strategy to individual fish, we created criteria using the location and date information from these detection histories. For the ocean-type life history, we assumed that any fish detected at a dam in the Columbia River prior to September 1st of the year in which it was tagged was an ocean-type juvenile. These criteria may capture some reservoir-type fish as well, as it is possible that some fish overwinter in reservoirs on the Columbia; however, this is the best assumption we can make given the data available. The only PIT detection site actually in the ocean is the estuary towed array, and too few fish are detected by this array to enable a quantitative analysis (Table 5.9). Additionally, the majority of fish that were known to be reservoir-type overwintered in Lower Granite Reservoir or Little Goose Reservoir on the Snake River (Connor, personal comm.). For the reservoir-type life history, we assumed that any fish detected at any juvenile bypass location between January 1st and June 1st of the year after it was tagged was a reservoir-type juvenile. We used only the detection sites located in the juvenile bypass systems to avoid confounding the data with returning minijacks. Additionally, the PIT dataset is likely unable to capture some reservoir-type fish, since the juvenile bypass systems are dewatered during winter, and therefore any fish passing a dam during the winter months will not be detected (Connor et al. 2005).

To expand the amount of data for this analysis, we included both presumed wild fall Chinook captured by beach seine by Connor in the years 1992-2000 and subyearling hatchery fall Chinook released into the Snake River by Connor in the years 1995, 1997, and 1998. Of a total of 31,531 tagged fish which were detected at least once by the PIT detection array, the records of 6,890 fish met the criteria for the ocean-type life history, and the records of 1,725 fish met the criteria for the reservoir-type life history. A single fish met the criteria for both life histories; the record of this fish was excluded from further analyses, resulting in a total of 6,889 ocean-type and 1,724 reservoir-type fish. A subset of these fish was selected using only the presumed wild fall Chinook captured and tagged by Connor for use in some analyses; this set of fish totaled 728 confirmed ocean-type fish and 374 confirmed reservoir-type fish.

5.3.2 Observed Differences in Modeled Statistics

Once sets of ocean-type and reservoir-type fish were identified, we compared the properties of the data and model predictions for the two sets of fish. Few of both the confirmed ocean-type and confirmed reservoir-type fish had T1 or T3 points from data, but all fish had a T0 and M0 data point; mass and date of tagging. In-river growth was modeled for all fish using the in-river growth model described in section 2.2.2; the few fish which had a T1 and M1 data point used an individually fitted in-river consumption rate for in-river growth, while the remainder of the fish used the mean fitted consumption rate of 0.56. Migration initiation dates T2m and T2a were predicted for all fish using the Mass-Growth and Age-Growth models. The yearly fitted parameters found for the Mass, Growth, & Catchability version of the Mass-Growth model were used for T2m predictions (see Table 3.7 for values). Mass at migration M2m and M2a was predicted for all fish using the in-river growth model and the predicted dates of migration

initiation. Consumption rate in the reservoir was predicted for all fish using both the MGRC and AGRC consumption rate models (Tables 5.4, 5.7); the MGRC model corresponding to Mass-Growth predicted migration and the AGRC model corresponding to Age-Growth predicted migration.

Statistically significant differences were found between ocean-type fish and reservoir-type fish in every statistic tested (Table 5.10). Reservoir-type fish, on average, are tagged later than ocean-type fish at a smaller size than ocean-type fish. Reservoir-type fish are also modeled to initiate migration later than ocean-type fish at a smaller size than ocean-type fish by both the Mass-Growth model and the Age-Growth model. However, regardless of the migration model used, reservoir-type fish are predicted to have a higher consumption rate once they enter Lower Granite Reservoir than ocean-type fish.

There was concern that comparing the overall means of the ocean-type and reservoir-type distributions was inappropriate, because significant year effects are observed in all of the statistics examined, and the distribution of fish in each life history category is not even across years (Table 5.11). To confirm if the trends observed in the overall dataset held on a yearly basis, yearly subsets of the data was examined for the years where significant numbers of both life history types are known : 1995, 1997, and 1998. Tables 5.12, 5.13, and 5.14 present the results of the comparisons for these years. While observed differences in M0, M2m, and M2a are considerably smaller in 1995, in all other respects, the patterns observed in the overall distributions hold in all three yearly comparisons.

5.3.3 Modeling the Cessation of Migration in Lower Granite Reservoir

The mechanisms informing the cessation of migration in reservoir-type juvenile fall Chinook are currently unknown; we used our models of migration to address this gap in our knowledge of salmon life history. In chapter 3 of this thesis, we described the mechanistic model of migration we created: the Mass-Growth model. This model specifies and fits threshold criteria in fish mass or growth efficiency that must be met to trigger migration; here, we postulate that a reversal of these criteria once a fish is migrating may result in a cessation of migration. The mass threshold is not a likely candidate for triggering this behavior; while the Wisconsin model can predict a negative energy balance at high water temperatures, we decided that it was unrealistic to model a fish losing enough mass to significantly compromise migration success. The theory informing fish mass as a criterion for migration postulates that larger size confers increased survivability to migrants by reducing vulnerability to gape-limited predators and increasing the fish's swimming speed (Thorpe et al. 1998). While fish under starvation conditions may lose muscle mass and lipid reserves, they do not shrink in overall size, meaning that there is no theoretical justification for predicting cessation of migration stemming from a loss of body mass. The growth efficiency threshold, however, can potentially explain cessation of migration. The theory informing the growth efficiency threshold postulates that growth efficiency provides an estimate of the benefit a fish is receiving from its current habitat; if the benefit drops below some threshold level, then the fish is forced to initiate migration regardless of how close to the threshold mass it is. Critically, in our models, the growth efficiency fish experience can change as a fish changes habitats. In particular, the temperature regime and fish's consumption rates are modeled to change as fish transition from the free-flowing reach of the Snake River into Lower Granite Reservoir. In the summer when fall Chinook are rearing in the Snake River, water

temperatures gradually increase to very high levels; in our models, this forces fish to migrate by driving growth efficiency below the *Gcrit* threshold. However, Lower Granite Reservoir receives cold water input from the Clearwater River, which is amplified in summer by coldwater flow releases from Dworshak Dam (Anderson 2000); this cold water persists into Lower Granite Reservoir creating a stratified water column (Cook et al. 2006, Tiffan et al. 2009). Fish migrating into Lower Granite Reservoir have access to this cooler water, which can improve growth efficiency (see Figures 2.8, 2.9). If a fish is forced to initiate migration due to falling below the *Gcrit* threshold while its mass is still below the mass threshold, then later enters a habitat in which its growth efficiency increases back above the *Gcrit* threshold, we postulate that the fish will arrest migration to take advantage of the growth opportunity until migration criteria are met again.

To test this hypothesis, we applied the Mass-Growth model and our model of growth in Lower Granite Reservoir to the records of fish with a confirmed life history. The Mass-Growth model predicts the initial migration from the rearing habitat individually for each fish; migration initiation begins when a fish grows larger than the mass threshold (mass > *Mcrit*) or when its growth efficiency drops below the growth efficiency threshold (growth efficiency < *Gcrit*). Since we assume that fish larger than the mass threshold will not shrink, only fish that left via the *Gcrit* threshold in the Mass-Growth leaving function are eligible to arrest migration upon entry to Lower Granite Reservoir. Based on our theory for cessation of migration, we would expect that reservoir-type fish would display a higher likelihood of leaving due to the *Gcrit* threshold than ocean-type fish, and we also expect the growth efficiency of reservoir-type fish that left by the *Gcrit* threshold to be more likely to rise back above the threshold for migration after reservoir entry.

We used the Mass-Growth model to predict T2m for 6,889 confirmed ocean-type fish and 1,724 confirmed reservoir-type fish and recorded the threshold that resulted in migration initiation for each fish. Of the 6,889 ocean-type fish, 2,549 initiated migration due to growth efficiency dropping below the threshold, while 4,340 initiated migration by growing larger than the mass threshold. Of the 1,724 reservoir-type fish, 860 initiated migration due to the growth efficiency threshold, while 864 initiated migration due to the mass threshold. Table 5.15 provides a contingency table of life history type and migration threshold; the Pearson's test of independence indicates that a significantly larger percentage of reservoir-type fish are modeled to initiate migration via the *Gcrit* threshold.

For the 2,549 ocean-type and 860 reservoir-type fish that initiated migration due to the *Gcrit* threshold, we then modeled their growth after entering Lower Granite Reservoir to examine whether each fish's modeled growth efficiency rose back above the *Gcrit* threshold. For each fish, growth was modeled and growth efficiency recorded for the first week after reservoir entry day T2m; if modeled growth efficiency rose above the growth efficiency threshold *Gcrit* (values of fitted *Gcrit* vary by year, see table 3.7) for any day during this period, the fish was modeled to arrest migration. Of 2,549 ocean-type fish, 1,798, or 70.5%, are modeled to arrest migration due to growth efficiency rising above *Gcrit* after entering Lower Granite Reservoir. Of 860 reservoir-type fish, 689, or 80%, are modeled to arrest migration. Table 5.16 provides a contingency table of life history and proportion of fish arresting or continuing migration; Pearson's test of independence indicates that reservoir-type fish were significantly more likely to be modeled to arrest migration.

Reservoir-type fish displayed a higher proportion of fish which initiated migration via *Gcrit* and a higher proportion of fish modeled to arrest migration after entering Lower Granite

reservoir than ocean-type fish; in both cases, the differences in proportions are statistically significant. However, significant numbers of confirmed ocean-type fish are modeled to arrest migration as well. The data confirms that these fish did not arrest migration in Lower Granite Reservoir for the duration of the summer, since they were detected at dams on the Columbia River prior to the end of their first summer. It is possible that these fish briefly arrested migration after entering Lower Granite Reservoir, but quickly grew into the mass threshold for migration and renewed migration. To examine this possibility, we used the reservoir growth model to model growth of both ocean-type and reservoir-type fish predicted to arrest migration and recorded the number of days required to reach the mass threshold and renew migration. The 1,796 ocean-type fish modeled to arrest migration took 5.8 days on average to grow to the mass threshold for migration; the 689 reservoir-type fish took 7.4 days on average. A Welch two-sample T-Test of the distributions of growth times between ocean-type and reservoir-type fish returned a T statistic of -11.3 with a P value less than 0.001, indicating that the difference in means is very statistically significant. This means that ocean-type fish are modeled to renew migration more quickly than reservoir-type fish after arresting migration in Lower Granite Reservoir.

Since these comparisons were conducted with a sample of fish that were mostly hatchery-spawned, it was decided to conduct the same tests on the smaller subset of only wild-reared fish. For each fish, three different model outcomes were possible. Firstly, a fish could be modeled to initiate migration via the *Mcrit* threshold (mass > *Mcrit*); this means the fish is not eligible to arrest migration and is modeled to be ocean-type. Secondly, a fish could initiate migration via the *Gcrit* threshold (growth efficiency < *Gcrit*), but not be modeled to arrest migration after reservoir entry (growth efficiency stays < *Gcrit*); this also results in a modeled ocean-type life

history as the fish is not modeled to arrest migration. The last possible model outcome is when a fish initiates migration via the *Gcrit* threshold and is then modeled to arrest migration after entering Lower Granite Reservoir; this outcome is a modeled reservoir-type life history. The model complex was used to predict migration initiation and growth after reservoir entry for the 728 confirmed ocean-type and 374 confirmed reservoir-type wild fish. Figure 5.7 displays the resulting life histories predicted by the model complex. Overall, the results were similar to those from the larger dataset including hatchery fish; majorities of fish of both life history types were correctly modeled to follow the right life history. Of 728 confirmed ocean-type fish, 425 migrated by *Mcrit*, and 72 migrated by *Gcrit* but did not arrest migration, resulting in 497 fish correctly modeled to be ocean-type. 231 ocean-type fish were modeled to arrest migration, incorrectly modeled to be reservoir-type. Of 374 confirmed reservoir-type wild fish, 88 migrated by Mcrit and 16 migrated by Gcrit but were not modeled to arrest migration, resulting in 104 fish incorrectly modeled to be ocean-type. 270 known reservoir-type fish were correctly modeled to arrest migration. Overall, 68% of known ocean-type fish and 72% of known reservoir-type fish were modeled to follow the correct life history.

5.4 Conclusions

Our modeling exercises identified statistically significant differences between ocean-type and reservoir type fish, and these differences are in the directions suggested by the theory informing our models. Fewer reservoir-type fish are modeled to grow larger than the mass threshold for migration initiation in-river (Table 5.15), more reservoir-type fish are modeled to arrest migration after entering Lower Granite Reservoir (Table 5.16), and reservoir-type fish take longer to reach the mass threshold for migration initiation after arresting migration. However,

while all of these differences are statistically significant, they are not extremely clear-cut. Based on our theory for migration initiation, we would expect ocean-type fish to reach the mass threshold for migration during the rearing period, meaning that they have no reason to arrest migration even if their growth efficiency improves after entering Lower Granite Reservoir. Two thirds of the ocean-type fish fall into this category, but a third does not, and a significant number of the remaining third are modeled to arrest migration, contrary to what we expect based on theory. Similarly perplexing, a significant portion of the confirmed reservoir-type fish do fall into this category, and will never be modeled to arrest migration by our models despite the fact that we know from data these fish did arrest migration. These disparities between theory and portions of the model predictions could simply be the result of imperfections in our modeling; the statistics produced for the reservoir comparisons are the result of a complex of models tracking in-river growth, consumption rate, migration initiation, converting fish length and mass, etc. None of these models are perfect; a number of assumptions and simplifications were made in the construction of each one, and it would not be surprising if the additive error were responsible for at least some of the disparity between theory and results.

Another possibility is that some of these reservoir-type fish really are reaching the mass threshold for migration, but are not initiating migration because the timing is off. Previous research into salmon migration has postulated that certain periods are important to successful migration (Scheuerell et al. 2009, Spence and Hall 2010); the theoretical framework proposed by Thorpe et al. (1998) and expanded upon by Mangle and Satterthwaite (2008) explicitly incorporates this idea by defining the ‘decision window’ when an individual decides whether to migrate and the actual initiation of migration as distinct points in time. Our modeling has shown that the reservoir-type fish tend to proceed on a later time schedule than ocean-type fish;

reservoir-type fish are tagged later (presumably indicating later emergence), they initiate migration later, they grow more slowly resulting in smaller mass at migration (Table 5.10), and they take longer to reach the migration mass threshold once in the reservoir. It is possible that a period analogous to the decision window exists for fall Chinook salmon, and reservoir-type salmon do not renew migration after reaching the threshold mass because the decision window has already passed by the time they reach it. This speculation is supported by empirical evidence of the size of reservoir-type migrants. Reservoir-type fish captured while migrating in the spring are much larger than ocean-type migrants; ocean-type smolts averaged 139 mm fork length, while reservoir-type smolts averaged 222 mm (Connor et al. 2005). These fish have clearly been much larger than the ocean-type migrants for a significant amount of time, as it is assumed that they do not grow very much during the winter months. The fact that they did not renew migration until the spring despite this size difference indicates that more than just a mass threshold is required for migration initiation, and the consistent timing difference in their early life history suggests that correct timing of reaching the bioenergetic thresholds is important.

5.4.1 The Ecology of Initiation of Migration in Fall Chinook Salmon

Previous research has broadly indicated that bioenergetic factors, including growth opportunity and growth rate, are the primary determinants of life history in salmonids, and that temperature plays a central role by impacting these bioenergetic factors (Brannon et al. 2004). Additional previous work has identified relationships between these factors and salmonid life history at various scales (Hutchings and Jones 1998, Metcalfe 1998, McCormick et al. 1998, Morinville and Rasumssen 2003), such as the model of Chinook life history created by Jager et al. (1997), in which timing of smoltification is triggered by accumulated degree-days- a proxy

for growth that incorporates temperature. The next steps to build on this research are to identify physiological mechanisms that quantify how environmental factors and biological processes interact to result in behavior, and how behavior and habitat combine to result in a particular life history strategy (Mangel and Satterthwaite 2008). The primary goal of this Master's research was to do this specifically for Snake River fall Chinook salmon; to create and parameterize a mechanistic model of migration initiation in fall Chinook and use this model to explore differences between the ocean-type and reservoir-type life history.

Starting with goals similar to our research, Thorpe et al. (1998) linked growth opportunity to life history via a quantitative theoretical framework incorporating bioenergetics in a model to predict salmon migration. We applied parts of this theory as the mass-based migration threshold of the Mass-Growth Model. This mass threshold represents the preparedness of a fish to undertake and survive migration to the ocean (Thorpe et al. 1998, Mangel and Satterthwaite 2008). Theoretical justifications for this threshold process involve balancing the relative benefits of staying in a freshwater environment versus a marine environment while taking into account the cost of and risk of mortality during the migration event- i.e., it is a sort of extension and physiological representation of a fitness maximization model (Werner and Gilliam 1984, Thorpe et al. 1998). For salmon, the ocean environment offers much greater growth opportunity than the freshwater environment, meaning that earlier migration to the ocean will yield benefits in the form of faster lifetime growth (Quinn 2005). However, migration is energetically costly, and exposure to size-selective predators during migration and after ocean entry means that larger size at migration confers significant survival benefits (Anderson et al. 2005, Duffy and Beauchamp 2008, Weitkamp et al. 2011). Thus, the mass threshold for migration represents a point of optimal fitness where the tradeoffs of migrating at a smaller mass are balanced with the benefits

of reaching the ocean earlier; as a genetic threshold, the optimal selection of the threshold magnitude occurs via evolutionary processes (Thorpe et al. 1998). The key to the operation of this mass threshold is that it is a process that operates within the physiology of individual fish, thus the fish needs no outside source of information to act on the threshold (Thorpe et al. 1998, Mangel and Satterthwaite 2008). In our modeling, the fitted values of the mass threshold ranged from around 7 grams to more than 11 grams (Table 3.7); this equates to roughly 80-100 mm fork length. The theory motivating this threshold suggests that fish larger than these fitted sizes should be prepared to initiate migration and smoltification. However, the fits span a fairly wide range; since these values are the independent fits of different years of data, they perhaps indicate phenotypic plasticity in the mass threshold responding to yearly variation in environmental conditions. Previous research has also hypothesized that significant plasticity exists in Chinook life history traits (Williams et al. 2008). Field data and prior research supports the values of the mass threshold we fitted in our modeling. Lower Granite Dam is the first location outside of the rearing habitat where juvenile fall Chinook are recaptured and remeasured (i.e., it is the earliest measure of the size of fall Chinook after initiating migration); in the PIT dataset used in our modeling, the minimum fork length of fall Chinook recaptured at Lower Granite Dam was 71 mm; however, of 1,156 fish recaptured, just 12 were smaller than 100 mm fork length, and the average fork length was 140 mm. Spring Chinook juveniles typically become active migrants between 80-120 mm fork length (Bjornn 1971). Additionally, a prior model of fall Chinook life history estimated a minimum size for smoltification of 70 mm (Jager et al. 1997).

However, as discussed in Chapter 3 of this thesis, the mass threshold alone was not sufficient to explain migration initiation in juvenile fall Chinook. We expanded upon the theory of Thorpe et al. to add a second bioenergetic process that can initiate migration: growth

efficiency. This process operates in the reverse of the theoretical underpinnings for the mass threshold; mass is treated as a requirement for successful migration, where surpassing the threshold indicates that a fish is biologically prepared to initiate migration. Growth efficiency, we propose, acts as an indicator of the favorability of the current environment to the fish, and dropping below a certain threshold indicates that the environment is becoming too hostile- the fish must initiate migration regardless of its bioenergetic preparedness. In particular, since growth efficiency is a bioenergetic process that is strongly sensitive to the high water temperatures that are stressful to Chinook salmon (see Figure 5.6), our research demonstrates that it can be used as an individually-based trigger to allow fish to avoid these unfavorable conditions. Previous work supports the theoretical basis for this process; Bellgraph et al. (2009) demonstrated in the laboratory that increasing temperatures will induce movement behavior in Chinook salmon, and several field studies have shown that in the wild, juvenile and adult Chinook salmon behaviorally avoid high water temperatures (Sauter et al. 2001, Goniea et al. 2006, Tiffan et al. 2009). The growth efficiency thresholds fitted in the most successful version of the Mass-Growth model (the Mass, Growth & Catchability version) are quite consistent; with the exception of 1994 and 1996, the fitted coefficients are around 0.3 (see Table 3.7). Since each year of data was fitted independently, the consistency of these fits indicates the suitability of a growth efficiency process for describing migration initiation. The magnitude of the resulting fits also bears some scrutiny; for consumption rates ranging from 0.5 to 0.7, the intersection with growth efficiency of 0.3 occurs at water temperatures between 17 and 19 degrees Celsius (Figure 5.6). As the mean fitted in-river consumption rate is 0.56, this means that the average fish in our model will be predicted to initiate migration via the growth efficiency threshold when temperatures exceed about 18 degrees Celsius (varying slightly depending on the exact growth

efficiency threshold fitted in a given year and the individual's mass). The theory informing the growth efficiency threshold indicates that this means that, for an average fish, water temperatures above about 18 degrees begin to become too stressful, and the growth opportunity available too low, to justify continued occupation of the current habitat. Empirical evidence from field studies supports this conclusion. Connor et al. observed that juvenile fall Chinook move offshore and become inaccessible to beach seine when river temperatures exceeded 18 degrees Celsius (Connor et al. 2002); presumably, these fish were initiating migration. Additionally, Tiffan et al. (2009) found that juvenile Chinook behaviorally selected temperatures from 16-20 degrees Celsius when in Lower Granite Reservoir. While the upper end of this temperature range is near or somewhat over the threshold we fitted in our modeling, Tiffan et al. also found that fish tended to increase their rate of downstream movement when they were occupying the upper end of this temperature range, as our modeling proposes.

In combination, the mass and growth efficiency thresholds parameterized in our modeling and the theory informing these thresholds reveal some patterns in predicted migration initiation of fall Chinook salmon. Firstly, the two processes for migration initiation produce different patterns in predicted migration. The mass threshold of the Mass-Growth model predicts migration in a diffuse, gradual pattern spread out over the rearing season (Figures 3.11, 3.12). This pattern arises due to individual differences in emergence date or growth rate, with individuals that emerge earlier or grow more rapidly reaching the threshold sooner, and vice versa. This result is fairly natural, and agrees with the theory of prior researchers. Brannon et al. proposed that much of the variation in salmon life history arises due to variation in growth opportunity; this was represented mechanistically via a mass threshold by Thorpe et al. (1998) and quantified by this research with the mass threshold in the Mass-Growth model. However,

The work of Brannon et al. and Thorpe et al. generally refers to timescales of a year or more, wherein faster or slower growth results in migration in an earlier year or a later year; in contrast, our modeling shows the same pattern, but on a much shorter timescale within a single rearing season. This difference between how prior researchers applied the mass threshold and how we apply it is important, as the within-season timing of when fish reach the mass threshold has consequences for Snake River fall Chinook due to the temperature regime of the rearing habitat. These consequences are made clear by the second migration initiation process in the Mass-Growth model- the growth efficiency process. The growth efficiency process shows markedly different patterns in the migration initiation predicted by the model (Figures 3.11, 3.12). While the mass process predicts gradual, diffuse migration initiation, the growth efficiency process predicts that almost all individuals initiate migration in a single, condensed group over a short period of just a few days. The fits of observed CPUE data indicate that this pulse of growth-efficiency driven migration occurs at the end of the rearing season, driving all remaining fish out of the rearing habitat; the theory motivating the threshold indicates that this point is when the river habitat has become too hostile to remain in due to rising temperatures. Thus, in the context of both processes operating simultaneously, the emergence timing and growth rate of individual fish has important consequences with regard to which process will ultimately result in migration. If a fish emerges too late or grows too slowly, it will be unable to reach the mass threshold before the growth efficiency threshold kicks in; these fish might be much smaller than the desired size for migration, but they have no choice other than to leave the rearing habitat.

5.4.2 The Reservoir-Type Life History and Reservoirs as Thermal Refuges

The recent emergence of the reservoir-type life history in juvenile fall Chinook in the Snake River is not yet completely understood, and it is important to proper management and recovery of the Snake River population to gain a better understanding of how and why this life history tactic operates (Connor et al. 2005, Williams 2008). Our modeling works towards this goal; we proposed, quantified, and tested individually-based, physiological mechanisms to explore juvenile fall Chinook life history by applying theory and trends identified by other researchers. Prior research outlines some general concepts for why the reservoir-type life history has emerged. In general, it is thought that changes in the timing of the fall Chinook rearing season has resulted in a desynchronization of salmon preparedness to migrate and the appropriate seasonal period to undergo migration (Williams et al. 2008). Dam construction denied fall Chinook access to their historical spawning grounds; salmon in the current habitat emerge from the gravel later, grow more slowly, and initiate migration later than before the dams were constructed (Krcma and Raleigh 1970, Connor et al. 2002, Connor and Burge 2003). These changes, along with slower juvenile migration through reservoir habitat as opposed to free-flowing habitat, have resulted in later passage of migrating juvenile fall Chinook salmon; currently, the majority of migrants pass Lower Granite Dam in July (Connor et al. 2002, Smith et al. 2003), about a month later than historically (Mains and Smith 1964). These delays in the timing of the juvenile life history have potentially severe consequences, as it is thought that the timing of arrival to the ocean is very important to survival (Scheuerell et al. 2009, Spence and Hall 2010), and migration during peak summer temperatures in August would expose juveniles to very stressful conditions throughout the Columbia and Snake Rivers (Sauter et al. 2001, Tiffan et al. 2003). Williams et al. (2008) proposed that the reservoir-type life history is likely to be

adopted by fish which have their timing and growth schedule delayed to the point that this synchronization is no longer likely. Our modeling of ocean-type and reservoir-type fall Chinook juveniles supports the hypothesis proposed by Williams et al. We found that, on average, juveniles that followed a reservoir-type life history had been tagged later and at smaller sizes than ocean-type juveniles, and our models of migration initiation predicted that reservoir-type juveniles initiate migration later on average as well (Tables 5.10, 5.12, 5.13, 5.14). Additionally, our modeling supports the hypothesis that fish that end up following a reservoir-type life history are not ready to migrate during their first summer. Our Mass-Growth model proposes that the mass threshold indicates preparedness to migrate; when we examined how ocean-type and reservoir-type fish were initiating migration, we found that a majority of ocean-type fish had surpassed the mass threshold for migration; in contrast, a majority of the reservoir-type fish did not surpass the mass threshold for migration, and were instead forced to initiate migration due to unfavorable environmental conditions- the growth efficiency threshold (Figure 5.7).

Habitat conditions in the reservoir provide the other half of the reservoir-type life history puzzle. Previous research has identified reservoirs and the temperature regimes in them as important thermal refuges during the summer months (Sauter et al. 2001, Tiffan et al. 2009). Our modeling provides physiologically-based, mechanistic explanations for why these behaviors occur. Water temperatures within the free-flowing portion of the Snake River upstream of the confluence with the Clearwater River are fairly homogenous (Anderson et al. 2000); meaning that when river temperatures rise above about 18 degrees Celsius, our Mass-Growth model predicts that juvenile Chinook throughout the rearing habitat are all forced to initiate migration via the growth efficiency process. In the absence of any habitat favorable for growth downstream of the rearing habitat, our model would predict that all fish would continue migration to the

ocean at this point, regardless of whether or not they had grown larger than the mass threshold. However, Lower Granite Reservoir receives significant input of cool water from the Clearwater River, supplemented by flow releases from Dworshak Dam on the Clearwater River (Cook et al. 2006). This significantly cooler water generally remains below 18 degrees Celsius year-round; peak summer temperatures do reach up to 19 degrees in some years. This cool water input partially mixes with warm Snake River water, but significant thermal stratification is observed within the impounded areas of Lower Granite Reservoir (Cook et al. 2006, Tiffan et al. 2009). Critically, radio tagging observations of juvenile fall Chinook have shown that individuals preferentially occupy cooler water in the thermocline around 17 degrees, and avoid the warmest water at the surface in Lower Granite Reservoir (Tiffan et al. 2009). This means that, in the context of our Mass-Growth model, fish that were forced to initiate migration within the rearing habitat by unfavorable temperatures can find favorable temperatures after entering Lower Granite Reservoir, resulting in modeled cessation of migration and a reservoir-type life history. In essence, our model quantifies a mechanism for why Lower Granite Reservoir and other reservoirs with thermally stratified water columns provide refuges for juvenile salmon that are not yet prepared to migrate, enabling the reservoir-type life history.

While we have represented migration as a simple on/off switch in our modeling for simplicity and ease of parameter estimation, the truth is that a continuum of migratory behavior and life history strategies exists in salmonids. Previous theory has noted the existence and importance of this continuum in the context of researching and managing salmonids (Thorpe et al. 1998, Mangel and Satterthwaite 2008). Previous research on Columbia basin salmon has demonstrated this continuum; Connor et al. (2003) identified four distinct migratory phases in juvenile fall Chinook, incorporating periods of continuous and discontinuous movement. Spring

Chinook commonly undertake partial migration into mainstem rivers as parr prior to the onset of the smolting migration (Bjornn 1971). This continuum of behavior applies to reservoir-type fall Chinook salmon; while we model these fish as arresting migration, reservoir-type juveniles still disperse downstream discontinuously throughout fall and winter. Few data exist on the passage rates of fall Chinook during these periods, as PIT tag detection systems in the Snake and Columbia Rivers are operated irregularly during the fall and dewatered completely during the winter (Marsh et al. 2004); however, what data exists shows that some fish do pass dams during fall and winter (Connor et al. 2004). Thus, migration may not be completely suppressed in reservoir-type individuals, or the fish may merely be dispersing downstream as passive particles. Our modeling does not implicitly capture this detail in its current form; however, an extension incorporating spatially-explicit movement rules or a hydrodynamic model could test the discontinuous downstream movement of reservoir-type fish. Though our modeling does not incorporate it, seasonal and timing considerations are very important to understanding the totality of the reservoir-type life history in fall Chinook salmon. A second complication of the reservoir-type life history that our modeling does not capture is the suppression of migration after arresting it in the reservoir. Reservoir-type fish continue to grow rapidly through the summer and fall, and at migration the following spring they are much larger than ocean-type smolts (Connor et al. 2005). Clearly these fish surpassed the mass threshold for migration sometime the previous year, but they did not renew migration and reach the ocean until spring. The ultimate reasons for the timing of ocean entry are clear; survival is highest during seasons when ocean conditions are most favorable (Schuerell et al. 2009, Petrosky and Schaller 2010, Spence and Hall 2010), however, an individually-based mechanism is necessary to represent this. Previous research has identified photoperiod as a potential mechanism individuals could use to time behavioral

switches (McNamara et al. 2011), and previous models of salmon life history have used photoperiod to time migration initiation (Thorpe et al. 1998). An extension of our Mass-Growth migration initiation model could incorporate a photoperiod based switch to inhibit migration after a certain point, which would capture why reservoir-type juveniles do not renew migration even though they may surpass the mass threshold for migration by late summer or fall.

5.4.3 Management Implications

The impounded water of the reservoir and the cool-water input from flow releases from Dworshak Dam are both critical to creating the stratified water column that provides juvenile fall Chinook a thermal refuge from high summer temperatures. While there is some variability by year and individual, our modeling predicts that temperatures very much above 19 to 20 degrees Celsius will likely force all juvenile Chinook to initiate migration, even if they are not physiologically prepared to migrate. Summer temperatures in the Snake River already reach well above this level, but in many years peak Clearwater River temperatures also approach this level. If managers of the Columbia River hydropower system wish to enable the continued existence of the reservoir-type life history, then our models suggest that at least some pool of water below about 18 degrees Celsius must be maintained within Lower Granite Reservoir or other reservoirs for the duration of the summer. If the thermal refuge fails, our model would predict that fish occupying it would be forced to renew migration. To prevent this occurrence will require careful management of water resources within the Snake River Basin; this is especially important in light of predicted climate changes in the Pacific Northwest (Schindler et al. 2008).

Enabling the reservoir-type life history in juvenile fall Chinook may be desirable for several reasons. Firstly, our models and the theory behind them suggest that fish that are

initiating migration via the growth efficiency threshold are not doing so because they are bioenergetically prepared to migrate, but to escape adverse local conditions. If there were no thermal refuges and these fish were forced to complete their ocean migration as subyearlings, they would likely experience high mortality from a number of sources. Firstly, fish migrating in late summer would be exposed to maximum summer temperatures throughout the Snake and Columbia Rivers and would incur significant thermal stress (Sauter et al. 2001, Smith et al. 2003); the work of Tiffan et al. (2003) demonstrates how much thermal stress fish can be exposed to in a homothermic reservoir. Secondly, these fish would likely be exposed to severe predation mortality during their migration due to their smaller size than fish that initiated migration due to the mass threshold and due to warm temperature regimes that favor salmon predators (Vigg et al. 1991, Petersen and Kitchell 2001). Lastly, these fish would be reaching the ocean at a non-ideal time in very late summer or fall, and would likely suffer severe mortality in the ocean (Duffy and Beauchamp 2008, Petrosky and Schaller 2010, Spence and Hall 2010, Weitkamp et al. 2011). In addition to this, recent research has demonstrated that reservoir-type juveniles have a high smolt-to-adult return ratio and potentially higher fitness than ocean-type juveniles (Williams 2008, Marsh et al. 2010). In light of the threatened status of Snake River fall Chinook, managers may wish to support the reservoir-type life history by maintaining thermal refuges during the summer, as lack of thermal refuges could have severe consequences for reservoir-type juveniles.

5.5 Chapter 5 Tables

Table 5.1

Table of individually fitted consumption rates resulting Mass-Growth model predicted reservoir entry. Year is the year in which the fish were tagged; # Fish is the number of fish in each year for which all necessary data was present and a consumption rate within Lower Granite Reservoir could be individually fitted. The mean and variance of the resulting fitted consumption rates is presented for each year.

Year	# Fish	Mean Fitted P	Variance in Fitted P
1992	2	0.77	0.016
1993	29	0.90	0.020
1994	8	1.13	0.17
1995	71	0.90	0.035

Table 5.2

Table of individually fitted consumption rates resulting Age-Growth model predicted reservoir entry. Year is the year in which the fish were tagged; # Fish is the number of fish in each year for which all necessary data was present and a consumption rate within Lower Granite Reservoir could be individually fitted. The mean and variance of the resulting fitted consumption rates is presented for each year.

Year	# Fish	Mean Fitted P	Variance in Fitted P
1992	2	0.80	0.026
1993	29	0.97	0.038
1994	30	1.40	0.099
1995	71	0.94	0.052

Table 5.3

Summary of the full MGRC model, the multivariate linear model of consumption rate in Lower Granite Reservoir using Mass-Growth modeled migration. T0 is the day a fish was tagged, M0 is the fish's mass on the tag day in grams, T2m is the modeled day a fish initiates migration predicted by the Mass-Growth model, and M2m is the fish's modeled mass predicted by the Wisconsin bioenergetics model on day T2m. T0 CPUE is the CPUE at the tag site on the tag date, CPUE^2 is a squared term of CPUE, T0 Temp is the daily mean temperature of the Snake River on the tag date, and Temp^2 is a squared term of temperature. T2 Temp 1, 2, and 3 are indices of temperature in Lower Granite Reservoir. T2 Temp 1 is the daily mean temperature of the scroll case reading at Lower Granite Dam on day T2m. T2 Temp 2 is the mean temperature for the first week after day T2m. T2 Temp 3 is the mean temperature for the first month after day T2m. Squared terms for all three temperature indices are included. T0:M0 and T2m:M2m are interaction terms. No parameter estimates are significantly different from zero at the 0.05 level.

Predictor	Estimate	Std. Error	T Statistic	P
Y-Intercept	-1.231	3.555	-0.346	0.730
T0	-0.00135	0.00462	-0.292	0.771
M0	-0.367	0.472	-0.777	0.439
T2m	0.00151	0.00465	0.324	0.747
M2m	0.150	0.307	0.487	0.627
T0 RKM	-0.000383	0.000522	-0.733	0.466
T0 CPUE	0.00190	0.00738	0.255	0.800
CPUE^2	-0.000120	0.000322	-0.373	0.710
T0 Temp	0.243	0.180	1.350	0.180
Temp^2	-0.00958	0.00682	-1.405	0.163
T2 Temp1	-0.500	0.333	-0.157	0.875
T2 Temp1^2	0.0162	0.0115	0.253	0.801
T2 Temp2	-0.0669	0.426	0.854	0.395
T2 Temp2^2	0.00350	0.0138	-0.622	0.535
T2 Temp3	0.289	0.338	-1.503	0.136
T2 Temp3^2	-0.00640	0.0103	1.409	0.162
T0:M0	0.0000286	0.0000370	0.773	0.442
T2m:M2m	-0.0000143	0.0000244	-0.583	0.561
			r^2: 0.458	**Adjusted r^2: 0.358**
			AIC: -379.7	**Parameters: 18**

Table 5.4

Summary of the reduced MGRC model, the multivariate linear model of consumption rate in Lower Granite Reservoir using Mass-Growth modeled migration. M2m is the fish's modeled mass predicted by the Wisconsin bioenergetics model on day T2m. T0 Temp^2 is the daily mean temperature in the Snake River on the day the fish was tagged, squared. T2 Temp 1 and 3 are indices of temperature in Lower Granite Reservoir. T2 Temp 1 is the daily mean temperature of the scroll case reading at Lower Granite Dam on day T2m. T2 Temp 3 is the mean temperature for the first month after day T2m. The squared term for T2 Temp 1 was retained. All parameter estimates are significantly different from zero at the 0.05 level.

Predictor	**Estimate**	**Std. Error**	**T Statistic**	**P**
Y-Intercept	4.475	1.073	4.169	6.4e-5
M2m	-0.0246	0.00724	-3.403	0.00095
T0 Temp^2	-0.00108	0.000446	-2.428	0.017
T2 Temp1	-0.627	0.0171	5.095	1.6e-6
T2 Temp1^2	0.0210	0.137	-4.569	1.4e-5
T2 Temp3	0.0870	0.00451	4.662	9.3e-6
			r^2: 0.405	**Adjusted r^2: 0.376**
			AIC: -393.5	**Parameters: 6**

Table 5.5

ANOVA Table of the reduced MGRC model, the multivariate linear model of consumption rate in Lower Granite Reservoir using Mass-Growth modeled migration. M2m is the fish's modeled mass predicted by the Wisconsin bioenergetics model on day T2m. T0 Temp^2 is the daily mean temperature in the Snake River on the day the fish was tagged, squared. T2 Temp 1 and 3 are indices of temperature in Lower Granite Reservoir. T2 Temp 1 is the daily mean temperature of the scroll case reading at Lower Granite Dam on day T2m. T2 Temp 3 is the mean temperature for the first month after day T2m. The squared term for T2 Temp 1 was retained. The F-statistics of T2 Temp 1 and T2 Temp 3 are significant at the 0.05 level; all other predictors are not statistically significant. All predictors combined explain 1.873 of 4.361 total variance in the response variable, fitted consumption rate.

Predictor	D.F.	SS	Mean SS	F	P
M2m	1	0.0146	0.0146	0.549	0.46
T0 Temp^2	1	0.00063	0.00063	0.0237	0.88
T2 Temp 1	1	1.273	1.273	48.017	3.6e-10
T2 Temp 1^2	1	0.00905	0.00905	0.341	0.56
T2 Temp 3	1	0.576	0.576	21.739	9.3e-6
Error	104	2.757	0.0265		
Total	109	4.631			

Table 5.6

Summary of the full AGRC model, the multivariate linear model of consumption rate in Lower Granite Reservoir using Age-Growth modeled migration. T0 is the day a fish was tagged, M0 is the fish's mass on the tag day in grams, T2a is the modeled day a fish initiates migration predicted by the Mass-Growth model, and M2a is the fish's modeled mass predicted by the Wisconsin bioenergetics model on day T2a. T0 CPUE is the CPUE at the tag site on the tag date, CPUE^2 is a squared term of CPUE, T0 Temp is the daily mean temperature of the Snake River on the tag date, and Temp^2 is a squared term of temperature. T2 Temp 1, 2, and 3 are indices of temperature in Lower Granite Reservoir. T2 Temp 1 is the daily mean temperature of the scroll case reading at Lower Granite Dam on day T2a. T2 Temp 2 is the mean temperature for the first week after day T2a. T2 Temp 3 is the mean temperature for the first month after day T2a. Squared terms for all three temperature indices are included. T0:M0 and T2a:M2a are interaction terms. No parameter estimates are significantly different from zero at the 0.05 level.

Predictor	Estimate	Std. Error	T Statistic	P
Y-Intercept	3.192	4.852	0.658	0.51
T0	-0.0181	0.0142	-1.278	0.20
M0	-0.0870	0.734	-0.119	0.91
T2a	0.0182	0.0142	1.276	0.20
M2a	-0.0418	0.469	-0.089	0.93
T0 RKM	0.0000655	0.000612	0.107	0.91
T0 CPUE	0.00516	0.00864	0.597	0.55
CPUE^2	-0.000127	0.000386	-0.328	0.74
T0 Temp	0.372	0.219	1.700	0.092
Temp^2	-0.0151	0.00815	-1.848	0.067
T2 Temp1	-0.172	0.279	-0.617	0.54
T2 Temp1^2	0.00639	0.00943	0.678	0.50
T2 Temp2	-0.431	0.371	-1.163	0.25
T2 Temp2^2	0.0131	0.0115	1.141	0.26
T2 Temp3	-0.205	0.542	-0.378	0.71
T2 Temp3^2	0.0105	0.0158	0.667	0.51
T0:M0	0.0000103	0.0000579	0.178	0.86
T2a:M2a	-0.00000059	0.0000368	-0.016	0.99
			r^2: 0.624	**Adjusted r^2: 0.568**
			AIC: -404.3	**Parameters: 18**

Table 5.7

Summary of the reduced AGRC model, the multivariate linear model of consumption rate in Lower Granite Reservoir using Age-Growth modeled migration. M2a is the fish's modeled mass predicted by the Wisconsin bioenergetics model on day T2a. T0 Temp is the daily mean temperature in the Snake River on the day the fish was tagged; T0 Temp^2 is the squared term. T2 Temp 2 and 3 are indices of temperature in Lower Granite Reservoir. T2 Temp 2 is the mean temperature of the scroll case reading at Lower Granite Dam for the first week after day T2a. T2 Temp 3 is the mean temperature for the first month after day T2a. The squared term for T2 Temp 2 was retained; the base term for T2 Temp 3 was dropped and only the squared term was retained. All parameter estimates except the intercept term are significantly different from zero at the 0.05 level.

Predictor	Estimate	Std. Error	T Statistic	P
Y-Intercept	3.738	2.358	1.585	0.11
M2a	-0.0380	0.00678	-5.608	1.3e-7
T0 Temp	0.420	0.193	2.173	0.032
T0 Temp^2	-0.0170	0.00727	-2.334	0.021
T2 Temp2	-0.800	0.270	-2.961	0.0037
T2 Temp2^2	0.0248	0.00826	3.007	0.0032
T2 Temp3^2	0.00476	0.000808	5.885	3.4e-8
			r^2: 0.597	**Adjusted r^2: 0.578**
			AIC: -417.2	**Parameters: 7**

Table 5.8

ANOVA Table of the reduced AGRC model, the multivariate linear model of consumption rate in Lower Granite Reservoir using Age-Growth modeled migration. M2a is the fish's modeled mass predicted by the Wisconsin bioenergetics model on day T2a. T0 Temp is the daily mean temperature in the Snake River on the day the fish was tagged; T0 Temp^2 is the squared term. T2 Temp 2 and 3 are indices of temperature in Lower Granite Reservoir. T2 Temp 2 is the mean temperature of the scroll case reading at Lower Granite Dam for the first week after day T2a. T2 Temp 3 is the mean temperature for the first month after day T2a. The squared term for T2 Temp 2 was retained; the base term for T2 Temp 3 was dropped and only the squared term was retained. The F-statistics of all predictors except T0 Temp^2 are significant at the 0.05 level. All predictors combined explain 7.466 of 12.499 total variance in the response variable, fitted consumption rate.

Predictor	D.F.	SS	Mean SS	F	P
M2a	1	1.389	1.389	34.50	3.6e-8
T0 Temp	1	0.200	0.200	4.97	0.028
T0 Temp^2	1	0.127	0.127	3.15	0.078
T2 Temp 2	1	4.096	4.096	101.73	< 2.2e-16
T2 Temp 2^2	1	0.260	0.260	6.45	0.012
T2 Temp 3^2	1	1.395	1.395	34.64	3.4e-8
Error	125	5.033	0.0403		
Total	131	12.499			

Table 5.9

Distribution of detections of wild juvenile fall Chinook by dam and by year. Total Detected = total number of fish detected in that year; numbers of detections at the various locations are not additive since fish can be detected at more than one location. LGD = Lower Granite Dam, LGS = Little Goose Dam, LMN = Lower Monumental Dam, IHA = Ice Harbor Dam, MCN = McNary Dam, JDA = John Day Dam, BON = Bonneville Dam, Traps = Snake and Clearwater River juvenile traps.

Year	Total Detected	LGD	LGS	LMN	IHA	MCN	JDA	BON	Traps
1992	68	39	20	0	0	9	0	0	1
1993	393	270	68	54	0	40	0	0	3
1994	340	202	60	64	0	52	5	0	1
1995	3479	2097	1344	1303	0	946	31	11	0
1996	203	145	76	45	0	27	2	1	0
1997	223	135	106	47	0	32	2	2	0
1998	1024	571	631	295	0	217	75	19	1
1999	1062	608	544	364	0	142	73	40	0
2000	507	336	269	145	2	142	31	11	1
Total	7299	4403	3118	2317	2	1607	219	84	7

Table 5.10

Table of overall mean values from data and modeled statistics for 6,889 confirmed ocean-type fish and 1,724 confirmed reservoir-type fish. The mean values of each statistic tested are presented for both ocean-type and reservoir-type categories; a Welch two-sample T-Test was performed between the distributions from the two life history types for each statistic. T0 and M0 are day of year of tagging and mass at tagging; T2m and T2a are the day of year of migration initiation predicted individually by the Mass-Growth model and the Age-Growth model respectively; M2m and M2a are the mass at migration initiation predicted by the in-river growth model, and MGRC P and AGRC P are the consumption rates in Lower Granite Reservoir predicted individually by the MGRC and AGRC consumption rate models.

Statistic	Ocean Type	Reservoir Type	T-Statistic	P
# Fish	6,889	1,724	-	-
T0	158.9	166.4	-27.2	< 2.2e-16
M0	7.39 g	5.27 g	32.9	< 2.2e-16
T2m	163.6	176.0	-46.6	< 2.2e-16
T2a	171.9	179.4	-33.1	< 2.2e-16
M2m	8.70 g	7.31 g	24.9	< 2.2e-16
M2a	11.19 g	8.13 g	40.8	< 2.2e-16
MGRC P	0.88	1.07	-38.0	< 2.2e-16
AGRC P	0.99	1.17	-29.6	< 2.2e-16

Table 5.11

Table of the number of confirmed ocean-type and reservoir-type fish in each year of data.

Year	# Ocean Type Fish	# Reservoir Type Fish
1992	6	3
1993	9	111
1994	3	108
1995	975	167
1996	19	11
1997	1163	863
1998	4384	403
1999	211	0
2000	119	58

Table 5.12

Table of mean values for the year 1995 from data and modeled statistics for 975 confirmed ocean-type fish and 167 confirmed reservoir-type fish tagged in 1995. The mean values of each statistic tested are presented for both ocean-type and reservoir-type categories; a Welch two-sample T-Test was performed between the distributions from the two life history types for each statistic. T0 and M0 are day of year of tagging and mass at tagging; T2m and T2a are the day of year of migration initiation predicted individually by the Mass-Growth model and the Age-Growth model respectively; M2m and M2a are the mass at migration initiation predicted by the in-river growth model, and MGRC P and AGRC P are the consumption rates in Lower Granite Reservoir predicted individually by the MGRC and AGRC consumption rate models.

Statistic	Ocean Type	Reservoir Type	T-Statistic	P
# Fish	975	167	-	-
T0	157.1	161.2	-7.0	3.2e-11
M0	4.52 g	4.42 g	0.77	0.45
T2m	169.3	172.5	-6.4	6.2e-10
T2a	171.7	175.4	-7.4	2.7e-12
M2m	7.24 g	6.92 g	3.0	0.0025
M2a	7.90 g	7.63 g	1.9	0.065
MGRC P	0.94	0.98	-5.3	2.7e-7
AGRC P	1.04	1.13	-7.4	3.3e-12

Table 5.13

Table of mean values for the year 1997 from data and modeled statistics for 1,163 confirmed ocean-type fish and 863 confirmed reservoir-type fish tagged in 1997. The mean values of each statistic tested are presented for both ocean-type and reservoir-type categories; a Welch two-sample T-Test was performed between the distributions from the two life history types for each statistic. T0 and M0 are day of year of tagging and mass at tagging; T2m and T2a are the day of year of migration initiation predicted individually by the Mass-Growth model and the Age-Growth model respectively; M2m and M2a are the mass at migration initiation predicted by the in-river growth model, and MGRC P and AGRC P are the consumption rates in Lower Granite Reservoir predicted individually by the MGRC and AGRC consumption rate models.

Statistic	Ocean Type	Reservoir Type	T-Statistic	P
# Fish	1,163	863	-	-
T0	164.1	167.5	-12.6	< 2.2e-16
M0	7.20 g	5.30 g	18.7	< 2.2e-16
T2m	169.9	179.6	-26.7	< 2.2e-16
T2a	175.9	180.3	-18.3	< 2.2e-16
M2m	8.70 g	7.79 g	14.8	< 2.2e-16
M2a	10.50 g	8.10 g	20.7	< 2.2e-16
MGRC P	0.93	1.08	-24.0	< 2.2e-16
AGRC P	1.01	1.11	-14.4	< 2.2e-16

Table 5.14

Table of mean values for the year 1998 from data and modeled statistics for 4,384 confirmed ocean-type fish and 403 confirmed reservoir-type fish tagged in 1998. The mean values of each statistic tested are presented for both ocean-type and reservoir-type categories; a Welch two-sample T-Test was performed between the distributions from the two life history types for each statistic. T0 and M0 are day of year of tagging and mass at tagging; T2m and T2a are the day of year of migration initiation predicted individually by the Mass-Growth model and the Age-Growth model respectively; M2m and M2a are the mass at migration initiation predicted by the in-river growth model, and MGRC P and AGRC P are the consumption rates in Lower Granite Reservoir predicted individually by the MGRC and AGRC consumption rate models.

Statistic	Ocean Type	Reservoir Type	T-Statistic	P
# Fish	4,384	403	-	-
T0	158.9	168.3	-26.6	< 2.2e-16
M0	8.21 g	5.70 g	20.8	< 2.2e-16
T2m	160.4	169.6	-29.4	< 2.2e-16
T2a	171.4	180.4	-31.1	< 2.2e-16
M2m	8.86 g	6.16 g	21.7	< 2.2e-16
M2a	12.19 g	8.46 g	26.0	< 2.2e-16
MGRC P	0.86	0.98	-31.3	< 2.2e-16
AGRC P	0.98	1.30	-31.3	< 2.2e-16

Table 5.15

Contingency table of life history type and the threshold of the Mass-Growth model that resulted in migration initiation date T2m. Of 6,889 ocean-type fish, 4340 initiated migration due to mass growing larger than *Mcrit*, while 2,549 initiated migration due to growth efficiency dropping below *Gcrit*. Of 1,724 reservoir-type fish, 864 initiated migration due to mass growing larger than *Mcrit*, while 860 initiated migration due to growth efficiency dropping below *Gcrit*. The Pearson's χ^2 test of independence is highly significant, indicating that life history affects the proportion of fish initiating migration by the two processes.

	Ocean-Type	**Reservoir-Type**	**Total**
Mcrit	4340	864	5204
Gcrit	2549	860	3409
Total	6889	1724	8613
	χ^2: 95.16		**P: < 2.2e-16**

Table 5.16

Contingency table of life history type and the number of fish which were modeled to arrest migration or continue migrating. Of 2,549 ocean-type fish which initiated migration via the *Gcrit* threshold and could arrest migration if their growth efficiency rose back above *Gcrit*, 1,798 were modeled to arrest migration, while 751 were modeled to continue migrating. Of 860 reservoir-type fish which initiated migration via the *Gcrit* threshold and could arrest migration if their growth efficiency rose back above *Gcrit*, 689 were modeled to arrest migration, while 171 were modeled to continue migrating. . The Pearson's χ^2 test of independence is highly significant, indicating that life history affects the proportion of fish which are modeled to arrest migration.

	Ocean-Type	**Reservoir-Type**	**Total**
Arrested Migration	1798	689	2487
Continued Migration	751	171	922
Total	2549	860	3409
	χ^2: 29.4		**P: 5.8e-8**

5.6 Chapter 5 Figures

Figure 5.1

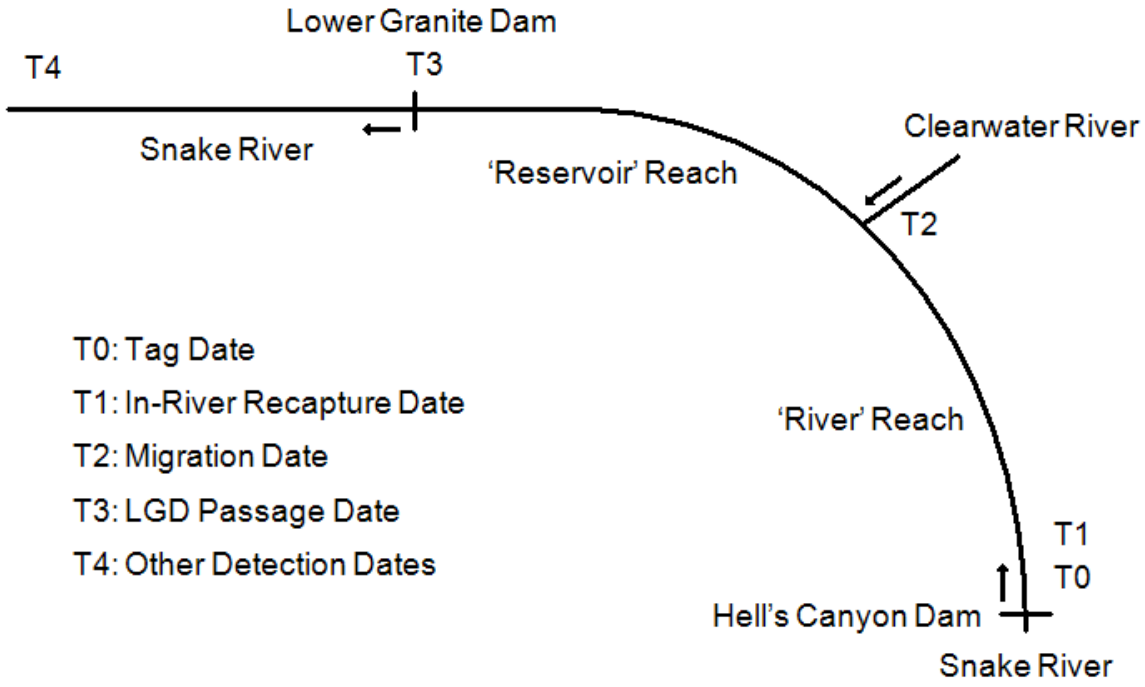

A diagrammatic depiction of the Snake River habitat relevant to our modeling. The direction of water flow and seaward migration of juvenile Chinook is indicated with arrows. The points important to our modeling are labeled; the Snake River habitat is broken into the 'River' and 'Reservoir' reaches, and the critical points in time T0-T4 indicate where in the habitat each event occurs.

Figure 5.2

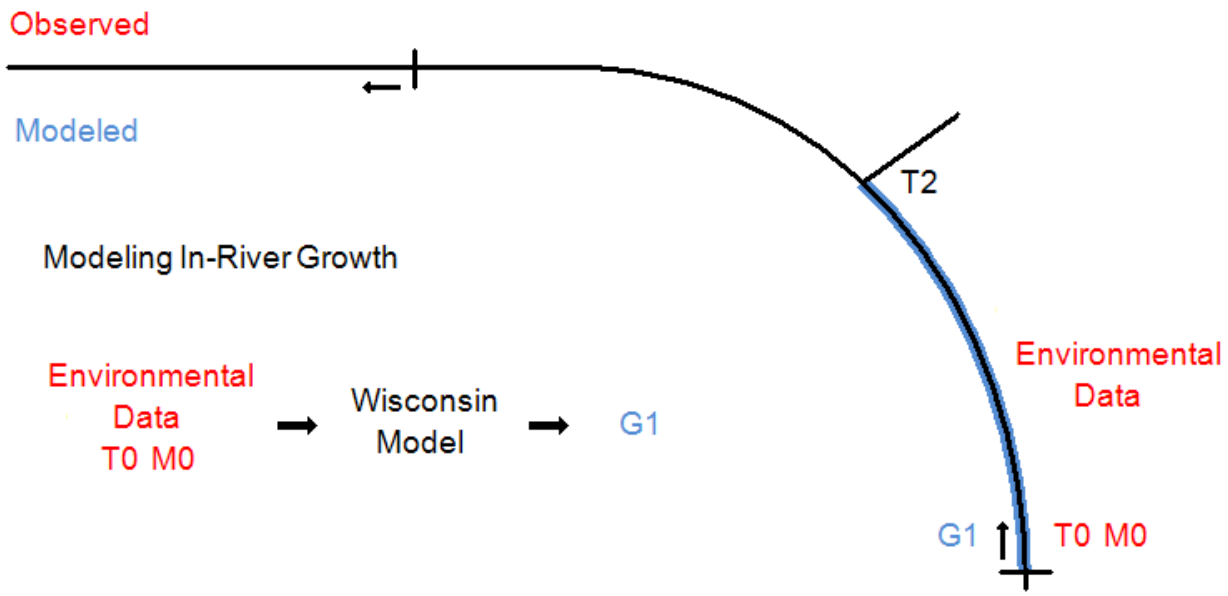

A diagrammatic depiction of our model of in-river growth. Tagging data for an individual fish and environmental data are input into the Wisconsin model, which produces modeled growth within the 'River' reach of the Snake River.

Figure 5.3

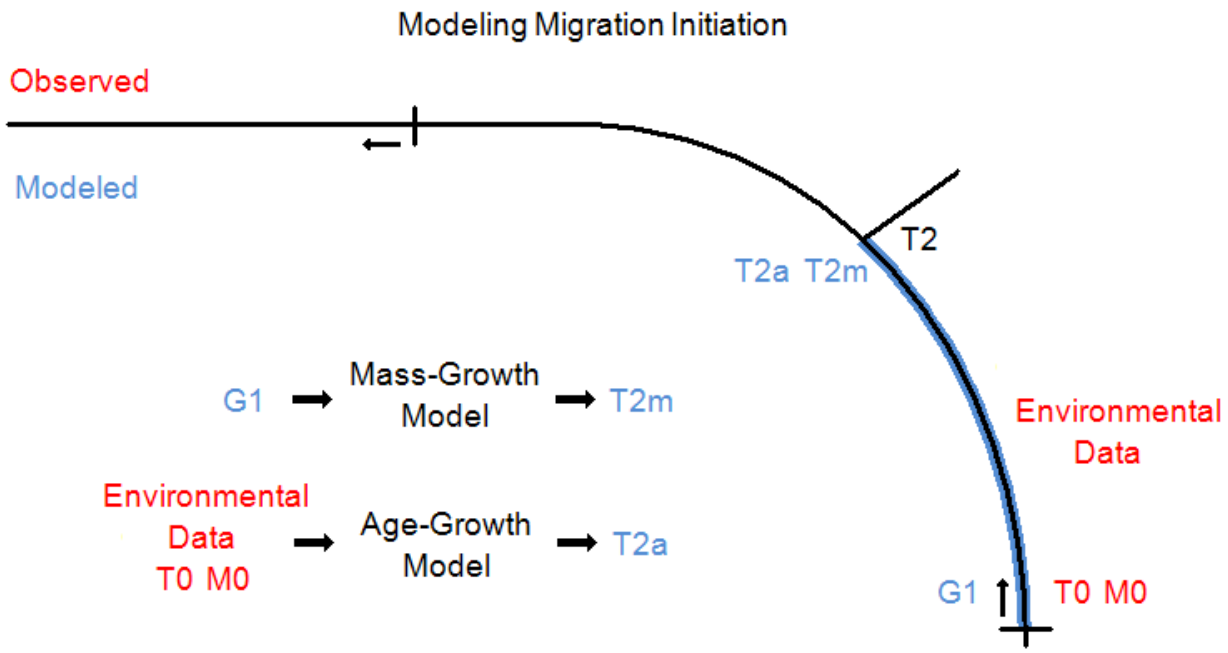

A diagrammatic depiction of our models of migration initiation. The Mass-Growth model uses a mechanistic process to predict day of migration initiation T2m from modeled growth and growth efficiency. The Age-Growth model uses a correlative model to predict day of migration initiation T2a using tagging and environmental data.

Figure 5.4

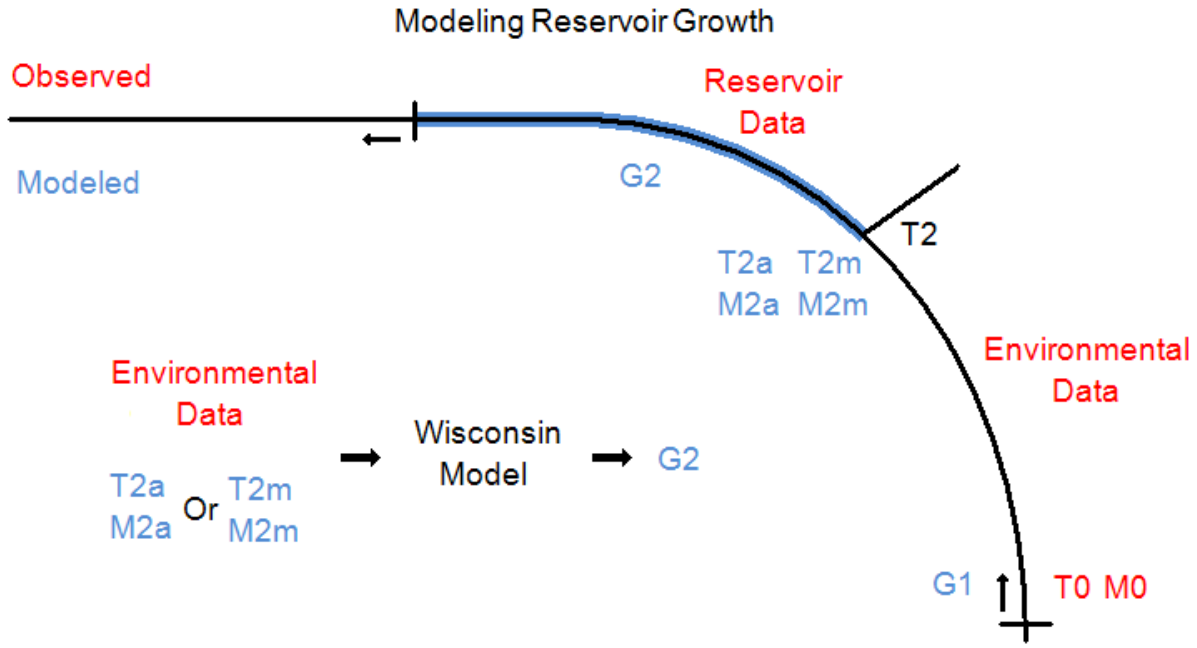

A diagrammatic depiction of the process of modeling growth in Lower Granite Reservoir. Environmental data from the reservoir and a starting time and mass generated from either the Mass-Growth or Age-Growth models are used as inputs to the Wisconsin Bioenergetics Model, which predicts growth. Environmental data in the reservoir includes temperature data from the scroll case reading at Lower Granite Dam and prey energy density.

Figure 5.5

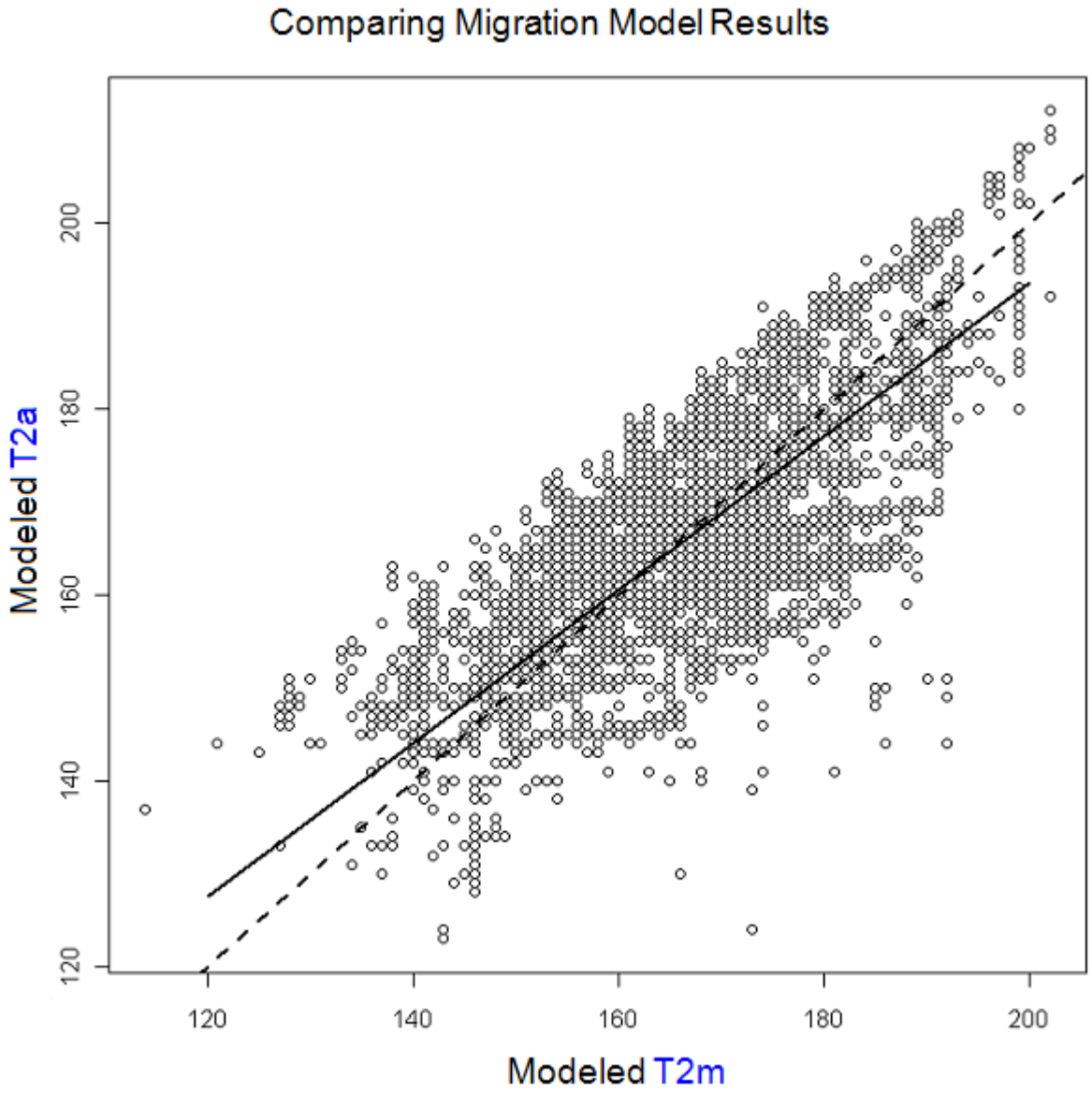

Comparison of the day of year of modeled T2a predicted by the Age-Growth model and modeled T2m predicted by the Mass-Growth model for a set of 7,438 fish. The one-to-one line is shown dashed. The solid line is the least-squares fitted linear model resulting from regressing modeled T2a against modeled T2m.

Figure 5.6

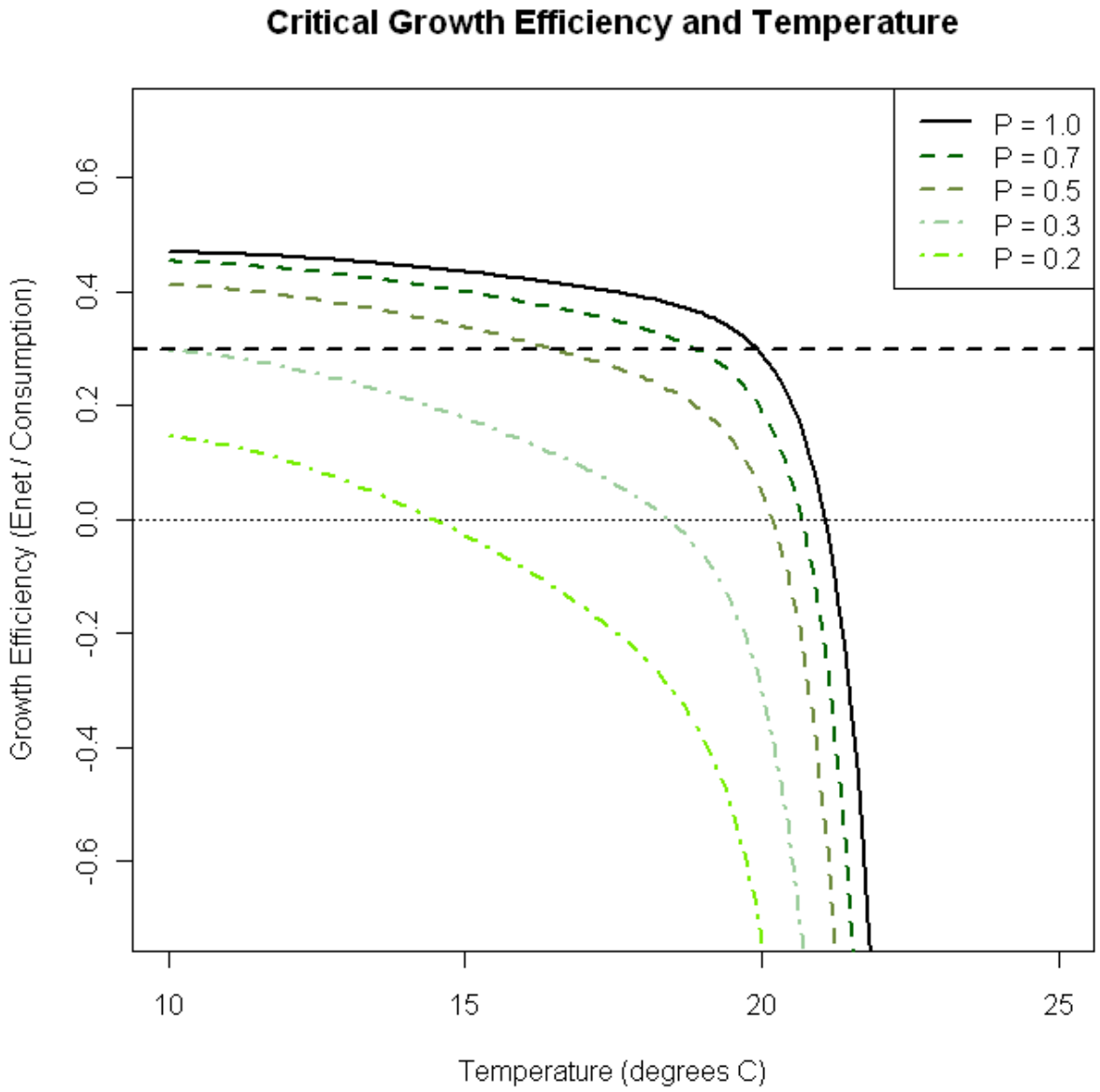

Plot of growth efficiency vs. temperature for multiple possible consumption rates (P). Growth efficiency of zero is the light dotted line; growth efficiency of 0.3 is the dark dashed line.

Figure 5.7

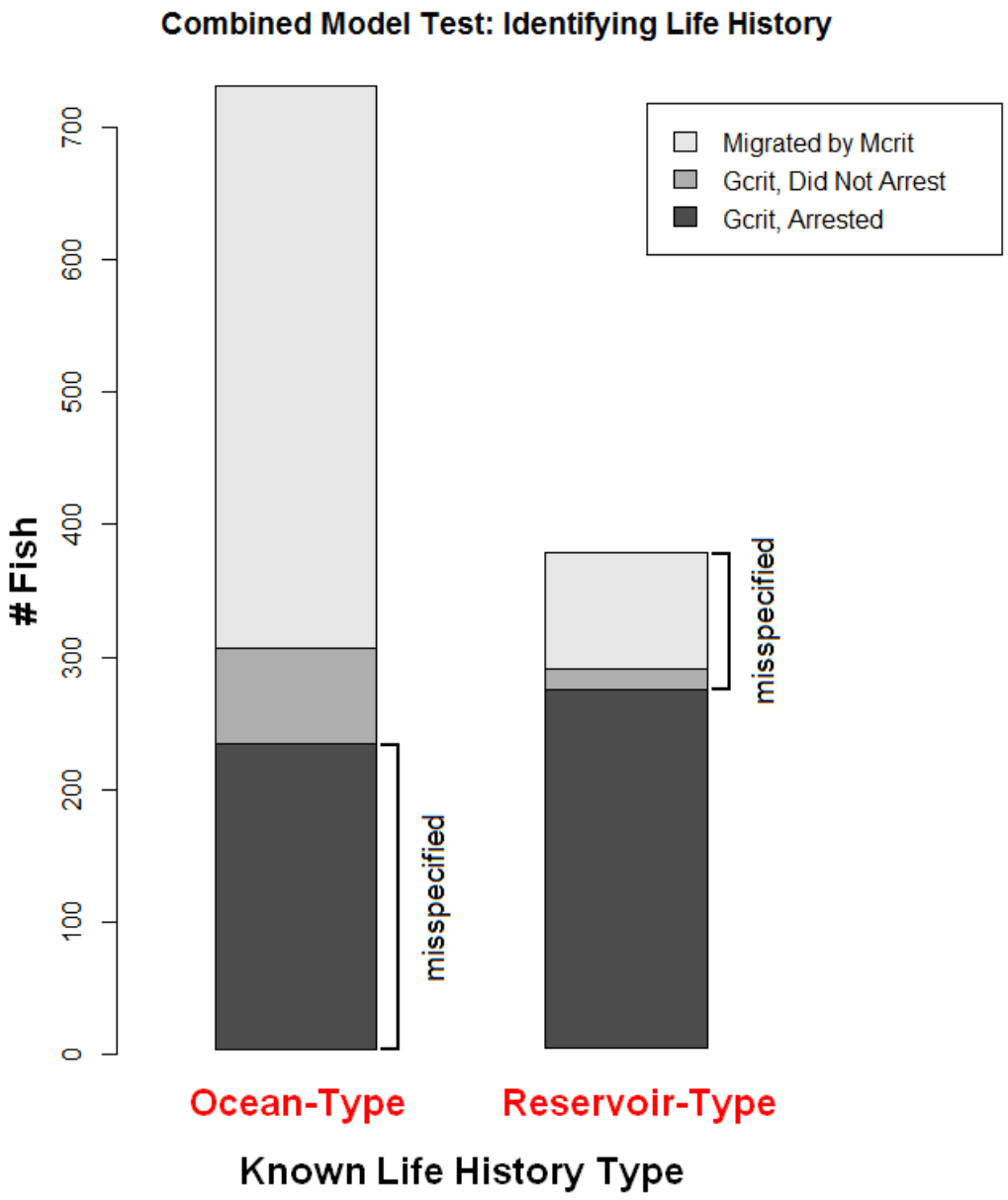

Plot of the life history outcomes predicted by the Mass-Growth model complex for 728 known ocean-type fish and 374 known reservoir-type fish. Three different model outcomes were possible: fish that migrated by the *Mcrit* threshold were modeled as ocean-type; fish that migrated by the *Gcrit* threshold but did not arrest migration were also modeled as ocean-type; fish that migrated by the *Gcrit* threshold and were modeled to arrest migration were modeled as reservoir-type. The fish in each known life history type that were modeled to follow the wrong life history are labeled as misspecified.

References

Anderson, J. J. 2000. Heat budget of water flowing through Hells Canyon and the effects of flow augmentation on Snake River water temperature. Columbia Basin Research, article available online at http://www.cbr.washington.edu/papers/jim/SRheatbudget.html

Anderson, J. J., Gurarie, E. and Zabel, R. W. 2005. Mean free-path length theory of predator-prey interactions: Application to juvenile salmon migration. Ecological Modeling 186:196-211.

Arreguin-Sanchez, F. 1996. Catchability: a key parameter for fish stock assessment. Reviews in Fish Biology and Fisheries 6:221-242.

Beer, W. N. 1998. Growth of Snake River Chinook salmon, draft. Columbia Basin Research, 70 electronic pages, article available online at http://www.cbr.washington.edu/papers/growth/fishgrow.html

Bellgraph, B. J., McMichael, G. A., Mueller, R. P. and Monroe, J. L. 2009. Behavioural response of juvenile Chinook salmon *Oncorhynchus tshawytscha* during a sudden temperature increase and implications for survival. Journal of Thermal Biology 35:6-10.

Bjornn, T. C. 1971. Trout and Salmon Movements in Two Idaho Streams as Related to Temperature, Food, Stream Flow, Cover, and Population Density. Transactions of the American Fisheries Society 100(3):423-438.

Bogacz, R. 2007. Optimal decision-making theories: linking neurobiology with behaviour. TRENDS in Cognitive Sciences 11(3):118-125.

Brannon, E. L., Powell, M. S., Quinn, T. P. and Talbot, A. 2004. Population structure of Columbia River Basin Chinook salmon and steelhead trout. Reviews in Fisheries Science 12:99-232.

Byrd, R. H., Lu, P., Nocedal, J. and Zhu, C. 1995. A limited memory algorithm for bound constrained optimization. SIAM Journal on Scientific Computing 16:1190–1208.

Carey, M. P., Sanderson, B. L., Friesen, T. A., Barnas, K. A. and Olden, J. D. 2011. Smallmouth Bass in the Pacific Northwest: A Threat to Native Species; a Benefit for Anglers. Reviews in Fisheries Science 19(3):305-315.

Chen, X., Thompson, M. B. and Dickman, C. R. 2004. Energy density and its seasonal variation in desert beetles. Journal of Arid Environments 56:559-567.

Connor, W. P., Burge, H. L., Waitt, R. and Bjornn, T. C. 2002. Juvenile life history of wild fall Chinook salmon in the Snake and Clearwater Rivers. North American Journal of Fisheries Management 22:703-712.

Connor, W. P. and Burge, H. L. 2003. Growth of wild subyearling fall chinook salmon in the Snake River. North American Journal of Fisheries Management 23:594-599.

Connor, W. P., Steinhorst, R. K., and Burge, H. L. 2003. Migrational behavior and seaward movement of wild subyearling fall chinook salmon in the Snake River. North American Jorunal of Fisheries Management 23:414-430.

Connor, W. P., Tiffan, K. and Sneva, J. 2004. Investigating Passage of ESA-listed Juvenile Fall Chinook Salmon at Lower Granite Dam during Winter when the Fish Bypass System is Not Operated. 2002-2003 Annual Report, Project No. 200203200, 75 electronic pages, BPA Report DOE/BP-00010474-1.

Connor, W. P., Sneva, J. G., Tiffan, K. F., Steinhorst, R. K. and Ross, D. 2005. Two alternative life history types for fall Chinook salmon in the Snake River basin. Transactions of the American Fisheries Society 134:291-304.

Cook, C. B., Dibrani, B., Richmond, M. C., Bleich, M. D., Titzler, S. and Fu, T. 2006. Hydraulic characteristics of the lower Snake River during periods of juvenile fall Chinook migration. Final Project Report 2002-2006, Project No. 2002-027-00, 176 electronic pages (BPA Report DOE/BP-00000652-29).

Curet, T. S. 1993. Habitat use, food habits and the influence of predation on subyearling Chinook salmon in Lower Granite and Little Goose reservoirs, Washington. Master’s thesis, University of Idaho.

Dauble, D. D. and Geist, D. R. 2000. Comparison of mainstem spawning habitats for two populations of fall Chinook salmon in the Columbia River basin. Regulated Rivers: Research & Management 16:345-361.

Dauble, D. D., Hanrahan, T. P., Geist, D. R. and Parsley, M. J. 2003. Impacts of the Columbia River Hydroelectric System on Main-Stem Habitats of Fall Chinook Salmon. North American Journal of Fisheries Management 23:641-659.

Deng, Z., Carlson, T. J., Dauble, D. D. and Ploskey, G. R. 2011. Fish Passage Assessment of an Advanced Hydropower Turbine and Conventional Turbine Using Blade-Strike Modeling. Energies 4:57-67.

Duffy, E. J. and Beauchamp, D. A. 2008. Seasonal Patterns of Predation on Juvenile Pacific Salmon by Anadromous Cutthroat Trout in Puget Sound. Transactions of the American Fisheries Society 137:165-181.

Feller, W. 1966. An Introduction to Probability Theory and Its Applications. Wiley, London.

Fritts, A. L. and Pearsons, T. N. 2008. Can non-native smallmouth bass, *Micropterus dolomeiu*, be swamped by hatchery fish releases to increase juvenile Chinook salmon, *Oncorhynchus tshawytscha*, survival? Environmental Biology of Fishes 83:485-494.

Geist, D. R., Deng, Z. and Mueller, R. P. 2009. Survival and growth of juvenile Snake River fall Chinook exposed to constant and fluctuating temperatures. Transactions of the American Fisheries Society, 139:92-107.

Gold, J. I. and Shadlen, M. N. 2007. The neural basis of decision making. Annual Review of Neuroscience 30:535-574.

Goniea, T. M., Keefer, M. L., Bjornn, T. C., Peerys, C. A., Bennett, D. H. and Stuehrenberg, L. C. 2006. Behavioral Thermoregulation and Slowed Migration by Adult Fall Chinook Salmon in Response to High Columbia River Water Temperatures. Transactions of the American Fisheries Society 135:408-419.

Groot C., Margolis, L. and Clarke, W. C. 1995. Physiological ecology of Pacific salmon. UBC Press, Vancouver, BC, Canada.

Gross, M. A. 1987. Evolution of diadromy in fishes. American Fisheries Society Symposium 1:14–25.

Hanrahan, T. P., Dauble, D. D. and Geist, D. R. 2004. An estimate of chinook salmon (*Oncorhynchus tshawytscha*) spawning habitat and redd capacity upstream of a migration barrier in the upper Columbia River. Canadian Journal of Fisheries and Aquatic Sciences 61:23-33.

Hansen, L. P. 1987. Growth, migration and survival of lake reared juvenile anadromous Atlantic salmon *Salmo salar* L. Fauna Norvegica Series A, 8:29-34.

Hanson, P. C., Johnson, T. B., Schindler, D. E. and Kitchell, J. F. 1997. Fish bioenergetics model 3.0. Center for Limnology, University of Wisconsin Sea Grant Institute, WISCU-T-97-001, Madison.

Harvey, C. J. and Kareiva, P. M. 2005. Community context and the influence of non-indigenous species on juvenile salmon survival in a Columbia River reservoir. Biological Invasions 7:651-663.

Healey, M. C. 1991. Life history of Chinook salmon (*Oncorhynchus tshawytscha*). Pages 312–393 *in* C. Groot and L. Margolis, editors, Pacific salmon Life Histories. UBC Press, Vancouver.

Hutchings, J. A. and Jones, M. E .B. 1998. Life history variation and growth rate thresholds for maturity in Atlantic salmon, *Salmo salar*. Canadian Journal of Fisheries and Aquatic Sciences 55(Supplement 1):22-47

Jager, H. I., Cardwell, H. E., Sale, M. J., Bvelhimer, M. S., Coutant, C. C. and Van Winkle, W. 1997. Modelling the linkages between flow management and salmon recruitment in rivers. Ecological Modelling 103:171-191.

Johnson, G. E. and Dauble, D. D. 2006. Surface Flow Outlets to Protect Juvenile Salmonids Passing Through Hydropower Dams. Reviews in Fisheries Science 14(3):213-244.

Krcma, R. F. and Raleigh, R. F. 1970. Migration of juvenile salmon and trout into Brownlee reservoir, 1962-65. Fishery Bulletin 68(2):203-217.

Luecke, C. and Brandt, D. 1993. Estimating the energy density of Daphnid prey for use with rainbow trout bioenergetics models. Transactions of the American Fisheries Society 122:386-389.

Madenjian, C. P., O'Connor, D. V., Chernyak, S. M., Rediske, R. R. and O'Keefe, J. P. 2009. Evaluation of a Chinook salmon bioenergetics model. Canadian Journal of Fisheries and Aquatic Sciences 61:627-635.

Mains, E. M. and Smith, J. M. 1964. The distribution, size, time, and current preferences of seaward migrant chinook salmon in the Columbia and Snake Rivers. Fisheries Research Papers, Washington Department of Fisheries 2:5-43.

Mangel, M. and Satterthwaite, W. H. 2008. Combining proximate and ultimate approaches to understand life history variation in salmonids with application to fisheries, conservation, and aquaculture. Bulletin of Marine Science 83(1):107-130.

Marsh, D. M., McIntyre, K. W., Sandford, B. P., Smith, S. G., Muir, W. D. and Matthews, G. M. 2010. Transportation of Snake River Fall Chinook Salmon 2008: Final Report for the 2004 Juvenile Migration. U.S. Army Corps of Engineers, Walla Walla District, Delivery Order E86960099, 54 electronic pages.

Marvin, D. and Nighbor, J. 2009. 2009 PIT Tag specification document. Pacific States Marine Fisheries Commission, 142 electronic pages.

Matthews, G. M. and Waples, R. S. 1991. Status review for Snake River spring and summer Chinook salmon. NOAA Technical Memorandum NMFS F/NWC-200.

McCormick, S. D., Hansen, L. P., Quinn, T. P. and Saunders, R. L. 1998. Movement, migration, and smolting of Atlantic salmon (*Salmo salar*). Canadian Journal of Fisheries and Aquatic Sciences 55(Supplement 1):71-92.

McNamara, J. M., Barta, Z., Klassen, M., and Bauer, S. 2011. Cues and the optimal timing of activities under environmental changes. Ecology Letters 14:1183-1190.

Metcalfe, N. B. 1998. The interaction between behavior and physiology in determining life history patterns in Atlantic salmon (*Salmo salar*). Canadian Journal of Fisheries and Aquatic Sciences 55(Supplement 1):93-103.

Morinville, G. R. and Rasmussen, J. B. 2003. Early juvenile bioenergetic differences between anadromous and resident brook trout (*Salvelinus fontinalis*). Canadian Journal of Fisheries and Aquatic Sciences 60:401-410.

Morinville, G. R. and Rasmussen, J. B. 2006. Does life-history variability in salmonids affect habitat use by juveniles? A comparison among streams open and closed to anadromy. Journal of Animal Ecology 75:693-704.

Muir, W. D. and Coley, T. C. 1996. Diet of yearling Chinook salmon and feeding success during downstream migration in the Snake and Columbia Rivers. Northwest Science 70:298-305.

Muir, W. D., Smith, S. G., Williams, J. G., Hockersmith, E. E. and Skalski, J. R. 2001. Survival Estimates for Migrant Yearling Chinook Salmon and Steelhead Tagged with Passive Integrated Transponders in the Lower Snake and Lower Columbia Rivers, 1993-1998. North American Journal of Fisheries Management 21:269-282.

Nelder, J. A. and Mead, R. 1965. A simplex algorithm for function minimization. Computer Journal 7:308–313.

NMFS (National Marine Fisheries Service). 1992. Threatened status for Snake River spring–summer Chinook salmon, threatened status for Snake River fall Chinook salmon. Federal Register 57:78(22 April 1992):14653–14663.

Petersen, J. H. and DeAngelis, D. L. 2000. Dynamics of prey moving through a predator field: a model of migrating juvenile salmon. Mathematical Biosciences 165:97-114.

Petersen, J. H. and Kitchell, J. F. 2001. Climate regimes and water temperature changes in the Columbia River: bioenergetic implications for predators of juvenile salmon. Canadian Journal of Fisheries and Aquatic Sciences 58:1831-1841.

Petrosky, C. E. and Schaller, H. A. 2010. Influence of river conditions during seaward migration and ocean conditions on survival rates of Snake River Chinook salmon and steelhead. Ecology of Freshwater Fish 19:520-536.

Quinn, T. P. 2005. The behavior and ecology of Pacific salmon & trout. University of Washington Press, Seattle.

Richter, A. and Kolmes, S. A. 2005. Maximum temperature limits for chinook, coho, and chum salmon, and steelhead trout in the Pacific Northwest. Reviews in Fisheries Science 13:23-49.

Ruiz, P. and Laplanche, C. 2010. A hierarchical model to estimate the abundance and biomass of salmonids by using removal sampling and biometric data from multiple locations. Canadian Journal of Fisheries and Aquatic Sciences 67:2032-2044.

Sauter, S. T., Crawshaw, L. I., and Maule, A. G. 2001. Behavioral thermoregulation by juvenile spring and fall chinook salmon, *Oncorhynchus tshawytscha*, during smoltification. Environmental Biology of Fishes 61:295-304.

Scheuerell, M. D., Zabel, R. W. and Sandford, B. P. 2009. Relating juvenile migration timing and survival to adulthood in two species of threatened Pacific salmon (*Oncorhynchus* spp.). Journal of Applied Ecology 46:983-990.

Schindler, D. E., Augerot, X., Fleishman, E., Mantua, N. J., Riddell, B., Ruckelshaus, M., Seeb, J. and Webster, M. 2008. Climate change, ecosystem impacts, and management for Pacific salmon. Fisheries 33(10):502-506.

Smith, S. G., Muir, W. D., Hockersmith, E. E., Zabel, R. W., Graves, R. J., Ross, C. V., Connor, W.P. and Arnsberg, B. D. 2003. Influence of River Conditions on Survival and Travel Time of Snake River Subyearling Fall Chinook Salmon. North American Journal of Fisheries Management 23(3):939-961.

Spence, B. C. and Hall, J. D. 2010. Spatiotemporal patterns in migration timing of coho salmon (*Oncorhynchus kisutch*) smolts in North America. Canadian Journal of Fisheries and Aquatic Sciences 67:1316-1334.

Stewart, D. J. and Ibarra, M. 1991. Predation and production by salmonine fishes in Lake Michigan, 1978-1988. Canadian Journal of Fisheries and Aquatic Sciences 48:909-922.

Stockwell, J. D., Bonfantine, K. L. and Johnson, B. M. 1999. Kokanee foraging: a Daphnia in the stomach is worth two in the lake. Transactions of the American Fisheries Society 128:169-174.

Sykes, G. E., Johnson, C. J. and Shrimpton, J.M. 2009. Temperature and flow effects on migration timing of Chinook salmon smolts. Transactions of the American Fisheries Society 138:1252-1265.

Tiffan, K. F., Haskell, C.A. and Rondorf, D. W. 2003. Thermal Exposure of Juvenile Fall Chinook Salmon Migrating Through a Lower Snake River Reservoir. Northwest Science 77(2):100-109.

Tiffan, K. F., Garland, R. D. and Rondorf, D.W. 2006. Predicted Changes in Subyearling Fall Chinook Salmon Rearing and Migratory Habitat under Two Drawdown Scenarios for John Day Reservoir, Columbia River. North American Journal of Fisheries Management 26(4):894-907.

Tiffan, K. F., Connor, W. P., Bellgraph, B. J., and Buchanan, R. A. 2008. Snake River fall Chinook salmon life history investigations, Annual Report 2008, Project No. 2002-03200, 55 electronic pages (BPA Document ID #P113402).

Tiffan, K. F., Kock, T. J., Connor, W. P., Steinhorst, R. K. and Rondorf, D. W. 2009. Behavioural thermoregulation by subyearling fall (autumn) Chinook salmon *Oncorhyncus tshawytscha* in a reservoir. Journal of Fish Biology 74:1562-1579.

Thorpe, J. E., Mangel, M., Metcalfe, N. B. and Huntingford, F. A. 1998. Modeling the proximate basis of salmonid life-history variation, with application to Atlantic salmon, *Salmo salar* L. Evolutionary Ecology 12:581-599.

Vigg, S., Poe, T. P., Prendergast, L. A. and Hansel, H. C. 1991. Rates of consumption of Juvenile Salmonids and Alternative Prey Fish by Northern Squawfish, Walleyes, Smallmouth Bass, and Channel Catfish in John Day Reservoir, Columbia River. Transactions of the American Fisheries Society 120(4):421-438.

Waples, R. S., Jones, R. P. Jr., Beckman, B. R. and Swan, G. A. 1991. Status review for Snake River fall Chinook salmon. NOAA Technical Memorandum NMFS F/NWC-201.

Waples, R. S., Zabel, R. W., Scheuerell, M. D., and Sanderson, B. L. 2007. Evolutionary responses by native species to major anthropogenic changes to their ecosystems: Pacific salmon in the Columbia River hydropower system. Molecular Ecology 17:84-96

Weitkamp, L. A., Orsi, J. A., Myers, K. W. and Francis, R. C. 2011. Contrasting Early Marine Ecology of Chinook Salmon and Coho Salmon in Southeast Alaska: Insight into Factors Affecting Marine Survival. Marine and Coastal Fisheries: Dynamics, Management, and Ecosystem Science 3:233-249.

Werner, E. E., Mittelback, G. G., Hall, D. J. and Gilliam, J. F. 1983. Experimental tests of optimal habitat use in fish: the role of relative habitat profitability. Ecology 64(6):1525-1539.

Werner, E. E. and Gilliam, J. F. 1984. The ontogenetic niche and species interactions in size-structured populations.

Williams, J. G. 2008. Mitigating the effects of high-head dams on the Columbia River, USA: experience from the trenches. Hydrobiologia 609:241-251.

Williams, J. G., Zabel, R. W., Waples, R. S., Hutchings, J. A. and Connor, W. P. 2008. Potential for anthropogenic disturbances to influence evolutionary change in the life history of a threatened salmonid. Evolutionary Applications 1:271-285.

Yates, D., Galbraith, H., Purkey, D., Huber-Lee, A., Seiber, J., West, J., Herrod-Julius, S. and Joyce, B. 2008. Climate warming, water storage, and Chinook salmon in California's Sacramento Valley. Climatic Change 91:335-350.